UNIVERSITY OF SOUTHAMPTON

FACULTY OF MEDICINE, HEALTH & LIFE SCIENCES
Cancer Sciences Division

B Cell Receptor Apoptosis: Signalling and Regulation

by

Matthew David Fox, BSc (Hons)

Thesis for the degree of Doctor of Philosophy

August 2005

UNIVERSITY OF SOUTHAMPTON

ABSTRACT

FACULTY OF MEDICINE, HEALTH AND LIFE SCIENCES; CANCER SCIENCES DIVISION

Doctor of Philosophy

B CELL RECEPTOR APOPTOSIS: SIGNALLING AND REGULATION

By Matthew David Fox

The response of B cells to contact with antigen is controlled by intracellular signals transmitted through the B cell receptor for antigen (BCR). At certain stages of B cell differentiation, these signals, generated by cross-linking the BCR, lead variously to proliferation, differentiation or cell death. This latter outcome is of interest with respect to immunotherapy of B cell tumours where monoclonal antibodies (mAb) can mimic antigenic contact. To date, research has focused on the production of mAb raised against specific idiotypic domains of tumour BCR. Unfortunately, although good clinical responses are seen with this so-called anti-idiotype approach, the unique specificity of these reagents renders them unfeasible as a cost effective means of large-scale tumour therapy. Therefore, reagents that are more generic are required, capable of targeting a range of different tumours. Similarly, it is still unclear which signals elicited from the BCR are important for initiating tumour cell death.

The following study was undertaken, using a variety of B cell lymphoma lines to investigate which properties of anti-BCR mAb are important for the induction of cell death. The data contained in this thesis demonstrates that the IgM region of the BCR is a potent inducer of apoptosis. Interestingly, only mAb raised against the Fcμ domain of mIgM could induce potent apoptosis. Although mAb raised against the Fdμ, light chains and Id domain of mIgM and mAb raised against the CD79 heterodimer did not induce apoptosis, all mAb induced activation of protein tyrosine kinase (PTK) signalling cascades, and release of intracellular calcium. What appears to be important is the kinetics of PTK and calcium signalling from the BCR such that anti-Fcμ mAb induce moderate, but prolonged PTK activation. In particular, the PTK Syk but not Lyn was shown to be regulated in this way.

Next, we sought the reason for the difference in signalling and apoptosis induced by the various mAb. After discounting the binding level and affinity of the mAb, we investigated the ability of the mAb to cause disruption of the BCR. Whilst anti-Fcμ mAb caused disruption of the BCR, leading to the dissociation of mIgM from the CD79 heterodimer, other mAb did not. It was postulated that this results in the CD79 heterodimer being retained at the cell surface for a longer period of time, causing prolonged signalling, which was demonstrated by flow cytometry. Conversely, other mAb specificities caused the whole BCR complex to be internalised leading to more rapid shut down of the PTK.

Another aspect of research into providing therapy for lymphomas relies on the further understanding of causative factors of disease. Previous studies have shown that an alternative transcript of CD79b is present in human B cells, and raised in tumour cells isolated from patients suffering from various B cell tumours. To assess whether this might be a central means of regulating deleterious BCR signals, we assessed whether this transcript was also present in normal and malignant mouse B cells. Using RT-PCR, sequencing and western blotting, we demonstrate for the first time that an alternative transcript of CD79b that lacks the whole of exon three (mΔCD79b) is also present in murine B cell lines and normal splenocytes. Research indicates that over-expression of this transcript inhibits BCR induced apoptosis, possibly through regulation of different PTK signalling cascades.

The data represented in this thesis help to explain why only certain mAb directed at the BCR have been successful in therapy and indicate a possible mechanism for their efficiency. In addition, that mΔCD79b does affect the activation of PTK generated through cross-linking BCR and remains a possible causative factor for B-CLL.

Table of Contents

List of Figures

List of Tables

Authorship declaration
I declare that this thesis represents entirely my work.

This thesis has not been submitted for any other degree.

Publications

Cragg MS, Chan HT, Fox MD, Tutt A, Smith A, Oscier DG, Hamblin TJ, Glennie MJ. (2002) The alternative transcript of CD79b is overexpressed in B-CLL and inhibits signaling for apoptosis. **Blood.** 100(9):3068-76.

Fox MD, Cragg MS, and Glennie MJ. (2005) Identification of an Alternative transcript of murine CD79b. **European Journal of Immunology.** (submitted)

Presentations

Parts of this work have been presented at:

M.D. Fox, M.S. Cragg and M.J. Glennie. Identification and characterisation of an alternative transcript of mouse B29.
Poster presentation; BSI Annual Congress, December 2002.

M.D. Fox, M.S. Cragg and M.J. Glennie. Identification and characterisation of an alternative transcript of mouse B29.
Keystone Symposia Scholarship award; Poster presentation, Lymphocyte signalling conference, January 2004.

M.D. Fox, M.S. Cragg and M.J. Glennie. Signalling and redistribution events in BCR induced apoptosis.
Poster presentation; Keystone Symposia, Lymphocyte signalling conference, January 2004.

Acknowledgements

Firstly I need to thank my parents, Chris and Barry, to whom this thesis is dedicated. It is with their encouragement that I have been enabled to realise my true potential. I also need to thank them for all the financial and emotional support they have given me over the past seven years. I also need to thank Hannah, Darren and the two 'mad' Nan's for all the support.

Next I would like to thank my supervisors; Martin Glennie and Mark Cragg for their help in guiding me through my PhD. I would also like to thank them for putting up with my sometimes erratic theories and allowing me to pursue areas of scientific research that have been of most interest to me.

A big thanks is needed to everyone in the Directors group at Tenovus not only for the support but also for putting up with an extremely 'cheeky chap'! Special thanks to Auntie Mo and Alison Tutt for preparing mAb and Claude Chan for help on the molecular biology front. Also to the 'young ones' for supplying excuses to go down the pub, and allowing us to sample a wide variety of burgers in most of the local establishments.

To Paul, Denise, Paul Junior, Sally, Squiggles, Mark and Caroline for all support, laughs over the past three years and for also making me feel welcome.

Finally, but no means least, to my future wife Jane, for not only putting up with me but also making the past three years the most enjoyable of my life. You are my light.

Abbreviations

Ab	Antibody
ADCC	Antibody Directed Cellular Cytotoxicity
Ag	Antigen
B-CLL	B cell Chronic Lymphocytic Leukaemia
BCR	B cell receptor
BLNK	B cell Linker protein
BM	Bone Marrow
BN-PAGE	Blue Native Polyacrylamide Gel Electrophoresis
Btk	Brutons Tyrosine Kinase
DAG	Diacylglycerol
EBV	Epstein Bar Virus
ER	Endoplasmic Reticulum
ERK	MAPK Extracellular signal Regulated Kinase
FCS	Foetal Calf Serum
FDC	Follicular Dendritic Cells
GC	Germinal Centre
GEF	Guanine nucleotide Exchange Factors
HRP	Horse Radish Peroxidase
HSC	Haematopoietic Stem Cells
Id	Idiotype
IgH	Ig-Heavy chain
IgL	Ig-Light chain
IL	Interlukin
IP3	Inositol 1,4,5-triphosphate
ITAM	Immunoreceptor Based Activation Motif
ITIM	Immunoreceptor Tyrosine-based Inhibitory Motif
JNK	c-jun NH2 –terminal Kinase
LMP2A	Latent Membrane associated Protein 2A
mAb	Monoclonal Antibodies
mIg	Membrane associated Immunoglobulin
mRNA	Messenger RNA
NFAT	Nuclear Factor of Activated T cells
PH	Plekstrin Homology domain
PIP_2	Phosphatidylinositol (3,4)-bisphosphate
PIP_3	Phosphatidylinositol (3,4,5)-triphosphate
PI3-K	Phosphatidylinositol 3-Kinase
PKC-β	Protein Kinase C-β
PLCγ2	Phospholipase Cγ2
PS	Phosphatidylserine
PTK	Protein Tyrosine Kinases
PTP	Protein Tyrosine Phosphatase
PVDF	Polyvinylidene Diflouride
RAG	Recombinase Activating Genes
SDS-PAGE	Sodium Dodecyl Sulphate Polyacrylamide Gel Electrophoresis
SHIP	SH2-domain containing phosphatidylinositol 5-Phosphate
SHP-1	SH2 domain containing protein tyrosine Phosphatase
SH2	Src-Homology 2 domain
siRNA	Short Inhibitory RNA
SOS	Sons of Sevenless
TdT	Terminal deoxynucleotidyl Transferase

Chapter 1

Introduction

1.1 B cell receptor for antigen

B cells are a pivotal part of the humoral immune system, allowing the host to effectively defend their environment from invading pathogens[1]. Possibly, the most important molecule expressed on the B cell surface is the B cell receptor (BCR) for antigen (Ag). The BCR plays a fundamental role in the activation of the B cell in response to foreign Ag and also regulating its development[2]. Both of these functions require appropriate signalling through the BCR. In addition, the BCR is responsible for delivering receptor bound Ag for processing and presentation via MHC class II molecules to helper T cells[3]. Both of these processes are required for complete B cell activation and mounting of an appropriate immune response.

The BCR is comprised of a membrane associated immunoglobulin (mIg) molecule non-covalently associated with the CD79 heterodimer. The association of these two molecules and their expression at the cell surface is critical to the activation of intracellular signalling pathways that are induced when the BCR is cross-linked by Ag[4, 5]. The structure and function of the BCR will now be discussed, along with current views on receptor redistribution in response to ligation.

1.1.1 Membrane bound immunoglobulin

Membrane Ig is expressed on the surface of normal B cells at 10^4-10^5 copies per cell, with the predominant isotypes being IgM and IgD[6], although all classes of immunoglobulin (IgM, IgD, IgG, IgE, and IgA) have been shown to exist as structurally distinct mIg forms on the B cell surface[7]. mIg consists of two Ig heavy chains forming a homodimer and two light chains each of which is covalently bound to one of the heavy chains[8]. The mIgM and mIgD are not capable of initiating signalling pathways following BCR cross-linking as the intracellular region of these two isotypes consists of only three amino acid residues; lysine, valine, lysine (KVK)[8]. The cytoplasmic domains of the other mIg isotypes express an extended number of residues of either 28 (IgG, IgE) or 14 (IgA) amino acids, and may be important in delivering istotype specific intracellular responses[9].

1.1.2 CD79 heterodimer

The CD79 heterodimer (CD79a and CD79b) is comprised of two structurally similar proteins linked by an extracellular disulfide bond[10]. CD79a and CD79b are encoded by the B cell specific genes *mb-1* and *B29* respectively, encoding proteins of 34kDa and 39kDa, depending on the glycosylation state of the protein[11-14]. The B cell specific gene *mb-1* is located at position 19q13.2 in the human genome and 7p20.1 in murine genome[13-15]. B29 is located at position 17q23.3 in the human genome and 11q106.13 in the murine genome[13-15]. Both proteins comprise an N-terminal leader sequence followed by either 109 (CD79a) or 129 (CD79b) amino acid extracellular domain[8, 15]. CD79b contains an additional exon (exon 2) encoding a small extracellular peptide before the main extracellular region[16]. The extracellular domains of CD79a and CD79b contain three and five cysteine residues respectively, along with one tryptophan and several other conserved residues found in proteins of the immunoglobulin super-family[15]. From this sequence data, prediction modelling indicates that the extracellular domains of CD79a and CD79b form an Ig-like domain with intra-domain disulfide bonds and with both proteins joined via an inter disulfide as shown in Figure 1.1[8, 16].

Both CD79 proteins also contain a 22 amino acid transmembrane domain containing either negatively charged (CD79a) or polar (CD79b) residues[8]. The C-terminal cytoplasmic domains of CD79a and CD79b consist of 61 and 48 amino acids containing four and two tyrosine residues, respectively[8]. The cytoplasmic domain of CD79a and CD79b contain a specific sequence known as the Immunoreceptor Based Activation Motif (ITAM), which is responsible for mediating the intracellular signalling cascade[4]. ITAM motifs are also found on the C-terminal domain of other important immune receptors including the T cell receptor for Ag and the γ-chain of the IgE Fc-receptor on mast cells[17]. All three types of receptor are activated by cross-linking leading to rapid tyrosine phosphorylation and calcium mobilisation within the cell[18]. The single ITAM motif located in the cytoplasmic domain of each CD79 protein consists of six conserved amino acid residues spaced over a 26 amino acid sequence ($D/EX_7D/EX_2YX_2LX_7YX_2L$)[4, 8]. Each ITAM motif contains two negatively charged residues and two tyrosine residues; mutation of the two tyrosine residues to alanines ablates the triggering of the intracellular signalling cascade in B cells[19, 20].

1.1.3 Association of mIg and CD79 heterodimer

It is known that the extracellular and transmembrane domains of CD79a and CD79b interact with mIg[8, 21]. The interaction between mIg and the CD79 heterodimer is both necessary

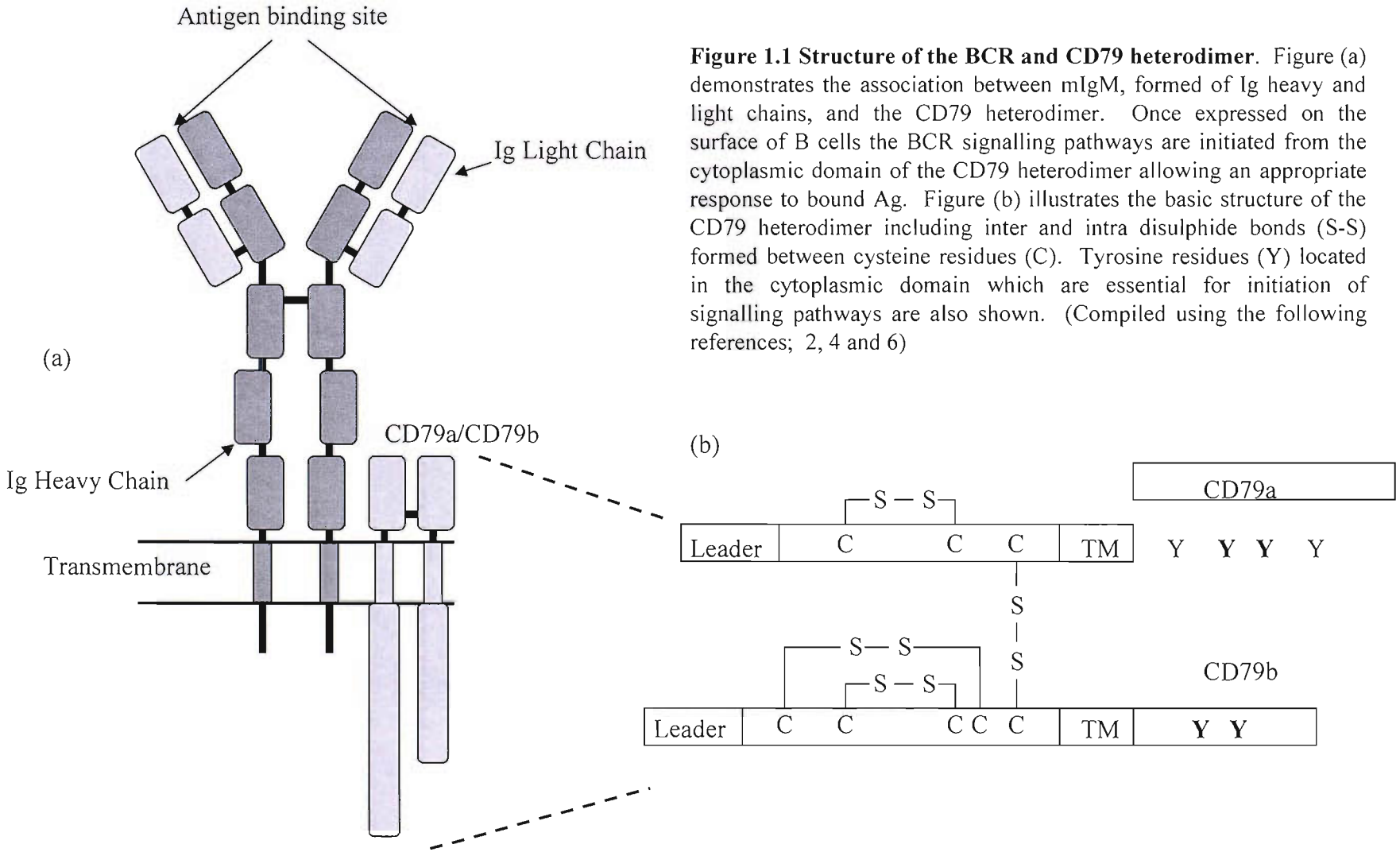

Figure 1.1 Structure of the BCR and CD79 heterodimer. Figure (a) demonstrates the association between mIgM, formed of Ig heavy and light chains, and the CD79 heterodimer. Once expressed on the surface of B cells the BCR signalling pathways are initiated from the cytoplasmic domain of the CD79 heterodimer allowing an appropriate response to bound Ag. Figure (b) illustrates the basic structure of the CD79 heterodimer including inter and intra disulphide bonds (S-S) formed between cysteine residues (C). Tyrosine residues (Y) located in the cytoplasmic domain which are essential for initiation of signalling pathways are also shown. (Compiled using the following references; 2, 4 and 6)

and sufficient for the release of the complete BCR from the endoplasmic reticulum (ER) and transport to the cell membrane[22].

Due to the short cytoplasmic domains of mIgM and mIgD it was proposed that the mIg must associate with a signalling complex to allow the transmission of intracellular signals upon receptor cross-linking[4]. Hombach, *et al.*,[22] showed that Myeloma cell lines that do not express mIg, would not express mIg at the surface even if transfected with mIgM DNA. However, repeated cloning and sorting lead to the isolation of one clone expressing mIgM at the cell surface. Further analysis revealed that the surface IgM molecule was there in the presence of an associated heterodimer which had been lacking from the other clones[23]. The finding that mIg is associated with an accessory heterodimer, allowing the expression of mIg at the cell membrane was also shown by other groups[24]. This heterodimer is now known as the CD79 heterodimer, and mIgM expression is dependent on the cellular expression and association of mIgM with CD79a and CD79b[21]. In fact mIg expression of all isotypes is dependent on the expression and association of the CD79 heterodimer[25].

Prediction modelling shows that if the transmembrane domain of mIg were to form an α-helix then one side of the helix would contain a large number of polar amino acid residues which are highly conserved among all mIg isotypes[26, 27]. These polar residues are required to be neutralised by protein-protein interactions. Therefore, it is predicted that polar residues located in the transmembrane domain of the CD79 heterodimer may provide this interaction[8]. This theory has been supported by the fact that mutation of the mIg transmembrane polar residues to non-polar residues prevents that association of mIg with the CD79 heterodimer[26-28]. Importantly, these and other experiments of this type have shown that although mutant mIg molecules are capable of escaping from the ER without CD79 and being expressed at the cell surface, cross-linking of these receptors fails to initiate intracellular signalling cascades[28, 29]. Studies investigating the glycosylation state of the CD79 heterodimer have reported that CD79a can be differentially glycosylated and this may account for the association of the CD79 heteromdimer with different mIg isotypes[26,27]. There have been no reported differences in the glycosylation state of CD79b, or of differences in the glycosylation state of CD79a and CD79b between species. It was also predicted that two CD79 heterodimers would associate with one mIg, due to the presence of two Ig heavy chains and the requirement to neutralise two sections of polar residues[8], however, recent evidence suggests that this may not be the case and only one CD79 heterodimer associates with one mIg molecule[30].

1.2 Activation of B cell signalling pathways

Cross-linking of the BCR upon ligation of mIg with Ag leads to the activation of intracellular signalling pathways. It is these signals, along with others from helper T cells, that then direct mature B cells to differentiate into plasma cells which secrete antibody (Ab) directed towards the initial Ags[4, 5]. B cells develop from a single progenitor cell giving rise to a large proportion of cells that express individual Ag specificity[31]. Inevitably, a large proportion of B cells develop containing a variable domain of the BCR specific for 'self' Ag. During development, B cells that bind 'self' Ag initiate signalling pathways that result in eradication of self reactive cells by the process of apoptosis, which is detailed in figure 1.2[2].

It has been known for some time that cross-linking of the BCR with multivalent Ag or monoclonal antibodies (mAb) that cause receptor aggregation leads to the activation of intracellular protein tyrosine kinases (PTK), release of intracellular calcium and the activation of nuclear transcription factors[32, 33].

Over the past decade research has allowed the discovery of specific PTK activated in response to BCR cross-linking. It is clear that specific PTK bind phosphorylated tyrosine residues located within the ITAM motifs of the CD79 heterodimer, which in turn become activated and subsequently activate other downstream PTK that lead to both release of intracellular calcium, and the activation of nuclear transcription factors. Nuclear transcription factors that are important in B cell responses to intracellular signalling pathways include; NF-κB, c-jun, nuclear Factor of Activated T cells (NFAT), c-Rel and Rel-A, activated by downstream effector molecules including the MAPK extracellular signal regulated kinase (ERK), c-jun NH2 –terminal kinase (JNK-1), and p38 MAPK[32]. Although the final stages of the B cell signalling pathway are reasonably well characterised the initiation events of BCR signalling have led to much disagreement within the field.

It is accepted that BCR activated intracellular signalling pathways originate from the CD79 heterodimer, however, the process of receptor signalling and PTK activation is complex. The main outline of B cell signalling pathways is detailed in Figure 1.3.

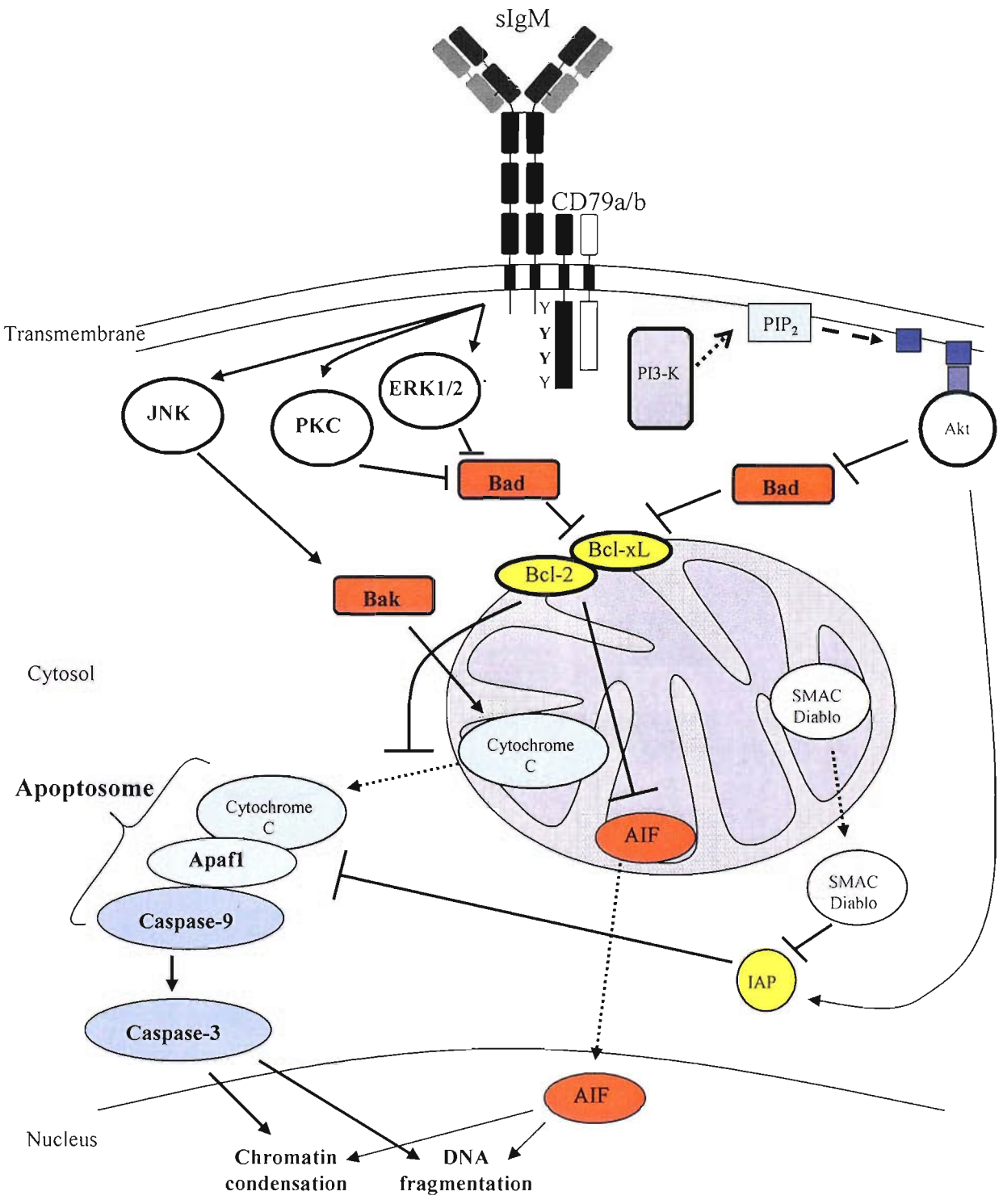

Figure 1.2 Apoptosis pathways leading from activation of the BCR. Cross-linking of the BCR on the surface of B cells in response to Ag leads to the activation of downstream molecules. Activation of these molecules can either lead to cell death or cell survival depending on the type of PTKs activated. The difference in the type of pro- or anti-apoptotic factors depends on the stage of B cell development and the severity of the PTK activated.

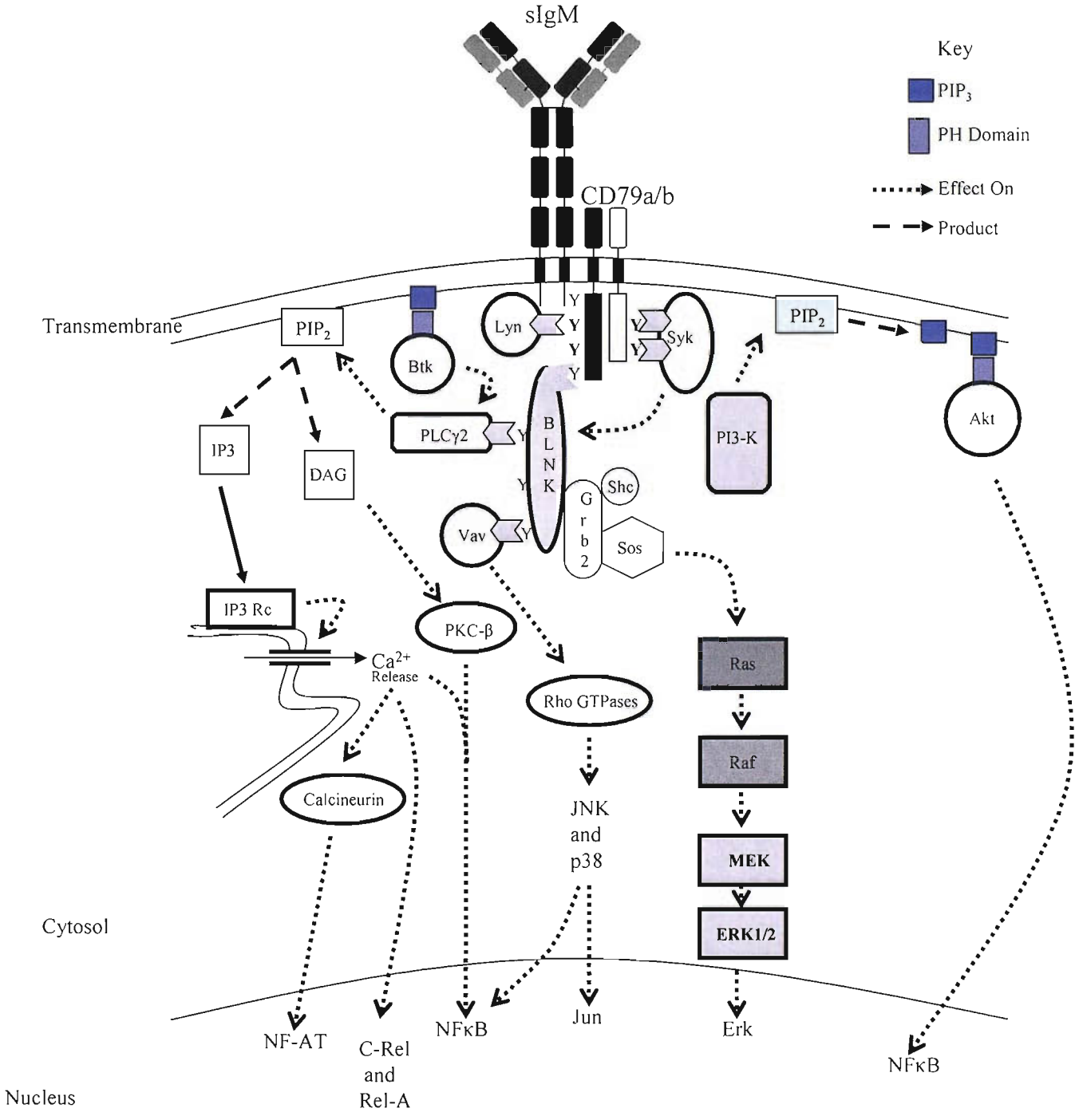

Figure 1.3 Activation of Intracellular Signalling Pathways. Cross-linking of the BCR on the surface of B cells in response to Ag leads to the activation of a variety of PTKs. Activation of these PTKs leads to the activation of intracellular signalling pathways ultimately leading to the activation of nuclear transcription factors within the cell nucleus. Complied using the following references; 8, 18, 21, 36, 38, 41, 44, 46, 48, 50, 53, 54, 56 and 62.

Signal transduction has been shown to proceed from the ITAM motifs located within the cytoplasmic domain of the CD79 heterodimer, and is dependent on the successful expression of the CD79 heterodimer with mIg[22]. Prevention of mIg associating with the CD79 heterodimer either by deleting the cytoplasmic domain of mIg, or mutating the polar residues located within the transmembrane region of mIg heavy chain also prevent the initiation of signalling pathways shown by the ablation of tyrosine phosphorylation[28, 29]. Activation of the initial PTK by CD79 leads to further PTK activation and the spreading of a signalling pathway within the cell leading to the activation of nuclear transcription factors[32]. Initiation of signalling pathways also rely on the interaction between PTKs and protein tyrosine phosphatases (PTP), which oppose the actions of PTKs[34]. It is the balance between PTKs and PTPs that allows the tight regulation of signalling pathways.

1.2.1 Src-family kinases

Once the BCR has clustered at the cell membrane in response to Ag or mAb, the tyrosine residues located within the ITAM motif of the CD79 heterodimer must be phosphorylated to allow signalling pathways to develop. Clark, *et al.*,[35] were among the first to demonstrate that the cytoplasmic domain of CD79a and CD79b bind PTK upon BCR cross-linking. Initial evidence indicated that the Src-family kinases were the first to phosphorylate and bind activated tyrosine residues located within the ITAM motif[36, 37]. Evidence showed that Src-family kinases that include Lyn, Fyn, Blk, and Fgr can bind phosphorylated tyrosine residues via their single Src-homology 2 (SH2) domain and become activated[4, 33].

Coupling of the CD79a and CD79b cytoplasmic domains to external ligands such as MHC class II or Platelet Derived Growth Factor Receptor shows that 80% of the phosphorylation first occurs at the N-terminus of the ITAM motif[38]. This suggested that Src-family kinases phosphorylate the N-terminus tyrosine residue located in the ITAM motif, bind and subsequently activate further downstream PTKs allowing the spread of signalling pathways[32].

1.2.2 Syk protein tyrosine kinase

Following the activation of Src-family kinases and the phosphorylation of both tyrosine residues located within the ITAM motif, it is traditionally thought that Syk, a non-Src like PTK is next to bind the ITAM motif. Syk binds via its two SH2 domains; importantly both SH2 domains are required to be bound for full activation of Syk[4]. However, recent controversial research suggests that binding of Syk to the ITAM motif is independent of

Src-family kinases. Rolli *et al.*,[39] suggest that Syk under certain conditions can phosphorylate both tyrosine residues located within the ITAM motif itself, allowing it to subsequently become fully activated by binding through both SH2 domains.

It is believed that Syk is tightly regulated by SH2 domain containing protein tyrosine phosphatase (SHP-1) which de-phosphorylates tyrosine residues within the ITAM motif preventing Syk binding and initiation of full signalling pathways[40, 41]. This theory suggests that the interaction of PTK such as Syk and regulation by PTP generates a low basal signal that sustains the life of the cell[42]. This new theory was proposed as a result of Syk knock out models that indicate binding of Syk to ITAM motifs is essential for completion of the signalling pathways and activation of downstream signalling effectors; ERK, JNK1 and p38[43, 44].

1.2.3 Adaptor proteins

The signal transduced from the ITAM motif of the activated BCR cannot be transported directly to the nucleus by Src-family or Syk PTKs. Therefore complex adaptor proteins including; phosphatidylinositol 3-kinase (PI3-K), the B cell linker protein (BLNK), Sons of Sevenless (SOS), Shc and Grb2 function to build a strong basis from which the signal can amplify and spread.

1.2.3.1 PI3-K

PI3-K remains the least well understood of all PTKs involved in B cell signalling. PI3-K is known to play a fundamental role in the B cell signalling pathway as PI3-K knockout models show abnormalities in B cell activation and development[45, 46]. Three classes of PI3-K exist, with class one remaining the most studied. PI3-K contains an SH2 domain that binds phosphorylated tyrosine residues within YXXM motif leading to its activation[47]. Activated PI3-K has the capability to phosphorylate phosphatidylinositol (3,4)-bisphosphate (PIP_2) to phosphatidylinositol (3,4,5)-triphosphate (PIP_3). The production of PIP_3 is important in aiding the recruitment of PTK to the plasma membrane that contain Plekstrin Homology (PH) domains[48, 49]. Recruitment of PH containing PTK including Akt (or PKB) and Brutons Tyrosine Kinase (Btk) are essential for activation of distinct signalling pathways. Although Btk is widely known to play a key role in calcium mobilisation, the activation of Akt is less well understood. Akt is known to be important in providing anti-apoptotic signals to the B cell by the activation of nuclear transcription factor NF-κB[50, 51].

PI3-K knock out models fail to show BCR activated phosphorylation of Akt and subsequently fail to activate NF-κB[52].

1.2.3.2 BLNK

The most well characterised adaptor protein to date in B cells is BLNK, which is phosphorylated shortly after the activation of Syk[53, 54]. BLNK is a cytoplasmic adaptor protein containing several N-terminal tyrosine phosphorylation sites, a proline rich stretch and consensus recognition motifs for SH3 domains and a C-terminal SH2 domain[32]. BLNK acts as a scaffold, recruiting various signalling proteins including Phospholipase Cγ2 (PLCγ2), Vav, Grb2, Nck, and Btk[55, 56].

BLNK binds to the phosphorylated tyrosine at the C-terminus of the CD79a cytoplasmic domain at position Y204, located outside of the ITAM motif[57]. Mutation of this tyrosine to phenylalanine prevents association of BLNK with the CD79 heterodimer, interrupting the intracellular signalling cascade[57]. BLNK knockout mice show severe Ab deficiency and a phenotype that matches X-linked agammaglobulinaemia in humans and X-linked Immunodeficiency in mice[53]; with B cell development blocked at the pro- to pre-B cell stage[58, 59].

1.2.4 Release of intracellular calcium

One of the earliest intracellular responses to BCR activation along with protein tyrosine phosphorylation is the increase in concentration of intracellular calcium[18]. Upon BCR activation, Btk migrates to the plasma membrane where it binds to PIP_3 via its N-terminal PH domain[60, 61]. Binding of Btk to the plasma membrane brings it within reach of activated PTKs allowing its phosphorylation by Src-family kinases and subsequent activation[62]. Although the activation of Btk is thought to be dependent on PI3-K due to the presence of a PH domain, recent evidence suggests that Btk translocation to the plasma membrane and subsequent activation is unaffected in PI3-$K^{-/-}$ murine models[63]. The loss of functional Btk expression has been linked with reported disease states in both murine and humans. Btk deficiency leads to impaired maturation of B cells between the pro- to pre-B stage, diminished Ig production, compromised T-independent immune response and a marked attenuation of sustained calcium signalling upon BCR activation[64, 65].

The most studied PTK involved in increasing the concentration of intracellular calcium is PLCγ2, with its activation dependent on the activation of PTKs including Syk and Btk. PLCγ2 binds phosphorylated tyrosine residues on BLNK via its SH2 domain, allowing its

recruitment to the plasma membrane[33]. Phosphorylation of PLCγ2, by Btk and Syk leads to its full activation allowing cleavage of PIP_2 to inositol 1,4,5-triphosphate (IP3) and diacylglycerol (DAG)[32]. IP3 binds to its receptor located within the ER, leading to the release of intracellular calcium stores and an increase in the concentration of cytosolic calcium[66, 67]. This sudden increase in cytosolic calcium also leads to the activation of calcineurin, de-phosphorylation and migration to the nucleus resulting in the activation of the nuclear transcription factor; NFAT[68]. Increased cytosolic calcium levels also promote the nuclear translocation of NK-κB, c-Rel and Rel-A transcription factors[32].

1.2.5 Activation of PKC

Activated DAG in the presence of calcium leads to the activation of protein kinase C-β (PKC-β)[4, 69]. Upon activation, PKC-β is recruited to the plasma membrane along with the IKK complex, which is comprised of the nuclear transcription factor NF-κB and its regulatory molecule IκB[70]. IκB negatively regulates NF-κB preventing translocation of the nuclear transcription factor from the cytosol to the nucleus[71, 72]. Recruitment of the IKK complex to the plasma membrane allows phosphorylation of IκB by PKC-β, targeting it for ubiquitination and degradation, releasing NF-κB and allowing it to translocate to the nucleus[70].

1.2.6 Activation of Rho-family GTPases

Vav, a member of the guanine nucleotide exchange factors (GEF) of the Rho family GTPases is phosphorylated upon BCR activation[73]. Vav phosphorylation allows the activation of Rho-family GTPases including Rac-1, RhoA and Cdc42[74]. Rho-family GTPases are induced to undergo GDP to GTP exchange, functioning as molecular switches to activate downstream signalling effectors such as MAPK; JNK and p38[43, 75]. The Rho-family of GTPases also promote site-specific actin polymerisation leading to alterations in plasma membrane structures allowing the capping of activated BCR and optimal calcium mobilisation[73]. Rho-GTPases also function to allow sustained hydrolysis of PIP_2 by stimulating the PIP 5-kinase that synthesises PIP_2[76].

1.2.7 Ras activation

Another GTPase involved in the activation of nuclear transcription factors following activation of B cell PTKs is the Ras GTPase. Following BCR activation the GEF SOS associates with the adaptor proteins Shc and Grb2 forming a complex of Shc-Grb2-SOS and its translocation to the plasma membrane[77]. BLNK plays a fundamental role in the

activation of Ras-GTP by recruiting Grb2[78], increasing concentrations of Grb2 and SOS are associated with BLNK upon BCR activation and pervanedate treatment of B cells[54]. Grb2 binds to BLNK via its N-terminal SH3 and SH2 domains and the C-terminal SH3 domain allows the binding of SOS via its proline rich domain. Translocation of SOS to the plasma membrane directly activates Ras-GTP allowing it to function as a GEF[32].

Ras-GTP recruits the serine/threonine kinase Raf (MAPKKK) to the plasma membrane for activation[43, 75]. Following activation, Raf phosphorylates the dual-specificity kinase MEK (MAPKK) which then phosphorylates and activates ERK (MAPK) which is responsible for regulating various cytoplasmic and nuclear effectors[43, 75].

There are two isotypes of Raf that are predominantly expressed in mammalian tissue, Raf-1 and B-Raf[79]. Initial research indicated that Raf-1 was required for downstream ERK activation and transcription of the immediate early genes egr-1 and c-fos[80, 81]. However, recent research indicates that Raf-1 deficient DT40 B cells only slightly down regulate ERK activity, where B-Raf deficient cells lose complete ERK activation and subsequent activation of NFAT, following BCR mediated activation[79].

1.2.8 Role of protein tyrosine phosphatases

The triggering of signalling pathways is controlled within the cell to prevent constant and inappropriate activation[34, 40]. B cell signalling pathways utilise PTPs to regulate the action of PTKs within the cell. Important PTKs controlled by PTPs include Src-family kinases and Syk[34]. The major PTPs involved in regulating BCR signalling are SHP-1, CD45 and the SH2-domain containing phosphatidylinositol 5-phosphate (SHIP)[82-84]. Interactions between PTPs and PTKs not only allow the initiation of the signalling pathway due to the removal of inhibitory phosphorylated tyrosine residues on signalling PTKs but also prevent activation in resting B cells and aid in setting a signalling transduction threshold[34, 40].

For example in resting B cells, Src-family kinases are prevented from undergoing spontaneous activation by a negative regulatory N-terminal tyrosine residue[40]. This residue upon phosphorylation by Csk family kinases prevents Src-family kinase phosphorylating and binding tyrosine residues located within the ITAM motif[85]. However, Src-family kinases can be activated in the presence of the PTP CD45, a transmembrane PTP which contains two cytoplasmic PTP domains[40, 82]. In B cells CD45 functions to dephosphorylate the negative regulatory tyrosine residue on Src-family kinases allowing

them to phosphorylate tyrosine residues and participate in the B cell signalling pathway[40]. CD45 knock out mice bare B cells that cannot activate Src-family kinases in response to BCR cross-linking [34].

Accessory proteins that contain cytoplasmic Immunoreceptor Tyrosine-based Inhibitory Motif (ITIM) also play an important role in preventing BCR signalling[34]. PTP including SHP-1 and SHIP have been shown to bind ITIM motifs of negatively regulatory proteins including the IgG Fc receptor; FcγRIIb and CD22[34, 84, 86]. Both molecules are required to control B cell activation, and mice that lack these inhibitory receptors exhibit high levels of circulating IgM and autoantbodies[40]. SHIP, although it does not directly control the activation of PTKs is important in preventing improper activation of the signalling pathway. SHIP regulates PIP_2, which is phosphorylated to PIP_3 by PI3-K. SHIP can dephosphorylate PIP_3 back to PIP_2 preventing the association of PH containing PTKs such as Btk and Akt with the plasma membrane in resting B cells and their activation by other PTKs[84].

Therefore, it can be seen that the interaction between PTKs and PTPs is essential not only to prevent activation of the B cell signalling pathways in resting B cell, but also in activating and maintaining the signalling pathway in activated B cells.

1.3 Role of the BCR in B cell development

As well as delivering the appropriate signal for B cell activation in the presence of foreign Ag, the BCR also plays a significant role in B cell development. In fact BCR signalling controls such diverse activities as apoptosis, anergy, proliferation and receptor editing during B cell development. B cells are generated from haematopoietic stem cells (HSC) in the liver during foetal life, and in the bone marrow (BM) in adult life[87]. From HSC, B cells develop along a well differentiated pathway from pro-B cells through the pre-B and immature stages to develop into mature B cells, as shown in Figure 1.4. B cell development is governed not only by the pre-programmed transcription factors but also signals delivered from the BCR[2]. These signals play a pivotal role during B cell development allowing B cell proliferation at the early stages. There is still much debate into whether B cell development within the BM relies on an external ligand, or whether intracellular signals are sufficient to drive development. The stages of B cell development will now be discussed including the importance of BCR signalling at each stage.

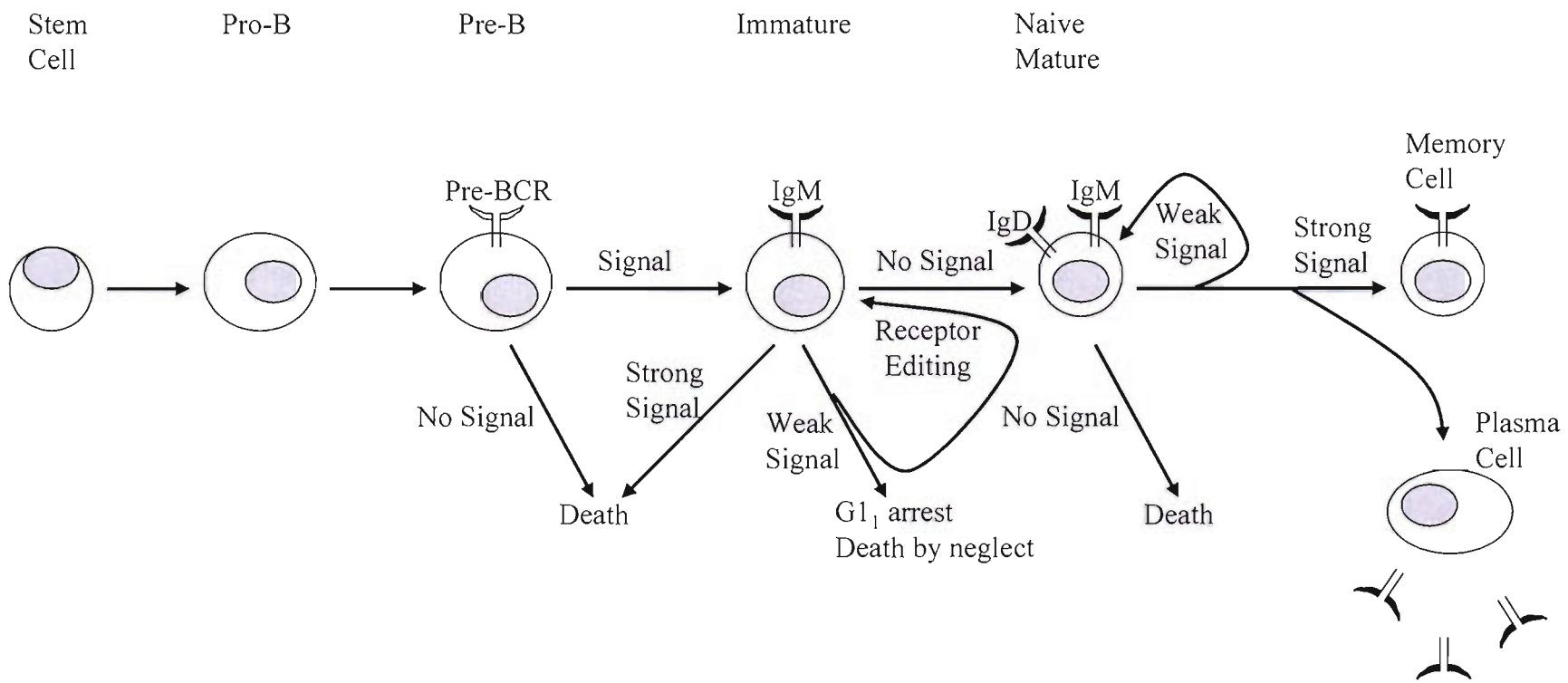

Figure 1.4 The Developmental progression of B cells. B cells originate in the bone marrow from stem cells, differentiate into pro-B cells and then into pre-B cells that express a pre-BCR. From the pre-B cell stage it is thought that signals derived from the BCR drives B cell differentiation allowing cells to mature. BCR signalling pathways are also important in selecting B cells that only recognise and react to foreign Ag allowing the production of high affinity Ab secreting plasma cells against the target. Complied using references 88, 90, 93 and 96.

1.3.1 Pro-B cell development

At the early stages of development stromal cells located in the BM are believed to play an important role in early B cell development due to their ability to secrete interlukin-7 (IL-7)[88]. HSC expressing the IL-7 receptor in the BM microenvironment are able to differentiate into early pro-B cell stage in the presence of the transcription factors E2A and early B cell factor[89]. Pro-B cells express the Pax-5 transcription factor, which is essential for maintaining B lineage commitment[87]. Pax-5 deficient pro-B cells are not capable of maturing past the pro-B cell stage[90]. The main characteristic of pro-B cells is the initiation of V(D)J recombination of the Ig-Heavy (IgH) chain under the expression of the recombinase activating genes (RAG-1 and RAG-2)[87]. Although pro-B cells do not express IgH chain at the cell surface, interest in the capability of pro-B cells to initiate intracellular signals allowing B cell development to progress has been fuelled by the discovery of the expression of the CD79 heterodimer on the surface of murine pro-B cells isolated from the BM of RAG-2 deficient ($RAG2^{-/-}$) mice[91]. These experiments showed that CD79b was expressed as either a monomer, or disulfide linked heterodimer at the cell surface, in the presence of four membrane molecules, of which one has been identified as the protein chaperone; calnexin[92]. Cross-linking of the pro-BCR with mAb directed to CD79b led to rapid, transient tyrosine phosphorylation of CD79a and intracellular signalling proteins[92]. mAb induced intracellular signalling allowed pro-B cells to differentiate to the small pre-B cell stage, when expressed in the presence of a μ transgene[92].

However, the presence of a CD79 heterodimer has yet to be identified on human pro-B cells. Research by Benlagha, *et al.*,[93] provided biochemical evidence that CD79 heterodimers do not reach the cell surface of human pro-B cells. More importantly the majority of CD79a and CD79b in pro-B cells are located in separate pools within the ER, and only a small fraction form heterodimers. It has been suggested that although the CD79 heterodimer must be incapable of arriving at the pro-B cell surface on human B cells, the CD79 heterodimer could still signal to allow B cell development as the Src family kinase Lyn was found to associate with CD79a and CD79b.

The formation of a pro-BCR that could initiate intracellular signals allowing the development of pro-B cells to the pre-B cell stage is hotly debated. It is not known whether pro-B cells are sufficient to generate their own signal to allow B cell development, or whether the BM microenvironment allows differentiation via ligand interactions, which have yet to be identified[94, 95]. To date, the majority of research has focused on the pro-B

cells capability to form intracellular signals to allow differentiation independent of ligand. Murine models that lack CD79b ($CD79b^{-/-}$) developed by Gong and Nussenzweig[96] showed a complete block in B cell development at the pro- to pre-B cell stage. If CD79b is then reintroduced into $CD79b^{-/-}$ mice under the control of RAG promoters, murine B cells develop to the pre-B cell stage[97]. CD79a knock out murine models ($CD79a^{-/-}$) show an absence of immature and mature B cells in murine BM, with the presence of B cells that express the pan-B cell markers $B220^{+}$ and CD19[98]. Bannish, *et al.*,[99] showed that retroviral transfection of a fusion protein containing the cytoplasmic domains of CD79a and CD79b fused to a lck domain that targets the construct to the inner-leaflet of the plasma membrane, could drive B cell differentiation from the pro-B cell stage to the immature B cell stage in mice that expressed B cells lacking IgM heavy chain. This evidence suggests that pro-B to pre-B cell differentiation is dependent on signals derived from either ITAM of the CD79 heterodimer and that this process is ligand independent.

1.3.2 Pre-B cell development

Pre-B cells are characterised by the expression of the pre-BCR at the cell surface[100]. The pre-BCR is comprised of mIgM heavy chain associated with a surrogate light chain (VpreB or λ5) and the CD79 heterodimer[101]. The pre-BCR functions as a key checkpoint regulator, triggering B cell proliferation in the presence of successful IgH chain rearrangement leading to its expression at the cell surface and the allelic exclusion of the second IgH chain locus[102]. Successful IgH chain gene rearrangement is associated with a down regulation of RAG expression at the messenger RNA (mRNA) and protein level[101]. RAG expression is subsequently up regulated allowing the recombination of the Ig-light (IgL) chain in the absence of terminal deoxynucletidyl transferase (TdT)[87]. Pre-B cells are also associated with the up regulation of the anti-apoptotic protein $Bcl\text{-}_{XL}$[103].

Truncation of the cytoplasmic domain of either CD79a or CD79b results in differences in functions of CD79a and CD79b in B cell development in respect that mIg being expressed at the surface with the absence of one ITAM motif. Torres and Hofen[104] showed that truncation of CD79a cytoplasmic domains ($CD79a^{\Delta c/\Delta c}$) did not prevent B cell developmental arrest at the early pro- and pre- B cell stages, suggesting that the single ITAM motif of CD79b is sufficient to drive B cell development. However, the numbers of peripheral B cells were severely reduced, and immature B cells expressed a BCR, which constitutively signalled. Truncation of the cytoplasmic domain of CD79b ($CD79b^{\Delta c/\Delta c}$) leads to B cell arrest at the immature stage, with cell death occurring by apoptosis[105].

There was however, a marked increase in the number of pro-B cells, indicating that the single cytoplasmic domain of CD79a was sufficient to trigger pre-B cell differentiation and proliferation. Crossing of CD79a$^{\Delta c/\Delta c}$ with CD79b$^{\Delta c/\Delta c}$ lead to developmental arrest at the pre-B cell stage indicating that the intracellular signals derived from the cytoplasmic domain of the CD79 heterodimer is crucial for B cell development, in agreement with data from the CD79a and CD79b whole molecule knock out models[105].

1.3.3 Immature B cell Development

Once the IgL chain has successfully rearranged and is expressed at the cell membrane along with IgH chain and the CD79 heterodimer, B cell differentiation progresses to the immature stage[2]. BCR expression and signalling are required at the pre-B cell stage to allow V(D)J recombinase-dependent IgL chain assembly, surface expression of the BCR and suppression of further gene rearrangements[106]. Up to the immature stage of B cell development, B cell differentiation and survival has relied on positive selection, where only B cells capable of generating an intracellular signal from the pre-BCR can proliferate, re-arrange the IgL chain and survive to differentiate to form immature B cells.

Immature B cells migrate from the BM to the spleen where they undergo important selection events before becoming selected into the pool of long lived Ag responsive mature B cells[2]. Only 5-10% of newly generated immature B cells are selected and survive to become mature B cells due to the removal of self reactive clones by cell death, anergy or neglect[107]. Immature B cells circulate in the spleen for three to four days, where they are constantly exposed to self Ag; the fate of individual B cells depends on how strongly the BCR binds Ag[108]. B cells that express a BCR that binds self Ag with high affinity are deleted by apoptosis[107]. B cells that express a BCR that binds Ag with an low affinity become anergic and eventually die by neglect, or they re-arrange their variable domains by a process known as receptor editing. If the new receptor does not bind at all then they progress to mature B cells[2, 107]. Immature B cells that do not bind 'self' Ag progress successfully to naïve mature B cells and up-regulate mIgD-BCR at the cell membrane[107].

On mature B cells mIgD-BCR is expressed, the level of mIgD-BCR is five to ten times higher then the mIgM-BCR, which is the predominant mIg expressed on immature B cells[109]. The increased expression of mIgD-BCR on mature B cells occurs despite a steady state production of mIgM which exceeds that of mIgD[109]. It has been shown that mIgD binds to the CD79 heterodimer more stably then mIgM, probably due to its transmembrane

domain, as the extracellular domains of CD79 form a tighter contact with the heavy chain of mIgM than mIgD[109].

1.3.4 Mature B cells

Naïve mature B cells circulate the secondary lymphoid organs searching for Ag. Once bound via the BCR the B cells become activated and migrate into Germinal Centre (GC) follicles where Ag dependent selection begins[110, 111]. Activated B cells differentiate into centroblasts that rapidly proliferate, and alter their BCR IgV region by somatic hypermuation in order to develop high affinity clones towards Ag presented by follicular dendritic cells (FDC)[110]. Centroblasts compete for Ag presented by FDC and those that bind with high affinity mature into centrocytes and migrate through the GC, whereas centroblasts that do not bind Ag presented by FDC or bind with low affinity are deleted by apoptosis[112]. Centrocytes present Ag to T helper cells that express CD40 ligand (CD154), which interacts with CD40 on the surface of B cells[113]. Interactions between CD40 and CD154 in the presence of cytokines secreted by the T helper cell leads to the expansion of cells and isotype switching[113]. These high affinity centrocytes differentiate into memory B cells or Ab secreting plasma cells depending on the length of exposure to CD154[113]. The overall accomplishment of the GC reaction is to generate memory B cells that secrete or express BCR with a high affinity domain associated to either IgM, IgG, IgA or IgE constant domains[112, 113].

1.4 Association of the BCR and lipid rafts

Following the binding of Ag to the BCR, cross-linking of receptors on the cell surface allows the transmission of intracellular signals leading to the transcription of a variety of genes associated with B cell activation. Until recently it was not clear how BCR cross-linking allowed triggering of intracellular signalling cascades. Evidence has shown that signalling receptors including the BCR associate with specialised lipid microdomains in the plasma membrane following cross-linking, as summarised in Figure 1.5[114]. These lipid microdomains, termed lipid rafts are composed of sphingolipids, cholesterol, and GPI linked proteins that exist on both the outer and inner leaflet of the plasma membrane[115]. Importantly, specific PTKs known to be involved in the initiation of intracellular signalling cascades such as Lyn are preferentially associated with lipid rafts[116].

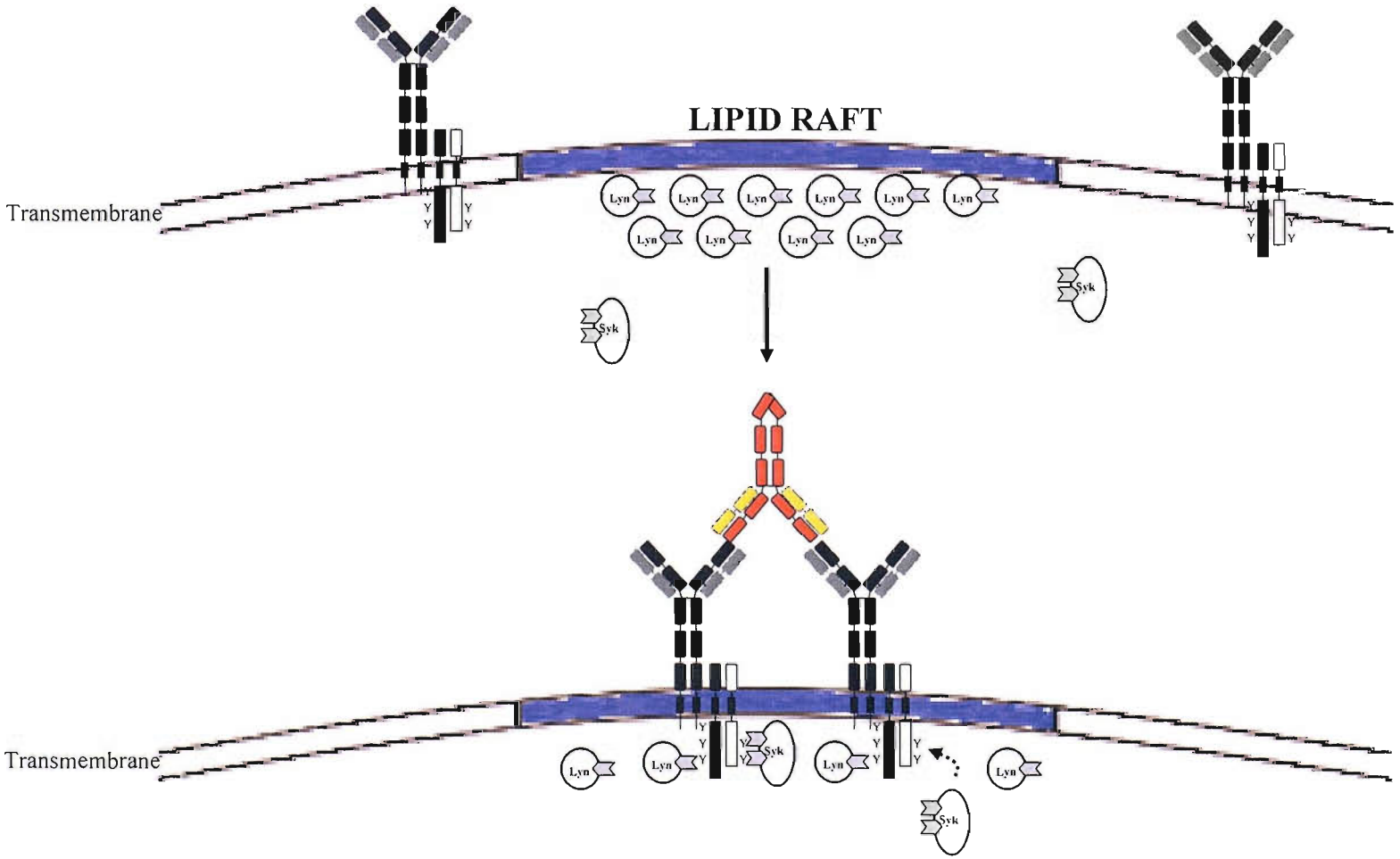

Figure 1.5 Translocation of cross-linked BCR into lipid rafts. In resting B cells the BCR remains outside of lipid rafts, that are rich in the PTK Lyn. Upon cross-linking the BCR with Ag or mAb, the BCR translocate into the lipid rich domain of the plasma membrane. This allows activation of PTK by the CD79 heterodimer on the BCR, leading to activation of further PTK and activation of a full signalling cascade. Compiled using references; 118, 120, 122 and 123.

Lipid rafts consist of sphingolipids that contain highly saturated lipid tails[114, 115]. These sphingolipids in conjugation with cholesterol make rafts less fluid then the remaining plasma membrane environment[114, 115]. This separation between specific sections of the plasma membrane means that detergents such as Triton X-100 can be used to solublise the more fluid sections of the plasma membrane, allowing isolation of the insoluble lipid rafts on sucrose density gradients[117]. This technique has indicated that many signalling receptors including the BCR associate with lipid rafts after ligation[118].

Initial research showed that mIg and CD79a do not associate with lipid rafts in untreated resting B cells, but that mAb receptor cross-linking caused translocation of mIg along with CD79 into lipid rafts[118]. Importantly, translocation of cross-linked BCR into lipid rafts occurred in conjunction with phosphorylation of CD79a and the Src-family PTK Lyn[118]. Following BCR cross-linking protein tyrosine phosphorylation occurs almost immediately, with maximum levels reached after about five minutes[29]. Therefore, it is predicted that cross-linked BCR can translocate into lipid rafts allowing the rapid phosphorylation and activation of PTKs in mature B cells.

The importance of the BCR translocating into lipid rafts following BCR cross-linking is highlighted in B cells where lipid rafts are disrupted. Synthetic agents that either remove membrane associated cholesterol or disrupt the association of the BCR with lipid rafts show greatly reduced levels of PTK phosphorylation after stimulation[117, 119]. At a more fundamental level, B cells infected with the Epstein Bar virus (EBV) show inhibition of BCR induced PTK phosphorylation due to the EBV latent membrane associated protein 2A (LMP2A) that resides within lipid rafts. LMP2A not only prevents translocation of the receptor to lipid rafts following cross-linking but also sequesters Lyn away from the BCR[120].

1.4.1 Importance of lipid rafts at different stages of B cell development

The association of the BCR with lipid rafts appears to be different at specific stages of B cell development. The pre-BCR expressed at the surface of pre-B cells is known to associate with lipid rafts in non-stimulated cells[121]. The association of the pre-BCR with lipid rafts and the association of the pre-BCR with Lyn suggests that lipid rafts may contribute to survival signals required to allow development of pre-B cells[121]. Disruption of lipid rafts in pre-B cells inhibits the recruitment of the PTKs PLCγ2, IP3 production and

pre-B cell calcium signalling. Cross-linking the pre-BCR allows more pre-BCR to translocate into lipid rafts[121], presumably leading to more potent signalling.

Unlike the pre- and mature BCR, the BCR expressed on the surface of immature B cells does not associate with lipid rafts either prior to or following cross-linking[122]. The non-association of the BCR with lipid rafts appears to correlate with an increased susceptibility to BCR induced apoptosis. This evidence suggests that lipid rafts may not only function as platforms for signal activation, they may also mediate important decisions of B cell fate during development, allowing decisions for survival in a signal transmission from a correctly assembled pre-BCR or deletion of self reactive immature B cells.

1.4.2 Role of lipid rafts in receptor internalisation

Lipid rafts function in B cells not only to mediate signal transduction in B cells in response to foreign Ag, but also to aid in internalisation of bound Ag for processing and presentation to helper T cells. It has been shown that B cells treated with Src family kinase inhibitors fail to internalise cross-linked BCR[123]. This evidence suggests that lipid rafts that include increased concentrations of the Src-family kinase Lyn may function to mediate the internalisation of cross-linked BCR[123, 124].

Recent evidence indicates that disruption of lipid rafts using chemical inhibitors or expression of LMP2A not only prevents the phosphorylation and activation of clathrin, but BCR internalisation is also inhibited[123]. Reduced levels of BCR internalisation following cross-linking was also observed in immature B cells, where the BCR is known not to translocate into lipid rafts[122, 123]. However, receptor internalisation of bound Ag, although mediated within lipid rafts, appears to be independent of lipid raft internalisation due to differences in kinetics observed for the internalisation of lipid rafts compared to the BCR[125].

1.5 BCR Oligomerisation- An alternative view

The recent evidence that suggests cross-linked BCR translocates to lipid rafts allowing initiation of intracellular signalling cascades has not been fully accepted. Evidence indicates that mice lacking Syk PTK fail to express B cells that develop beyond the pro-B cell stage, where mice that lack Src-family kinases express B cells which are capable of developing up to the immature stage of B cell development[44, 126, 127]. This suggests that

Syk PTK is the major regulator of BCR induced activation, and that if receptors were held in an oligomeric form, activated Syk could proceed to activate multiple ITAM motifs very quickly.

Schamel and Reth[30] indicate that prior to BCR translocation to lipid rafts, BCR may exist as oligomeric structures on the B cell surface. This was shown by B cell lines that co-expressed the mIgM-BCR with two different forms of CD79a, wild type and flag tagged CD79a (flagCD79a). Cross-linking the BCR with anti-flag mAb lead to the phosphorylation of both flagCD79a and wild type CD79a. As only one CD79 heterodimer associates with one mIg the activation and phosphorylation of WT-CD79a in response to anti-flag mAb suggests that the BCR may form oligomeric structures. This theory is not in line with the conventional cross-linking hypothesis which indicates that only two receptors are cross-linked in response to Ab leading to activation and signal transduction. Reth *et al.*,[128] have utilised gel assays to show that BCR complexes on the B cell surface are larger then that predicted for a monomeric receptor and instead are more likely to represent dimeric or larger oligomeric structures.

The oligomeric receptor model relies on the fact that BCR of the same isotype are clustered at the cell membrane where the ITAM motifs of the CD79 heterodimer are constantly activated and inactivated by PTKs and PTPs. Binding of Ag to the receptor disturbs the oligomeric receptor structure moving PTPs from the local vicinity and allowing PTKs to phosphorylate the CD79 ITAM motifs, bind, and subsequently activate further surrounding PTKs leading to activation of the signalling pathway[41, 42]. The oligomeric receptor model also allows for signal spreading, in that other ITAM motifs within the oligomeric BCR although not bound by Ag could easily become activated by surrounding activated PTKs leading to an overall increase in PTK activation and triggering of the signalling cascade[42].

1.6 Association of the CD79 heterodimer with malignancy

The function of the CD79 heterodimer in BCR responses to Ag and B cell development has been discussed. The CD79 heterodimer has also been associated with specific disease states, most notably B cell chronic lymphocytic leukaemia (B-CLL). B-CLL is a disorder characterised by an increase of aberrant, monoclonal B lymphocytes in the spleen and peripheral blood, and is the most common leukaemia in the Western World[129]. B-CLL cells show a low proliferative rate and prolonged life span suggesting their primary

alteration is a defect in apoptosis[130]. B-CLL are characterised by the expression of the cell surface markers CD5, CD23, CD19 and low levels of sIgM/sIgD and CD79b[131, 132]. B-CLL has also been divided into two sub-groups depending on the mutation status of the Ig variable regions[133]. Between 50 to 70% of B-CLL cells indicate that they have undergone variable gene hypermutation, a phenomenon characteristic of normal B cells that have undergone a T cell dependent GC reaction. B-CLL cells showing IgV hypermutation are associated with a benign clinical course compared to the more aggressive non-mutated B-CLL cases[133].

One group reported that various point mutations were observed in the B29 gene, mainly in areas encoding the conserved transmembrane and cytoplasmic domains[134]. These authors also reported that there was a direct correlation between decreased CD79b expression at the mRNA level and decreased expression of surface mIg in B-CLL cells. However, familial studies have indicated that such mutations are not hereditary where B-CLL is observed between generations[135]. Other groups have not reported the specific mutations of CD79b as detailed in early work indicating major discrepancies between different research groups[136, 137].

From the lack of an obvious mutation within the B29 gene that could lead to the development of B-CLL some research groups have speculated that an alternative, truncated transcript of CD79b may have a functional role in B-CLL. Hashimoto, *et al.*,[138] showed that as well as full-length transcripts, alternative transcripts of CD79a and CD79b existed in human B cell lines and normal human B cells. The alternative transcripts of CD79a and CD79b both show deletions in the extracellular domain, in the case of CD79b the whole of exon three is spliced out leading to the formation of a truncated extracellular domain (hΔCD79b)[138] (see Figure 1.4). Koyama, *et al.*,[139] also showed the presence of hΔCD79b in normal B cells, with activated B cells expressing an increase in the relative expression of hΔCD79b. Deletion of exon 3 in ΔCD79b prevents the formation of heterodimers with CD79a due to the loss of the vital cystiene residues, meaning that ΔCD79b may exist as a monomer within B cells[138]. Interestingly hΔCD79b still contains a functional cytoplasmic ITAM motif and therefore could participate in intracellular signalling. It has also been shown that in B-CLL, increased ratios of hΔCD79b to CD79b have been observed linking a possible physiological role of the alternative transcript in the biology of these cells[140, 141].

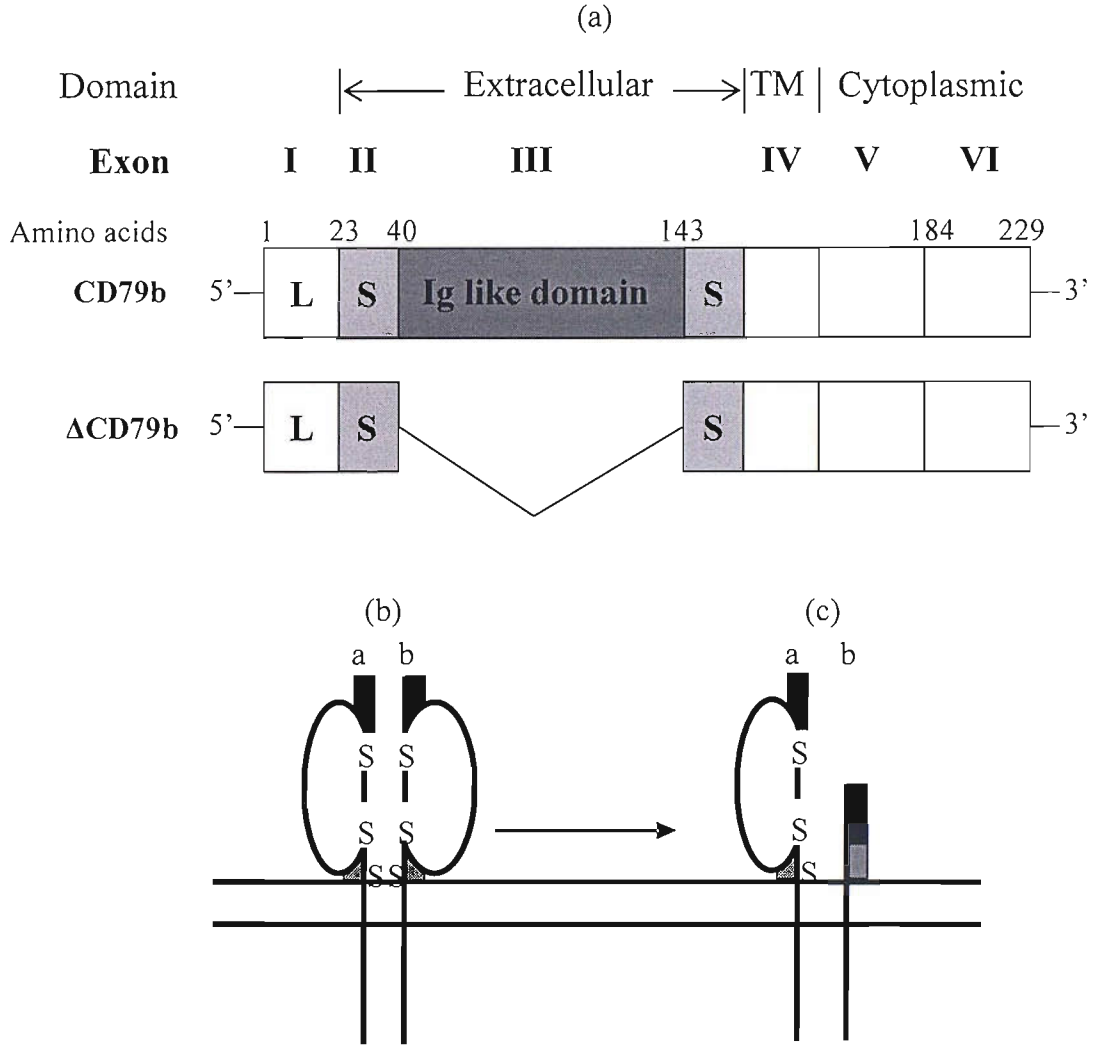

Figure 1.6 Schematic representation of the alternative transcript of CD79b. The alternative splice site located in the genomic sequence suggests the presence of an alternative transcript of CD79b that would lack the whole of exon 3, leading to the formation of a truncated extracellular (immunoglobulin-like) domain (a). Figures (b) and (c) show the schematic representation of CD79b and the alternative CD79b transcript if successfully expressed at the cell surface.

Therefore, it appears that one major candidate for aberrant function of B cells in B-CLL could result from the up-regulation in alternative splicing of CD79b to yield ΔCD79b. The primary function of ΔCD79b could be to interfere with BCR signalling cascades preventing apoptosis, or by preventing expression of the BCR at the cell membrane. Both are characteristics of B-CLL cells.

1.6.1 Alternative splicing

The human genome comprises around 40,000 genes, only twice that seen in the simple worm; *Caenorhabditis elegans* (19, 000 genes)[142]. How then, does this relatively small increase in the number of genes explain the vastly increased sophistication of humans? The answer is the way genes are regulated, transcribed and the control of post-transcriptional processing[142, 143]. The processs of alternative splicing between genes could lead to the generation of large numbers of proteins from a limited numer of genes. The process of alternative splicing could also lead to the accidental alteration of proteins that could still have a functional, but deleterious role within the cell. This process could account for the generation of an alternative transcript of CD79 in both human and murine B cells.

In eukaryotic cells, DNA is transcribed to pre-mRNA and then to mRNA before export from the nucleus and translation into protein. Post-transcriptional processing at the pre-mRNA stage provides additional mRNA and protein diversity allowing the generation of multiple isoforms of a single gene[144]. Of post-transcriptional processing events, splicing and polyadenylation are the major processes that allow the generation of diversity on genetic function.

Most eukaryotic genes are comprised of long sequences of DNA known as 'introns' that separate short coding regions of DNA (exons). Mature mRNA consists of aligned exons which are spliced together, removing intervening introns[143, 145]. This process known as splicing occurs within the splicesome, a multi-unit complex of proteins and RNA within the nucleus[146]. The splicesome is also responsible for selection of splice sites and splicing of different splice sites in alternative splicing[146, 147]. The average exon contains 150 nucleotides (nt), compared to introns that can contain between 3,500nt and 500,000nt[146]. Therefore, the splicing machinery must be able to recognise small exon sequences located within vast intronic RNA[146]. Moreover, the sequences that encode for splice site regions which are spliced together are poorly conserved and introns contain large numbers of cryptic splice sites that match the loose 5' or 3' splice-site consensus[148]. Cryptic splice sites are normally avoided by the splicing machinery, but, can be selected for splicing when

normal splice sites are altered by mutations[146]. Once the correct exons are recognised by the splicesome, the flanking splice sites must be joined in the correct 5' to 3' order to prevent exons being missed out of the completed sequence[149].

Alternative splicing appears to be a tightly regulated process in a cell type or developmental stage specific manner[150]. Uncontrolled splicing can have disastrous effects, 15% of human genetic diseases are caused by mutations that destroy functional splice sites or generate new ones[150, 151]. Although splicing of eukaryotic genes is well understood, explaining why specific splice sites are selected for splicing has proven difficult.

1.7 Aims

The aims of this project were to investigate the mechanisms of intracellular signalling generated by mAb binding to the BCR. It is of interest to understand why certain mAb raised against specific domains of the BCR can induce cell death, where as mAb raised against others cannot. We propose that mAb that can induce cell death affect the type of PTK activated and the kinetics of PTK activation following BCR cross-linking. If this were proven then it would be advantageous to understand what happens to the BCR upon mAb binding.

Another aspect of this thesis is to investigate if an alternative transcript of CD79b that lacks exon three (ΔCD79b) is present in murine B cells. Our hypothesis is that over-expression of ΔCD79b in murine B cells would inhibit B cell death. This inhibition of cell death would probably be caused by interference in PTK activation. Ultimately the long term aim from this research would be to generate a transgenic mouse that overexpresses either murine or huaman ΔCD79b. This would enable us to detail if ΔCD79b plays a significant role in both the development of B cells and the development of specific disease states.

2.1 Cell culture materials

All cell lines were cultured in RPMI (Roswell Park Memorial Institute) 1640 medium (Invitrogen, Gibco, UK), supplemented with 100 U/ml penicillin and streptomycin (Invitrogen, Gibco), 50 U/ml amphotericin B (Fungizone; Squibb and Sons, UK), 2 mM L-glutamine (Invitrogen), 1 mM pyruvate (Invitrogen) and 10% Foetal Calf Serum (FCS; Invitrogen, Gibco, UK). Murine cell lines were cultured in the above media with the addition of 50 mM 2- meceptoethanol (2-ME, Sigma, Poole, UK).

2.2 Cell lines

Human cell lines Ramos-EHRB, BL-60, Daudi, HEK-293T, murine B cell lines WEHI-231, A20, (ECACC) $\pi BCL_1^{(152)}$ (ECACC), and the COS-7 cell line (ECACC) were maintained in culture medium as described above at 37°C in a 5% CO_2 humidified incubator. Media was replaced every 2-3 days. As cell lines can differentiate over prolonged periods of culturing, cell lines used were replaced from stock every 3 weeks to prevent cells becoming insensitive to stimulation through the BCR. This is important, especially when investigating signalling pathways in cultured cell lines.

2.3 Cell quantitation

Cell concentrations were determined using Coulter Industrial D Cell counter (Coulter Electronics, Bedfordshire, UK)

2.4 Antibodies

The majority of mAb used in this study have been raised 'in-house', other Ab supplied are noted. Specificities of the anti-human mAb are as follows: anti-human irrevant isotype matched control specific for the plant toxin saporin (CP1/17), anti-Fcμ (M15/8, ZL7/5, Mc244G10), anti-Fdμ (XG9, MA5, M2E6), anti-λ light chain (Mc24IC6, M15/2), anti-CD79a (ZL7/4), anti-CD79b extracellular domain (AT105/1), anti-CD79b cytoplasmic domain (AT107/2), anti-EHRB idiotype (ZL16/1), anti-Daudi idiotype (ZL15/27) and sheep anti-human μ chain polyclonal Ab (Jackson Laboratories, USA).

Specificities of the anti-mouse mAb were: irrelevant isotype matched control for the anti-mouse CD3 (KT3), anti-μ (Mc39/12), anti-κ light chain (HB58), rabbit anti-mouse IgG

polyclonal Ab (Jackson Laboratories), and hamster anti-mouse CD79b labelled with Fluorescein Isothiocyanate (FITC) (HM79-11, Serotec, UK).

Ab used for immunoblotting experiments included mouse anti-Csk-binding protein (Cbp) (or phosphoprotein assocaiated with glycosphingolipid-enriched microdomains (PAG)) (kind gift V Horejsi, Prague), anti-phosphotyrosine (4G10) and mouse anti-Syk (4D10.1) (Upstate, UK), goat anti-human IgM labelled with Horse Radish Peroxidase (HRP) (Southern Biotech, Cambridge Bioscience, UK), rabbit anti-phospho-threonine (P-Thr-Polyclonal, Cell Signaling Technology, UK) rabbit anti-rat Ig-HRP labelled, anti-rabbit Ig-HRP labelled (Sigma), anti-mouse Ig-HRP labelled (Amersham Biosciences, UK), anti-hamster HRP labelled (Southern Biotech), anti-β-actin (Sigma), mouse anti-CD20 (7D1 , Serotec) anti-ACTIVE MAPK, anti-ACTIVE p38, and anti-ERK (Promega, Southampton, UK) and goat $F(ab')_2$ anti-mouse Ig-FITC labelled (Dako, UK).

2.5 Preparation of cDNA

cDNA was prepared from $1x10^7$ cells. Lymphocytes prepared from the spleens of naive Balb/c and CBA mice, or spleens from terminal mice bearing the BCL_1 or A31 tumours (Balb/c and CBA respectively) were provided by Dr Jamie Honeychurch (University of Southampton, UK). Cells were pelleted by centrifugation at 200g for 5 minutes. mRNA was extracted by using the Quickprep-micro mRNA purification kit according to the manufacturers' instructions (Amersham Biosciences). mRNA was converted to cDNA using the first-strand cDNA synthesis kit (Amersham Biosciences), in a final volume of 15 µl. cDNA samples were stored at -20°C.

2.6 PCR

DNA amplification was performed as follows. Briefly, 1µl of each primer (see table 2.1) (100 ng/ml) was added to 1 µl of cDNA with 2.5 µl of optimised reaction buffer and 0.5 µl of dNTP mix, in a total volume of 24.5 µl. This mixture was then pulse spun and 0.5 µl of Taq polymerase (5 U/µl) (Promega) added, before a further pulse spin.

PCR was performed using a PTC-100 thermal control system (MJ Research Inc, UK). DNA was denatured at 95°C for 5 minutes, followed by 30 cycles of; denaturing at 95°C for 30 seconds, annealing at the appropriate temperature for 1 minute, and elongation for 2 minutes at 72°C. A final elongation reaction of 10 minutes was performed to ensure formation of full-length transcripts.

PCR products were mixed with 2.5 µl gel loading buffer, and 25 µl of each sample loaded into agarose gels containing ethidium bromide and separated at 120 V, along with 1 kB marker (Gene-ruler, MBI-Fermentas, UK) to allow estimation of fragment size. DNA was visualised under UV light and a photographic record taken.

Primer	Sequence	T_M
mCD79b Forward Primer	5' GAC TCG AGC AGT GAC CAT GGC CAC ACT Xho1	61.9°C
mCD79b full-length Reverse Primer	3' GTG CGG CCG CAG AGT TGA GC GGA TGA Not1	61.9°C
mCD79b Extracellular Reverse Primer	5' ATC TTT CAG TGT GTT CCG CCG CTT CAG	61°C
YFP-mCD79b Forward Primer	5' GGG AAT TCG GTA CCA GCA ATG ACA AGC EcoR1	60.7°C
YFP-mCD79b Reverse Primer	3' GGG GAT CCT CAT TCC TGG CCT GGA TGC BamH1	60.7°C

Table 2.1 – PCR primers utilised for the detection and amplification of mCD79b and mΔCD79b from murine B cells. Primers are shown with underlined text corresponding to the restriction enzyme site.

2.7. Cloning, DNA amplification and sequence analysis

2.7.1 Cloning

PCR was performed as described above but using *Pfu* polymerase to minimise the number of replication errors. PCR products were visualised on 2% agarose gels and the PCR product corresponding to the correct size was excised from the gel. DNA was extracted from the gel using Qiaex II gel extraction kit (Qiagen, UK) in a final volume of 20 µl. 4 µl of extracted DNA was incubated with 1 µl of salt solution and 1 µl of TOPO II blunt sequencing vector (Invitrogen), for 5 minutes at room temperature. One vial of TOP10 chemically competent cells (Invitrogen) was added and the sample incubated on ice for 30 minutes. Cells were heat shocked at 42°C in a water bath for 45 seconds before being placed directly onto ice for a further 2 minutes, allowing the incorporation of plasmid DNA into cells. One ml of SOC medium (2% w/v tryptone, 0.5% w/v yeast extract, 10mM sodium chloride, 2.5 mM potassium chloride, 10 mM magnesium chloride, 10mM

magnesium sulphate, 20 mM glucose (Sigma)), was added and the mixture incubated for one hour at 37°C with agitation.

Following one hour incubation at 37°C, expanded cultures were spun for 10 minutes at 6000g and bacterial pellets re-suspended in 150 µl SOC medium and spread on kanamycin (50 µg/ml) treated agar plates. Agar plates were incubated for 16-18 hours at 37°C. Following incubation, eight colonies were selected and expanded for 6 to 8 hours in 5 ml of L-broth containing kanamycin (50 µg/ml). Cultures were spun at 6000g for 10 minutes at 4°C, and plasmid DNA extracted from bacterial pellets using the mini-prep DNA extraction kit (Qiagen), giving a final volume of 50 µl plasmid DNA.

2.7.2 Restriction digests

Plasmid DNA was checked for the presence of the correct DNA insert using restriction enzymes. Briefly, 8 µl of plasmid DNA was incubated at 37°C for 2 to 4 hours, or overnight, in the presence of 2 µl of the appropriate reaction buffer, and 1 µl of the appropriate restriction enzymes (see table 2.1) (Promega). Following incubation, DNA was visualised using 2% agarose gels. Samples that contained the correct sized DNA insert were used for DNA sequencing reactions

2.7.3 Sequencing

4 µl of plasmid DNA was used for each sequencing reaction with the addition of 2 µl of BigDye (Applied Biosciences, UK), 2 µl of 10x reaction buffer, and 2 µl of T7 or SP6 primer (1 pM/ml). PCR reactions were performed for 3 hours using the standard BigDye protocol consisting of 25 cycles of; denaturing at 96°C for 10 seconds, annealing at 50°C for 5 seconds and elongation at 60°C for 4 minutes, samples were then cooled to 4°C.

DNA from each PCR reaction was then precipitated as follows. To 10 µl of PCR reaction, 1 µl of 3M sodium acetate and 25 µl of 100% ethanol was added in a 1.5 ml microfuge tube (Eppendorf, UK). Samples were incubated on ice for 10 minutes; DNA was pelleted by centrifugation at 16,000g for 30 minutes at 4°C, then washed in 250 µl of 70% ethanol, and re-pelleted for 10 minutes. Ethanol was removed and the DNA pellet was re-suspended in 2 µl of loading buffer (1:4 of dextran:formaldehyde). DNA sequence samples were run by the HIT group, (University of Southampton), and analysed using Chromas software.

2.7.4 Cloning of expression vectors

Briefly, following sequencing plasmid DNA from the mini prep was digested for 2 hours with the appropriate restriction enzyme as mentioned in section 2.7.2. The expression vector was also linearised using the appropriate restriction enzymes; 2 µl of vector was digested for 2 hours at 37°C, in a final volume of 20 µl. All restriction products were separated on agarose gels and DNA of the correct size extracted as detailed in section 2.7.1. In a transformation tube, 12 µl of digested DNA was ligated with 12 µl of linearised expression vector for 16 to 18 hours in the presence of T4 ligase buffer and T4 ligase (Promega). Ligated DNA was transformed into JM109 chemically competent cells (Promega) as detailed in 2.7.1 and spread onto ampicillin (100 µg/ml) treated agar plates. Colonies were expanded, plasmid DNA extracted and the presence of inserts identified using restriction digests.

2.7.5 Maxipreps

Colonies containing the correct sized insert were picked and expanded in 5 ml of ampicillin treated L-Broth (100 µg/ml) for 6 to 8 hours at 37°C with agitation. Starter cultures were expanded by the addition of 150 ml of ampicillin treated L-Broth and incubated for a further 16 to 18 hours. Cultures were spun down at 6000g for 15 minutes at 4°C, plasmid DNA was extracted from bacterial pellets using maxi-prep Hi speed DNA extraction kit (Qiagen) in a final volume of 500 µl. Plasmid DNA concentration was quantified using the GeneQuant analysis system (Amersham Biosciences).

2.8 Transfection of cell lines

2.8.1 DEAE transfection of COS-7 cells.

24 hours prior to transfection, $1x10^7$ COS-7 cells were seeded into plastic flasks and incubated overnight. For each transfection 10 µg of DNA was used in the presence of 40 µl Diethylaminoethyl-dextran (DEAE-dextran; 400 µg/ml final), 100 µM Chloroquin (Sigma) and 10 ml of RPMI 1640 medium without the addition of supplements.

For each transfection, supernatant was removed from COS-7 cells and the DNA mix (detailed above) added, for a maximum of 4 hours at 37°C in a 5% CO_2 humidified incubator. The reaction mix was then removed, and cells washed once with sterile phosphate buffered saline (PBS), before being shocked with 10 ml of 10% Dimethyl sulfoxide (DMSO) in PBS for a maximum of 3 minutes at room temperature. The DMSO

solution was removed and cells washed twice with sterile PBS, before the addition of complete medium, and then incubated at 37°C as described above. After 24 to 48 hours incubation, COS-7 cells were harvested by washing twice with PBS followed by incubating with 10 mM ethylenediametetraacetic acid (EDTA) in PBS for 10 minutes at 37°C.

2.8.2 Electroporation

For electroporation, $1x10^7$ cells were washed twice in RPMI medium without supplements, re-suspended in a final volume of 800 µl, and transferred to a 4 mm electroporation cuvette (Flowgen, UK) with the addition of 25 µg of the appropriate plasmid DNA. Samples were cooled on ice for 10 minutes before being electroporated using a gene pulse II electroporator (Bio-Rad, UK), at 0.3 mV, 960 microfarads (µF) for approximately 20 ms. Immediately after transfection, the cuvette was gently disturbed and placed onto ice for 10 minutes. Following this, cells were incubated for 10 minutes at room temperature in 10 ml of cold RPMI medium containing supplements and 10% FCS. Electoporated samples were made up to a final volume of 30 ml with complete RPMI medium at room temperature and incubated for 72 hours at 37°C in a 5% CO_2 humidified incubator.

Following 72 hours incubation, cells containing the inserted DNA vector were selected using the appropriate selection medium. Cells were plated out across 96-well flat-bottomed plates (Nunc, UK) (100 µl/per well) and 200 µl of the appropriate selection medium added. Plates were returned to the 37°C humidified incubators and checked on a regular basis. Positive clones were selected, expanded and tested to ensure that cells expressed the gene of choice.

2.8.3 Lipionic transfection

24 hours prior to transfection, $2x10^5$ cells per well were transferred to a six well tissue culture dish in RPMI medium without antibiotics. On the day of transfection 2 to 6 µg of DNA was diluted in 500 µl of serum-free medium. 10 to 30 µl of GenePORTER (Gene Therapy Systems, Cambridge Bioscience, UK) was diluted in 500 µl of serum-free medium, added to the diluted DNA and incubated for 30 minutes at room temperature. Following incubation, culture medium was removed from the cells and the DNA-GenePORTER mixture was carefully added, and the mixture incubated for 3 to 5 hours at 37°C. The DNA-GenePORTER mix was then removed from the cells and 2 ml of RPMI containing 10% FCS was added per well and the plates incubated for 24 to 48 hours at 37°C in a 5% CO_2 humidified incubator prior to analysis.

2.9 siRNA

Briefly, siRNA was set up according to manufacturer's protocol to utilise the pSILENCER siRNA vector system (Ambion, USA). Hairpin siRNA template oligonucleotides designed to span the splice site between exons two and four located on mΔCD79b were dissolved in 100 µl distilled water, and adjusted to a final concentration of 1µg/µl in TE buffer (10 mM Tris, 1 mM EDTA. Diluted siRNA oligonucleotides were then annealed and ligated into the pSILENCER 2.0-U6 plasmid as detailed in the manufacturer's protocol. Plasmids were transformed into TOP10 *E.coli,* and colonies tested by sequence analysis to determine whether the mΔCD79b siRNA oligonucleotide was inserted in the vector. Correct vectors were expanded and isolated by Maxiprep techniques (see section 2.7.5).

2.10 SDS PAGE analysis

2.10.1 Sample preparation

2.10.1.1 Whole cell lysates

For preparation of whole cell lysates, $4x10^6$ cells were spun at 200g for 5 minutes at 4°C, and cell pellets lysed in 100 µl NP-40 lysis buffer (150 mM NaCl, 10 mM Tris, 2.5 mM EDTA), bovine serum albumin (BSA; 1 mg/ml) 1% Nonident P-40 (NP-40; v/v), 1 mM Phenylmethylsulphonylflouride (PMSF), 2.5 mM iodoacetamide and 1% (v/v) aprotonin (Sigma). Cells were incubated on ice for 30 minutes, and nuclear material removed by centrifugation at 16,000g for 15 minutes at 4°C. Supernatants were removed and mixed with an equal volume of 2x sodium dodecyl sulphate (SDS) sample buffer (62.5 mM Tris-HCl (pH 6.8), 2% w/v SDS, 10% glycerol, 50 mM dithiothreitol (DTT) and 0.05% bromophenol blue (Sigma)). Samples were then heated to 95 to100°C for 5 minutes and placed at room temperature before loading. 10 µl of sample (equivalent to $2x10^5$ cells) was loaded per lane.

2.10.1.2 Lipid raft preparation

To allow the detection of specific proteins in lipid raft membranes, cell lysates were separated through sucrose density gradients. $1x10^8$ cells were washed and re-suspended in 500 µl/ml of complete medium, cells were then pre-warmed for 5 minutes at 37°C. The relevant Ab was re-suspended to give a final concentration of 0.5 µg/10^6 cells in 500 µl medium. Antibody was also pre-warmed 5 minutes at 37°C. After 5 minutes the pre-warmed Ab was added to the cells and incubated for the appropriate time at 37°C. Cells were washed once in compete medium then immediately lysed in 750 µl of cold lysis buffer

(5 ml of MES buffer (250 mM MES, 1.5 M sodium chloride, titrated to pH 6.5 with sodium hydroxide), 1% Triton X-100, 5.75 mM PMSF, 0.06% aprotonin (w/v) and, 0.025 mM EDTA (Sigma)) for 40 minutes on ice. The lysed cell solution was mixed with an equal volume of 80% sucrose (w/v in MES buffer) and transferred into a 5 ml ultracentrifuge tube (Sorvall, UK) and layered with 750 µl of 30% sucrose, 500 µl of 20% sucrose, 500 µl of 10% sucrose and then the tube filled with 5% sucrose (all w/v in MES buffer). Layered samples were then centrifuged at 45,000g for 16 to 18 hours at 4°C.

Post-centrifugation, sequential 500 µl aliquots were removed from the tube, the first removed being denoted as fraction one, and either analysed immediately or stored at -20°C. Samples were mixed with an equal volume of 2x SDS-loading buffer (see section 2.10.1.1) and separated using SDS-PAGE (see below)

2.10.1.3 Pellet/lysate analysis

A modified method for observing movement of proteins from lipid soluble fractions into lipid insoluble fractions was recently reported by Deans *et al.*,[153]. Following treatment of $4x10^6$ cells with the relevant mAb, samples were washed once in PBS before being lysed in 1% TX-100 lysis buffer (section 2.10.1.1) for 15 minutes on ice. Insoluble material was pelleted by centrifugation at 16,000g for 15 minutes at 4°C. Supernatant was removed and termed the lysate or lipid soluble fraction, and diluted with the addition of 25 µl of SDS loading buffer. The pelleted insoluble material (pellet or lipid insoluble fraction) was carefully washed four times in ice cold lysis buffer, and denatured in 60 µl SDS loading buffer, in order to give an approximately equal number of cell equivalents to the lysate fraction. Samples were resolved on SDS-PAGE gels and immunoblotted for presence of specific proteins as detailed below.

2.10.1.4 Protein tyrosine phosphorylation experiments.

$4x10^6$ cells were resuspended in 1 ml of complete medium and incubated in a 1.5 ml microfuge tube (Ependorf) for 15 minutes at 37°C in a water bath. Following pre-incubation the relevant Ab was added and the cells incubated for the appropriate time at 37°C. Cells were then spun at 16,000g for five seconds, supernatant removed and 1 ml of cold PBS added. Cells were spun down at 500g for 10 minutes at 4°C, supernatant removed and cell pellets lysed in cold NP-40 lysis buffer, as detailed in section 2.9.1.1 with the addition of 1 mM sodium orthovanadate (Sigma), or the appropriate concentration of activated sodium orthovanadate (pervanadate). Sodium orthovanadate was activated

following the method of Gordon, J [154]. Samples were run on SDS-PAGE gels and blotted as detailed below.

2.10.1.5 Immunoprecipitation

2.10.1.5.1 Phosphorylated PTK

Cells were prepared as detailed above in section 2.9.1.1. Following lysis of cell pellets in TX-100 lysis buffer, supernatant was removed and incubated overnight at 4°C with 2 µg of anti-tyrosine mAb (4G10) with constant agitation. Protein G-Sephrose beads (15 µl of packed suspension) were added to the sample, which was then incubated for a further 2 hours at 4°C. The beads were then washed four times with cold lysis buffer and the sample boiled in sample buffer (15 µl). The precipitated protein was separated by SDS-PAGE and blotted as detailed below. Protein A or protein G beads were used depending on the specificity of mAb used for immunoprecipiton experiments. For phosphorylated PTK, the mAb 4G10, is raised in mouse and can only be immunoprecipitated with Protein G coated sepharose beads.

2.10.1.5.2 Isolation of BCR complexes from detergent lysates

To determine whether the mAb used to bind specific BCR components could also immunoprecipitate whole BCR complexes in detergent lysates, $4x10^6$ EHRB cells were lysed in 1% digitonin lysis buffer for 30 minutes on ice. Insoluble material was pelleted by centrifugation at 16,000g for 15 minutes at 4°C. Supernatants were removed and 2 µg of the relevant mAb added and incubated overnight at 4°C with agitation. Protein A-Sephrose beads (20µl of packed suspension) were added to the sample, which was then incubated for a further 2 hours at 4°C. The beads were washed four times with ice cold lysis buffer, boiled in SDS sample buffer (20 µl) and immunoprecipitated protein resolved by SDS-PAGE. BCR complexes were probed for the presence of mIgM and CD79b as detailed below.

2.10.1.5.3 Surface bound BCR complexes

To determine whether mAb bound to cell membrane could immunoprecipitate surface BCR complexes, $4x10^6$ cells were treated with the relevant mAb (10 µg/ml) for 30 minutes on ice. Samples were then washed twice in PBS and either lysed or heated to 37°C in a water bath for the relevant time. Samples were lysed for 30 minutes with 1% digitonin lysis buffer on ice, and insoluble material removed as detailed above. Supernatant was incubated overnight with protein A-Sephrose beads (20 µl) at 4°C with agitation. The following day

beads were washed four times in ice cold lysis buffer, boiled in SDS loading buffer, separated by SDS-PAGE and BCR complexes blotted for as detailed below.

2.10.2 I^{125} radiolabeling surface proteins

Another method for measuring the surface proteins of cells bound by mAb is to radiolabel surface proteins. For this, we followed the method of Spencer and Nicoloff [154]. Briefly, 10^7 cells were washed into PBS and mixed with 200 μM lactoperoxidase, 0.5 mCi Na[^{125}I] and 0.03% H_2O_2 on ice. After gentle mixing for 5 minutes, 20 μM lactoperoxidase and 0.03% H_2O_2 were added followed by three additions of 0.03% H_2O_2 on ice. Samples were then washed four times in ice cold PBS containing lactoperoxidase. Follwowing this cells were incubated with mAb either before or after lysing cells in buffer containing TX-100 detergent asdetailedin sections 2.10.1.5.2 and 2.10.1.5.3. Samples were then resolved by SDS-PAGE (section 2.10.3)

2.10.3 SDS PAGE gel analysis

SDS-PAGE was performed using a mini-gel system (Hoeffer SE-250, Hoeffer, UK). In all cases both the resolving and stacking gels were prepared using 30% (w/v) acrylamide: 0.8% (w/v) bisacrylamide stock solution (National Diagnostics; Atlanta, USA) containing 0.1% (w/v) SDS. Resolving gels at 10, 12.5 or 15% acrylamide were made using a 1.5 M Tris Base pH 8.7 stock solution. The 3% acrylamide stacking gel was made using a 0.5 M Tris base pH6.8 stock solution. The polymerisation reaction was catalysed with N N N' N'-tetramethylethylene (TEMED, Sigma) at final concentrations of 0.05% and 0.1% for the resolving and stacking gels respectively. The reaction was initiated with a fresh 10% (w/v in distilled water) solution of ammonium persulfate (APS), added at a final concentration of 0.4% in resolving gels and 1.0% in stacking gels.

Gels were run at a constant current of 20 mA or constant voltage of 100 V per gel, until samples had entered the resolving gel. This was increased to 40 mA or 200 V until markers (Rainbow markers; Amersham Biosciences) had reached the required position. Gel running apparatus was water cooled throughout.

2.11 Blue Native PAGE

2.11.1 Blue Native PAGE gel preparation

The method for preparation of blue native PAGE (BN-PAGE) gels follows that originally described by Schagger, *et al.*,[155], modified by Schamel and Reth[30] for use on small SDS-

PAGE gel systems (1 mm thickness). First, all equipment and glassware was cleaned with distilled water to remove any trace of SDS. 16% and 5.5% resolving acrylamide mixtures were then prepared using 49.5% (w/v) acylamide: 3% (w/v) bisacrylamide stock solution (Bio-Rad). All gels contained 3x buffer (200 mM e-amino caproic acid, 150 mM bis-tris pH 7.0; Sigma), and distilled water. The 16% resolving gel also contained glycerol (26%). The 16% mix was added into the first chamber of a gradient-pouring device, and the 5.5% mix into the second chamber together with a magnetic stirrer. 10% APS and TEMED were added to catalyse the reaction, and the connection between the chambers opened, allowing generation of a gradient resolving gel. After polymerisation, the stacking gel was poured (using same mixture as for the 5.5% resolving gel).

2.11.2 Sample preparation

$4x10^6$ cells, either treated or not, were lysed in lysis buffer containing either 1% (w/v) digitonin or increasing concentrations of thesit (v/v) detergent dissolved in lysis buffer containing 500 mM e-amino caproic acid, 20 mM tris HCl pH7.4, 2 mM EDTA and 10% (v/v) glycerol (Sigma). Samples were lysed for 30 minutes on ice, and insoluble material removed by centrifugation at 16,000g for 30 minutes at 4°C. Lysates were then directly run on BN-PAGE gels, or incubated overnight with protein A-Sephrose beads at 4°C with agitation. The following day immunoprecipitated protein was washed four times in ice-cold lysis buffer and protein eluted from beads using titrated 0.1 M tris-glycine buffer.

2.11.3 Running samples on BN-PAGE gels

After pouring the BN-PAGE gels, the following steps were performed at 4°C. Samples and markers were applied to relevant lanes and carefully overlaid with blue cathode buffer (50 mM tricine, 15 mM bis-tris, 0.02% Coomassie blue G 250, pH7.0 at 4°C; Sigma). The remainder of the inner chamber was filled with blue cathode buffer, and the outer chamber was with anode buffer (50 mM Bistris pH7.0 at 4°C; Sigma). Gels were run at a constant current of 20 mA or constant voltage of 100 V per gel, until samples had entered the resolving gel. This was increased to 40 mA or 200 V until the running front reached the middle of the separating gel. The blue cathode buffer was then exchanged for colourless electrode buffer (as for blue cathode buffer without Coomassie blue G250). Gels were then removed and protein detected by staining with Coomasie stain. For immunoblotting, gels were prepared as noted below, with the addition of 0.01% SDS to the transfer buffer.

2.12 Western blotting

For western blot analysis, polyvinylidene diflouride (PVDF) membranes (Sigma) were pre-activated by immersing in 100% methanol for 15 seconds, followed by immersing in distilled water for 2 minutes, and incubated in transfer buffer. Proteins were transferred to membranes in transfer buffer (20% (v/v) methanol, 25 mM tris, 192 mM glycine) for one hour at 400 mA (constant current) using a semi-dry transfer system (TE 22 system; Hoeffer). The tank was water cooled throughout transfer. Following transfer, gels were routinely Coomassie stained to determine relative levels of loaded protein. Transfer was deemed to have been successful when Rainbow markers could be seen on the PVDF membrane.

The PVDF membranes were blocked overnight at 4°C, to prevent non-specific binding using 5% low-fat milk powder or 5% BSA (Sigma), in tris buffered saline with 0.1% Tween-20 (TBS/T) (Sigma) with constant rotation using a roller mixer (Spiramix; Jencons, UK).

Following blocking, the membrane was rinsed twice in TBS/T, followed by one 15 minute and two 5 minute washes. The primary antibody was diluted to the desired concentration in TBS/T and incubated with the membrane for 1 hour at room temperature with constant rotation. Following primary antibody incubation the membrane was extensively washed as described above before incubating with the relevant secondary antibody conjugated to horse radish peroxidase (HRP) (Amersham Biosciences), at the desired concentration in TBS/T, for 1 hour at room temperature with rotation.

The membrane was washed in TBS/T once for 15 minutes incubation and four times for 5 minutes before the addition of Supersignal Chemiluminescent reagent (Pierce, UK); Supersignal reagent was added to the membrane surface on a flat surface for 5 minutes. Excess reagent was then removed and the membrane was placed in an appropriate film cassette (Kodak, UK), and protein bands visualised by exposing light sensitive film paper (Hyperfilm; Amersham Biosciences) for the desired length of time under safe light conditions. Films exposed to the treated membrane were developed and fixed under safe-light conditions before analysis.

2.13 Calcium signalling

$1x10^7$ cells were washed twice in serum free RPMI and loaded with 20μM INDO-1-AM (Sigma; made up in 0.2% plurionic-F127) by incubating at 37°C for 30 minutes, then

washed twice in serum free RPMI and re-suspended in 5 ml RPMI containing 10% FCS. Cells were rested for 30 minutes in the dark at room temperature. For analysis of calcium flux generation, the cells were analysed by flow cytometry using a FACS Vantage. After establishing the basal level of calcium, cells were stimulated with various mAb and assessed for a change in the fluorescent ratio.

2.14 Fluorescent microscopy

Cells were suspended at a final concentration of $5x10^5$ cells/ml, in complete medium following the appropriate treatment. PLL coated slides (BDH, Poole, UK) were used for all preparations. The cytospin cassette was assembled with holder and filter in place and 100 µl of cell suspension was slowly loaded into the holder the slides spun for 5 minutes at 100 g with acceleration set at low. Slides were washed twice in PBS and fixed with 3.7% freshly prepared paraformaldehyde for 10 minutes at room temperature. Slides were washed once more in PBS before staining with propidium iodide (PI, 10 µg/ml in PBS), for five minutes in the dark. Excess PI was removed and slides were washed once more in PBS. A few drops of mowiol mountant were placed on the fixed cells, and a cover slip gently lowered on top, and slides left to set at 4°C in the dark prior to analysis.

2.15 Apoptosis experiments

2.15.1 Annexin V FITC; PI assay

As cells apoptose, they translocate phosphatidylserine (PS) from the inner to the outer layer of the plasma membrane. Annexin V is a phospholipid binding protein with affinity for PS. Therefore, binding of Annexin V to the external surfaces of a cell is indicative of apoptosis. Following incubation with the appropriate mAb, $1x10^5$ cells were washed in PBS and re-suspended in 110 µl of binding buffer (10 mM HEPES, pH 7.4, 140 mM NaCl, 2.5 mM calcium chloride), containing 1 µg/ml FITC-annexin V (Pharmingen, UK), and subsequently assessed by flow cytometry using a FACScan.

2.15.2 DioC6 analysis

DioC6 was used to measure cells that were in a later stage of apoptosis, compared with those detected by annexin V staining. DioC6 is incorporated into mitochondria, and released as mitochondrial membranes lose their electrostatic potential during apoptosis. Following incubation with the appropriate mAb, $1x10^6$ cells were removed and 25 µl of DioC6 solution added (20 nM final concentration). Cells were incubated at 37°C for 30

minutes before being spun down and re-suspended in 200 µl of PBS containing PI. Samples were analysed using a FACScan as detailed above.

2.15.4 Analysis of DNA fragmentation and growth arrest.

Samples were analysed essentially as described by Nicoletti, *et al.*,[156]. Briefly, $5x10^5$ cells were centrifuged for 5 minutes at 500g. Cells were washed once in PBS, re-suspended in hypotonic fluorochrome solution (50µg/ml PI, 0.1% sodium citrate, 0.1% (v/v) Triton X-100) and stored in the dark at 4°C overnight. Samples were then analysed using a FACScan flow cytometer and PI fluorescence detected on FL2 channel.

2.16 Modulation of surface BCR

Cells were plated at $1.5x10^5$ cells/well in a 96 well, flat-bottomed plate and left for 1 to 2 hours at 37°C in a humidified incubator. At relevant time points Ab at the required concentration was added to the wells and the cells re-incubated at 37°C for the required time. For short 1 to15 minute time points cells were incubated in a water bath. Prior to flow cytometric analysis, samples were washed twice in PBS containing 1% BSA (w/v) and 0.1% azide (PBS/BSA/azide). Cells were then incubated with the relevant FITC conjugated secondary Ab for 20 minutes in 100 µl of PBS/BSA/azide. Cells were then washed once more in PBS/BSA/azide and analysed.

Chapter 3

The effect of anti-BCR antibodies on receptor induced apoptosis and intracellular signalling in B cell lines.

3.1 Introduction

In-vitro studies have shown that cross-linking the BCR on the surface of B cells can induce growth arrest and apoptosis in certain cell lines[157]. The maturation state of the cell line is of importance, with immature B cells that express high levels of mIgM on the cell surface being susceptible to anti-BCR induced cell death[2]. This observation led workers to assess whether mAb directed to the BCR could induce inhibitory signals within B lymphoma cells[158, 159]. Vuist, *et al.*,[160] showed that in Non-Hodgkins lymphoma, mAb directed at the idiotype (Id) of mIgM can be used as an effective immunotherapeutic target. More importantly, this work demonstrated that anti-Id mAb caused an increase in protein tyrosine phosphorylation only in tumour cells taken from patients that had responded with a partial or complete remission. These data, along with results from *in vitro* cell lines, have indicated that mAb directed at the BCR may induce immunotherapy by transmitting inhibitory intracellular signals to the tumour cells, rather than through more conventional effector mechanisms, such as complement or antibody directed cellular cytotoxicity (ADCC)[161, 162].

The *in vitro* Burkitt's lymphoma cell line Ramos is thought to have been derived from GC type B cells[158]. The Ramos cell line is sensitive to growth inhibition and apoptosis when stimulated with mAb directed at mIgM and, therefore, is a good model for analysing inhibitory signalling effects[158]. EHRB is a cell line derivative of Ramos which is particularly sensitive to these signals[141, 158]. Previous work in our laboratory has shown that mAb directed at the Fab domain (Fdμ, Ig-light chain, and Id itself) and the CD79 heterodimer have little effect on growth inhibition in these cells[159]. In this section the aim is to try to understand why mAb directed at the Fcμ domain of mIgM (Figure 3.1), are efficient at inducing growth inhibition, why mAb directed at other regions of the same receptor are not, whether this growth inhibition is predominantly due to the induction of apoptosis, and how this understanding might be applied to immunotherapy.

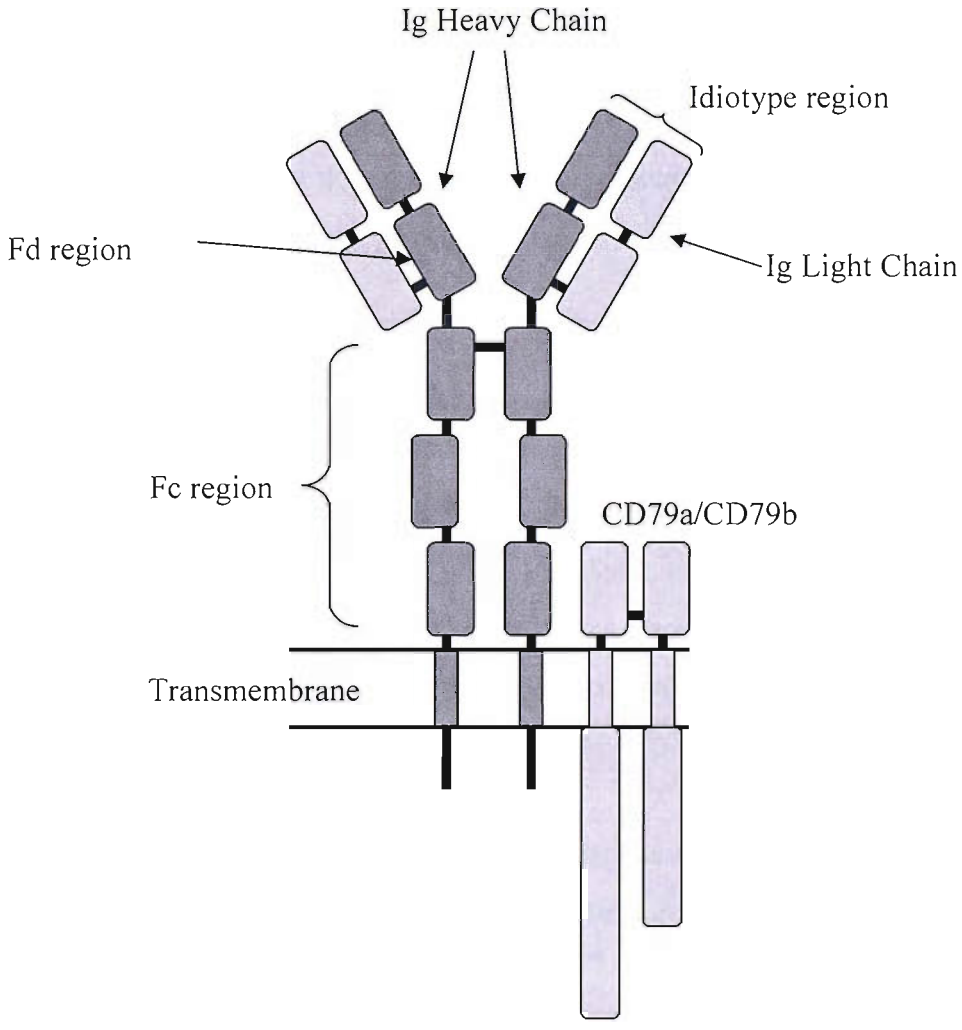

Figure 3.1 Domains of the BCR. Schematic representation of the mIgM BCR showing domains where different mAb bind.

3.2 Results

3.2.1 Measurement of BCR induced apoptosis.

Previous work in our laboratory has shown that the anti-Fcμ mAb, but not other anti-BCR mAb, can induce potent growth inhibition of EHRB cells (Figure 3.2)[158]. Therefore, in our initial experiments it was decided to confirm these observations and assess whether growth inhibition was due to apoptosis. Initially, EHRB cells were stimulated with either an irrelevant non-binding control mAb (CP1/17) or a polyclonal Ab raised against human mIgM (10 μg/ml) for 24 hours at 37°C, and levels of BCR induced apoptosis assessed using a variety of techniques as detailed in section 2.15.

3.2.1.1 Use of AnnexinV and PI to detect early apoptosis.

An early measure of apoptosis is the increased availability of phosphatidyl serine (PS) at the cell surface. PS is normally confined to the inner leaflet of the plasma membrane, however, as cells undergo apoptosis the PS flips to the outer side of the plasma membrane. PS at the cell surface can be detected using FITC labelled annexin V, which binds specifically to PS in the presence of calcium. Figure 3.3a, clearly shows that EHRB cells stimulated with the anti-μ polyclonal Ab give increased binding of annexin V compared with cells treated with the control mAb, confirming an increased level of PS at the cell surface.

A later stage of cell death is when the plasma and nuclear membranes of the cell become compromised, a process known as secondary necrosis. To measure this, the DNA fluorochrome PI can be used. Although PI is unable to enter healthy cells, in cells undergoing secondary necrosis PI enters and binds to DNA, causing it to fluoresce. Therefore, to discriminate between early and late stages of apoptosis, PI was added to samples along with annexin V. A typical example of this analysis is shown in Figure 3.3b. As expected, the anti-μ treatment resulted in a larger proportion of PI positive cells compared to the control samples, showing that secondary necrosis was induced following treatment with the anti-μ polyclonal Ab. However, it should be noted that the number of PI positive cells is lower than the number of annexin V positive cells, indicating that annexin V is also capable of detecting cells at the early stages of apoptosis.

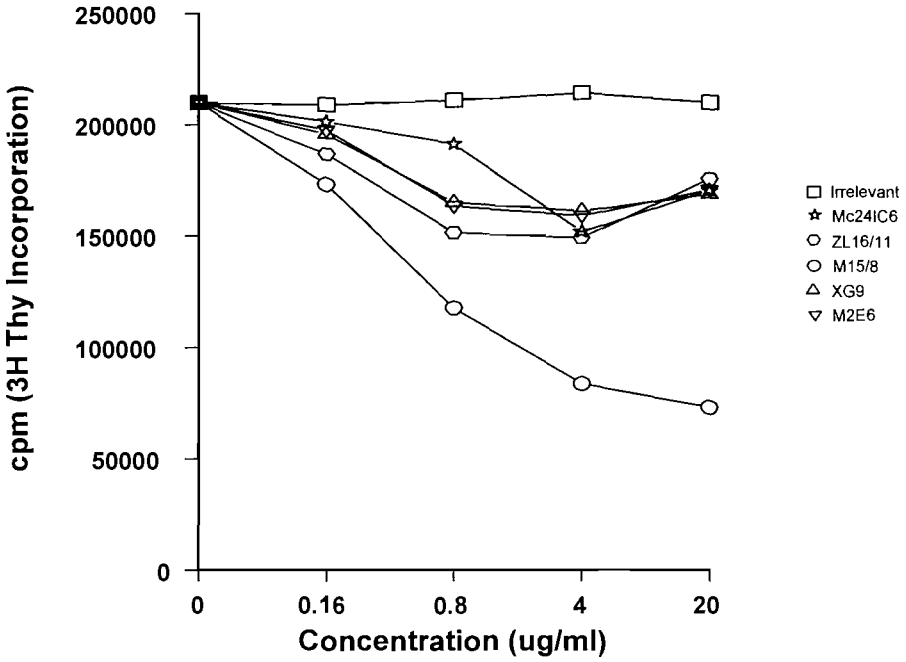

Figure 3.2 Growth inhibition of EHRB cells stimulated with various mAb directed at different domains of the mIgM. EHRB cells were treated with various concentrations of anti-BCR mAb. Control (CP1/17), anti-Fcμ (M15/8), anti-Fdμ (XG9 and M2E6), anti-λ (Mc24IC6) and anti-Id (ZL16-11). Growth inhibition was determined by reduction in ability of cells to divide using [^{3}H] thymidine. Figure courtesy of Dr Mark Cragg.

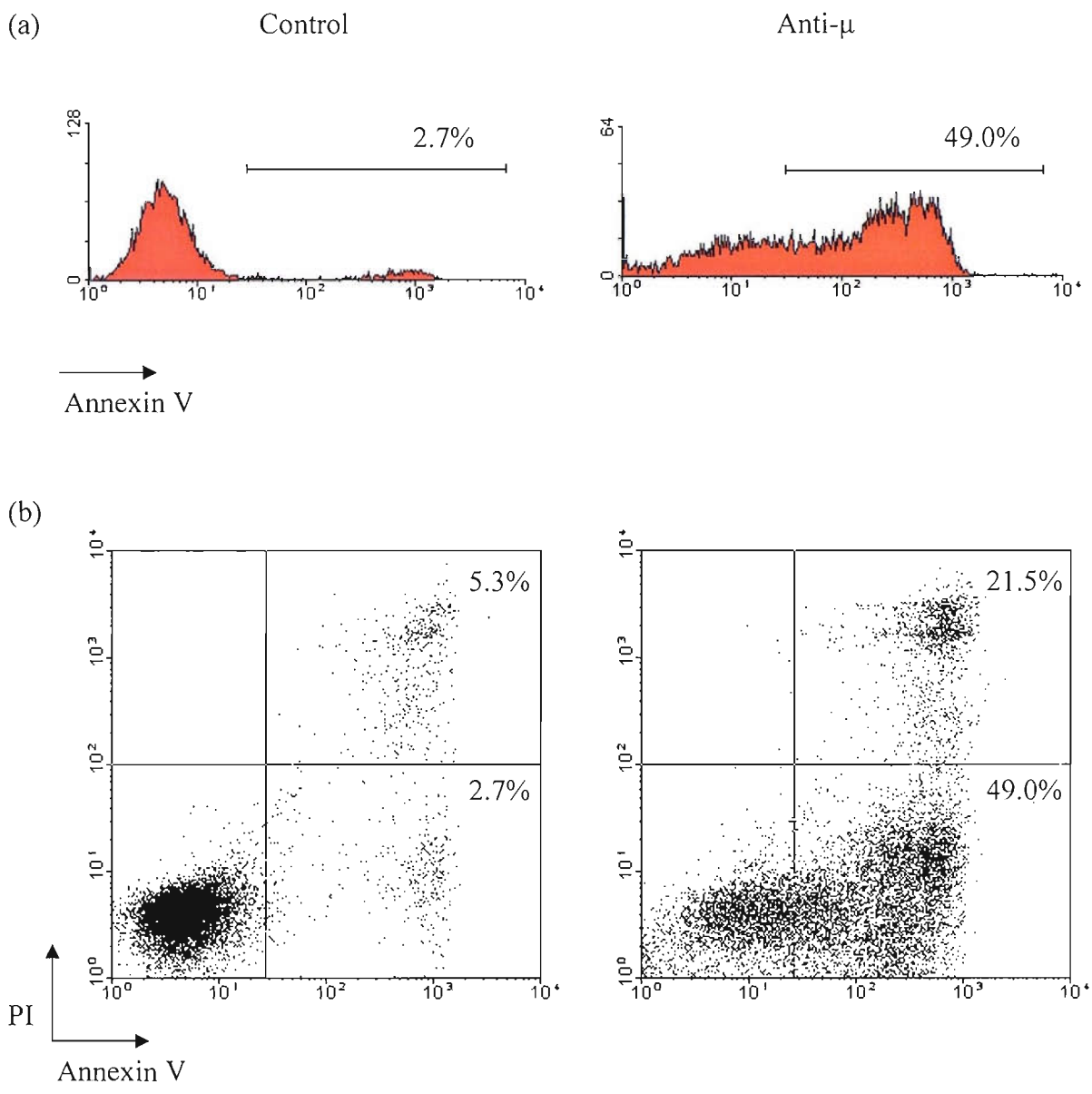

Figure 3.3 Measurement of BCR induced apoptosis using AnnexinV and PI. 1x10^5 EHRB cells were treated with either control (CP1/17) mAb or anti-μ polyclonal Ab (10 μg/ml) for 24 hours at 37°C in a humidified incubator. Levels of cellular apoptosis were measured using FITC labelled AnnexinV by flow cytometry (a) (note the axis between the two plots is different). To assess levels of secondary necrosis, cells were stained with FITC labelled Annexin V and PI and assessed by flow cytometry (b). Representation of at least three independent experiments.

3.2.1.2 DioC6 analysis.

Another stage of apoptosis involves the loss of the mitochondrial membrane potential. To assess mitochondrial membrane potential the reporter dye DioC6 dye can be used. When incubated with cells this fluorescent dye becomes incorporated into healthy mitochondria. However, the fluorescence is lost when the mitochondrial membrane potential is reduced during apoptosis, as shown in Figure 3.4. Cells treated with the anti-μ polyclonal Ab induced apoptosis as measured by a loss of DioC6, shown as gated population, compared to cells treated with the control mAb.

3.2.1.3 Measurement of cell cycle arrest and DNA fragmentation.

At later stages of apoptosis, the nucleus becomes dismantled and DNA fragmentation occurs. To assess DNA fragmentation we used a hypotonic PI buffer to lyse the cells and measure DNA content. This technique has the advantage of also revealing cell cycle distribution of the cell population, providing information of any cell cycle arrest. Following 24 hours stimulation with the anti-μ polyclonal Ab, growth inhibition in EHRB cells can clearly be observed as an increased number of cells in the G_1 stage of the cell cycle, with fewer cells present in the S and G_2/M stages (Figure 3.5a), with 11% DNA fragmentation compared with 1% in the control. At 48 and 72 hours (Figures 3.5b and 3.5c, respectively), the level of DNA fragmentation clearly increase to 27% and 37% respectively.

Together these data convincingly show that Ab specific for mIgM can induce apoptosis in the EHRB cell line.

3.2.2 The effect of mAb concentration on BCR induced apoptosis in EHRB cells.

Following the confirmation that a polyclonal anti-μ Ab clearly induced apoptosis, we decided to determine whether mAb raised against specific domains of mIgM could also induce apoptosis. First, to assess how sensitive the EHRB cell line is to BCR induced apoptosis, cells were treated with increasing concentrations of control (CP1/17) and anti-Fcμ (M15/8) mAb. As the concentration of the anti-Fcμ mAb increased, so the levels of BCR induced apoptosis increased, as shown by annexin V/PI and DioC6 staining (Figure 3.6). The results showed that the optimal concentration of anti-Fcμ mAb to induce apoptosis was 10 μg/ml.

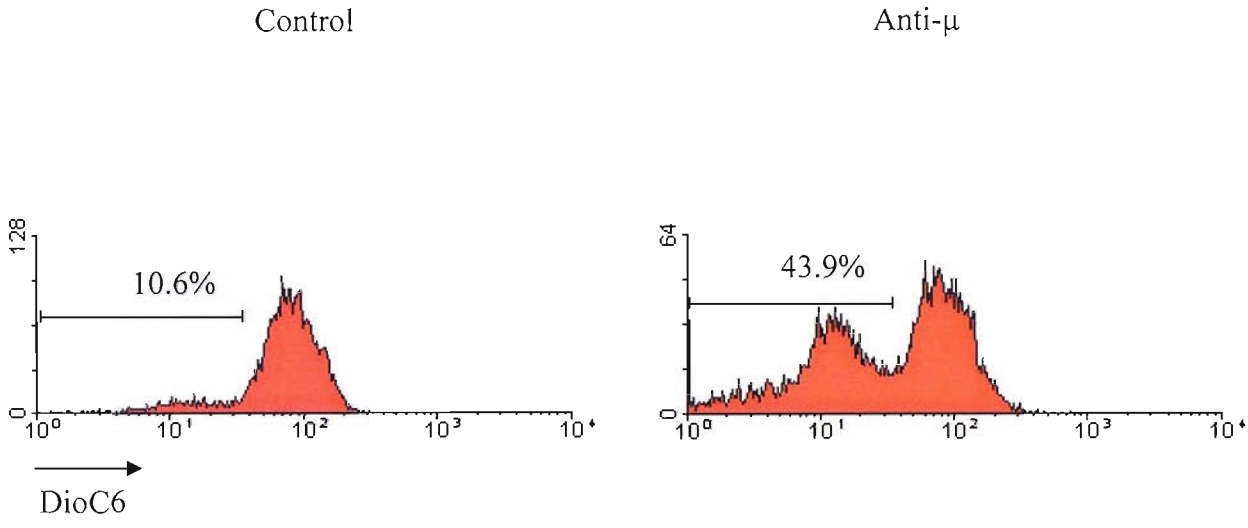

Figure 3.4 Measurement of BCR induced apoptosis using DioC6. $1x10^5$ EHRB cells were treated with either control (CP1/17) mAb or anti-μ polyclonal Ab (10 μg/ml) for 24 hours at 37°C in a humidified incubator. Levels of cellular apoptosis were measured using DioC6. Representation of at least three independent experiments. (note the axis between the two plots is different).

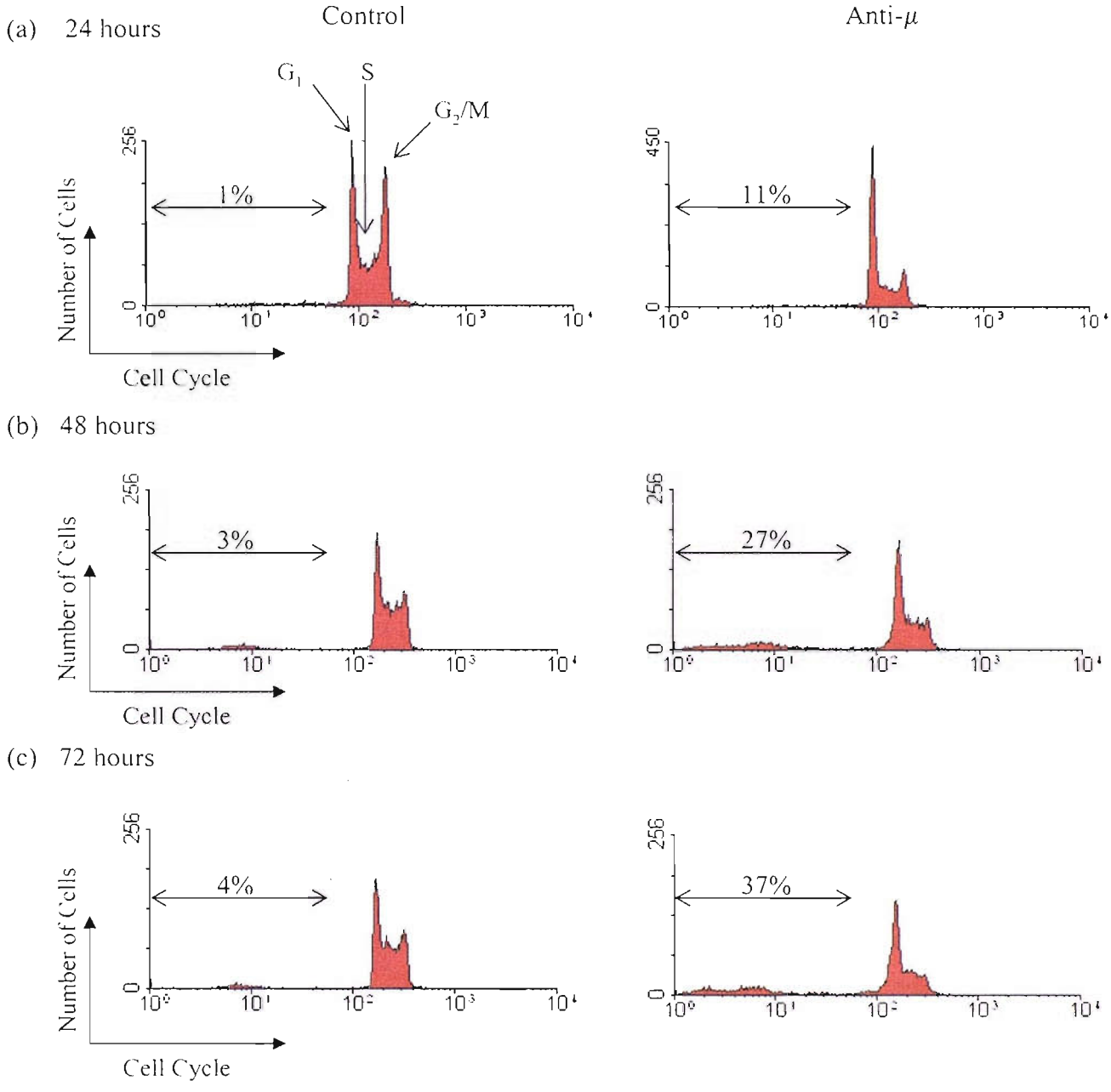

Figure 3.5 Measurement of BCR induced growth arrest and DNA fragmentation. 5x10^5 EHRB cells were treated with either control (CP1/17) mAb or anti-μ polyclonal Ab (10 μg/ml) for 24 (a), 48 (b) or 72 (c) hours at 37°C. Following incubation, cells were washed twice in PBS followed by addition of hypotonic PI overnight at 4°C. The level of cells in specific stages of the cell cycle was assessed by flow cytometry, together with levels of DNA fragmentation, and shows arrest in cell cycle at the G_1 stage after anti-μ Ab treatment, with decreased numbers of cells progressing to the S and G_2/M stages of the cell cycle. Representation of at least three independent experiments. (note the axis between the plots is different, depending on the treatment and time of experiment).

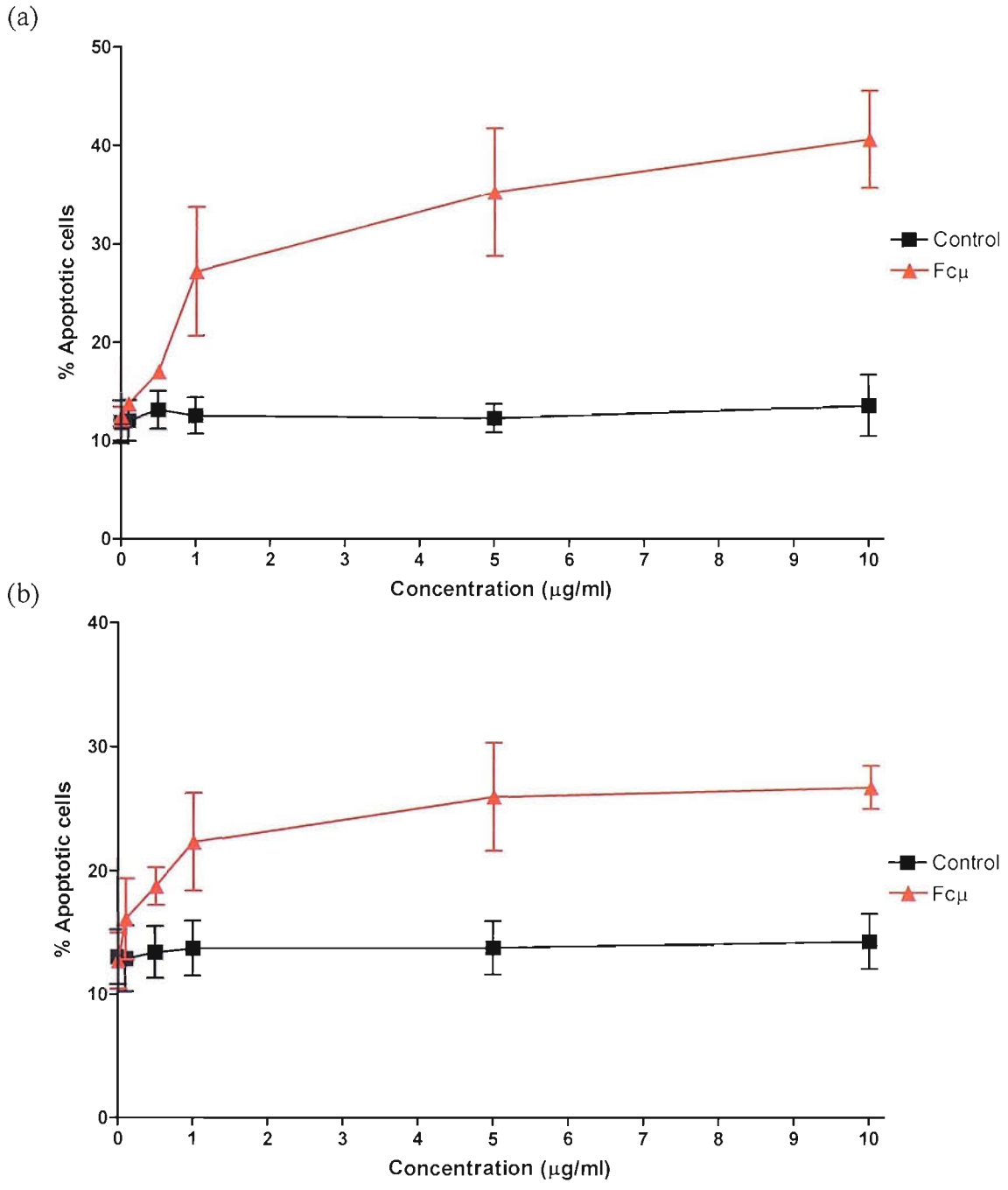

Figure 3.6 Effect of increasing concentrations of anti-Fcµ mAb on EHRB BCR induced apoptosis. $2x10^5$ EHRB cells were treated with either control (CP1/17) or anti-Fcµ (M15/8) mAb at various concentrations for 24 hours at 37°C in a humidified incubator. Levels of cellular apoptosis were analysed by flow cytometry using either AnnexinV PI (a) or DioC6 (b) staining. Mean values ± SD of three independent experiments.

3.2.3 The kinetics of BCR induced apoptosis in EHRB cells.

In addition to assessing the effect of the anti-Fcμ mAb concentration on BCR induced apoptosis it was necessary to look at the kinetics of the process. EHRB cells were treated with either: control (CP1/17), anti-Fcμ (M15/8) mAb or polyclonal anti-μ Ab for 6, 24, 48 or 72 hours at 37°C in a humidified incubator. Following stimulation, levels of apoptosis were assessed using annexin V/PI. Figure 3.7 shows that the level of BCR induced apoptosis increased with time of exposure to either anti-Fcμ or polyclonal anti-μ Ab. Interestingly after six hours incubation, the level of BCR induced apoptosis was already quite high with 40% and 30% cells staining positive when treated with the anti-Fcμ and polyclonal anti-μ Ab, respectively. These levels increased as the incubation time increased from 24 to 72 hours.

3.2.4 The effect of mAb directed at different domains of mIgM on BCR induced apoptosis in EHRB cells.

As both a polyclonal Ab and anti-Fcμ mAb clearly induced apoptosis, we decided to observe whether mAb raised against different domains of mIgM could also induce apoptosis. EHRB cells were treated with either: control mAb (CP1/17), mAb directed at the Fdμ (XG9), λ light chain (Mc24IC6) or Fcμ (M15/8) domain of mIgM. All mAb were of IgG_{2a} isotype, removing the possibility of any isotype specific effects of the mAb. Levels of BCR induced apoptosis were assessed using annexin V/PI and DioC6. Figure 3.8 shows that only the anti-Fcμ mAb induced high levels of apoptosis compared with cells treated with control mAb, with mAb directed at the Fdμ and λ light chain domains inducing low levels of apoptosis.

To check whether this phenomenon was particular to a single antibody rather than a domain-specific effect, we tested a wider range of mAb. EHRB cells were treated for 24 hours with different mAb (10 μg/ml) directed at the Fcμ (M15/8, ZL7/5, Mc244G10), Fdμ (MA5, XG9, M2E6), or λ light chain (Mc24IC6, M15/2) domains of mIgM, along with control mAb (CP1/17) or polyclonal anti-μ Ab. Figure 3.9 shows that all three mAb directed at the Fcμ domain of mIgM induced apoptosis similar to that obtained with the polyclonal anti-μ Ab. Monoclonal Ab against the Fdμ or λ light chain domains of mIgM clearly did not induce substantial levels of apoptosis above that seen with the control.

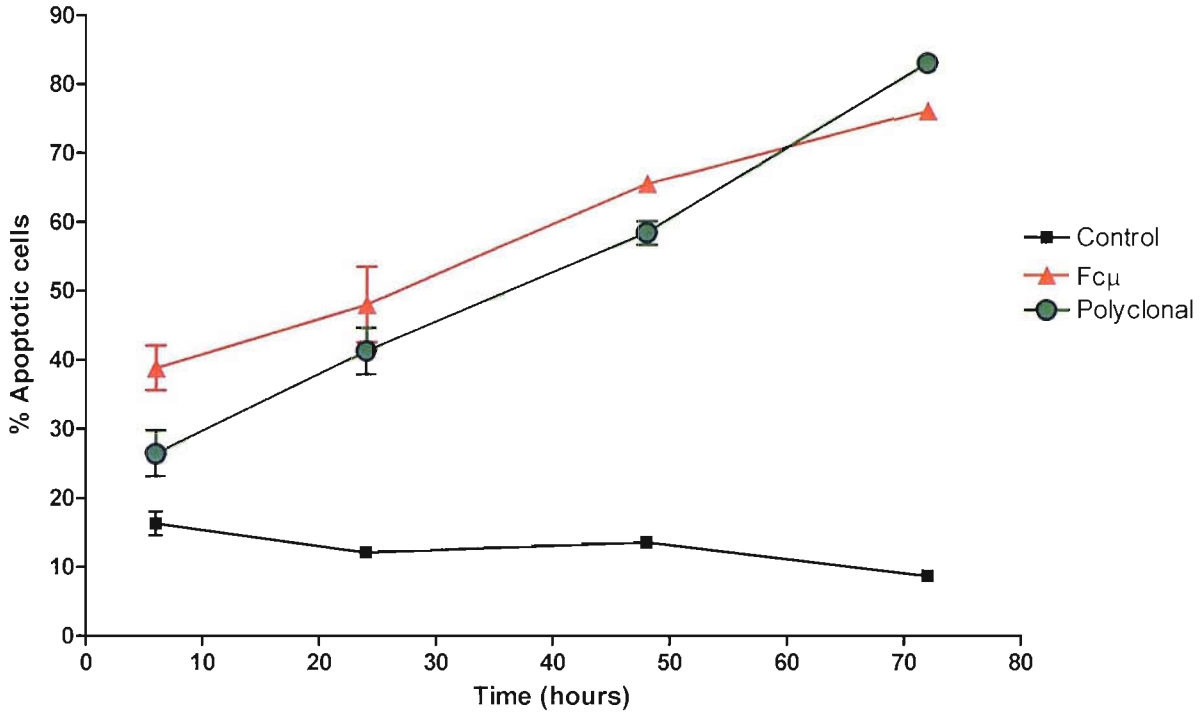

Figure 3.7 Kinetics of BCR induced apoptosis. $1x10^5$ EHRB cells were treated with either control (CP1/17), anti-Fcμ (M15/8) mAb or polyclonal anti-μ Ab (10 μg/ml) for 6, 24, 48, or 72 hours at 37°C. Levels of BCR induced apoptosis were assessed by flow cytometry using annexin V/PI staining. Mean values ± SD of three independent experiments shown.

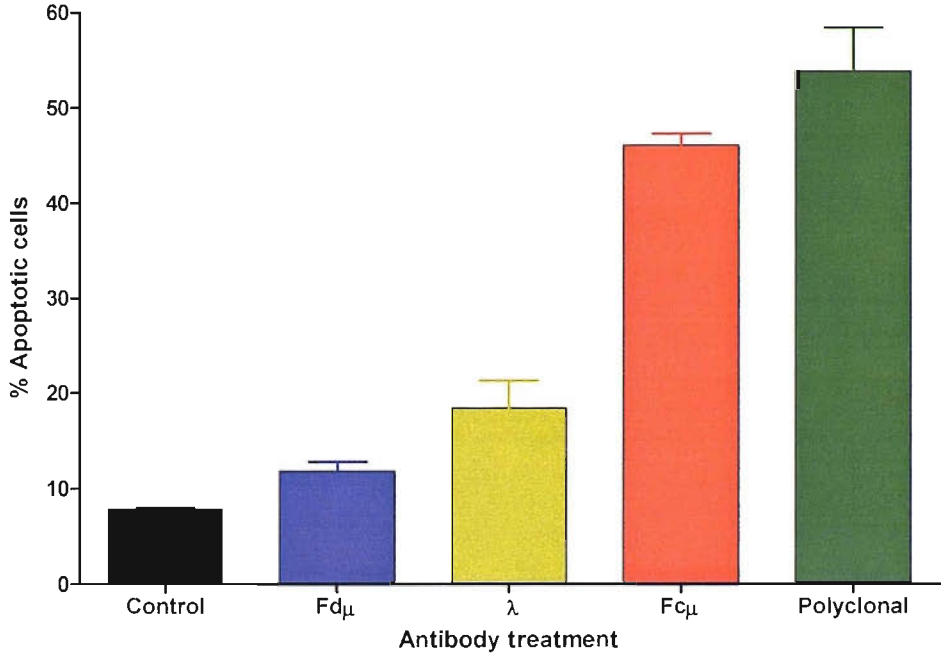

Figure 3.8 Apoptosis induced by antibodies recognising different regions of mIgM on EHRB cells. $2x10^5$ EHRB cells were treated with various Ab (10 μg/ml) directed at different domains of mIgM for 24 hours at 37°C. Levels of cellular apoptosis were measured using FITC labeled annexinV and PI by flow cytometry. Mean values ± SD given for three independent experiments. Antibodies used were: control (CP1/17), anti-Fdμ (XG9), anti-λ (Mc24IC6), anti-Fcμ (M15/8), and polyclonal anti-μ Ab.

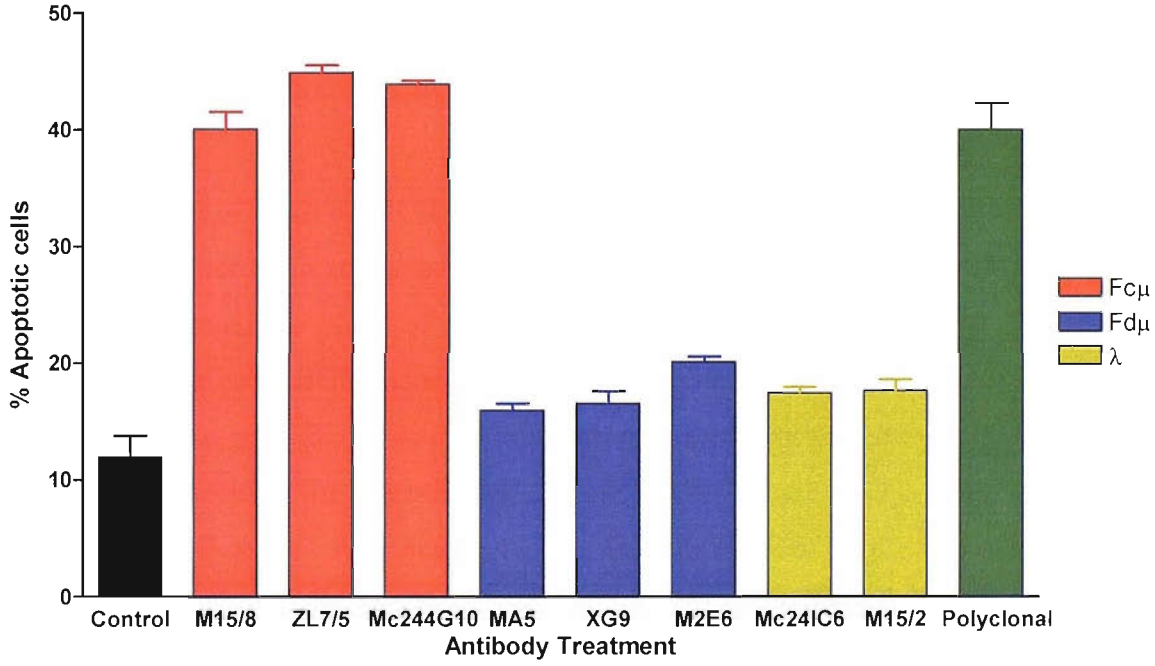

Figure 3.9 Effect of mAb directed to similar domains of mIgM on BCR induced cellular apoptosis. 1x10^5 EHRB cells were treated with various mAb (10 μg/ml) for 24 hours at 37°C. The level of BCR induced apoptosis was analysed by flow cytometry with FITC labeled AnnexinV and PI. Mean values ± SD of three independent experiments. Cells treated with the following Ab; Control (CP1/17), anti-Fcμ (M15/8, ZL7/5 and Mc244G10), anti-Fdμ (MA5, XG9, and M2E6), anti-λ (Mc24IC6 and M15/2) and polyclonal anti-μ Ab.

3.2.5 The effect of anti-CD79a and b mAb on BCR induced apoptosis in EHRB cells.

The CD79 heterodimer is an appealing target for mAb therapy of B cell lymphomas, due to its expression on all B cell sub groups, apart from plasma cells[94, 163]. CD79 also represents the signalling component of the BCR and as intracellular signalling may correspond with therapy, we decided to investigate the effects of mAb directed at the CD79 heterodimer on apoptosis induction. EHRB cells were incubated with either control (CP1/17) mAb, anti-CD79a (ZL7/4), anti-CD79b (AT105/1), either alone, or in combination at a final concentration of 10 μg/ml, with anti-Fcμ mAb (M15/8) used as a positive control. Figure 3.10 shows that where the anti-Fcμ mAb induces apoptosis as measured by annexin V/PI or DioC6 staining, mAb directed to the CD79 heterodimer fail to induce apoptosis compared with the control mAb. Interestingly, a mixture of CD79a and CD79b mAb was unable to induce substantial levels of apoptosis. To confirm that this was not simply a mAb specific phenomenon, a number of different mAb to CD79a and b were tested and also shown not to induce apoptosis (data not shown).

3.2.6 The effect of mAb on BCR induced apoptosis in various human B cell lines.

To assess whether mAb recognising the Fcμ domain of the BCR is always able to induce apoptosis we tested the effect of these mAb on a range of cell lines. The EHRB cell line was most sensitive to BCR-induced apoptosis when stimulated with either the anti-Fcμ or polyclonal anti-μ Ab. BL-60 and Daudi were also sensitive and showed 45% and 35% of cells staining positive for annexin V/PI, respectively (Figure 3.11). The Raji cells were insensitive to all mAb. Anti-Fcμ mAb was the most potent of all mAb used on EHRB, Daudi and BL-60 cell lines. The Daudi cells were also sensitive to anti-Id mAb which induced about 40% apoptosis. Interestingly, the BL-60 cells also appeared to be slightly more sensitive to BCR induced apoptosis when stimulated with mAb directed at the CD79 heterodimer and Fdμ domains of mIgM, compared with EHRB cells. Although the levels of apoptosis were relatively low compared to that induced by the anti-Fcμ or polyclonal anti-μ Ab.

3.2.7 The BCR phenotype of human B cell lines.

It is clear that most cell lines are sensitive to anti-Fcμ mAb. However, to understand why cell lines exhibit different responses it was decided to assess the BCR phenotype of the different cell lines. EHRB, Daudi, BL-60, and Raji cells were incubated with the relevant mAb and levels of bound Ab measured indirectly by flow cytometry using FITC-labelled secondary Ab. Table 3.1 shows mean levels of expression ± SD from three independent

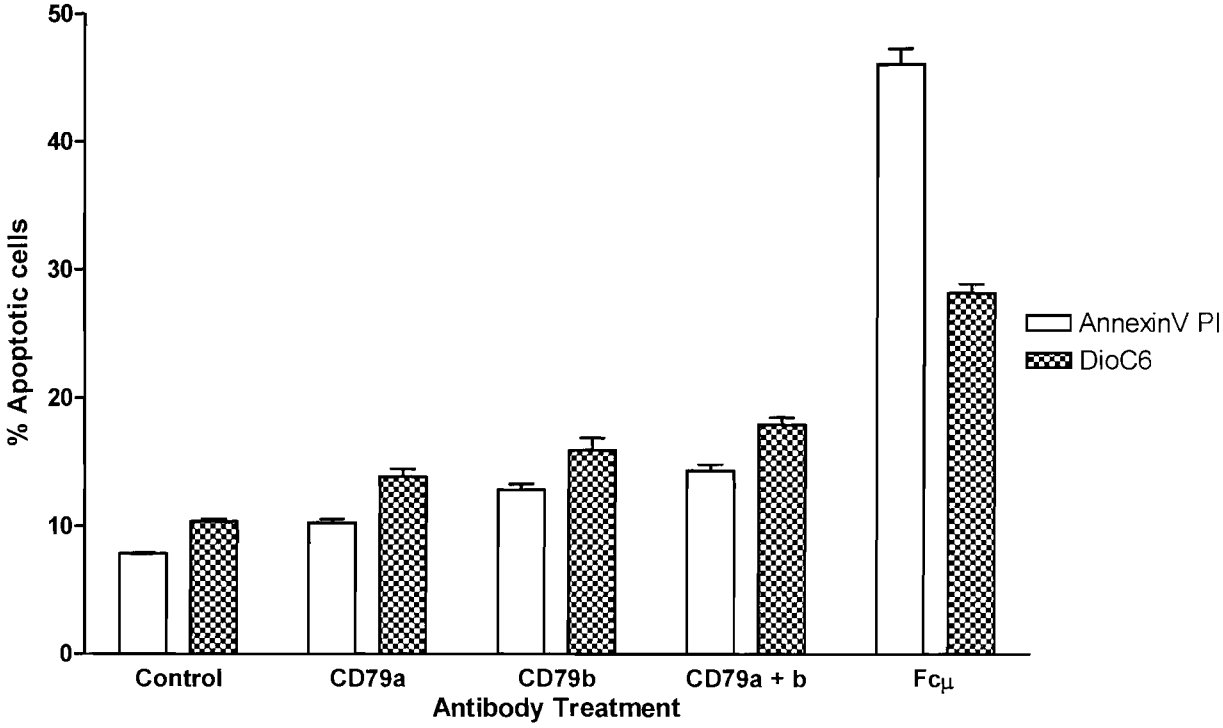

Figure 3.10 Apoptosis induced by antibodies directed to different regions of the CD79 heterodimer on EHRB cells. $2x10^5$ EHRB cells were treated with various Ab (10 μg/ml) directed at different domains of the CD79 heterodimer or the Fcμ domain of mIgM for 24 hours at 37°C. Levels of cellular apoptosis were measured using FITC labeled AnnexinV/PI, or DioC6 by flow cytometry. Mean values ± SD given for three independent experiments. Antibodies used were; control (CP1/17), anti-CD79a (ZL7/4), anti-CD79b (AT105/1), anti-CD79a + b (ZL7/4 + AT105/1), and anti-Fcμ (M15/8).

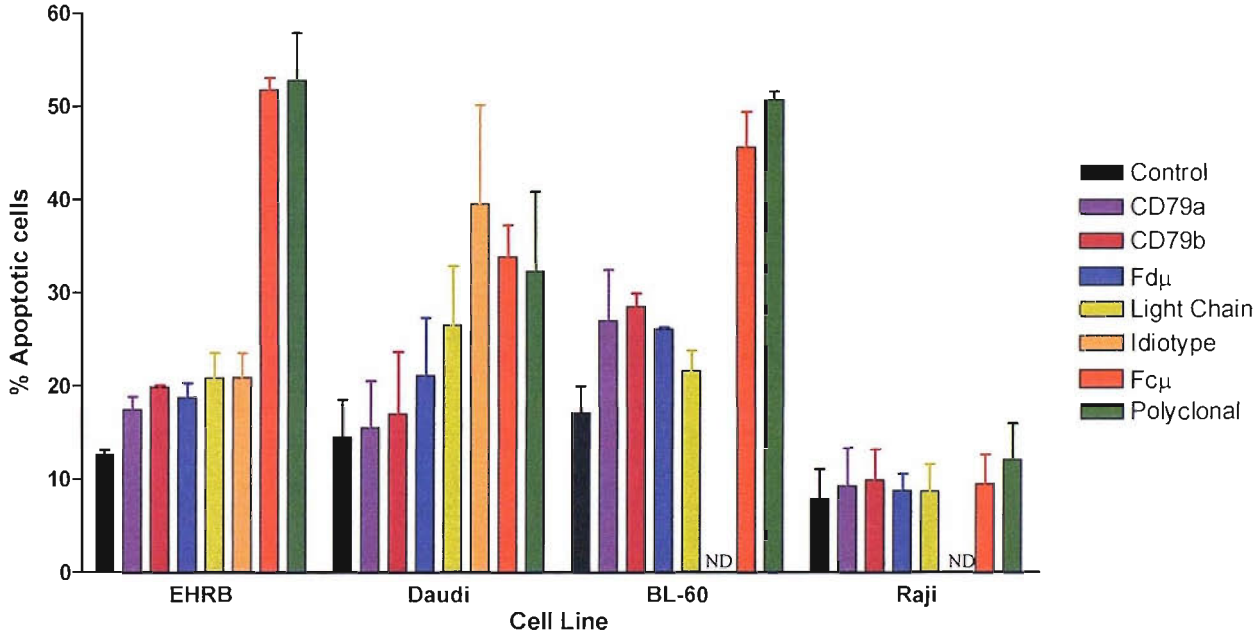

Figure 3.11 Effect of BCR induced apoptosis on human B cell lines. $1x10^5$ cells were treated with various mAb (10 μg/ml) for 24 hours at 37°C. Samples were then analysed for levels of BCR induced apoptosis by flow cytometry using FITC labelled AnnexinV/PI staining. Cells were treated with the following mAb; Control (CP1/17), Fcμ (M15/8), CD79a (ZL7/4), CD79b (AT105/1), Fdμ (XG9), light chain (EHRB; Mc24IC6, other cell lines; K35), idiotype (EHRB; ZL16/1 and Daudi; ZL15/27, no idiotype mAb was available for BL-60 and Raji cell lines) or polyclonal anti-μ Ab. Mean values ± SD for three independent experiments.

	EHRB		Daudi		BL-60		Raji	
Surface Antigen	Mean	SD	Mean	SD	Mean	SD	Mean	SD
Control	**3.4**	0.5	**3.3**	0.3	**3.7**	0.8	**4.0**	1.1
mIgM	**234.1**	11.9	**217.1**	34.7	**125.4**	11.8	**35.5**	1.4
CD79a	**140.1**	15.4	**99.5**	20.2	**77.9**	21.5	**19.6**	3.8
CD79b	**164.2**	38.0	**125.1**	22.5	**103.7**	30.8	**24.7**	0.9
CD19	**110.3**	3.1	**313.1**	61.8	**231.9**	58.6	**142.1**	17.8
CD22	**52.6**	0.1	**100.3**	16.1	**64.5**	7.1	**57.6**	10.0
mIgD	**8.4**	1.3	**4.5**	1.1	**6.4**	1.9	**3.8**	0.8

Table 3.1 Surface Phenotype of human B cell lines. $1x10^5$ EHRB cells were treated with various Ab (10 μg/ml) directed at B cell surface Ag's for 30 minutes at 4°C. Samples were washed and levels of surface bound mAb measured on flow cytometry using FITC labeled goat anti-mouse F(ab')2 Ab. Cells were treated with the following primary Ab: control (CP1/17), anti-mIgM (Fcμ, M15/8), anti-CD79a (ZL7/4), anti-CD79b (AT105/1), anti-CD19 (RFB9), anti-CD22 ( ), and anti-mIgD (KK2.1). Mean values from three independent experiments with SD.

experiments. The results show that EHRB cells express the highest levels of mIgM followed by Daudi and BL-60, which also showed the same ranking for expression of the CD79 heterodimer, measured using anti-CD79a and CD79b mAb. The Raji cells however, expressed relatively low levels of mIgM at the cell surface.

The surface expression of two proteins known to help regulate intracellular signals generated from the BCR was also assessed; the positive regulating protein CD19, and the negative regulating protein CD22. The Daudi cell line expressed the highest levels of CD19 and CD22 followed by BL-60 and Raji, with EHRB cells expressing the lowest levels. Surface levels of mIgD were also assessed, but expression was very weak on all four lines.

3.2.8 Protein tyrosine phosphorylation in the presence of anti-BCR Ab.

We were interested to understand how mAb directed at the Fcμ domain of the BCR can induce apoptosis. Early experiments in this laboratory, and other published research[5, 18] showed that cross-linking the BCR with mAb can induce intracellular signals. We wanted to know whether the mAb that induce apoptosis produced a different signalling pattern compared with mAb that do not. One of the earliest intracellular responses to BCR cross-linking is an increase in levels of protein tyrosine phosphorylation[164]. Therefore, it was decided to investigate if mAb directed at different domains of the BCR induced different tyrosine phosphorylation patterns. Previous work indicates that tyrosine phosphorylation in response to anti-BCR Ab peaks at around five minutes[28]. Therefore, EHRB cells were stimulated with various mAb for 5 minutes at 37°C, lysed as detailed in the methods section (2.10.1.3), separated on 12.5% SDS-PAGE gels, transferred to PVDF membranes and probed for the presence of proteins containing phosphorylated tyrosine residues using the mAb 4G10, and an anti-mouse HRP linked secondary Ab as described in section 2.12.

Figure 3.12 indicates that mAb directed to all domains of the BCR gave robust responses, in terms of tyrosine phosphorylation, compared with cells treated with the control mAb. Polyclonal anti-μ Ab and anti-Id mAb induced the highest levels of protein tyrosine phosphorylation, followed by mAb directed at the Fdμ, λ and CD79a domains of the BCR. Surprisingly, mAb directed at the Fcμ domain of mIgM induced the lowest levels of protein tyrosine phosphorylation along with the anti-CD79b mAb. It was also interesting to note that individual phosphorylated proteins could be observed on the gels, and differences in the level of phosphorylation of these proteins could be observed between samples. In the

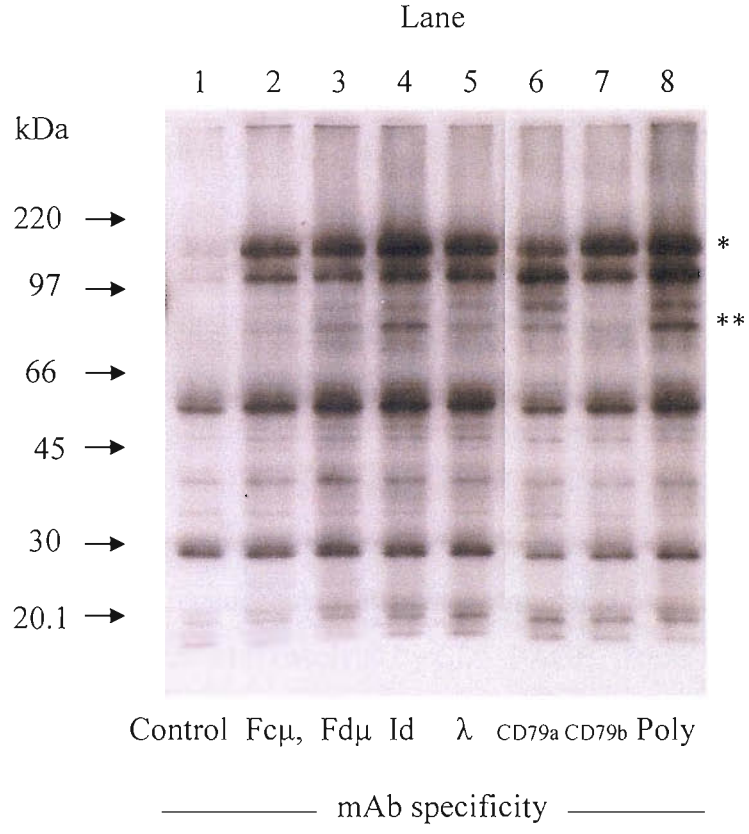

Figure 3.12 Tyrosine phosphorylation patterns in EHRB cells stimulated with various anti-BCR Ab. EHRB cells were stimulated with the appropriate antibody for 5 minutes at 37°C, lysed and separated on 12.5% SDS-PAGE gels. Proteins were then transferred to PVDF membrane and probed for the presence of phosphorylated tyrosine residues using the mAb 4G10 (1 μg/ml) and an appropriate HRP conjugated secondary Ab. Cells were stimulated with the following Ab: lane 1 CP1/17; lane 2 M15/8; lane 3 XG9; lane 4 ZL16/1; lane 5 Mc24IC6; lane 6 ZL7/4; lane 7 AT105/1; and lane 8 polyclonal anti-μ Ab. All antibodies were used at a final concentration of 10 μg/ml. This gel is representative of at least three independent experiments

highest molecular weight range, between 97 and 220kD, less induction of protein tyrosine phosphorylation was observed in cells treated with anti-CD79a mAb compared to the other mAb (*). Between 66 and 97kD different levels of protein tyrosine phosphorylation activation were also observed. (**).

3.2.9 PTK activation in EHRB cells treated with anti-BCR mAb.

From Figure 3.12, it was clear that specific proteins were differentially activated by the binding of mAb directed at different domains of the BCR. We therefore, decided to investigate the activation of specific PTK following BCR cross-linking and observe any differences following stimulation with the different mAb.

3.2.9.1 Activation of Akt.

The first PTK we investigated was Akt, a downstream target for PI3-K, with a molecular weight of 60 kD. PI-3K activation was observed in cells that do not undergo apoptosis[46]. PI3-K phosphorylates PIP_2 to PIP_3 at the plasma membrane, allowing PTK containing PH domains, like Akt, to bind and become activated[48, 49]. Akt is known to be important in providing anti-apoptotic signals to the B cell by the activation of nuclear transcription factor NF-κB as previously mentioned[50-52]. Cells were stimulated with mAb directed at different domains of the BCR and samples resolved by SDS-PAGE. Blots were then probed for the presence of active Akt using a phospho-specific mAb (detecting phospho-Thr308) and HRP labelled secondary Ab. Figure 3.13, shows that there is little difference in the levels of activated Akt when cells were stimulated with mAb directed at different domains of the BCR. Interestingly, levels of activated Akt were also high in cells treated with control mAb.

3.2.9.2 Activation of Lyn.

As no differences were observed in the levels of Akt activation, the activation of the early PTK Lyn, a member of the Src family of kinases, was investigated. Lyn has a molecular weight of between 53 and 56 kD and its activation is important for initiation of the downstream signalling cascade through the BCR[35-37]. To investigate the activation of Lyn, proteins containing phosphorylated tyrosine residues were immunoprecipitated from the supernatant of EHRB cells which had been stimulated for 5 minutes at 37°C, as detailed in section 2.10.1.5.1. Lysates were also immunoblotted for the presence of total Lyn prior to immunoprecipitation to show that the same levels of Lyn protein was present in each lysate. Immunoprecipitated tyrosine phosphorylated proteins were then immunoblotted for Lyn.

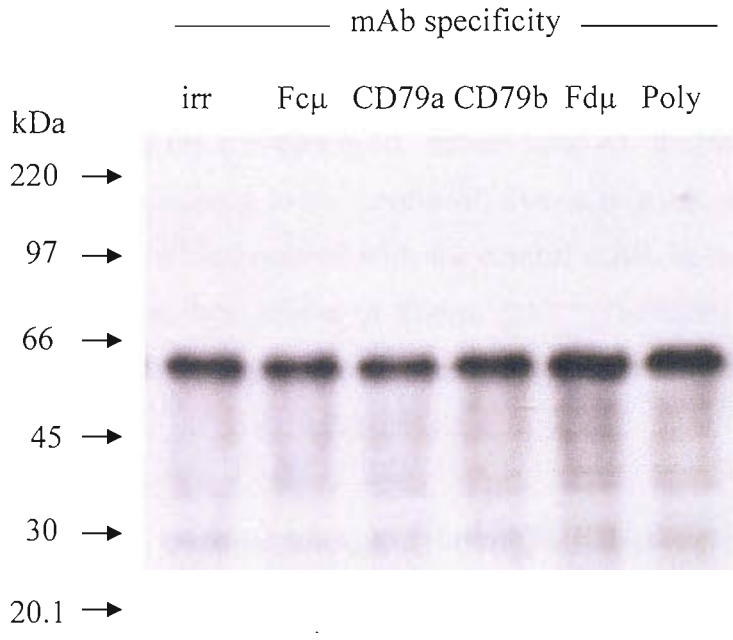

Figure 3.13 Akt activation in EHRB cells stimulated with anti-BCR mAb. $4x10^6$ EHRB cells were stimulated with various mAb (10 μg/ml) for five minutes at 37°C. Cells were then lysed and resolved on 12.5% SDS-PAGE gels, proteins were transferred to PVDF membrane and immunoblotted for levels of activated Akt. Cells were treated with the following mAb: irr (CP1/17); anti-Fcμ (M15/8); anti-CD79a (ZL7/4); anti-CD79b (AT105/1); anti-Fdμ (XG9); and Poly (polyclonal anti-μ) Ab. Representation of at least three separate experiments.

The results in Figure 3.14 show that cells treated with the different anti-BCR mAb showed little difference in levels of activation of Lyn. As with Akt, the resting levels of Lyn phosphorylation was high in EHRB cells treated with the control mAb.

3.2.9.3 Activation of Syk

The next PTK investigated for activation by anti-BCR mAb was Syk, another early PTK that is known to be essential for activation of downstream PTK. Proteins containing phosphorylated tyrosine residues were immunoprecipitated from EHRB cell lysates, as described above, and immunoblotted for Syk. Figure 3.15, shows that cells treated with the polyclonal anti-μ Ab induced the highest levels of Syk activation, followed by cells treated with the anti-CD79a and the anti-Fdμ mAb. Monoclonal Ab directed at the Fcμ and CD79b domains of the BCR induced lower levels of Syk activation, with minimal levels of activation observed in cells stimulated with the control mAb, in line with the total protein tyrosine phosphorylation data shown in Figure 3.12. Therefore, as differences in Syk phosphorylation were observed when cells were treated with different mAb, Syk activation could be important in the induction of apoptosis.

3.2.10 The kinetics of tyrosine phosphorylation in EHRB cells treated with various anti-BCR mAb.

Following the initial observation that all of the anti-BCR mAb tested induced protein tyrosine phosphorylation and activation of specific PTK, it was important to follow the kinetics of tyrosine phosphorylation. EHRB cells were incubated with the various anti-BCR mAb and then protein tyrosine phosphorylation assessed after 1, 5, 15 and 60 minutes incubation. Figure 3.16 again shows that all of the anti-BCR mAb gave robust phosphorylation responses, compared with cells treated with the irrelevant mAb or mAb directed at the surface protein CD19 (lanes 1 and 10 respectively). At each time point, the polyclonal anti-μ Ab (lane 6) induced the highest level of tyrosine phosphorylation, with maximum phosphorylation observed after 5 minutes stimulation. Monoclonal Ab directed at the Fdμ, λ light chain, and Id domains (lanes 3, 4and 5 respectively) induced a higher level of protein tyrosine phosphorylation following stimulation for 1 and 5 minutes compared with cells treated with the anti-Fcμ mAb (lane 2). However, the anti-Fcμ mAb appears to induce higher levels of protein tyrosine phosphorylation following 15 and 60 minutes of stimulation. Thus, anti-Fcμ has a slower rate of PTK phosphorylation, compared with the other anti-BCR mAb which do not induce apoptosis.

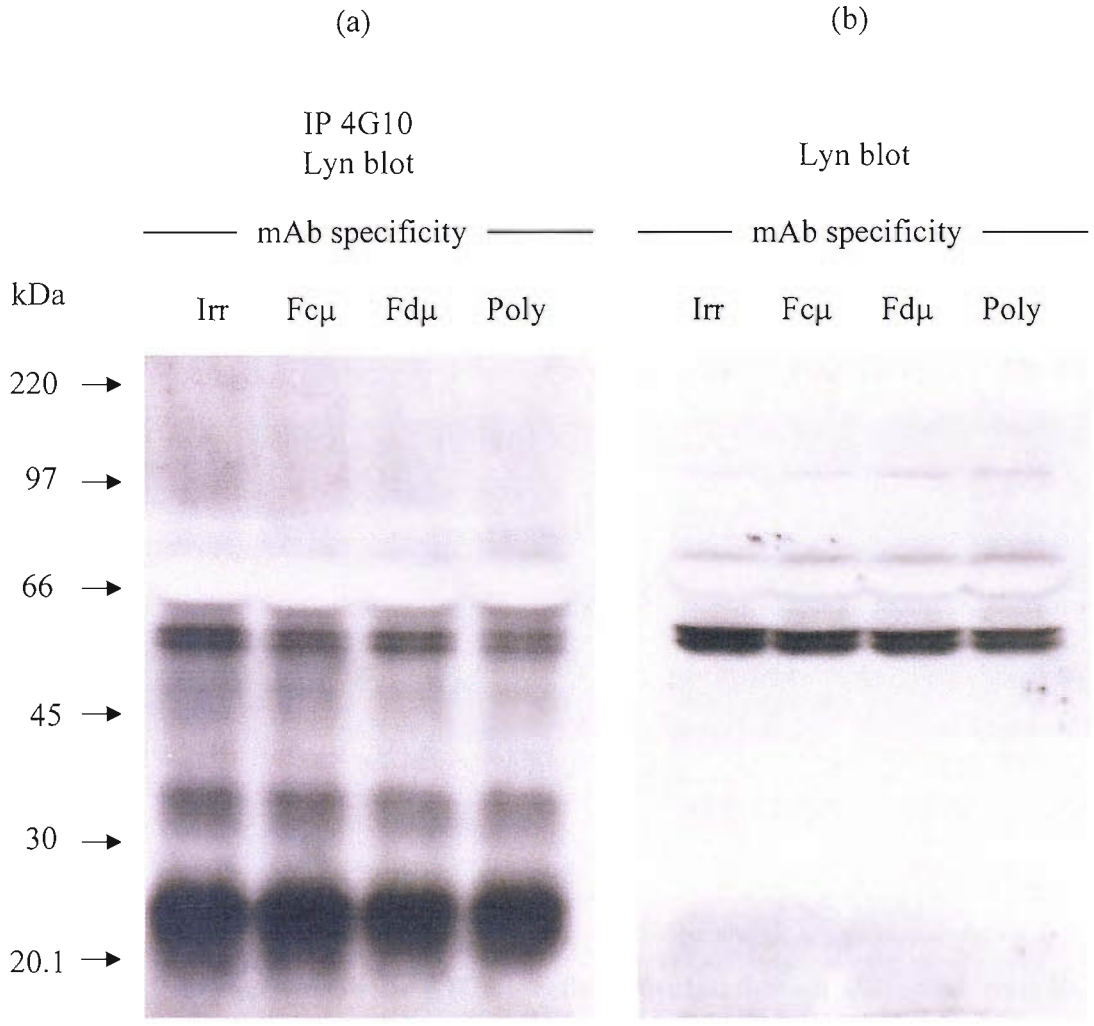

Figure 3.14 Lyn activation of EHRB cells stimulated with anti-BCR mAb. $4x10^6$ EHRB cells were stimulated with various mAb (10 μg/ml) for five minutes at 37°C. Cells were then lysed and proteins containing phosphorylated tyrosine residues were immunoprecipitated overnight at 4°C with 4G10 mAb (2 μg), bound by protein G coupled to sephrose beads for two hours at 4°C. Immunoprecipites were resolved on 12.5% SDS-PAGE gels, transferred to PVDF membrane and immunoblotted for activated Lyn (a). A small sample of cell lysates were used as controls for the total level of Lyn (b). Cells were treated with the following mAb: Irr (CP1/17); Fcμ (M15/8); Fdμ (XG9); and Poly (polyclonal anti-μ Ab). Representation of at least three separate experiments.

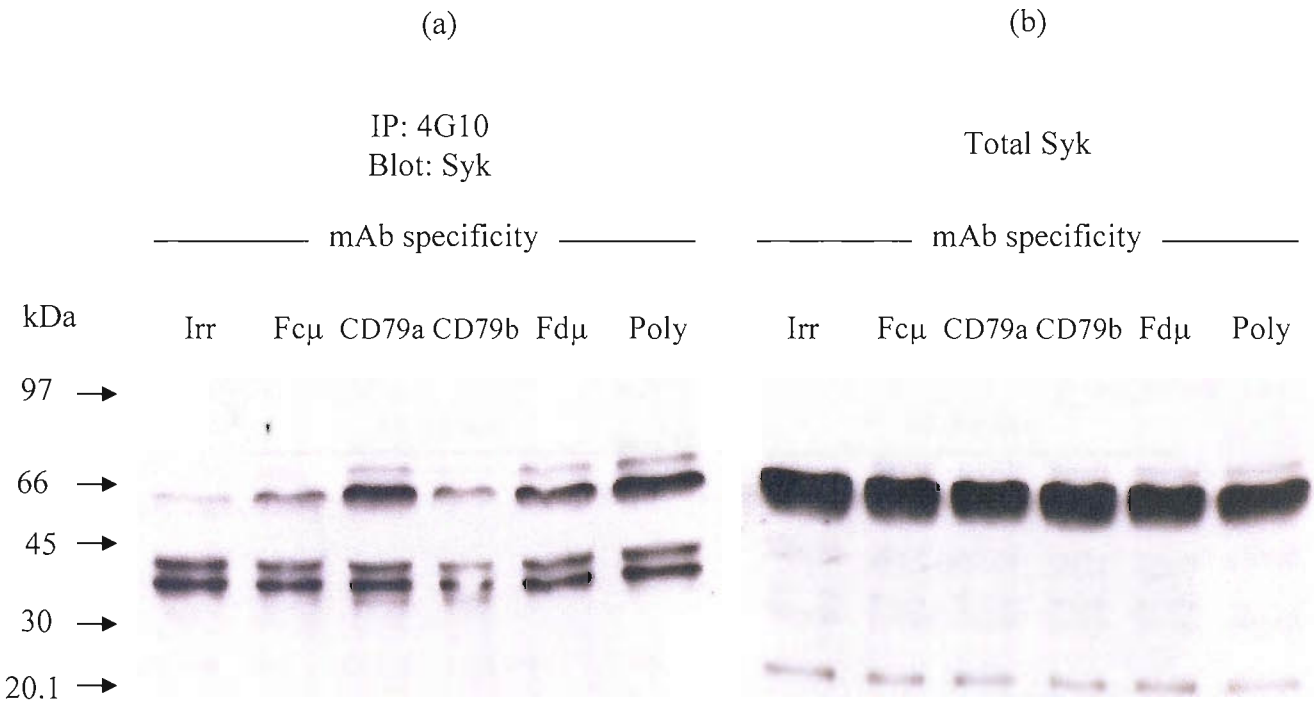

Figure 3.15 Syk activation in EHRB cells stimulated with different anti-BCR mAb. 4x10^6 EHRB cells were stimulated with various mAb (10 μg/ml) for five minutes at 37°C. Cells were then lysed and proteins containing phosphorylated tyrosine residues were immunoprecipitated by incubating overnight at 4°C with 4G10 mAb (2 μg) followed by protein G bound to sephrose beads for two hours at 4°C. Immunoprecipitates were resolved on 12.5% SDS-PAGE gels, transferred to PVDF membrane and immunoblotted for activated Syk (a). Samples of cell lysates were used as controls for the total level of Syk (b). Cells were treated with the following mAb: Irr (CP1/17); Fcμ (M15/8); CD79a (ZL7/4); CD79b (AT105/1); Fdμ (XG9); and Poly (polyclonal anti-μ Ab). Representative of at least three separate experiments.

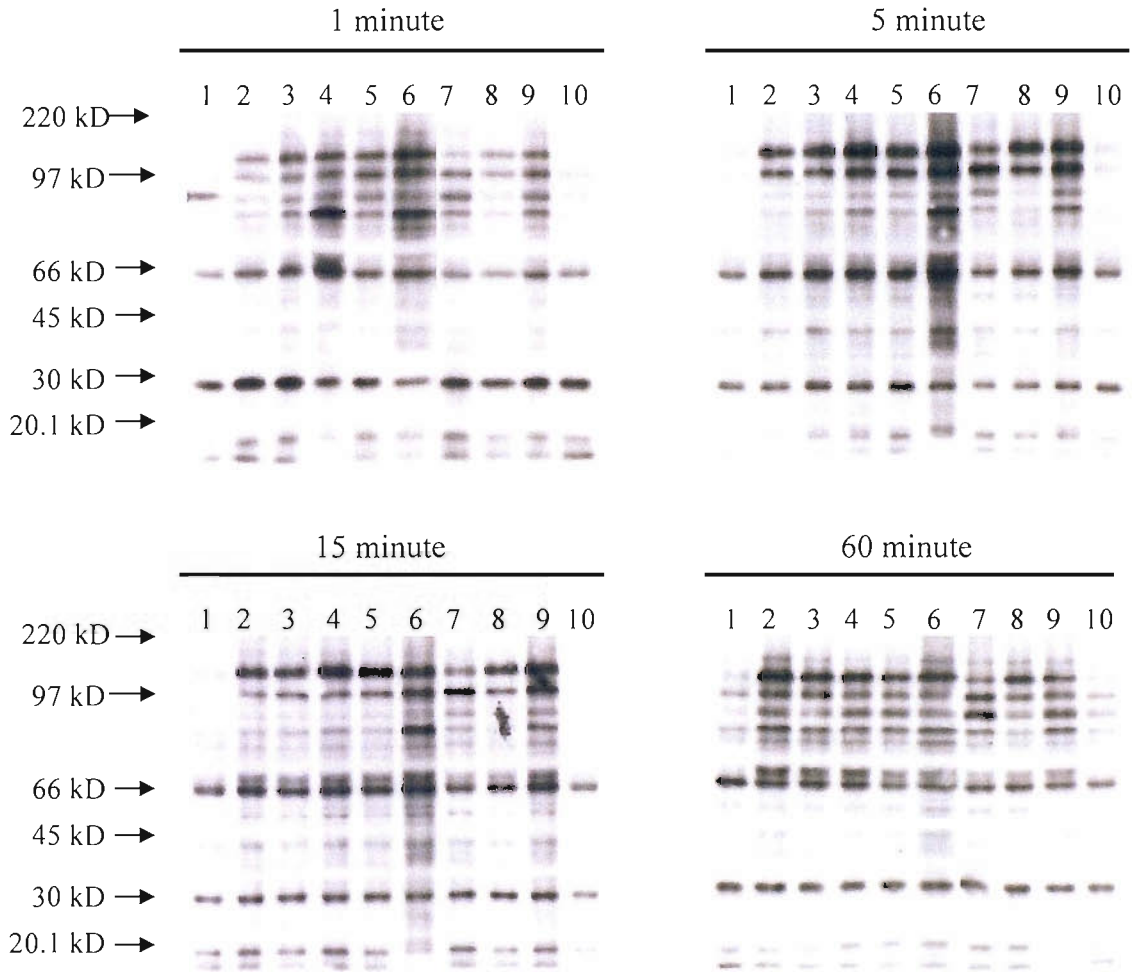

Figure 3.16 The kinetics of tyrosine phosphorylation in EHRB cells stimulated with anti-BCR mAb. EHRB cells were stimulated with the appropriate mAb (10 μg/ml) for the times shown at 37°C. Cells were then lysed and protein separated on 12.5% SDS-PAGE gels. Protein was transferred to PVDF membrane and probed for the presence of phosphorylated tyrosine residues using the mAb 4G10 (1 μg/ml) and HRP labelled secondary Ab. Cells were stimulated with the following: lane 1, irrelevant control (CP1/17); lane 2, anti-Fcμ (M15/8); lane 3, Fdμ (XG9); lane 4, anti-λ (Mc24IC6); lane 5, is anti-Id (ZL16/1); lane 6, polyclonal anti-μ Ab; lane 7, anti-CD79a (ZL7/4); lane 8, anti-CD79b (AT105/1); lane 9, anti-CD79a + b (ZL7/4 + AT105/1); and lane 10, anti-CD19 (RFB9). Representative of three independent experiments.

Monoclonal Ab directed towards the CD79 heterodimer also gave robust signalling, with anti-CD79a mAb inducing more tyrosine phosphorylation at all time points compared to cells treated with anti-CD79b (lanes 7 and 8 respectively). When cells were treated with a combination of the anti-CD79a and CD79b mAb (lane 9) the level of tyrosine phosphorylation exceeded that seen in cells stimulated with either mAb alone, or cells treated with mAb directed at the mIgM. Only the polyclonal anti-μ Ab gave more robust phosphorylation.

3.2.11 The kinetics of Lyn activation in EHRB cells treated with various anti-BCR mAb.

As the patterns of total protein tyrosine phosphorylation differed with time and Ab stimulation, it was decided to investigate the kinetics of early PTK activation. First, we investigated the kinetics of activation of Lyn. Cells were treated with mAb directed at the Fcμ (M15/8), Fdμ (XG9), CD79 heterodimer (ZL7/4 and AT105/1 in combination), polyclonal anti-μ Ab, and a control (CP1/17) mAb, for 3, 15, 60 and 120 minutes at 37°C, before immunoprecipitation of phosphorylated tyrosine residues from cell lysates and immunoblotting for Lyn (Figure 3.17a). Fortuitously, immunoprecipitated mouse light chain from the 4G10 mAb also immunoblotted alongside activated Lyn and was used as a loading control, as shown in Figure3.14. This was due to cross reactivity of the secondary Ab binding to the mAb which was raised in either the same or similar species. Figure 3.17b shows that all of the mAb tested gave a maximum level of Lyn activation at 15 minutes, which then decreased by 60 and 120 minutes. From the densitometry results shown in Figure 3.17b, for each mAb, the maximum density obtained was taken as 100% activation, and densities obtained at the other time points expressed as a percentage of this value and shown in Figure 3.17c. This plot indicates that there was no clear difference in kinetics between mAb recognising different domains of the BCR.

3.2.12 The kinetics of Syk activation in EHRB cells treated with anti-BCR mAb.

As levels of phosphorylated Syk appear to differ when EHRB cells are treated with different mAb for 5 minutes, we next followed the kinetics of Syk activation. Cells were treated with polyclonal anti-μ Ab and control mAb together with mAb directed at Fcμ (M15/8), Fdμ (XG9) and the CD79 heterodimer (ZL7/4 and AT105/1 in combination). After 3, 15, 60 and 120 minutes at 37°C, cells were lysed immunoprecipitated for phosphorylated tyrosine residues and immunoblotted for Syk (Figure 3.18a). Again mouse heavy chain from 4G10 mAb was used as a loading control, as shown in Figure 3.15.

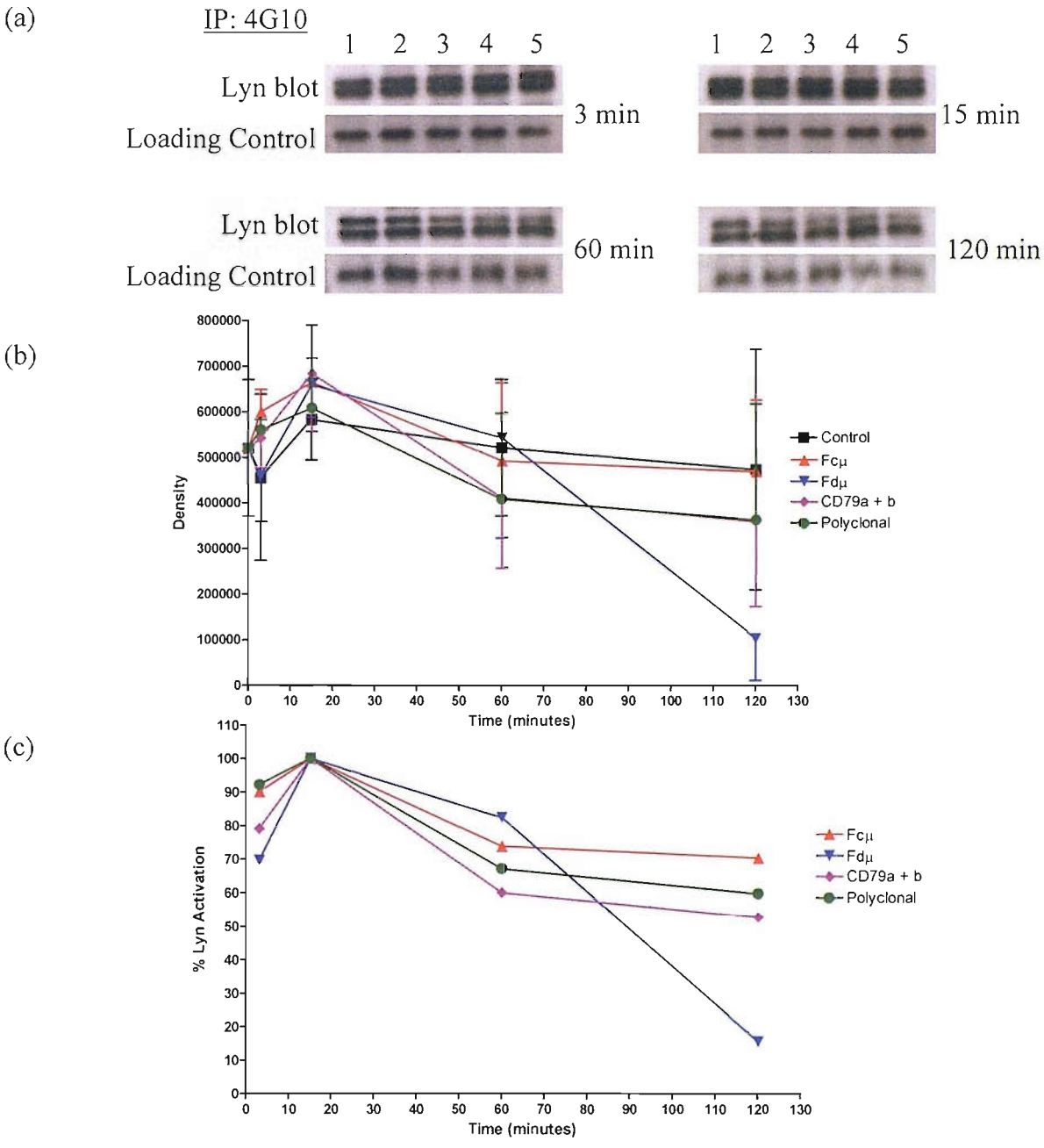

Figure 3.17 The kinetics of Lyn activation in EHRB cells stimulated with various mAb directed at BCR. EHRB cells were stimulated with the appropriate mAb (10 μg/ml) for the times shown at 37°C, before being lysed and phosphorylated PTK immunoprecipitated. Proteins were separated on 12.5% SDS-PAGE gels, proteins were transferred to PVDF membrane and probed for the presence of activated Lyn (a). Levels of Lyn activation were quantitated using densitometry (b). The results show mean values ± SD for three independent experiments. Levels of activated Lyn activation were normalised to the maximum levels of activation (c). Cells were stimulated with the following: lane 1, irrelevant control (CP1/17); lane 2, anti-Fcμ (M15/8); lane 3, Fdμ (XG9); lane 4, anti-CD79a + b (ZL7/4 + AT105/1); and lane 5, polyclonal anti-μ Ab.

(a)

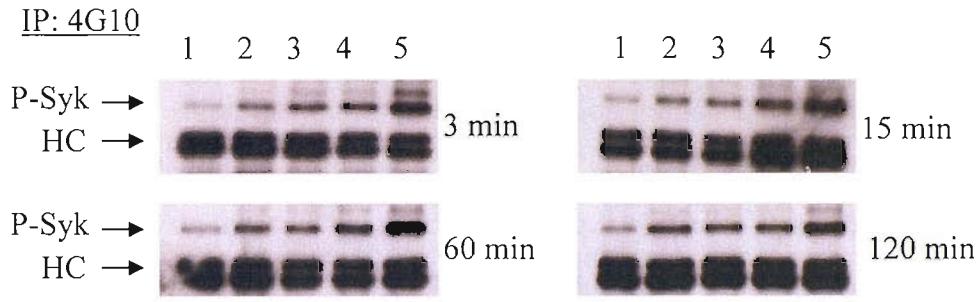

(b)

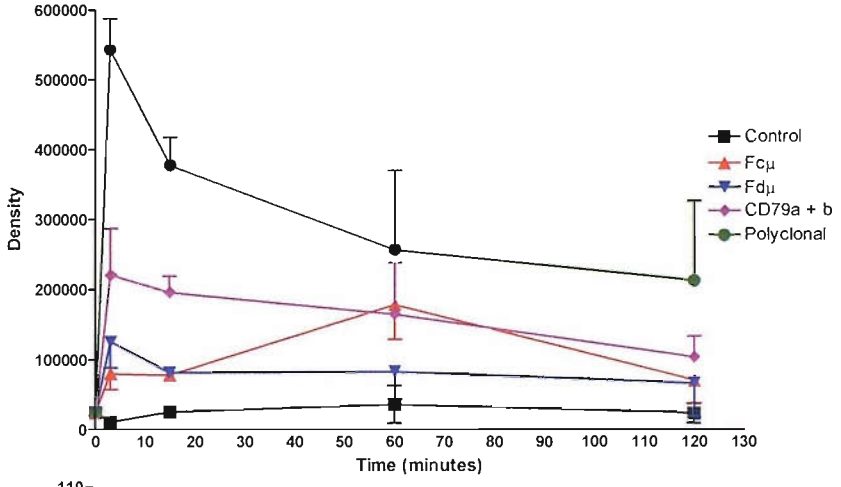

(c)

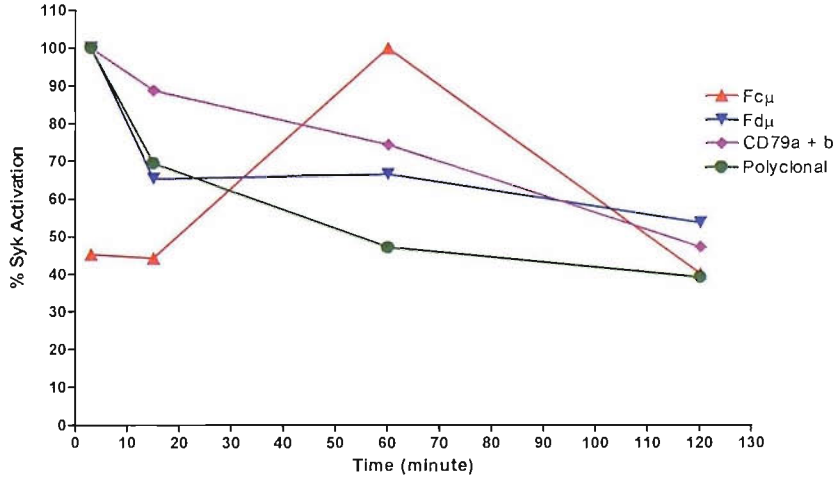

Figure 3.18 The kinetics of Syk activation in EHRB cells stimulated with various mAb directed at the BCR. EHRB cells were stimulated with the appropriate mAb (10 μg/ml) for the times shown at 37°C, before being lysed and phosphorylated PTK immunoprecipitated. Proteins separated on 12.5% SDS-PAGE gels, transferred to PVDF membranes and probed for the presence of activated Syk (a). Levels of Syk activation were quantitated using densitometry and (b) shows mean values ± SD for three independent experiments. Levels of Syk activation from (b) were normalised to maximum levels obtained when cells were treated with individual mAb (c). Cells were stimulated with the following: lane 1, irrelevant control (CP1/17); lane 2, anti-Fcμ (M15/8); lane 3, Fdμ (XG9); lane 4, anti-CD79a + b (ZL7/4 + AT105/1); and lane 12,polyclonal anti-μ Ab.

The levels of Syk activation shown in Figure 3.18a were quantified by densitometry and the results are shown in Figure 3.18b, again the maximum levels of activated Syk were calculated as detailed above (Figure 3.18c). Polyclonal anti-μ Ab induced the highest level of Syk activation, reaching a maximum level at 3 minutes and then declining. Monoclonal Ab directed at the Fdμ domain of mIgM heavy chain and the CD79 heterodimer induced a maximum level of Syk activation 3 minutes after stimulation, which then decreased over time. Although a combination of the anti-CD79 mAb induced more Syk activation compared to the anti-Fdμ mAb, these levels were lower then the level of Syk activated with the polyclonal anti-μ Ab (Figure 3.18b). Figure 3.18b and c show that the anti-Fcμ mAb activates low levels of Syk following stimulation for 3 and 15 minutes compared to cells stimulated with anti-Fdμ and anti-CD79 mAb. However, Syk activation reaches a maximum by 60 minutes. These results show that the anti-Fcμ mAb induced slower and more protracted levels of Syk activation compared to the other mAb. Anti-Fcμ mAb induced maximum levels of Syk activation after 60 minutes stimulation, compared to cells treated with the other anti-BCR Ab.

3.2.13 The induction of calcium flux in EHRB cells by anti-BCR mAb.

Following investigation of tyrosine phosphorylation in EHRB cells treated with different anti-BCR mAb, it was decided to investigate a later stage in the BCR signal transduction cascade. Following tyrosine phosphorylation and activation of proximal PTK, PLCγ2 becomes activated, hydrolysing PIP_2 to IP3. IP3 then binds to IP3 receptors in the cell, causing intracellular calcium to be released[66, 67]. Notably Syk is pivotal in activating PLCγ2 and regulating intracellular calcium signalling upon BCR cross-linking. Therefore, we wished to observe how calcium flux compared to Syk activation following BCR ligation with our panel of mAb. To assess calcium signalling, EHRB cells were pre-loaded with the calcium binding reporter dye INDO-1-AM as detailed in section 2.13. They were then stimulated with mAb directed at different regions of the BCR and levels of intracellular calcium flux assessed over time by flow cytometry.

The levels of calcium flux induced with anti-BCR mAb showed that the polyclonal anti-μ, and the and anti-λ mAb induced higher initial peaks of calcium flux. This was followed by the anti-Fdμ mAb, which stimulated an initial calcium flux that was comparable to that observed when cells were treated with either anti-CD79a or anti-CD79b mAb. Interestingly, the initial calcium flux observed when cells were treated with the anti-Fcμ were lower (Figure 3.19). However, similar to the observation with Syk activation it is

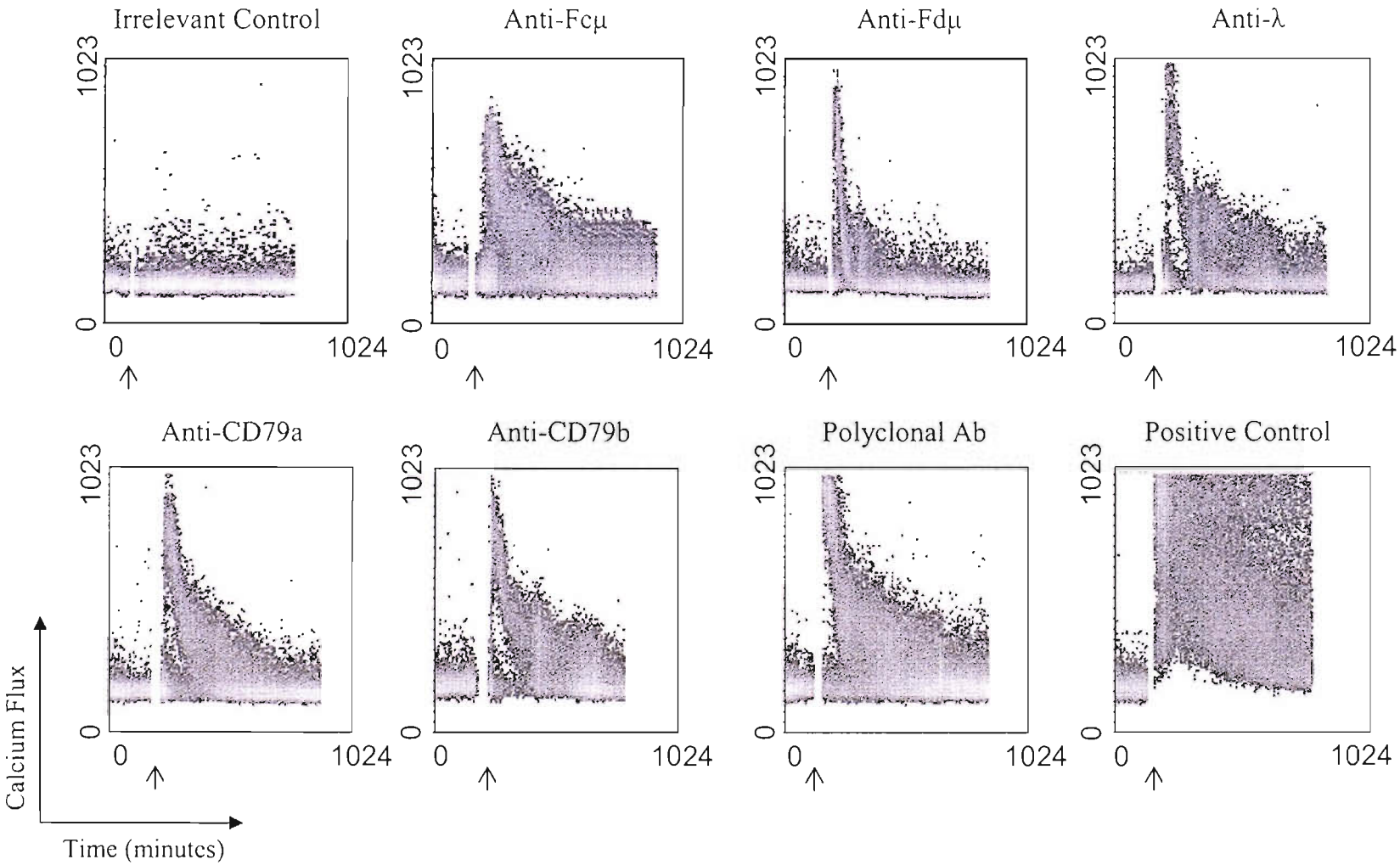

Figure 3.19 Calcium flux of EHRB cells stimulated with mAb directed at BCR. 1x10^7 cells EHRB cells were washed twice in serum free RPMI and loaded with 20μM INDO-1-AM. Cells were then incubated at 37°C for 30 minutes before being washed twice in serum free RPMI and re-suspended in 5ml RPMI (containing 10% FCS). Cells were rested for 30 minutes in the dark at room temperature. For analysis of calcium flux generation, the cells were assessed using a FACS Vantage. After establishing the basal level of calcium, cells were stimulated with various mAb (10μg/ml) at point shown (→), and level of calcium flux assessed over time (minutes). Cells were treated with; Irrelevant control (CP1/17), anti-Fcμ (M15/8), anti-Fdμ (XG9). Anti-λ (Mc24IC6), andti-CD79a (ZL7/4), anti-CD79b (AT105/1) and a positive control ionomycin.

apparent that anti-Fcμ mAb induces a prolonged level of calcium flux compared to other mAb raised against the BCR. These prolonged, elevated levels of calcium flux were similar to those observed when cells were treated with the polyclonal anti-μ Ab, which also leads to cellular apoptosis.

3.2.14 Correlation between the induction of apoptosis *in vitro* and the induction of therapy *in vivo*

Finally, after establishing that different mAb induce different levels of cellular apoptosis *in* vitro, it was of interest to investigate if these mAb could provide therapy from tumour *in vivo*, and to ask if there was any correlation between *in vitro* and *in vivo* activity. Therefore, we established a xenograft model of *in vivo* tumour therapy with the Ramos tumour cells in SCID mice. After establishing a robust and reproducible model system we performed immunotherapy experiments with the different mAb. Groups of age and gender matched SCID mice were treated with $2.5x10^6$ tumour cells on day 0. At day seven post-tumour, separate cohorts of mice were treated with the various mAb. Animals treated with the control mAb were culled between days 30 and 35 following symptoms of rear leg paralysis following tumour cell infiltration. Tumour-bearing animals treated with the anti-Fcμ mAb were protected for greater than 100 days. However, the other mAb failed to provide any long term protection and all mice succumbed to tumour within a 70 day period (Figure 3.20). This data shows that the therapeutic potency *in vivo* correlates with the *in vitro* data, such that the anti-Fcμ mAb which induced significant levels of growth arrest and cellular apoptosis produced therapy in vivo.

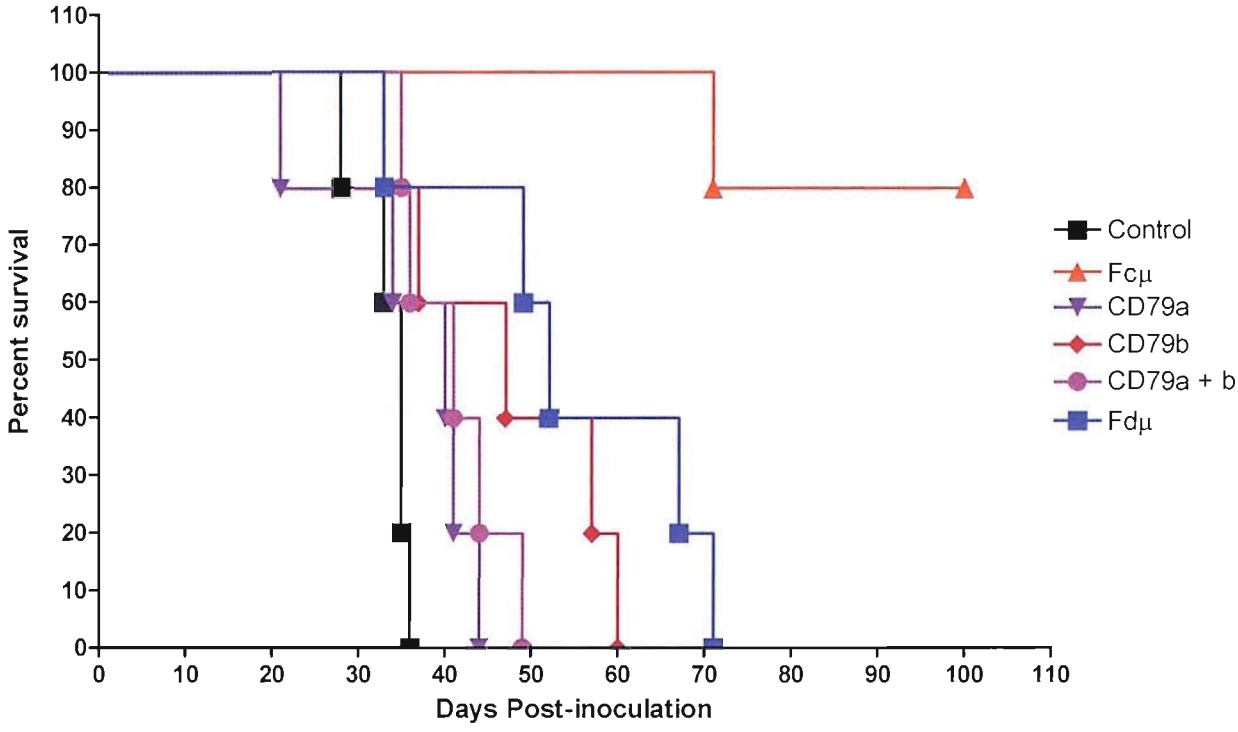

Figure 3.20 The effect of mAb treatment on human B cell xenografts *in vivo*. SCID xenografts were established with $2.5x10^6$ tumour cells (EHRB) i.v. on day 0. At day 7 groups of five mice were treated with various mAb (100 μg) i.v. and survival recorded for each group. mAb used were: control (PBS), Fcμ (M15/8), CD79a (ZL7/4), CD79b (AT105/1), CD79a + b (ZL7/4 + AT105/1), and Fdμ (XG9). Representative of at least two independent experiments.

3.3 Discussion

To investigate mAb for therapy against B cell lymphomas we utilised EHRB cells, a sub-line of the well characterised B cell line, Ramos. Ramos-EHRB cells are thought to reflect a GC like B cell line and have previously been shown by us and others to be sensitive to BCR induced apoptosis[158, 165, 166]. Importantly, it should be noted that most other studies utilise polyclonal reagents to induce cell death. Work carried out previously in our laboratory, showed that cell lines stimulated with various mAb directed at different domains of the BCR have varying ability to induce growth inhibition[158]. Subsequent work, detailed in this chapter has shown that at least a proportion of this inhibition is due to the induction of apoptosis as confirmed by annexin V/PI and DioC6 staining. Although some groups have questioned the use of annexin V for the measurement of apoptosis of mouse B cells *in vivo*[167, 168], we believe it provides an accurate measure for the induction of early stages of apoptosis. Later stages of cell death were also observed, such as PI positivity indicative of loss of plasma membrane integrity and DNA fragmentation, indicative of nuclear disintegration.

Our results showed that mAb directed at the Fcμ domain of mIgM (Cμ2-Cμ4) leads to induction of apoptosis while mAb directed at the Fdμ (Cμ1) or λ light chain (Cλ1), have little effect.

One possible difference between the different mAb is their binding affinity, this could potentially be of importance for the induction of apoptosis. Some reports suggest that high affinity anti-Fdμ and anti-Fcμ mAb are less efficient at inducing *in vitro* B cell death compared to anti-Fcμ mAb with moderate binding affinities[165, 169]. However, the anti-Fcμ mAb used in this study have similar binding affinities compared to the anti-Fdμ mAb and therefore, in this case affinity alone cannot explain the differences in apoptosis induction with these reagents[158, 159].

Another interesting therapeutic target for mAb on B cells is the CD79 heterodimer, which is expressed on all B cell types apart from plasma cells [94, 163]. As discussed in previous sections, the BCR is thought to be comprised of one mIg molecule non-covalently associated with one CD79 heterodimer [128]. Therefore, it might be expected that mAb directed at the extracellular domains of CD79a or CD79b should be able to cross-link BCRs

and cause equivalent levels of apoptosis. This appears not to be the case as observed in Figure 3.8, and previously reported data [159].

Monoclonal Ab raised against the BCR were also tested on other Ramos like B cell lines including Daudi and BL-60, alongside EHRB. Data showed that the EHRB cell line was only sensitive to BCR induced apoptosis when treated with anti-Fcμ mAb and polyclonal Ab. The Daudi cell line was sensitive to anti-Fcμ mAb and polyclonal Ab. However, it was also sensitive to mAb raised against the Id domain. Overall, the level of BCR induced apoptosis observed in Daudi cells was reduced compared to that seen in the EHRB cell line. The BL-60 cell line showed similar characteristics compared to the EHRB cell line, in that anti-Fcμ and polyclonal Ab induced the highest levels of apoptosis compared to control mAb.

To investigate why the different cell lines show different levels of susceptibility to anti-Fcμ mAb, the phenotype of other surface proteins important in activation of PTK was analysed. One explanation for the reduced sensitivity of Daudi cells to BCR induced apoptosis when treated with anti-Fcμ mAb may be due to the increased expression of CD22 at the cell surface. CD22 contains an active cytoplasmic ITIM motif that recruits PTP upon phosphorylation of the ITIM motif by activated Src family kinases[170]. Increased expression of CD22 could directly lead to a reduction in levels of signalling from the BCR and therefore, less apoptosis.

It is known that cross-linking mIgM induces intracellular signals shown by phosphorylation of tyrosine residues on important cellular substrates including PTKs[164]. Previous results from clinical studies showed a correlation between the protein tyrosine phosphorylation responses of *ex- vivo* stimulated NHL cells (stimulated with the patient specific anti-Id) and subsequent response of the patient[160]. In this study we have shown that all mAb directed at the mIgM and CD79 heterodimer domains of the BCR induce robust levels of tyrosine phosphorylation, as previously reported[159, 160]. However, not all of these mAb induce robust apoptosis, implying that the early induction of protein tyrosine phosphorylation is not in itself sufficient for apoptosis. Indeed, kinetic studies indicate that at early time points, mAb directed at Fdμ, λ light chain and Id domains of mIgM induce higher levels of protein tyrosine phosphorylation than does anti-Fcμ mAb. However, with the anti-Fcμ mAb, the level of protein tyrosine phosphorylation peaks at a later time point, and appears to remain elevated for longer periods of time.

These early tyrosine phosphorylation events were confirmed when looking at the activation of intracellular calcium flux. Monoclonal Ab directed at Fdμ, λ and Id domains induce a higher level of calcium flux compared to cells stimulated with anti-Fcμ mAb. However, activation of Syk as indicated by its increased phosphorylation status confirms the observation made with the global tyrosine phosphorylation immunoblots, that anti-Fcμ mAb induces moderate Syk activation, which peaks at one hour post stimulation, compared to other mAb that peaked at three minutes. These sustained levels of signalling may contribute to the final outcome of apoptosis.

As previously discussed Syk is a key signalling molecule required for the activation of downstream PTK, release of intracellular Ca^{2+} and subsequent activation of downstream nuclear transcription factors[101, 171]. Activation of specific nuclear transcription factors determines cell fate[172]. It is known that BCR induced cell death requires activation of PLCγ2 and release of intracellular Ca^{2+}, leading to the activation of JNK-1 [43]. In immature murine B cell lines, it has been shown that prolonged intracellular signalling induced by cross-linking the BCR, as shown by increased tyrosine phosphorylation is associated with the induction of apoptosis, [173]. This apoptosis also correlates with a reduction in the time of activation of ERK2, which is thought to be important for cell survival. As such, cells rescued from BCR induced apoptosis by the addition of CD40 ligand show reduced kinetics of protein tyrosine phosphorylation and prolonged activation of ERK2[174].

Activation of the Src family kinase Lyn, is thought to be important for activation of intracellular signalling cascades of B cells upon BCR cross-linking[175]. According to the theory proposed by Pierce, *et al.*,[114] cross-linked BCR translocate into cholesterol rich lipid domains of the plasma membrane (lipid rafts), that also appear to be rich in the Src family kinase Lyn. However, from our data, Lyn appears to be already activated in resting EHRB cells and only slightly enhanced following mAb stimulation. As little difference is seen between any of the mAb used and levels of Lyn activation, this suggests that Lyn is not essential for the activation of intracellular signalling cascades that are important for apoptosis. Potentially, Src kinases such as Lyn may be more important in modulating B cell responses to BCR cross-linking during B cell maturation[175].

These results follow other research that has shown that Lyn is not important for initial activation of intracellular signalling cascades following cross-linking BCRs, but is more important for tuning the B cell response to antigen [126, 127]. As such, B cells deficient in Syk

fail to release intracellular Ca^{2+} upon BCR cross-linking and more importantly fail to mature past the pro B cell stage of development[44]. On the other hand, Lyn deficient B cells are capable of maturing to naïve mature B cells[176] illustrating that Lyn is not essential in the signalling necessary to provide full development Furthermore, Lyn deficient B cells are hyper sensitive to BCR cross-linking by Ag or Ab, leading to increased populations of auto reactive B cells[177]. Research using GFP-tagged Syk and Lyn transfected into DT-40 cell lines deficient for Syk and Lyn has shown that upon BCR cross-linking Syk is required for capping of cross-linked BCR, where Lyn is required for mIgM internalisation[127].

Finally, it was interesting to observe that *in vitro* apoptosis data corresponds with *in vivo* therapy. SCID xenograft models using EHRB tumour cells show that only anti-Fcμ mAb can protect against tumour. Other mAb directed against the BCR cannot protect from *in vivo* tumour, suggesting an importance in anti-Fcμ mAb at providing therapy by inducing cellular apoptosis to tumour.

In conclusion, it can be seen that mAb directed at the BCR of the EHRB cell line that can induce high levels of apoptosis *in vitro*, also protect against *in vivo* tumour models. Interestingly, although all mAb directed at the BCR induce substantial protein tyrosine phosphorylation, this does not correlate with either in vitro apoptosis or therapeutic efficacy in vivo. In fact, mAb that do not induce apoptosis induce a higher level of signal than anti-Fcμ at early time points. However, both mAb that induce apoptosis (anti-Fcμ mAb and polyclonal anti-μ Ab) are able to sustain protein tyrosine phosphorylation for longer periods of time. For example, Syk activation was elevated for up to one hour after pro-apoptotic BCR stimuli.

Chapter 4

BCR modulation and aggregation on human B cell lines treated with monoclonal Ab.

4.1 Introduction

The proximal event in BCR signalling is the cross-linking of the BCR with Ag or Ab. Two recent theories have proposed how intracellular signalling pathways are activated upon cross-linking of the BCR. The first theory suggests that the BCR exists as an oligomeric complex at the cell surface[30, 42]. Research indicates that these oligomeric complexes are constantly being activated, and rapidly deactivated by Syk, and SHP, respectively[39]. Upon Ag or Ab binding to the BCR, it has been proposed that the oligomeric structure is distorted, preventing SHP from de-phosphorylating Syk, allowing initiation of the intracellular signalling cascade[42, 128]. This indicates that it is Syk which is vital for activation of intracellular signalling cascades, by activating and then binding to the ITAM motifs located within the cytoplasmic domain of the CD79 heterodimer[39].

The second theory regarding the activation of intracellular signalling cascades has focused on the translocation of cross-linked BCR into lipid rafts[118]. Pierce, *et al.*,[114, 116, 178] have shown that BCR translocate from the lipid soluble to the lipid insoluble region of the plasma membrane following ligation. Furthermore, it has been shown that Lyn is constitutively present in lipid rafts and, therefore, potentially the key PTK for activation of BCR intracellular signalling [118]. As well as the possibility of lipid rafts functioning as platforms for the activation of intracellular signalling pathways, research has also suggested that involvement of the BCR with lipid rafts is important during B cell development[118, 119, 122], and for internalisation of cross-linked BCR[123].

In the previous chapter, it was clearly demonstrated that mAb which bind to different regions of the BCR induce greatly differing levels of apoptosis. Therefore, it was of interest to investigate the binding properties of the anti-BCR mAb in an attempt to better understand why only certain mAb can induce apoptosis. Interestingly, Elliott, *et al.*,[179] have suggested that anti-BCR mAb that give therapy bind bigamously between separate BCR, whereas anti-BCR that do not give therapy bind monogamously to a single BCR complex. However, this property was not demonstrated to be linked to the induction of apoptosis and has never formally been proven.

As differences in signalling appear to be linked to the induction of apoptosis, it was also of interest to determine the nature of the BCR complex bound by the panel of anti-BCR mAb. Research has shown that the BCR from anergic B cells is disrupted, with the CD79 heterodimer not associated with mIgM[180, 181]. Therefore, it is possible that certain anti-BCR cause a disruption to the BCR structure, preventing complete activation of the intracellular signalling cascade, leading to the induction of apoptosis. For these reasons, in this chapter the nature of the BCR complex was assessed before and after binding with our panel of anti-BCR mAb. In addition, the hypothesis that the varying levels of apoptosis induced by the different mAb might be explained by variable redistribution of the BCR components into lipid rafts was explored.

4.2 Results

4.2.1 Comparison of the binding of various anti-BCR mAb to EHRB cells.

From the previous chapter, it was clear that the anti-Fcμ mAb may induce apoptosis by prolonging intracellular signals. Therefore, it was of interest to investigate whether the extended signalling was related to the binding properties of the different anti-BCR mAb. Therefore, in preliminary experiments EHRB cells were incubated with mAb directed at the Fcμ (M15/8), Fdμ (XG9), λ light chain (Mc24IC6), and Id (ZL16/1) domains of mIgM, and with mAb directed at the CD79a (ZL7/4) and CD79b (AT105/1) domains of the CD79 heterodimer. Levels of bound mAb were assessed using FITC labelled goat anti-mouse $F(ab')_2$.

Figure 4.1 shows that EHRB cells bind twice as much mAb directed at the Fdμ, λ light chain and Id domain of mIgM compared with the anti-Fcμ mAb. The binding mAb directed at the CD79 heterodimer was lower, about half the level of that with anti-Fcμ mAb. This data was consistent with a model where the anti-Fcμ mAb binds bigamously between BCR, as less mAb binds compared to the anti-Fdμ mAb which could bind monogamously to a single BCR, as shown in Figure 4.2.

4.2.2 The effect of anti-BCR mAb on modulation of the BCR on EHRB cells.

Clearly, mAb binding levels could not explain the prolonged signalling with the anti-Fcμ mAb shown in the previous chapter. An alternative reason for the prolonged signalling could be that the BCR bound by the anti-Fcμ mAb could remain at the cell surface for longer, allowing a prolonged intracellular signal to be delivered. To test this theory the panel of anti-BCR mAb were bound to EHRB cells, cells were washed and then analysed for levels of bound mAb using a goat anti-mouse $F(ab')_2$ over a period of 60 minutes. Figure 4.3 shows that although the anti-Fdμ and anti-λ mAb initially bound at higher levels than the anti-Fcμ mAb, the bound levels appeared to fall at an increased rate over time (Figure 4.3a). When levels of the bound mAb were expressed as a percentage of the initial amount bound (Figure 4.3b), the level of bound anti-Fdμ mAb fell at a slower rate compared to the fall of bound levels of the anti-Fcμ and the anti-λ mAb. Suggesting little difference in the rate of BCR modulation upon binding of anti-BCR mAb directed at the mIgM region. This modulation of the mIgM on the cell surface could be caused by internalisation of mIgM. However, this could not be proved, so the term modulation is used from here on.

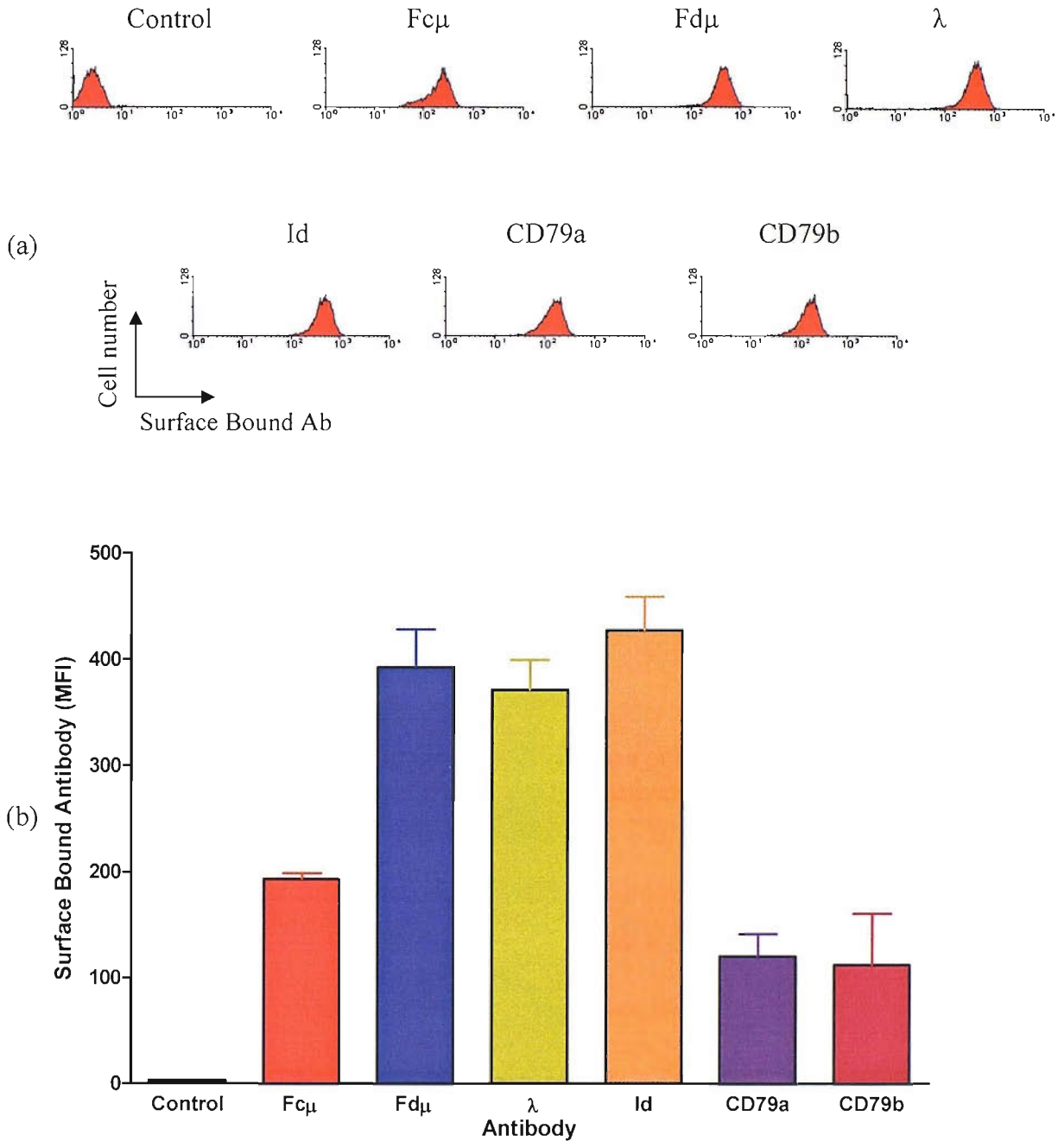

Figure 4.1 Levels of surface bound mAb on EHRB cell line. 1x10^5 EHRB cells were treated with the relevant anti-BCR mAb (10 μg/ml) for 30 minutes at room temperature. Samples were then washed twice and levels of mAb bound to surface of EHRB determined by flow cytometry using FITC labelled goat anti mouse F(ab')$_2$. FACS plots from one experiment show levels of bound Ab (a). Mean values ± SD from three independent experiments are shown (b). Control Ab: CP1/17, Fcμ: M15/8, Fdμ: XG9, λ: Mc24IC6, Id: ZL16/1, CD79a: ZL7/4, and CD79b: AT105/1.

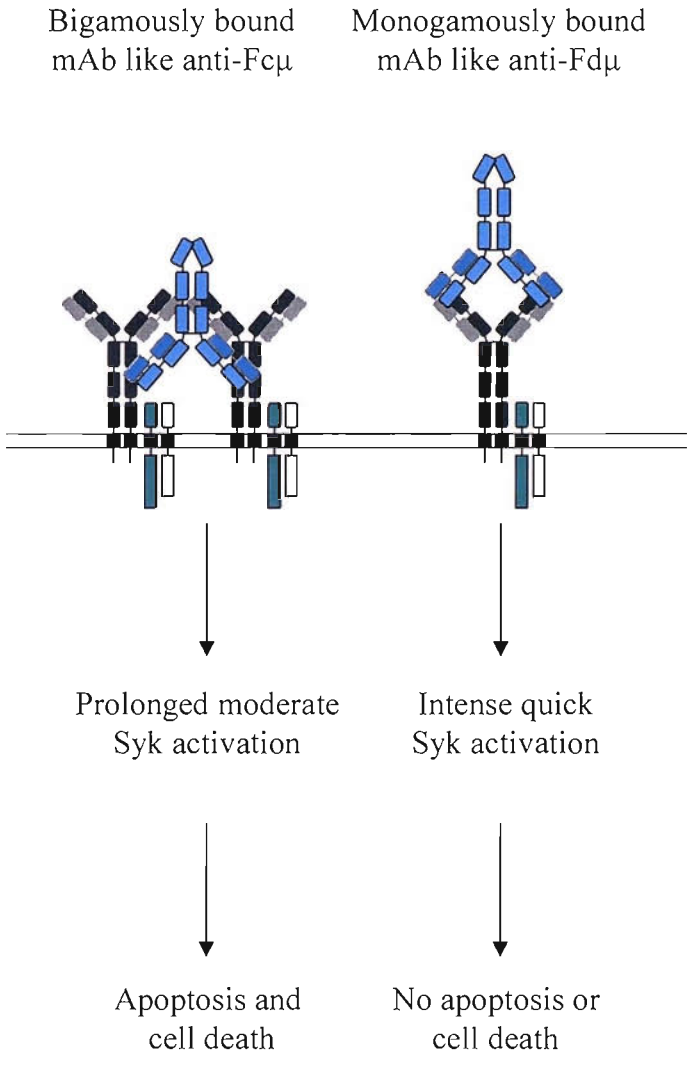

Figure 4.2 How different mAb may bind on the cell surface and how they may mediate different effects. Schematic representation of how mAb might bind to the BCR. Bigamously bound mAb (i.e. anti-Fcμ) bind between two BCRs, activate moderate but prolonged intracellular signals that lead to cellular apoptosis. Monogamously bound mAb (i.e anti-Fdμ, anti-λ and anti-Id) bind to one BCR, induce rapid intense intracellular signals that do not lead to cellular apoptosis.

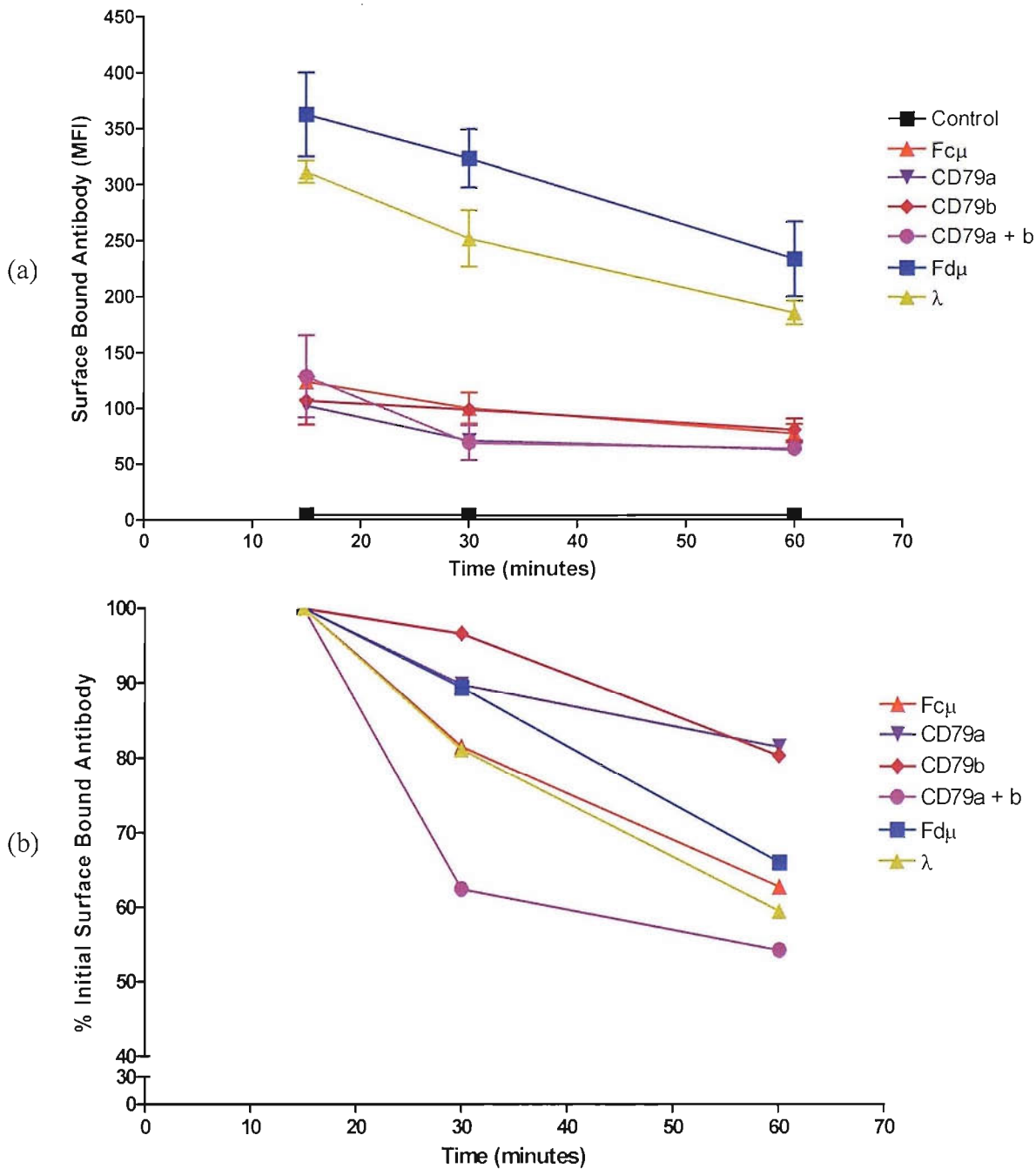

Figure 4.3 Kinetics of mAb internalisation by EHRB cells after binding by anti-BCR mAb. EHRB cells ($2x10^{5}$) were treated with the relevant mAb (10 μg/ml) for times indicated at 37°C. Cells were then removed, washed twice and assessed for levels of mAb bound to surface of EHRB cells analysed by flow cytometry using FITC labelled goat anti mouse $F(ab')_2$. (a) shows levels of surface bound mAb from FACS data, mean values ± SD from three independent experiments. (b) Mean values from (a) were normalised to 100% for mAb bound maximums. Control mAb: CP1/17, Fcμ: M15/8, CD79a: ZL7/4, CD79b: AT105/1, CD79a + b: ZL7/4 + AT105/1 (final concentration 10 μg/ml), Fdμ: XG9, and λ: Mc24IC6.

As a second method of observing BCR internalisation, EHRB cells were treated with the anti-BCR mAb, and the remaining mIgM quantified using FITC-labelled anti-Id (ZL16/11) mAb. This technique actually measures the level of BCR remaining at the cell surface, and is possible as anti-Id mAb is not blocked from binding by the other mAb specificities (data not shown; Dr M. Cragg, personal communication). Figure 4.4 shows that cells treated with the polyclonal anti-μ Ab induce rapid mIgM modulation, with only 40% of the original mIgM remaining on the cell surface 15 minutes after stimulation. Monoclonal Ab directed at various domains of mIgM (Fcμ, Fdμ, and λ) induce comparable rates of modulation over a 1 hour period. Monoclonal Ab directed at the CD79 heterodimer induced low rates of mIgM internalisation, with 85% of mIgM remaining at the cell surface when cells were treated with anti-CD79b mAb following stimulation for 60 minutes. Treatment of EHRB cells with the anti-CD79a and b mAb in combination induced more rapid mIgM internalisation, comparable to mAb directed at the mIgM domain.

The rate of BCR modulation over a 24 hour period was also assessed using the same techniques as described above. EHRB cells were also incubated with the same mAb over a 24 hour period. After 1 hour of incubation, it appears that the proportion of mIgM modulated when treated with the anti-Fcμ mAb is greater then that observed when cells were treated with the anti-Fdμ mAb. However, the proportion of mIgM modulated between 4 and 24 hours incubation with the mAb was similar, with between 20 and 30% of mIgM remaining at the cell surface (Figure 4.5). The surface level of each mAb remained on the cell surface over the 24 hour period, except cells treated with a combination of the mAb directed at CD79 heterodimer, where an increased loss in bound mAb was observed following incubation for 4 hours.

As well as investigating the rate of mIgM modulation from the cell surface, we also investigated the rate of CD79 modulation following binding of the anti-BCR mAb (Figure 4.6). EHRB cells treated with the polyclonal anti-μ Ab induced rapid modulation of both CD79a and CD79b as observed with modulation of mIgM. Similar results were observed with the anti-Fdμ and the anti-λ mAb, albeit with slightly slower kinetics. Interestingly, cells treated with mAb directed at the Fcμ induced slower modulaiton of CD79a and CD79b compared to cells treated with other mAb. In combination, these data suggests that the anti-Fcμ mAb leads to a more rapid modulation of IgM compared to CD79, implying that CD79 remains at the cell surface without IgM.

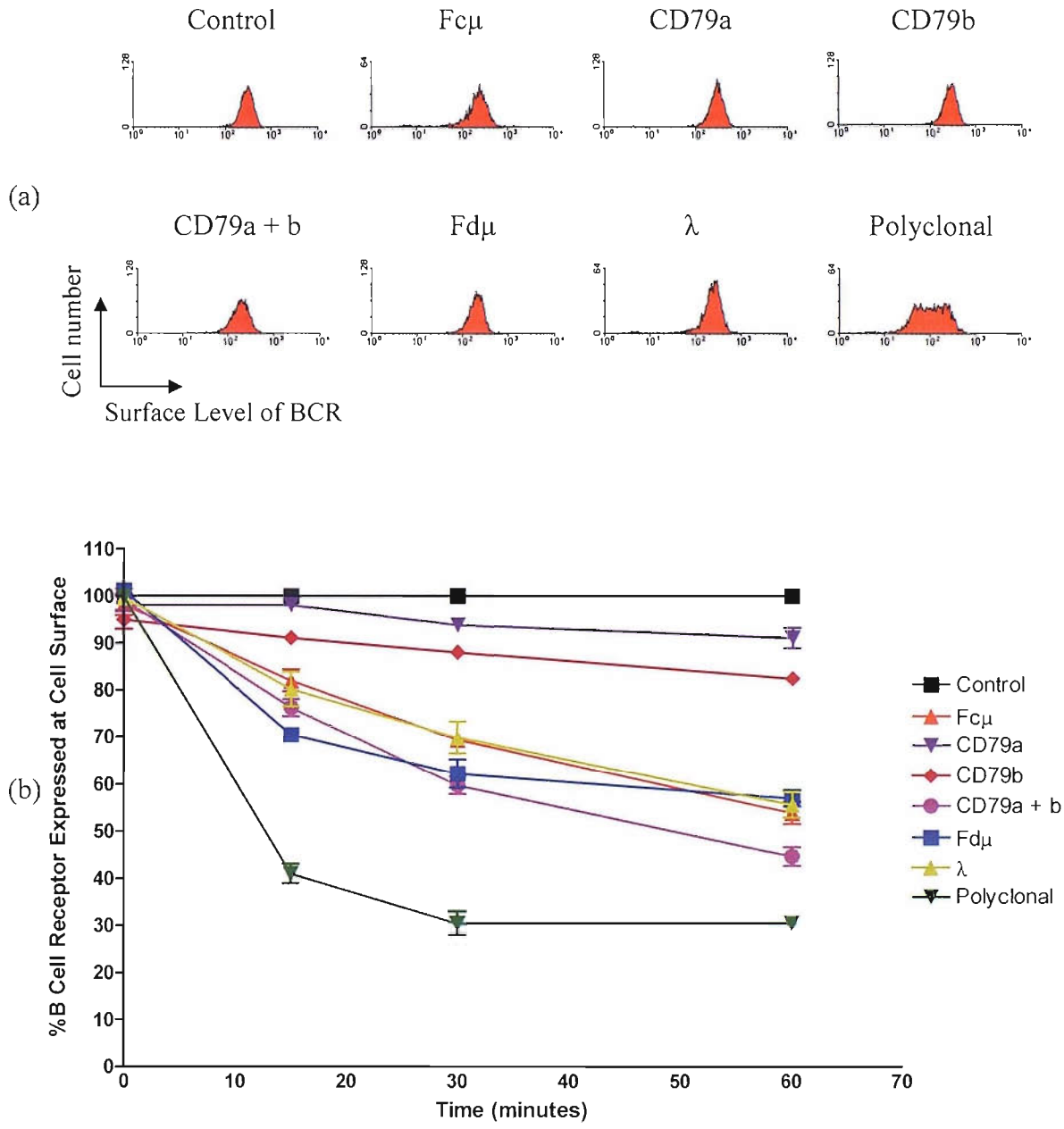

Figure 4.4 Kinetics of BCR modulation on EHRB cells following binding of anti-BCR mAb. EHRB cells ($2x10^5$) were treated with the relevant Ab (10 μg/ml) for the times indicated at 37°C. Cells were removed, washed twice in PBA and assessed for levels of BCR present at the cell surface by flow cytometry using FITC labelled anti-Id (ZL16/1). (a) Surface expression of the BCR at the cell surface following exposure to anti-BCR Ab for 60 minutes. (b) Levels of surface BCR expressed. Levels of surface BCR expressed as a percentage of control at each time point, mean values ± SD from three independent experiments. Control Ab: CP1/17, Fcμ: M15/8, CD79a: ZL7/4, CD79b: AT105/1, CD79a + b: ZL7/4 + AT105/1 (final concentration 10 μg/ml), Fdμ: XG9, λ: Mc24IC6, and Polyclonal is commercial anti-μ Ab.

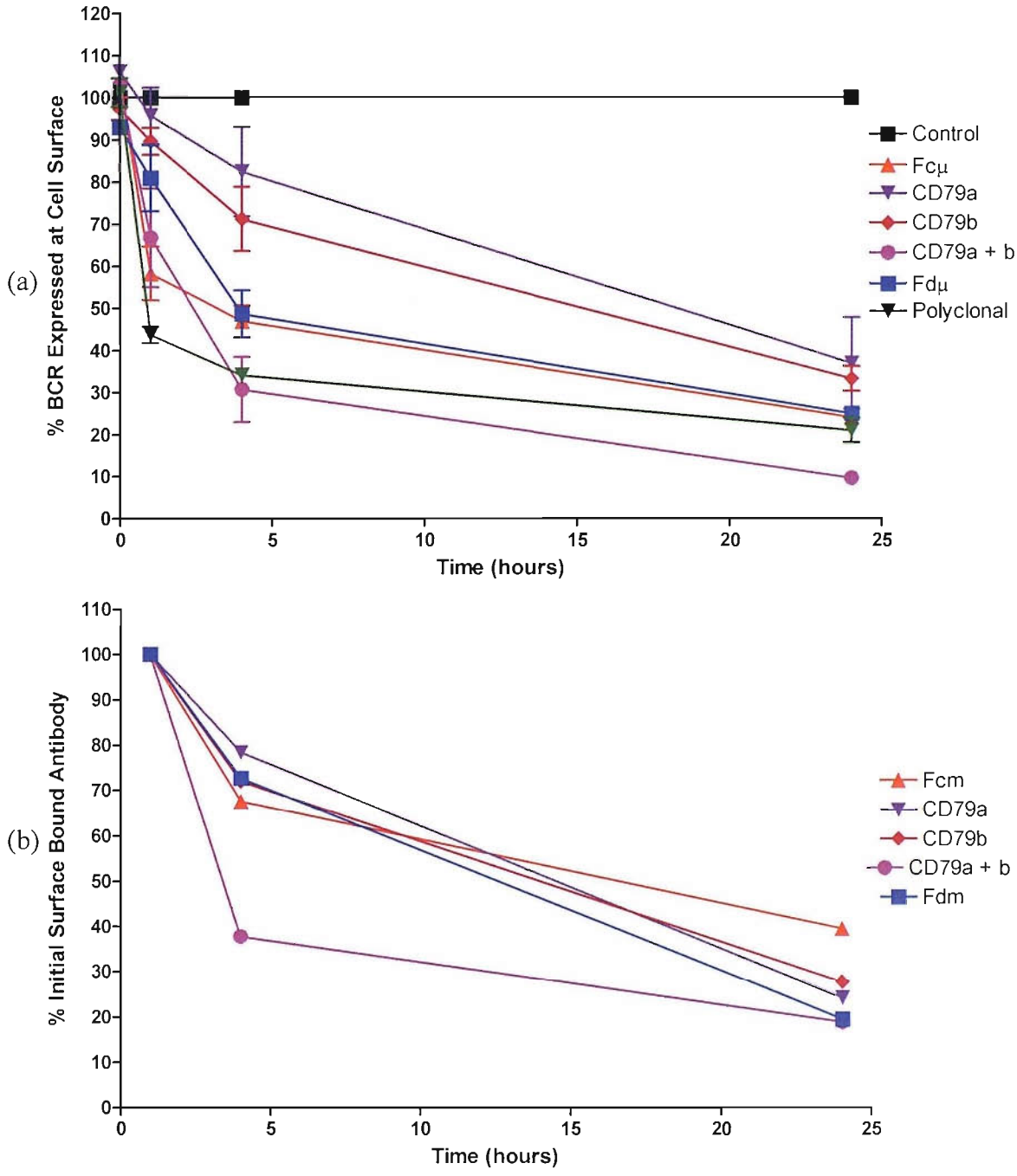

Figure 4.5 BCR modulation on EHRB in presence of Ab for 24 hours. EHRB cells ($2x10^5$) were incubated with the relevant Ab (10 μg/ml) for times indicated at 37°C in a humidified chamber. At relevant times, cells were removed, washed twice in PBA and assessed for levels of BCR present at the cell surface (a) mean value ± SD from three independent experiments. (b) Levels of bound mAb expressed as maximum level of mAb bound at 15 minutes, calculated from one of three independent experiments, Ab and reagents used as detailed in Figure 4.1.

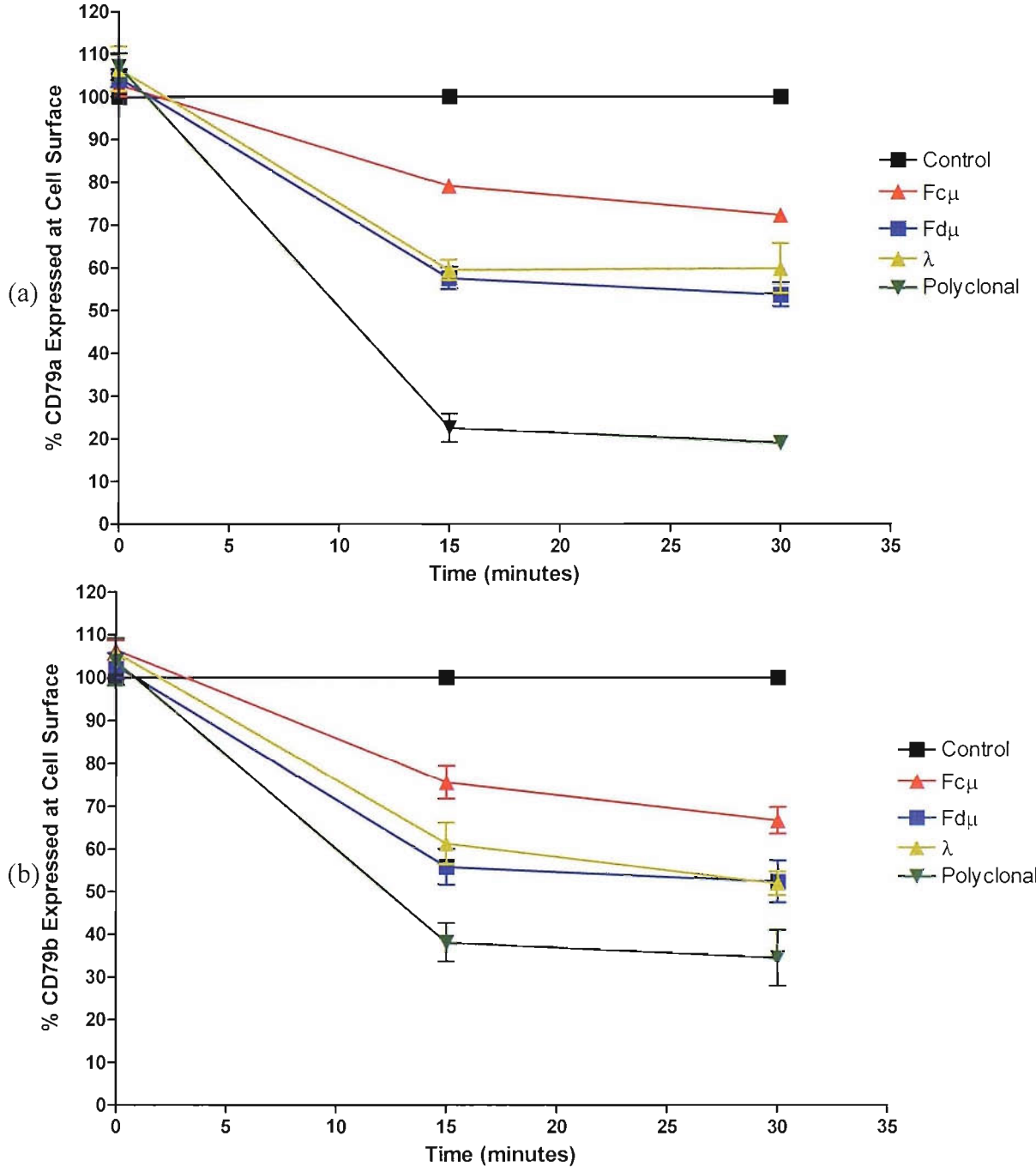

Figure 4.6 Levels of CD79a and CD79b expressed at the cell surface on EHRB following BCR modulation. EHRB cells ($2x10^5$) were treated with the various mAb as detailed in Figure 4.1, for times indicated at 37°C. At relevant times, cells were removed, washed twice and assessed using flow cytometry for surface levels of CD79a and CD79b using FITC labelled anti-CD79a (ZL7/4) (a), or FITC labelled anti-CD79b (AT105/1) (b). Levels of expression were normalised to cells treated with control mAb, and are mean values ± SD from three independent experiments.

4.2.3 The effect of BCR internalisation on B cell lines.

As shown in the previous chapter, *in vitro* BCR induced apoptosis varied between different cell lines. Therefore, it was interesting to investigate the kinetics of mIgM modulation on Daudi and BL-60 cells treated with the anti-BCR mAb. Figure 4.7 shows that Daudi cells treated with the panel of anti-BCR mAb have much lower rates of mIgM modulation than EHRB cells (Figure 4.4). Even treatment of Daudi cells with polyclonal anti-μ Ab had little effect, with 65% of mIgM remaining at the cell surface following treatment for 60 minutes. On the other hand, mIgM modualtion on BL-60 cells was more rapid, with only 25% of mIgM remaining at the cell surface following treatment with polyclonal anti-μ Ab for only 15 minutes (Figure 4.8). Anti-Fcμ mAb also showed rapid modualtion of IgM over the 60 minute incubation period on BL-60 cells, similar to when the anti-CD79a and b mAb were used in combination, which was more rapid than observed on EHRB treated cells. Surprisingly, modualtion of mIgM on BL-60 cells treated with the anti-Fdμ mAb was reduced compared to on EHRB cells.

4.2.4 Detecting the BCR complex when bound by mAb.

Given the differences in the kinetics of modulation of mIgM, CD79a and CD79b from the surface of EHRB cells, we wanted to investigate whether the whole BCR complex remains intact when stimulated with the anti-BCR mAb. Initially, EHRB cells were lysed in 1% digitonin lysate buffer and mAb added to see if whole BCR complexes could be immunoprecipitated. First we determined whether whole BCR complexes could be immunoprecipitated with the different anti-BCR mAb. EHRB cells were lysed in 1% digitonin, mAb added and the complexes pulled out by the addition of protein A coupled to sepharose 4B.

Figure 4.9, shows that all the anti-BCR mAb directed at the mIgM domain immunoprecipitated equal amounts of IgM from the cell lysate and that this was associated with CD79b. Monoclonal Ab directed at the CD79 heterodimer immunoprecipitated less IgM. However, more IgM was immunoprecipitated when anti-CD79a and b mAb were used in combination. Anti-CD79a mAb only immunoprecipitated small amounts of CD79b, compared to the other mAb used. CD79b appeared as a doublet when immunoblotted from immunoprecipitated complexes. Both of these bands were regarded as CD79b as this anti-CD79b mAb also immunoprecipitated the same doublet from EHRB cells.

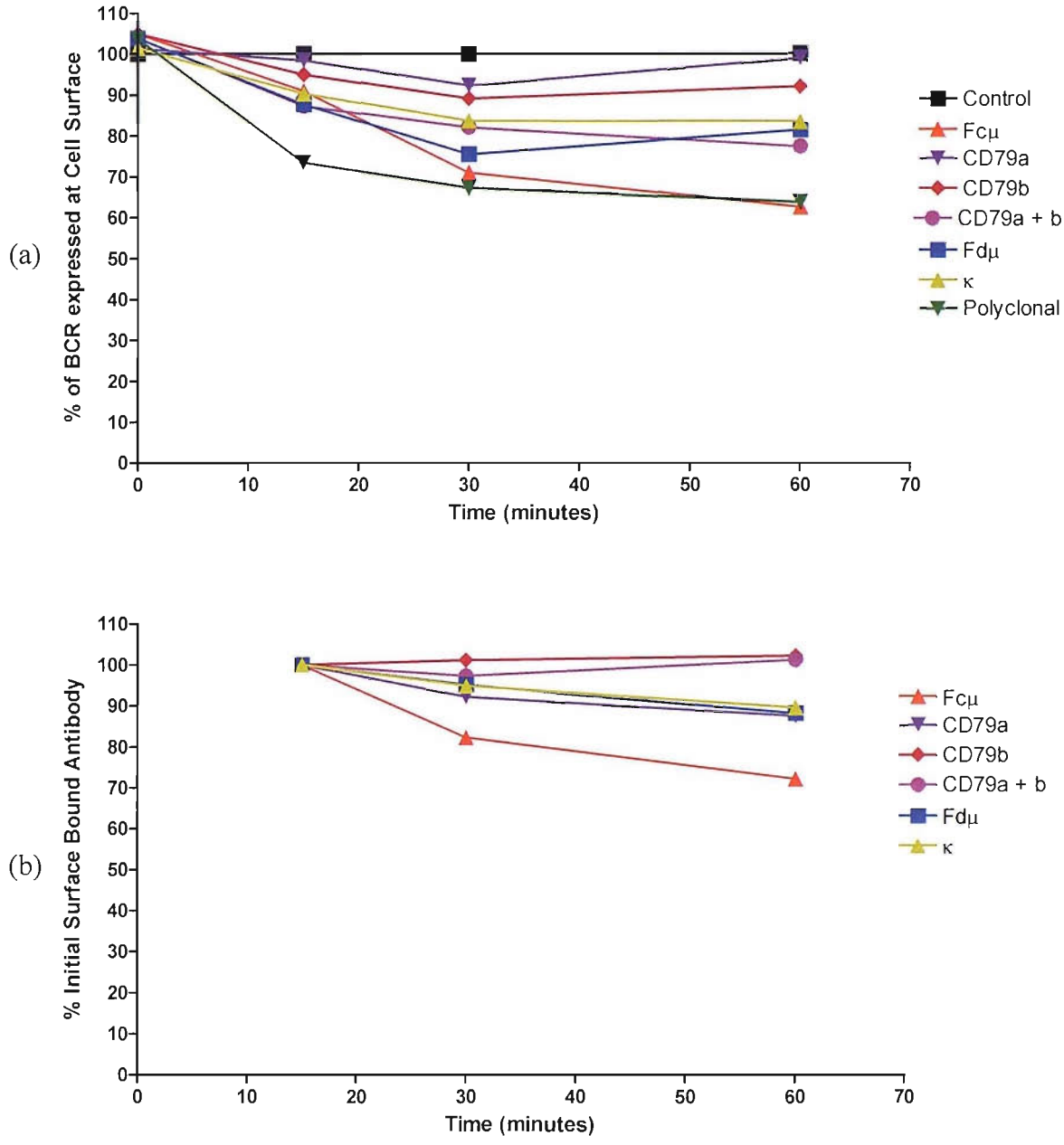

Figure 4.7 BCR internalisation on Daudi cell line following treatment with various Ab. Daudi cells ($2x10^5$) were incubated with the relevant Ab (10 μg/ml) for the times indicated at 37°C. At relevant times, cells were removed, washed twice and assessed for levels of BCR present at the cell surface using FITC labelled anti-Id (ZL15/27) (a), or levels of bound mAb using FITC labelled goat anti-mouse $F(ab')_2$ (b). Cells were analysed by flow cytometry and levels of BCR present normalised to cells treated with control mAb. The mAb used were as detailed in Figure 4.1.

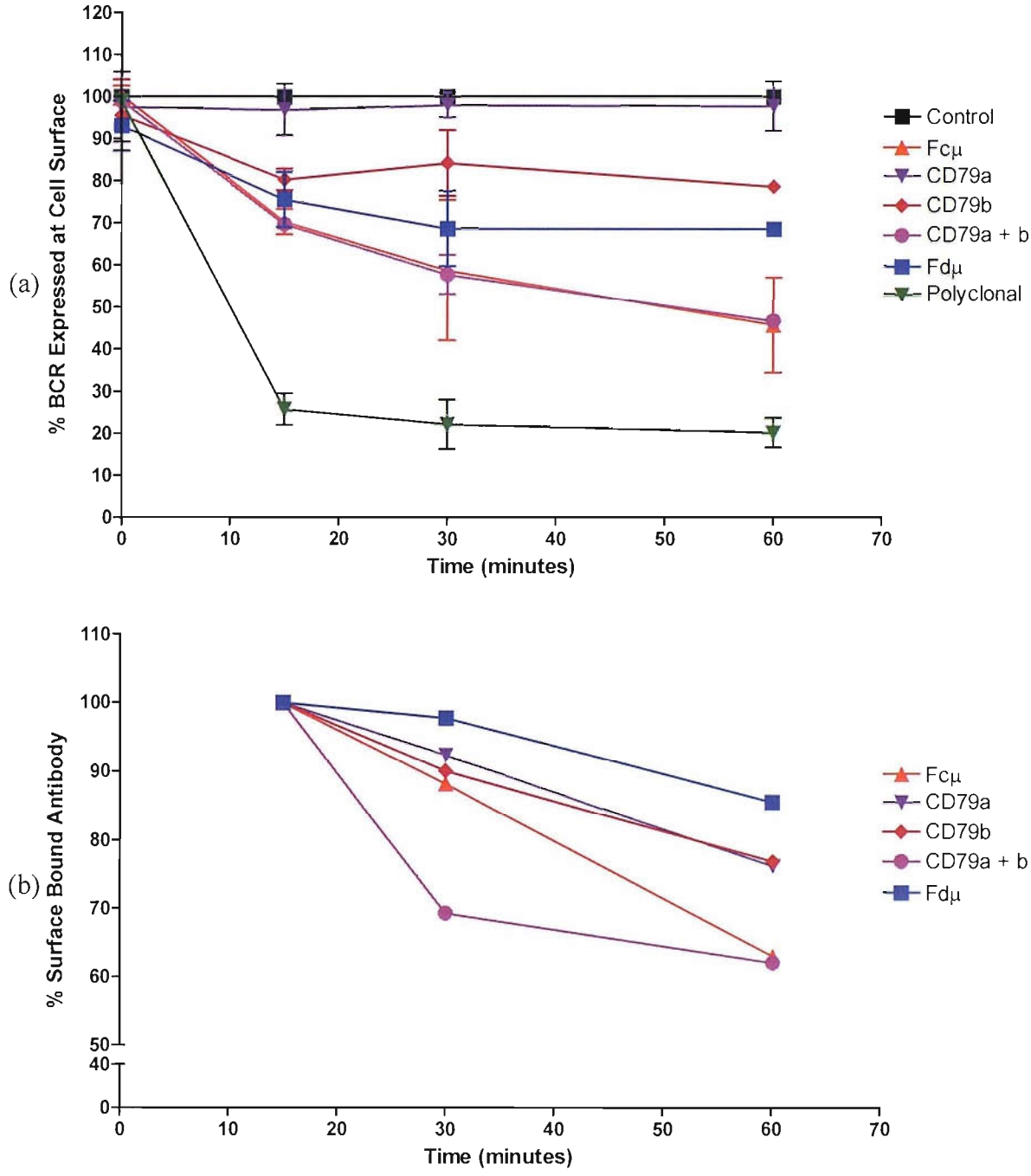

Figure 4.8 BCR modulation on BL-60 cell line following treatment with various Ab. BL-60 cells ($2x10^5$) were incubated with the relevant Ab (10 μg/ml) for the times indicated at 37°C. At relevant times, cells were removed, washed twice and assessed for levels of BCR present at the cell surface using FITC labelled anti-Fcμ (Mc244G10) (a), mean values ± SD from three independent experiments. Levels of bound mAb assessed using FITC labelled goat anti-mouse $F(ab')_2$ (b). Cells were analysed by flow cytometry and levels of BCR present normalised to cells treated with control mAb. The mAb used were as detailed in Figure 4.1.

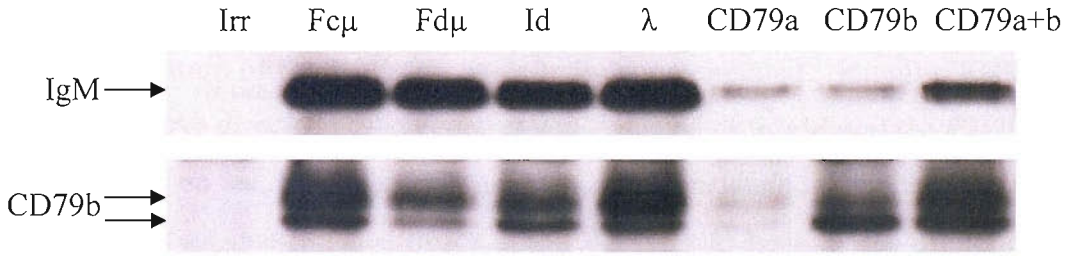

Figure 4.9 Immunoprecipitaion of BCR complexes from EHRB cell lysate with various mAb. EHRB cells ($4x10^6$) were treated with 10 μg/ml mAb following lysis in 1% digitonin and 2 hours incubation at 4°C with agitation. 20 μl protein A coupled to sepharose beads was added and samples incubated overnight at 4°C with constant agitation. Immunoprecipitated protein was resolved on 12.5% SDS-PAGE gels and levels of IgM and CD79b were identified using HRP directly labelled anti-μ Ab, or anti-CD79b (AT107/2) mAb and a relevant HRP labelled secondary Ab. mAb used are as follows: Irr, CP1/17: Fcμ, M15/8: Fdμ, XG9: Id, ZL16/1: λ, Mc24IC6: CD79a, ZL7/4: and CD79b, AT105/1. Representative of three independent experiments.

4.2.5 Detecting BCR complexes bound at the cell surface using different mAb.

Since we could use mAb to pull down complete BCR complexes from cell lysates of EHRB cells, we next wanted to investigate if the BCR remained intact after binding of the mAb to the cell surface. Before we could investigate the type of BCR immunoprecipitated from the surface of EHRB cells we needed to develop a method that could be confidently used within the laboratory.

4.2.5.1 Development and optimising a method for immunoprecipitating BCR from the surface of EHRB cells.

4.2.5.1.1 Influence of mAb binding time on BCR immunoprecipitate.

The first step was to investigate ti BCR could be immunoprecipitated from the cell surfaces, and to also investigate whether the incubation time of the mAb had an influence on the amount and nature of the BCR that were immunoprecipitated. Initially, EHRB cells were treated with mAb directed at the Fcμ and Fdμ domains of mIgM and the CD79 heterodimer for 30 minutes on ice, before being washed and then incubated for 1, 5, 15 or 60 minutes at 37°C. Cells were then washed in ice cold PBS prior to lysis in 1% digitonin, complexes were pulled out with protein A, and immunoblotted as detailed above.

Figure 4.10 shows that cells treated with the anti-Fcμ mAb immunoprecipitated more mIgM compared with cells treated with the anti-Fdμ mAb. Only relatively small amounts of mIgM were immunoprecipitated when cells were treated with a combination of mAb directed at the CD79 heterodimer. Interestingly, unlike cells treated with the anti-Fdμ mAb, mIgM complexes immunoprecipitated with the anti- Fcμ mAb failed to show the presence of CD79b. Cells treated with the anti-CD79b mAb alone, immunoprecipitated CD79b complexes, but cells treated with CD79a failed to immunoprecipitate any BCR complexes. Importantly, the length of time cells were incubated with the mAb had no affect on the amount and nature of proteins immunoprecipitated; this suggests that the BCRcomplex immunoprecipitated by the anti-BCR mAb may be due to the binding of the mAb and not a cellular response.

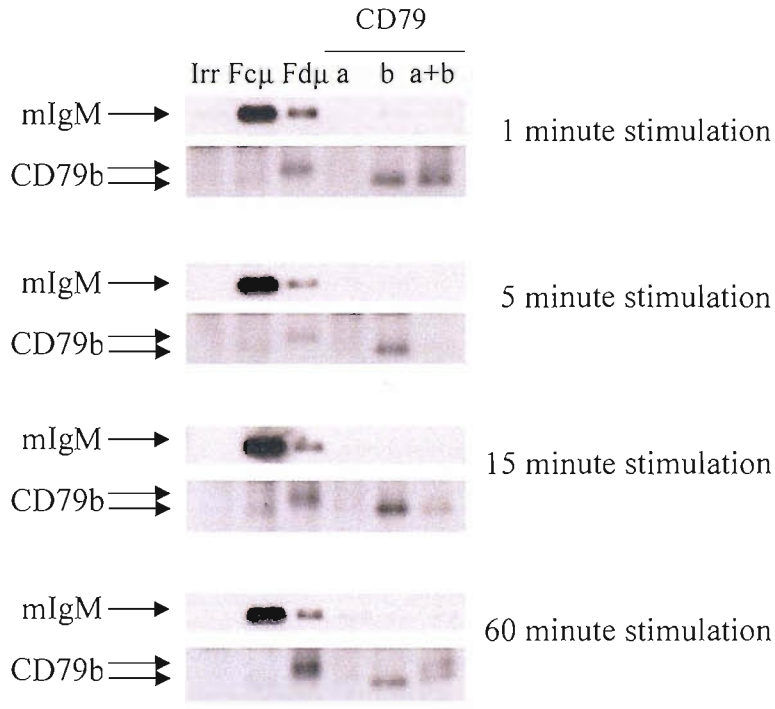

Figure 4.10 Influence of mAb binding time on immunoprecipitated BCR complexes. EHRB cells ($4x10^6$) were treated with the relevant mAb (10 μg/ml) for 30 minutes on ice, samples were then washed once and incubated for times indicated at 37°C. Cells were then removed and washed twice before being lysed in 1% digitonin. Lysates were incubated with 15 μl protein A beads overnight at 4°C with constant agitation. Protein A beads were washed four times in ice cold lysis buffer and bound protein separated on 12.5% SDS-PAGE gels, transferred to PVDF membranes and probed for the presence of mIgM and CD79b. Cells were stimulated with the following mAb: Irrelevant control, CP1/17: Fcμ, M15/8: Fdμ, XG9, CD79a, ZL7/4, CD79b, AT105/1, and CD79a + b, ZL7/4 + AT105/1. Representative of three independent experiments.

4.2.5.1.2 Influence of mAb binding time at 4°C on immunoprecipitated BCR from EHRB cells.

Since at 37°C incubation times did not influence the amount of BCR immunoprecipitated with each anti-BCR mAb, it was important to determine whether this was influenced by the initial binding at 4°C. To address this, EHRB cells were incubated with the various mAb at 4°C for 15, 30 or 60 minutes. Aliquots of the cells were then washed and assessed for levels of bound mAb, while incubating the remainder of the samples for 5 minutes at 37°C. Figure 4.11 shows that increasing the binding time at 4°C had little effect on the level of mAb bound, as assessed by flow cytometry, or the amount of mIgM immunoprecipitated. Monoclonal Ab directed at the Fcμ domain of the BCR still bound more mIgM than the other mAb used even when bound at 4°C.

4.2.5.1.3 The effect of increasing the number of washing steps before cell lysis on levels of BCR immunoprecipitated.

Another factor that could affect the amount of mIgM immunoprecipitated with the anti-BCR mAb was the possibility that any free mAb remaining after stimulation might capture intracellular IgM released when the cells were lysed. To address this question, the number of wash steps following incubation of the cells at 37°C with the different anti-BCR mAb was increased. EHRB cells were incubated with the anti-BCR mAb, washed once as before in PBS prior to incubation at 37°C. Samples where then washed, either once, or three times in ice cold PBS prior to lysis. Figure 4.12, shows that increasing the number of washes had little effect on the levels of immunoprecipitated mIgM. Therefore, the BCR aggregate observed when cells are treated with the anti-Fcμ mAb is not caused by free mAb binding to cytosolic/unbound IgM after cell lysis. However, by increasing the washing steps, the amount of mIgM and CD79b immunoprecipitated by anti-λ and CD79b mAb decreased, suggesting that these mAb could be binding BCR complexes in the cell lysate. Samples were also probed for the presence of IgM and CD79b in cell pellets and supernatant that did not bind to protein A, in all samples the levels expressed were the same. Therefore, it was decided that in the main experiments a total of two washes would be appropriate as the majority of unbound protein and mAb would be washed away.

(a)

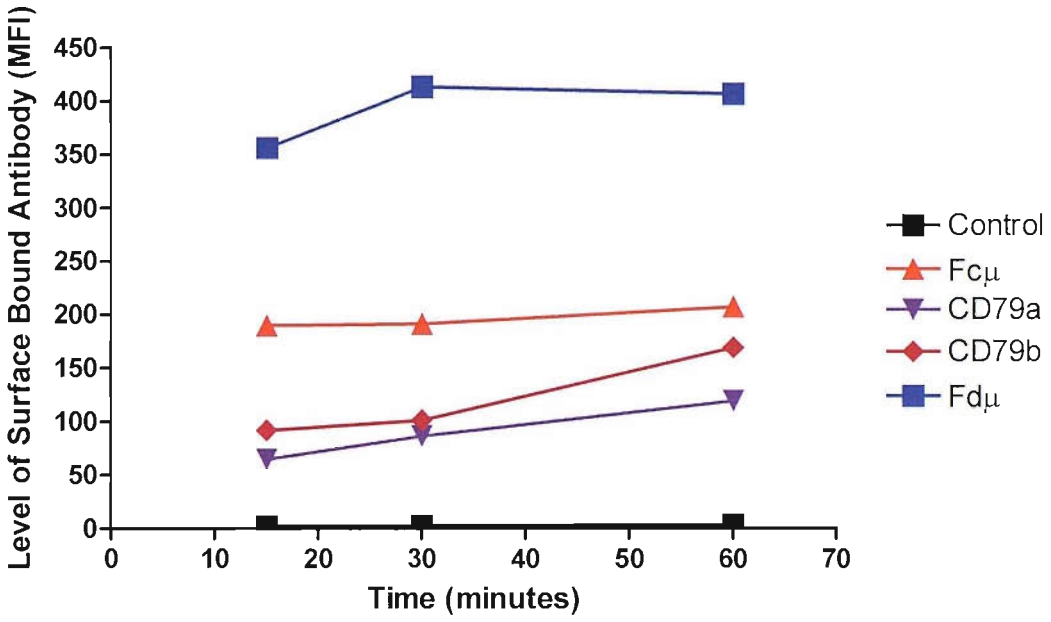

(b)

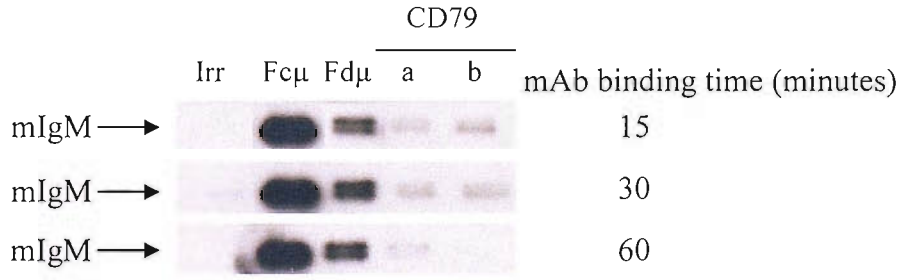

Figure 4.11 Does binding time for anti-BCR mAb at 4°C influence the immunoprecipitated BCR complex. $4x10^6$ EHRB cells were treated with various mAb on ice for times indicated. 25μl of each sample was removed, washed twice in PBA and levels of bound mAb assessed by flow cytometry using FITC labelled goat anti-mouse $F(ab')_2$ (a). The remainder of each sample was washed once in PBS prior to incubation for 5 minutes at 37°C in a pre-warmed water bath. Samples were washed twice in ice cold PBS before being lysed in 1% digitonin. Surface bound mIgM immunoprecipitates were identified as detailed in Figure 4.6 (b). Irr (CP1/17l), Fcμ is M15/8, Fdμ is XG9, CD79a is ZL7/4, and CD79b is AT105/1. Representative of three independent experiments.

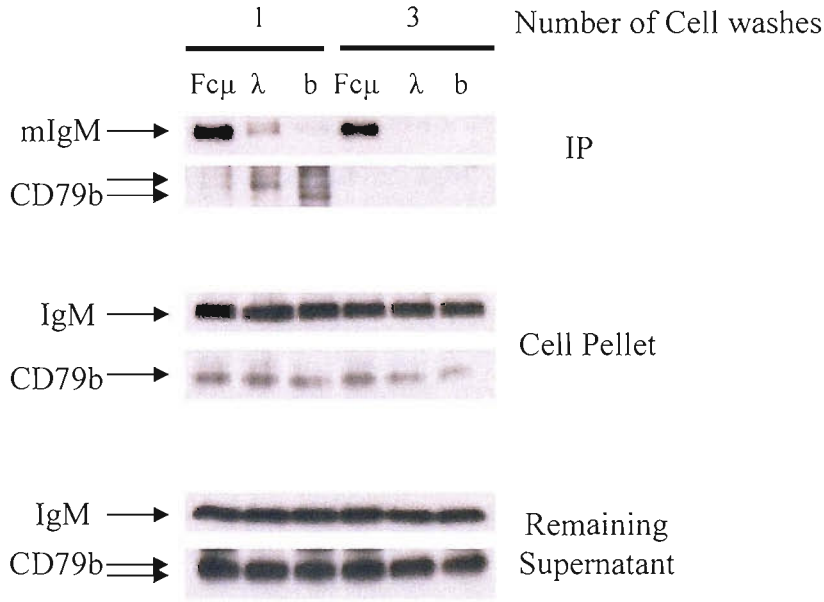

Figure 4.12 Effect of increasing the number of washing steps on levels of BCR immunoprecipitated with different mAb. $4x10^6$ EHRB cells were treated with relevant mAb for 30 minutes on ice, samples were washed once in PBS prior to a five minute incubation at 37°C in a pre-warmed water bath. Samples were then washed either once or three times in ice cold PBS before lysis and immunoprecipitation of surface bound BCR complexes. Cell debris pellets remaining from the lysis step were solubalised in 100μl of 2xSDS-LB and separated on 12.5% SDS-PAGE gels, transferred to PVDF membranes and bound protein probed for presence of IgM and CD79b. Remaining supernatant samples were levels of IgM or CD79b that did not bind to Protein A beads following overnight incubation, again protein was separated on 12.5% SDS-PAGE gels prior to immunoblotting for IgM and CD79b. Cells were treated with the following mAb; Fcμ is M15/8, λ is M24IC6, and b (CD79b) is AT105/1. Representative of at least three independent experiments

4.2.5.1.4 Effect of metabolic inhibitors on immunoprecipitated surface BCR.

The next experiment was set up to investigate if inhibition of cellular metabolism had any affect on the nature of the BCR complex immunoprecipitated with the different anti-BCR mAb. Cells were either incubated with or without the metabolic inhibitors azide and 2-deoxy glucose (2-DG), prior to incubation with mAb. These metabolic inhibitors prevent energy dependent events such as modulation of cross-linked BCR, allowing us to observe if the nature of the BCR complex immunoprecipitated with the various mAb is due to a direct binding phenomenon rather than an energy dependent cellular response. Figure 4.13, shows the same patterns of BCR immunoprecipitation as observed previously with the anti-Fcμ mAb immunoprecipitating significantly more IgM than the other mAb regardless of treatment with the metabolic inhibitor.

In addition, the cell lysate supernatant that did not bind to protein A (representing BCR that was not bound by the initial treatment with the anti-BCR mAb) and cell pellet (representing the digitonin insoluble material) were also probed for the presence of IgM and CD79b. In all of the samples, the levels of IgM and CD79b immunoblotted were the same, probably due to cytoplasmic IgM and CD79b.

4.2.5.1.5 The effect of altering the concentrations and volumes of protein A and G on BCR aggregates.

One possible explanation for the increased amount of mIgM immunoprecipitated with the anti-Fcμ mAb compared to the other anti-BCR mAb was that the protein A loaded sepharose beds were in some way limiting. To investigate if this was the case, two experiments were devised: one to alter the amount of protein A beads used, and a second to alter the concentration of protein A loaded on the sepharose beads. Initially, EHRB cells were treated with the relevant mAb for 30 minutes on ice, washed twice with PBS, lysed in 1% digitonin and then incubated over night with increasing volumes of protein A coated sephrose beads (10 mg protein A coupled per ml of sephrose beads).

Figure 4.14 shows that increasing the volume of protein A added to treated cell lysates caused a slight decrease in the amount of mIgM immunoprecipitated with anti-Fcμ mAb. However, as before, the two anti-Fcμ mAb used (M15/8 and ZL7/5) both immunoprecipitated more mIgM complexes then the anti-Fdμ, anti-λ or anti-Id mAb. Therefore, although increasing the amount of protein A used should allow more anti-BCR mAb to bind it had no affect on the amount of mIgM immunoprecipitated. This suggests

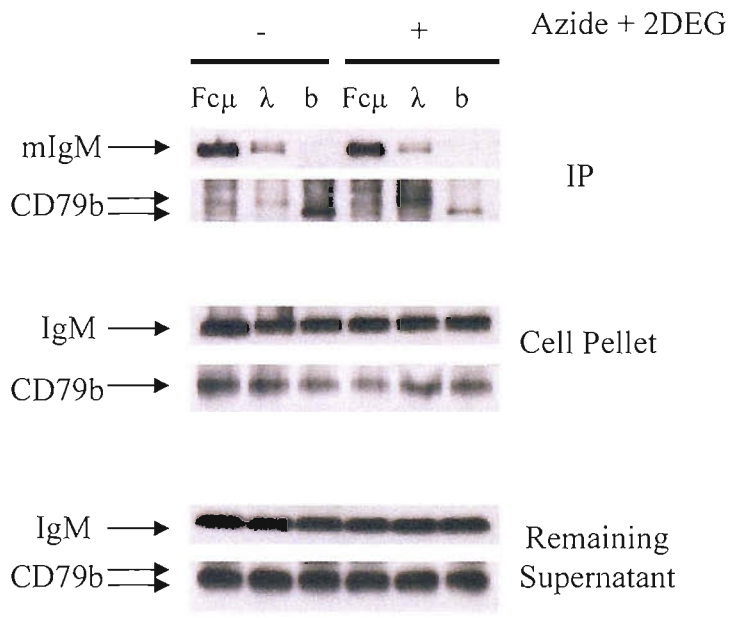

Figure 4.13 Effect of treating EHRB cells with metabolic inhibitors on levels of BCR immunoprecipitated. $4x10^6$ EHRB cells were treated with or without 1% Azide and 20 mM 2DEG for 30 minutes on ice, prior to incubation with various mAb for 30 minutes on ice, samples were washed once in PBS prior to a 5 minute incubation at 37°C in a pre-warmed water bath. Samples were then washed twice in ice cold PBS before lysis and immunoprecipitation of surface bound BCR complexes. Cell debris pellets remaining from the lysis step were solubalised in 100μl of 2xSDS-LB and separated on 12.5% SDS-PAGE gels, transferred to PVDF membranes and bound protein probed for presence of IgM and CD79b. Remaining supernatant samples were levels of IgM or CD79b that did not bind to Protein A beads following overnight incubation, again protein was separated on 12.5% SDS-PAGE gels prior to immunoblotting for IgM and CD79b. Cells were treated with the following mAb; Fcμ is M15/8, λ is M24IC6, and b (CD79b) is AT105/1. Representative of at least three independent experiments

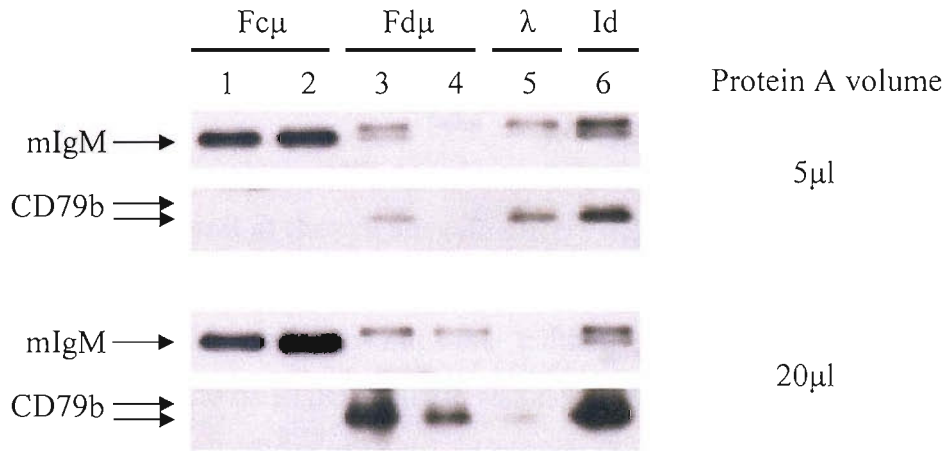

Figure 4.14 Effect of different mAb classes and protein A volumes on BCR immunoprecipitates. $4x10^6$ EHRB cells treated with various mAb directed to different regions of mIgM for 30 minutes on ice. Lysed cell samples were incubated overnight with increasing volumes of protein A (10 mg/ml). Immunoprecipitated mIgM and CD79b was assessed. Cells were treated with the following mAb; lane 1 is M15/8, lane 2 is ZL7/5, lane 3 is XG9, lane 4 is M2E6, lane 5 is Mc24IC6, and lane 6 is ZL16/1. Representation of three independent experiments.

that the 20 μl of protein A coated sephrose beads was not limiting the amount of BCR complex immunoprecipitated with the anti-BCR mAb.

To address this question from another perspective, Protein A and G were coupled to sephrose beads at two different concentrations: either 10 mg or 2 mg of protein per ml of sephrose beads. Figure 4.15, shows that coupling less protein A to the beads had little effect, reducing the amount of IgM complexes immunoprecipitated with anti-Fdμ and anti-λ mAb, but not affecting mIgM complexes immunoprecipitated with anti-Fcμ mAb. These results were also observed when the concentration of protein G was altered, although the initial amount of mIgM complexes immunoprecipitated was less then that observed when protein A was used.

4.2.6 BCR complexes bound at the cell surcafe differs depending on the mAb used.

Follwing on from the investigation into the method for immunoprecipitating BCR complexes from the surface of EHRB cells it was decided to investigate BCR complexes immunoprecipitated with all of the mAb raised against the BCR. One important note for this experiment, was that the commercially available polyclonal anti-μ Ab used in apoptosis and modulation studies could not be used in these experiments, as it is raised in a different species (goat), and consists of $F(ab')_2$ fragments. As such, it could not be immunoprecipitated with protein A coated beads. Therefore, it was decided to see if a combination of mAb directed at mIgM on EHRB cells could mimic the polyclonal anti-μ Ab and induce high levels of apoptosis. To test this, EHRB cells were treated with: control, anti-Fcμ, anti- Fdμ, or a mAb mixture (anti-Fdμ, λ and Id). Cells treated for 24 hours showed that the anti-Fcμ mAb induced highest levels of apoptosis measured with annexin V/PI. Cells treated with the mAb mixture induced higher levels of apoptosis when compared to that seen in cells treated with the anti-Fdμ and control mAb, Figure 4.16a.

Once we had identified that a mixture of the anti-BCR specific mAb could induce apoptosis, we then proceeded to investigate the surface bound BCR complexes immunoprecipitated with the different mAb. To immunoprecipitate surface bound BCR complexes, EHRB cells were treated with mAb directed at the Fcμ, Fdμ, λ light chain and Id domain of mIgM along with mAb directed at the CD79a and CD79b domains of the CD79 heterodimer, either alone or in combination. EHRB cells were also treated with the mAb mixture detailed above consisting of: Fdμ, XG9; λ, Mc24IC6; and anti-Id, ZL16/1 mAb. Cells were treated with

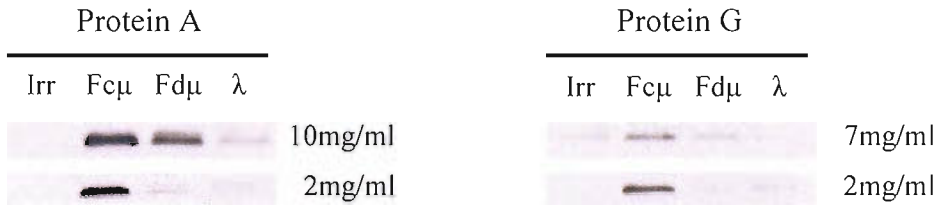

Figure 4.15 Effect of altering the concentration of protein A and G bound to sepharose beads on BCR immunoprecipitates. $4x10^6$ EHRB cells were treated with various mAb for 30 minutes on ice, lysed and surface bound mIgM immunoprecipitated with protein A or G sepharose coupled at either 10 or 2 mg/ml of sepharose beads. Immunoprecipitated mIgM was immunoblotted as detailed above. Cells treated with the following mAb, Irr is CP1/17, Fcμ is M15/8, Fdμ is XG9, and λ is Mc24IC6. Representative of three independent experiments.

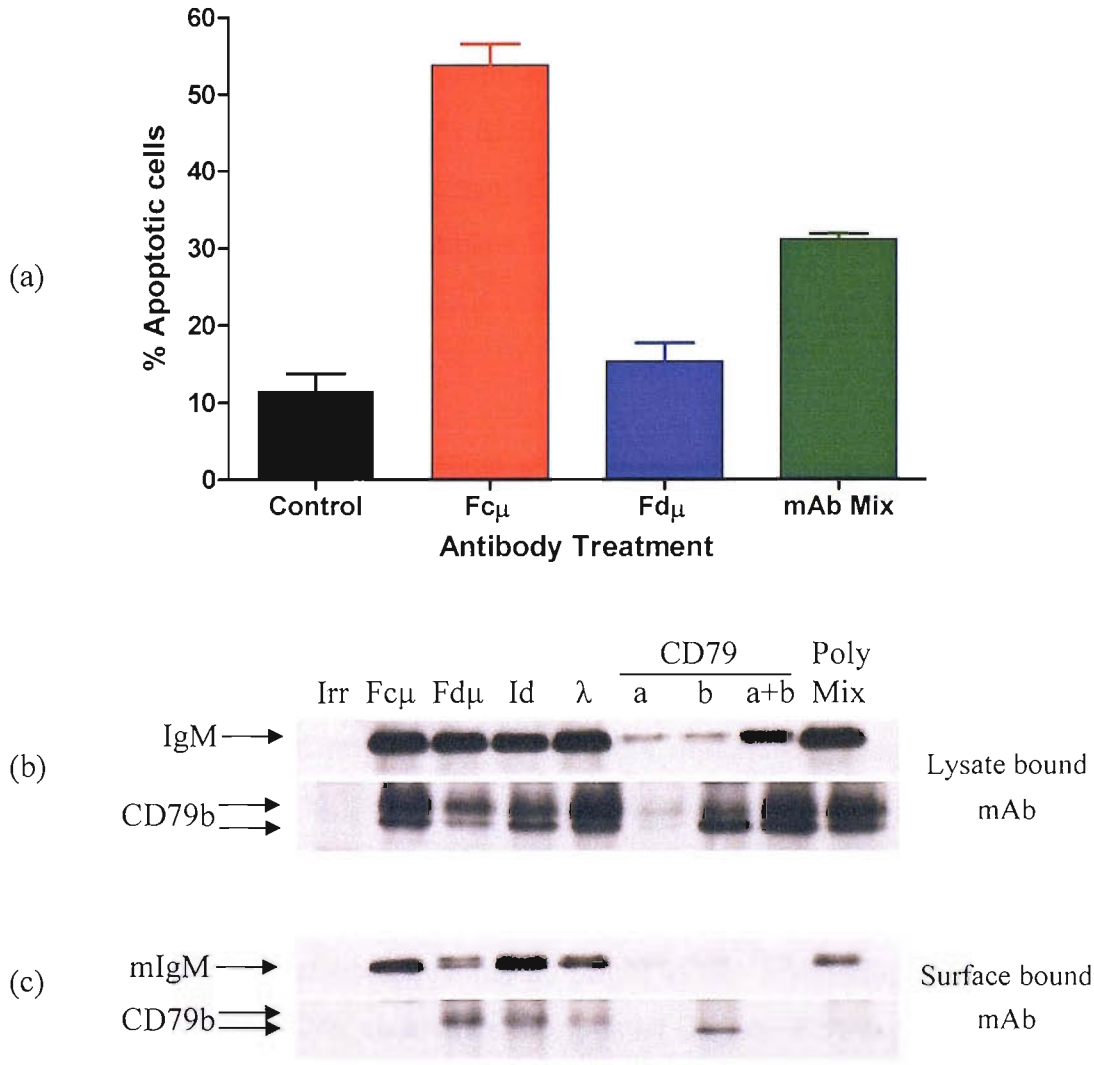

Figure 4.16 Use of a mAb mixture on BCR aggregation from EHRB cells. (a) EHRB cells ($2x10^5$) cells were treated with the relevant mAb at a final concentration of 10 μg/ml for 24 hours. The levels of apoptosis were assessed by flow cytometry using annexin V/PI staining and the values given are for mean percentages of apoptotic cells ± SD treated with the following mAb from three independent experiments: control, CP1/17: Fcμ, M15/8; Fdμ, XG9; the mAb mixture was a combination of XG9, Mc24IC6 and ZL16/1. $4x10^6$ EHRB cells were treated with 10 μg/ml mAb for 30 minutes on ice, washed once and incubated for 5 minutes at 37°C. Cells were then washed twice in ice cold PBS prior to lysis in 1% digitonin (Surface bound b) and incubation overnight with 15 μl protein A beads. For lysate bound samples (c), $4x10^6$ cells per treatment were lysed in 1% digitonin and mAb added to the lysate (10 μg/ml) for one hour at 4°C with agitation. Following this 15 μl protein A was added and samples incubated overnight at 4°C with constant agitation. Levels of immunoprecipitated mIgM and CD79b were identified as detailed in Figure 4.9. Monoclonal Ab used are as follows: Irrelevant control, CP1/17: Fcμ, M15/8, Fdμ, XG9, Id, ZL16/1, λ,Mc24IC6, CD79a, ZL7/4: CD79b, AT105/1, CD79a + b, ZL7/4 + AT105/1, and mAb mix is the defined mAb mixture. Representative of three independent experiments.

the relevant mAb for 30 minutes on ice, washed once in PBS and incubated for 5 minutes at 37°C. Cells were then washed twice in ice cold PBS prior to lysis in 1% digitonin lysate buffer. Cell lysates were incubated overnight with protein A coupled to sepharose 4B beads to immunoprecipitate mAb bound to the surface BCR complex. Immunoprecipitated complexes were resolved on 12.5% SDS-PAGE gels and probed for the presence of BCR complexes using Ab directed at human IgM or CD79b. As controls, to demonstrate that all mAb could immunoprecipitate complete BCR complexes from cell lysates, BCR complexes were immunoprecipitated from EHRB cell lysates without pre-binding of mAb as described above.

Figure 4.16b shows that as described above, when mAb is added to cell lysates, mAb directed at the mIgM, including the defined mAb mixture, immunoprecipitate large amount of IgM, compared to mAb directed at the CD79 heterodimer. Monoclonal Ab directed at the mIgM domain of the BCR also immunoprecipitated CD79b from cell lysates which appears as doublets. However, when mAb were pre-bound to the cell surface prior to lysis (Figure 4.10c), different mIgM and CD79b were immunoprecipitated from EHRB cells. Anti-Fcμ mAb appears to immunoprecipitate the most mIgM from the cell surface. This was followed by the anti-Id mAb. Monoclonal Ab directed at the Fdμ, λ light chain, and the mAb mixture, immunoprecipitated smaller amounts of mIgM, with mAb directed at the CD79 heterodimer immunoprecipitating no mIgM at all. Interestingly, mAb: anti-Fdμ, -λ light chain, -Id and -CD79b, co-immunoprecipitated CD79b. However, the anti-Fcμ and the mAb mixture failed to co-immunoprecipitate any CD79b with mIgM. Interestingly, the CD79b immunoprecipitated with surface bound mAb was not a doublet, as immunoprecipitated from cell lysates. Monoclonal Ab directed at the CD79b domain of the BCR immunoprecipitated a CD79b molecule from the cell surface that was slightly smaller in molecular weight than that immunoprecipitated with surface bound anti-Fdμ, λ and Id mAb, but within the size of the doublet immunoprecipitated from the cell lysate.

4.2.7 The nature of BCR complexes immunoprecipitated from radio-labelled EHRB cells.

Another way of addressing whether free mAb may be binding to intracellular IgM when EHRB cells are lysed is to pre-label surface proteins. Proteins immunoprecipitated with mAb can then be examined by SDS-PAGE to observe if they are surface of intracellular proteins. Therefore, we decided to radio-label surface proteins on EHRB cells with the radioisotope I^{125}. In this way, intracellular BCR proteins are excluded from the analysis as

they are not labelled. Briefly $1x10^8$ EHRB cells were radio-labelled with 1mC of I^{125}. EHRB cells were then treated with the anti-BCR mAb before or after lysis with 1% digitonin. Figure 4.17a shows that when the anti-Fcμ mAb was pre-bound to the surface of the cell only mIgM was immunoprecipitated without associated CD79a and b, compared with complete BCR complexes when the mAb is added to pre-lysed cells (Figure 4.17b). Monoclonal Ab raised against the Fdμ and λ-light chain domain of mIgM immunoprecipitated complete BCR complexes when bound to the cell surface and also when added to pre-lysed cells. The amount of immunoprecipitated mIgM was reduced compared to cells treated with the anti-Fcμ mAb as shown previously. These data indicate that the higher level of IgM immunoprecipitated with anti-Fcμ mAb is not due to mAb binding to intracellular BCR proteins. As before, these data show that the anti-Fcμ mAb binds to mIgM from the surface of EHRB cells and causes the dissociation of the CD79 heterodimer.

4.2.8 The effect of temperature on BCR immunoprecipitated with anti-BCR mAb.

Until now samples had always been warmed to 37°C following binding of the anti-BCR mAb to observe the nature of immunoprecipitated BCR complexes. As metabolic inhibitors had no affect on the ability of the anti-BCR mAb to immunoprecipitate BCR complexes, we next investigated the possibility that the nature of the BCR complex immunoprecipitated by the different anti-BCR mAb was entirely due to initial mAb binding and not secondary to a membrane redistribution event. This hypothesis suggests that the BCR complex immunoprecipitated by the anti-Fcμ mAb may form just by binding the mAb to cells on ice. To address this suggestion, EHRB cells were incubated with mAb for 30 minutes on ice and then either heated to 37°C for 5 minutes or lysed straight away (Figure 4.18). Interestingly, heating the cells to 37°C for 5 minutes had no affect on the ability of the anti-Fcμ to immunoprecipitate mIgM, and the anti-Fcμ mAb immunoprecipitated large amounts of mIgM that was not associated with CD79b when incubated with cells on ice, independent of the subsequent incubation period at 37°C. This suggests that the anti-Fcμ mAb can cause disassociation of mIgM from the CD79 heterodimer directly upon binding to the BCR complex, independent of any other cellular process.

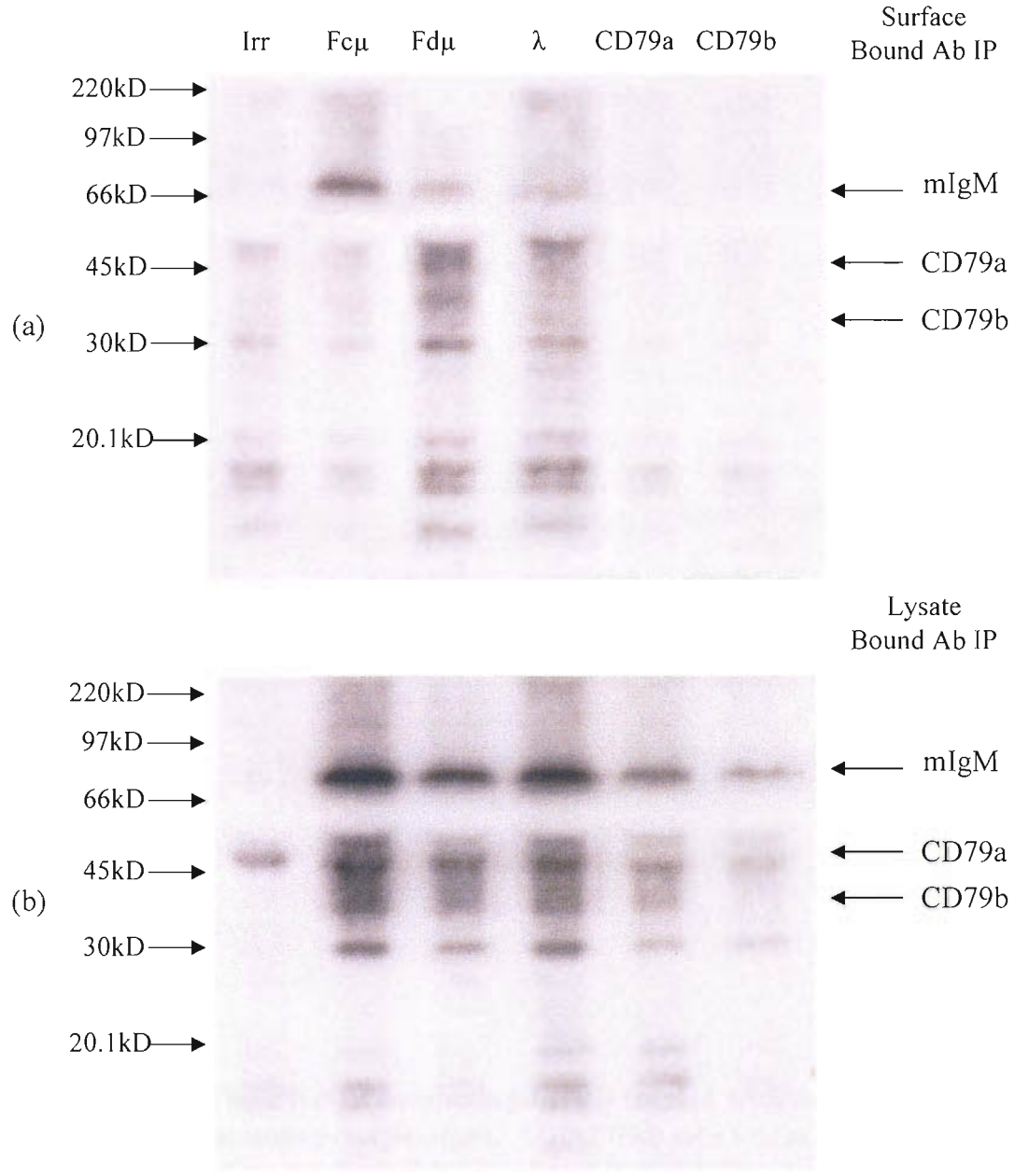

Figure 4.17 Immunoprecipitation of BCR by surface bound or lysate bound mAb from radio-labelled EHRB. $1x10^8$ EHRB cells were radio-labelled with 1mCu of I^{125}. Cells were then either treated with mAb (10 μg/ml) prior to lysis in 1% digitonin, or mAb was added to lysis buffer to investigate levels of labelled surface protein immunoprecipitated. Cells were treated with the following mAb: Irr is CP1/17, Fcμ is M15/8, Fdμ is XG9, λ is MC24IC6, CD79a is Zl7/4 and CD79b is AT105/1. Representative of several experiments.

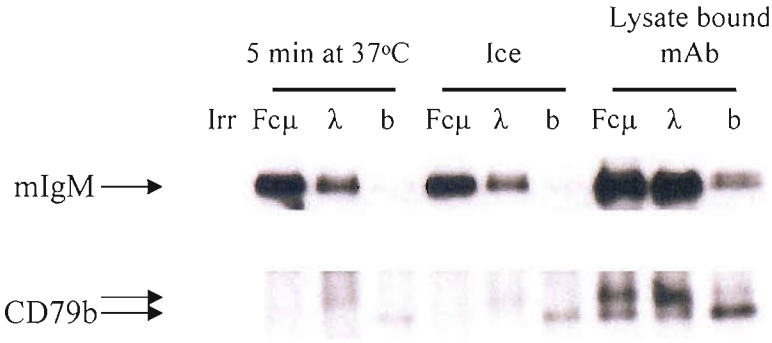

Figure 4.18 The effect of incubating EHRB treated with mAb at 37°C and 4°C on BCR immunoprecipitations. 4x10^6 EHRB cells treated with relevant mAb for 30 minutes on ice and then either washed once in PBS before incubating at 37°C for 5 minutes in a pre-warmed water bath, or washed twice in ice cold PBS prior to lysis in 1% Digitonin. EHRB cells were also lysed in 1% digitonin prior to addition of mAb as detailed in Figure 4.7 (WCL). Levels of mIgM and CD79b immunoprecipitated with surface bound and lysate bound mAb were analysed as detailed in Figure 4.6. Cells were treated with the following mAb; Irr is CP1/17, Fcμ is M15/8, λ is Mc24IC6, and b (CD79b) is AT105/1. Representative of three independent experiments.

4.2.9 The effect of binding similar levels of anti-BCR mAb on immunoprecipitated BCR from EHRB cells.

As shown previously, not all the anti-BCR mAb bound to the same level on EHRB cells, for example nearly twice as much of the anti-Fdμ mAb bound compared to the anti-Fcμ mAb (Figure 4.1). Therefore, we were interested to know, whether, when all the anti-BCR mAb were bound at the same level, they could immunoprecipitate the same amount of the BCR complex. To address this question, we performed binding experiments with each of the anti-BCR mAb to determine the concentrations required to give similar levels of bound mAb at the cell surface, as measured by staining with anti-mouse FITC Ab. To allow direct comparison of all of the anti-BCR mAb we adjusted the binding levels to that achieved when cells were incubated with saturating levels of the anti-CD79b mAb (10 μg/ml: Figure 4.19a). The immunoprecipitation experiments were then repeated using these concentrations of the anti-BCR mAb (Figure 4.19b). These experiments clearly showed that under these conditions all of the mAb immunoprecipitated similar amounts of IgM, except the anti-Fcμ mAb, which as before, immunoprecipitated high levels of IgM. Decreasing the concentration of the anti-Fcμ mAb had no affect on the amount of IgM immunoprecipitated, when compared to with cells incubated with saturating concentrations of the mAb.

4.2.10 Use of BN-PAGE for BCR aggregation analysis

From the extensive immunoprecipitation and SDS-PAGE experiments detailed above used to analyse the nature of the BCR complexes bound by the different mAb, it is clear that the anti-Fcμ mAb immunoprecipitated more mIgM then the other anti-BCR mAb. Interestingly, the anti-Fcμ mAb also failed to immunoprecipitate CD79b, suggesting that these anti-BCR mAb disrupt the BCR complex upon binding. To address the structure of the BCR complex more closely and investigate this theory further we decided to use a method that would allow the resolution of intact BCR complexes, rather than the SDS-PAGE method that disrupts the BCR complexes prior to resolution. For this reason we used Blue native PAGE (BN-PAGE)[30, 155] to investigate the BCR complexes immunoprecipitated with the anti-BCR mAb. BN-PAGE allows the separation of complete BCR complexes on native gels, with mIgM associated with the CD79 heterodimer. In addition to confirming the nature of the BCR complexes, BN-PAGE should also allow us to identify the size of the BCR complexes immunoprecipitated by the bound mAb, depending on the migration distance through BN-PAGE gels.

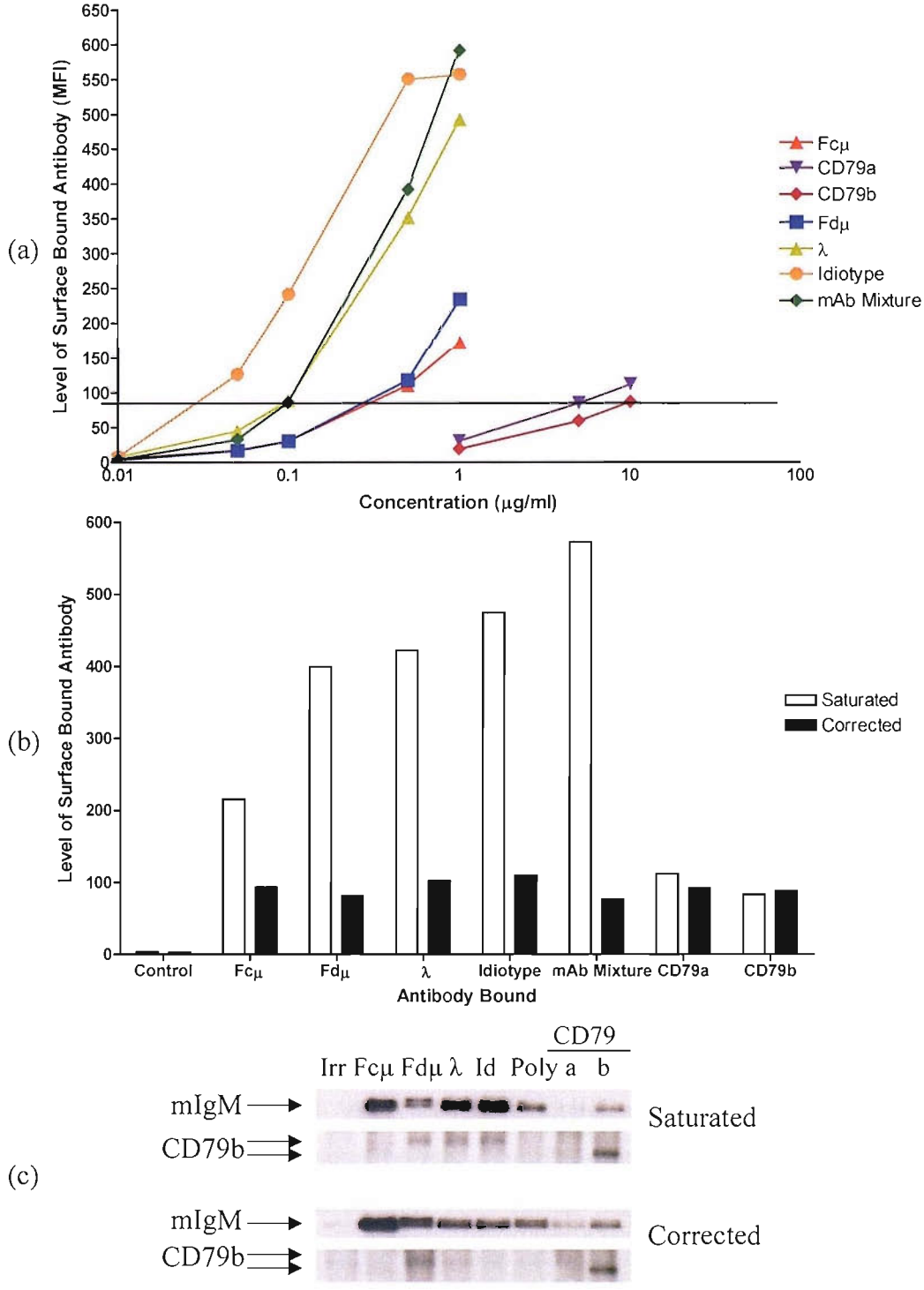

Figure 4.19 Immunoprecipitation BCR after binding equivalent levels of mAb on the surface of EHRB cells. (a) $1x10^5$ EHRB cells were treated with titrating concentrations of various mAb for 30 minutes on ice and levels of bound mAb assessed by flow cytometry. (b) $4x10^6$ EHRB cells were treated with either saturating (10μg/ml) mAb or the concentration of mAb required to give a binding level equal to that with saturated anti CD79b mAb for 30 minutes on ice. Following incubation, 25μl samples were removed to assess levels of bound mAb. (c) Samples were lysed in 1% digitonin and bound BCR complexes incubated overnight with protein A. Samples were probed for the presence of immunoprecipitated IgM and CD79b as detailed in Figure 4.6. Cells were treated with the following mAb; Irr is CP1/17, Fcμ is M15/8, Fdμ is XG9, λ is Mc24IC6, Id is ZL16/1, Poly is polyclonal mixture, CD79a is ZL7/4, and CD79b is AT105/1. Representative of three independent experiments.

Prior to performing these experiments, we needed to optimise the BN-PAGE method, to refine both the concentration and type of markers to use and to determine the volume of cell lysate that could be resolved using these gels (Figure 4.20a). Following extensive preliminary experimentation, Amersham Native markers along with ferritin at 2.5 mg/ml appeared to be the best, allowing identification of large complexes up to 880kD and smaller complexes down to 66kD. In order to obtain the maximum capacity of the BN-PAGE gels for resolving the cell lysates, increasing concentrations of EHRB cells were lysed in BN-PAGE lysis buffer and separated. Figure 4.20b, shows that the gel system could resolve lysates from up to $8x10^6$ cells and therefore, should be adequate to resolve the amount of protein loaded using our method.

Another problem we predicted was the release of immunoprecipitated complexes from protein A. When resolving immunoprecipitated protein through SDS-PAGE, samples are denatured in SDS loading buffer, releasing bound protein from protein A coated beads. However, when using BN-PAGE, samples cannot be denatured as this would lead to the break up of immunoprecipitated protein complexes. Therefore, further experiments were carried out to determine the best method to allow disassociation of the bound mAb from protein A. Figure 4.21a shows that a tris-glycine elution buffer with a pH of pH2.5 gave optimal elution of bound mAb. However, since it was thought that at this low pH, disruption of the BCR complex would occur, a tris-glycine buffer with pH4.5 was chosen for the experiments as this was still able to elute the majority of the mAb.

To see if our method worked, we treated $4x10^6$ EHRB cells with irrelevant control, anti-Fcμ or anti-Fdμ mAb for 30 minutes on ice. Samples were then washed twice in PBS before being lysed in 1% digitonin BN-PAGE lysis buffer. Supernatants were incubated over night with protein A coupled to sephrose and samples were then washed four times in lysis buffer before the addition of 20 μl of 0.1 M tris-glycine elution buffer and incubated for 30 minutes at room temperature. Samples were then resolved through 16 to 5.5% gradient BN-PAGE gels, protein transferred to PVDF membrane and immunoblotted for mIgM using HRP-labelled anti-μ Ab. Figure 4.21b shows that pH4.5 elution buffer allows disassociation of BCR complexes from protein A coated sepharose beads. Samples eluted using the pH2.5 elution buffer showed increased levels of eluted mIgM, which appeared to smear through the upper section of the gels, whereas the pH7.0 elution buffer eluted very little of the bound mIgM. For these reasons, in subsequent BN PAGE experiments, $4x10^6$ cells were lysed per

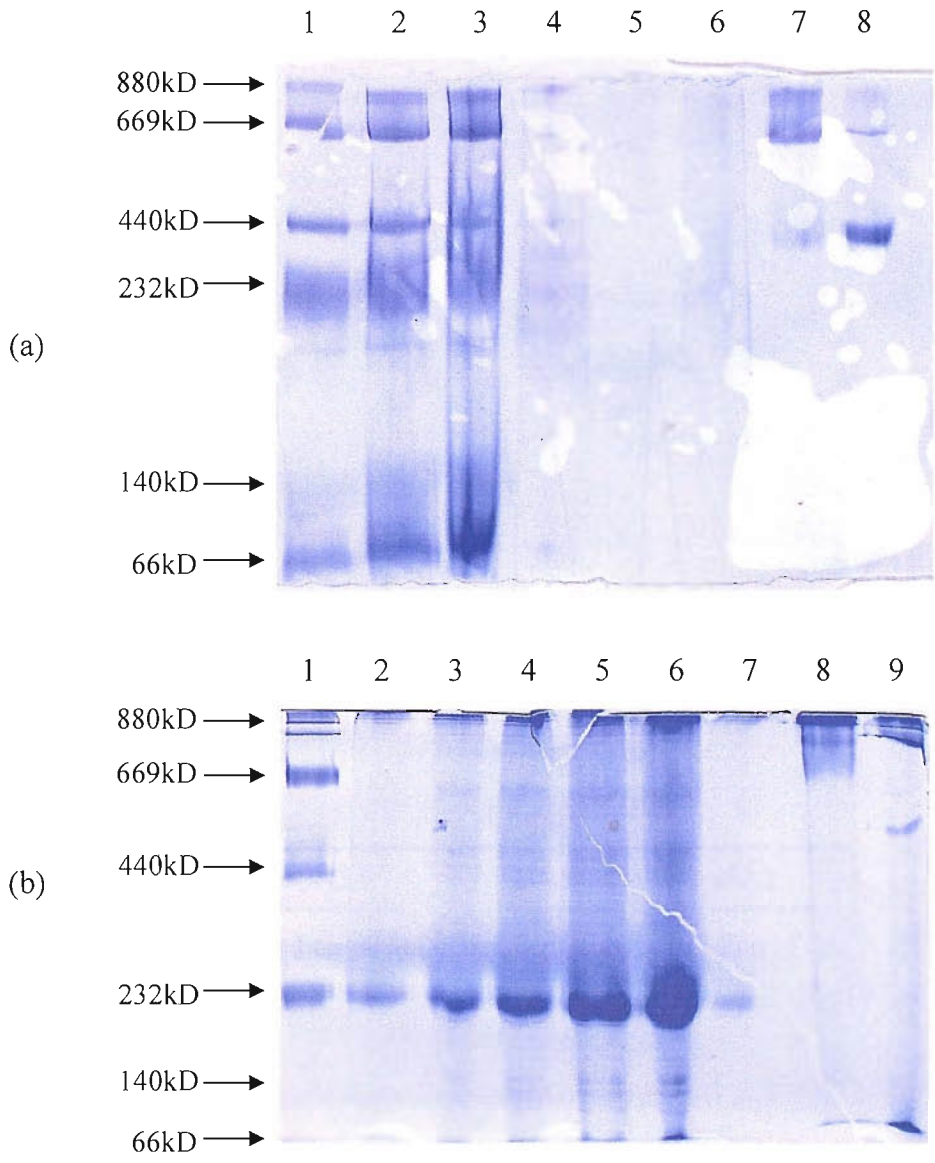

Figure 4.20 Optimisation of BN-PAGE for cell lysate concentration and markers. (a) Various markers at a final concentration of 2.5 mg/ml were separated by BN-PAGE followed by staining with Coomassie blue stain. Gel loaded as follows; lane 1 is Amersham Native marker (ANm, 5µl), lane 2 is ANm (10µl), lane 3 is ANm (20µl), lane 4 is Ig mixture (10µl), lane 5 is aldolase (158kD, 10µl), lane 6 is catalase (232kD, 10µl), lane 7 is thyroglobulin (670kD, 10µl), and lane 8 is ferritin (880 and 440kD, 10µl). (b) EHRB cells at different concentrations were lysed in 1% digitonin and separated on BN-PAGE followed by protein staining using Coomassie blue. Gel loaded as follows; lane 1 is 10µl ANm, lane 2 is $0.75x10^5$ EHRB, lane 3 is $1.5x10^5$ EHRB, lane 4 is $3x10^5$ EHRB, lane 5 is $6x10^5$ EHRB, lane 6 is $12x10^5$ EHRB, lane 7 is empty, lane 8 is thyroglobulin and catalase (20µl), and lane 9 is feretin and fldolase (20µl). Representative of at least two independent experiments.

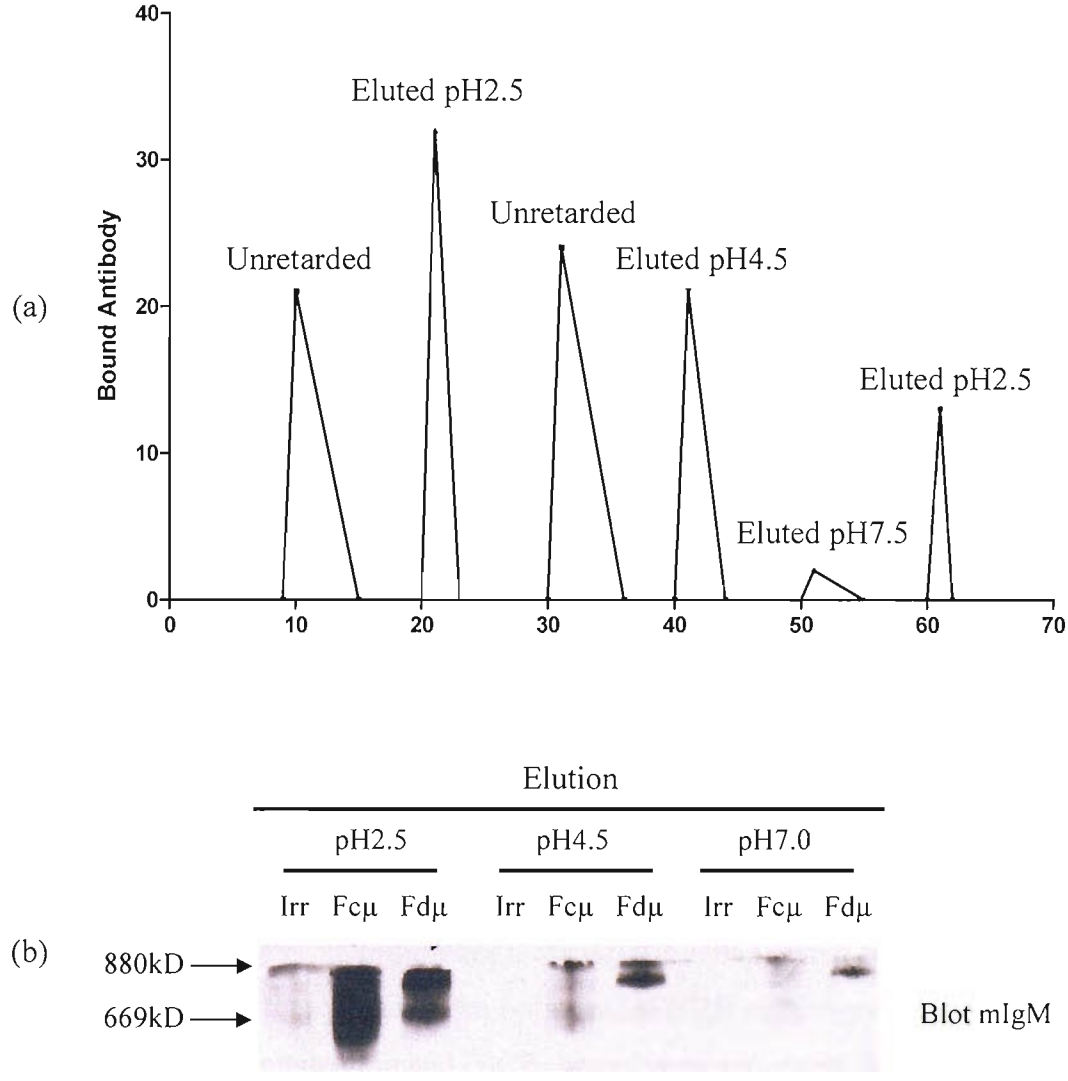

Figure 4.21 Comparison of elution of BCR/mAb complexes from protein A beads using various pH buffers. (a) Anti-μ mAb M15/8 (1.6 mg/ml) was loaded onto a Seph4B protein A column (10 mg/ml), and then bound mAb was eluted using various 0.1M tris-glycine buffer of various pH. (b) $4x10^6$ EHRB cells were treated with various anti-BCR mAb for 30 minutes on ice prior to lysis using 1% digitonin and BCR complexes were immunoprecipitated overnight using protein A coated beads. Protein A beads were then washed four times with ice cold lysis buffer, and incubated with 20 μl 0.1M tirs-glycine buffer at various pH (2.5, 4.5 or 7.0), for 30 minutes at room temperature. Protein A beads were then pulse spun, and 10 μl supernatant separated on BN-PAGE gels, and immunoblotted for presence of mIgM as detailed in Figure 4.16. Cells were treated with the following mAb; Irr is CP1/17, Fcμ is M15/8, and Fdμ is XG9. Representative of at least three independent experiments.

sample and pH 4.5 elution buffer was used to elute the immunoprecipitated BCR complexes.

As well as resolving immunoprecipitated complexes, whole cell lysates were also assessed by BN-PAGE. It was thought that aggregation of large BCR complexes from EHRB cells treated with the anti-BCR mAb may be able to be distinguishable in these cells, compared with cells treated with the control mAb. In addition, samples were resolved as complete complexes or denatured with SDS prior to running them on BN-PAGE. Figure 4.22 shows the results obtained from EHRB cells treated with control, anti-Fcμ or anti-Fdμ mAb. Anti-Fcμ mAb immunoprecipitated a mIgM complex of higher molecular weight compared to that immunoprecipitated with the anti-Fdμ mAb. However, when SDS was added multiple smaller bands of mIgM were observed. This appeared similar when BCR complexes were immunoprecipitated with either the anti-Fcμ or the anti-Fdμ mAb. Interestingly, as with the SDS-PAGE analysis, more mIgM was immunoprecipitated when EHRB cells were treated with anti-Fcμ mAb compared to anti-Fdμ or control treated cells. Whole cell lysates from cells treated with the different anti-BCR mAb showed the presence of multiple IgM complexes. As no differences were observed between the results with anti-Fcμ and anti-Fdμ mAb, whole cell lysates were not investigated further.

4.2.11 BN-PAGE analysis of complexes from EHRB cells treated with mAb

Once the BN-PAGE technique had been optimised, EHRB cells were treated with the anti-BCR mAb and immunoprecipitated BCR complexes separated by BN-PAGE. Two different concentrations of resolving gels were used to ensure optimal resolution. Figure 4.23, shows that as with SDS-PAGE gels, cells treated with the anti-Fcμ mAb immunoprecipitated mIgM but no CD79b, although the mIgM complex immunoprecipitated was again of a higher molecular size then the BCR complex immunoprecipitated with the anti-Fdμ mAb (IgM and CD79b migrated at the same position). A complete BCR complex was shown by the presence of mIgM and CD79b which when immunoblotted, were detected. In cells treated with the anti-λ, anti-Id and the mAb mixture, complete BCR complexes were immunoprecipitated, shown by mIgM and CD79b that both immunoblotted at the same position on the BN-PAGE gel. Interestingly, the amount of CD79b immunoblotted from cells treated with the mAb mixture, used to mimic the polyclonal reagent, was reduced, compared to cells treated with the other anti-BCR mAb directed at mIgM, again in accordance with the SDS-PAGE results. Cells treated with the anti-CD79b

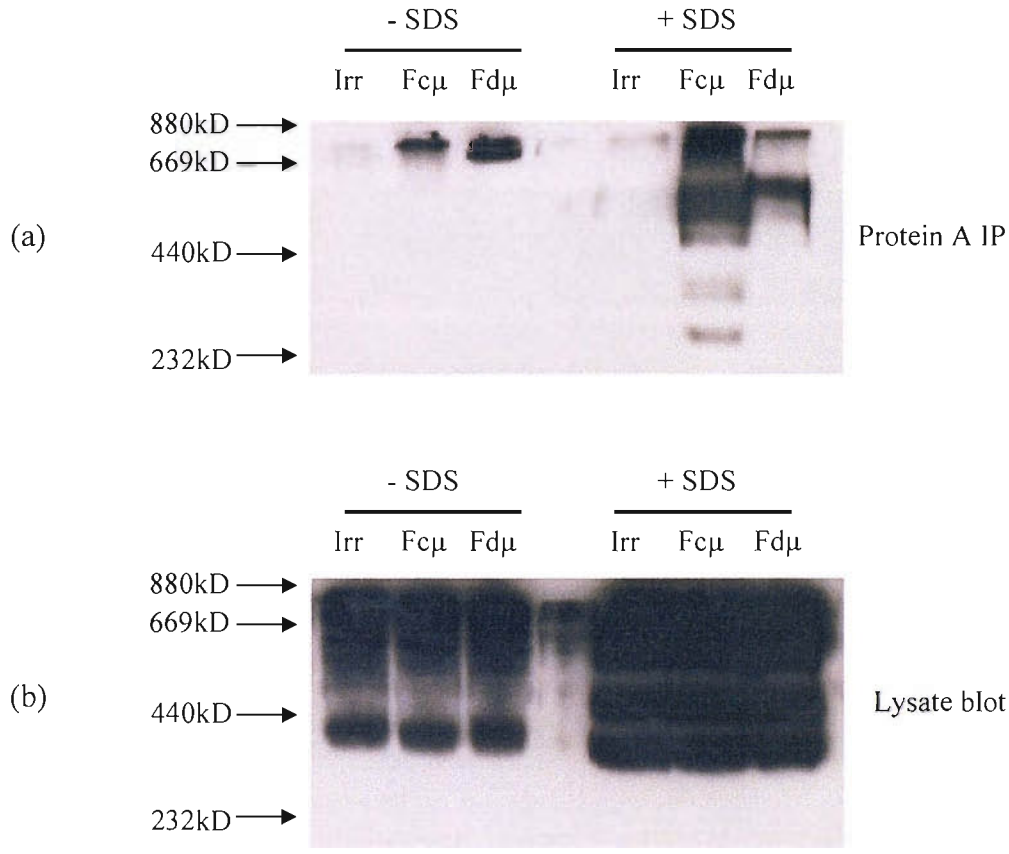

Figure 4.22 Separation of BCR complexes immunoprecipitated from EHRB cell line using BN-PAGE. $4x10^6$ cells treated with various mAb for 30 minutes on ice prior to lysis in 1% digitonin buffer. BCR complexes were then either immunoprecipitated overnight with protein A (a) or lysate was directly separated by BN-PAGE gels following incubation with or without 10% SDS (b). Immunoprecipitated samples were eluted off protein A beads using 0.1M tris-glycine buffer, pH4.5. BCR complexes were immunoblotted for presence of IgM as detailed in Figure 4.16. Cells were treated as follows; - is CP1/17, Fcμ is M15/8 and Fdμ is XG9. Representative of three independent experiments.

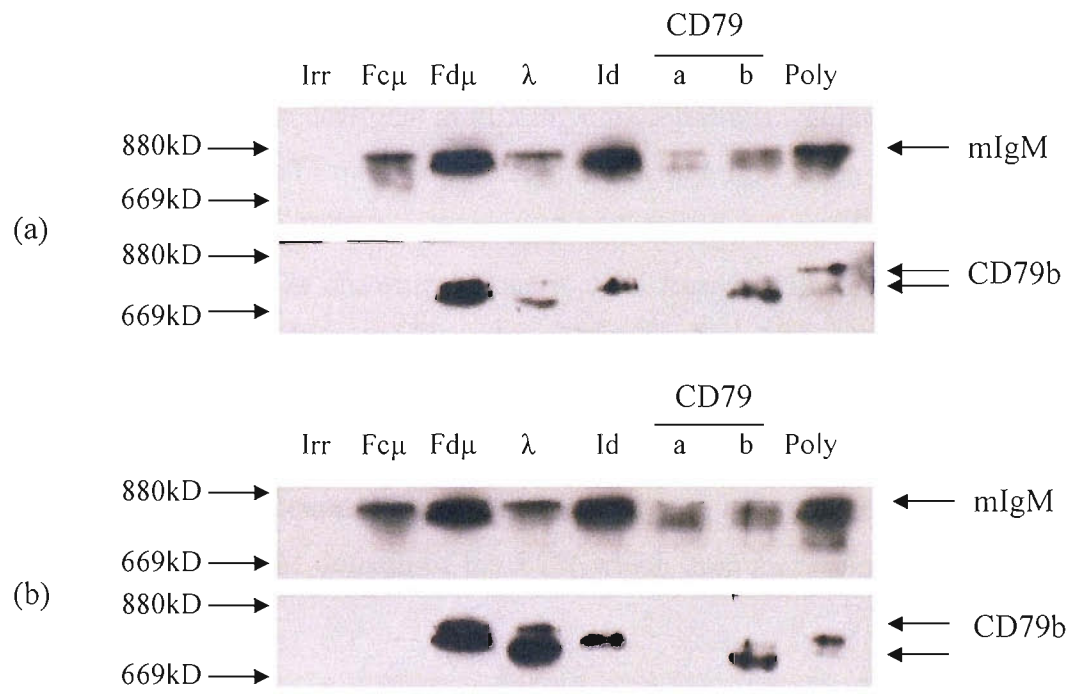

Figure 4.23 BN-PAGE analysis of BCR complexes immunoprecipitated from EHRB cells treated with various mAb. $4x10^6$ EHRB cells were treated with various mAb prior to lysis in 1% digitonin. Bound BCR complexes were immunoprecipitated with protein A beads overnight at 4°C. BCR complexes were eluted from beads using 0.1M tris-glycine buffer pH4.5 and separated by either 16-5.5% BN-PAGE (a), or 12.5-5.5% BN-PAGE gels (b). Separated protein was immunoblotted for presence or mIgM and CD79b as described previously. Cells were treated with the following mAbs; Irr is CP1/17, Fcμ is M15/8, Fdμ is XG9, λ is Mc24IC6, Id is ZL16/1, a is ZL7/4, b is AT105/1, and Poly is polyclonal mixture. Representative of at least two independent experiments.

mAb immunoprecipitated CD79b, but only small amounts of mIgM, where the anti-CD79a mAb only appeared to immunoprecipitate small amounts of mIgM not associated with CD79b. Interesingly, the size of the CD79b protein immunoprecipitated varied depending on the anti-BCR mAb used. The anti-CD79b and anti-λ mAb immunoprecipitated a smaller protein compared to the anti-Fdμ, anti-Id and polyclonal anti-μ Ab.

4.2.12 The use of thesit detergent to investigate BCR complexes

Following the successful application of BN-PAGE, it was decided to use thesit detergent, a slightly stronger non-ionic detergent at titrating concentrations. This was to investigate the strength of the association of the CD79 heterodimer with mIgM when BCR complexes were immunoprecipitated from EHRB cells treated with either the anti-Fcμ or anti-Fdμ mAb. Figure 4.24 shows that, as shown previously, cells treated with the anti-Fcμ mAb only immunoprecipitated mIgM complexes and not CD79b. Anti-Fdμ mAb immunoprecipitated complete BCR complexes, which were not disrupted as the concentration of thesit in the lysis buffer increased. Therefore, anti-Fcμ mAb appears to only immunoprecipitate large mIgM complexes not associated with CD79b, compared to cells treated with other anti-BCR mAb directed at the mIgM domain of the BCR which immunoprecipitated complete BCR complexes.

4.2.13 The association of BCR with lipid rafts from EHRB cells treated with the anti-BCR mAb.

Another method used to investigate the effect of mIgM cross-linking on B cell activation is sucrose density gradient centrifugation. This method allows analysis of protein translocation into lipid insoluble fractions of the plasma membrane rafts, upon cross-linking mIgM with mAb[118]. Following treatment of EHRB cells with either: anti-Fcμ, anti-Fdμ, or polyclonal anti-μ Ab, cells were lysed with 1% TX-100 lysis buffer, layered onto continuous sucrose gradients and separated overnight by centrifugation at 45,000 rpm. Sequential 0.5 ml fractions were removed and resolved by SDS-PAGE. The BCR in each fraction was probed using anti-μ and anti-CD79b Ab. Figure 4.25 shows that the majority of IgM resides in the lipid soluble fractions (5 to 10) when cells were treated with the control mAb. However, when cells were treated with either the anti-Fcμ, or polyclonal anti-μ Ab, small amounts of IgM translocated into the lipid insoluble fractions (Fractions 1 to 4). These fractions were confirmed to be the lipid insoluble fractions by the use of an anti-PAG mAb. PAG has previously been shown to have a higher expression in the lipid insoluble fractions of the plasma membrane. The PAG fraction is highest in fraction 3 indicating that

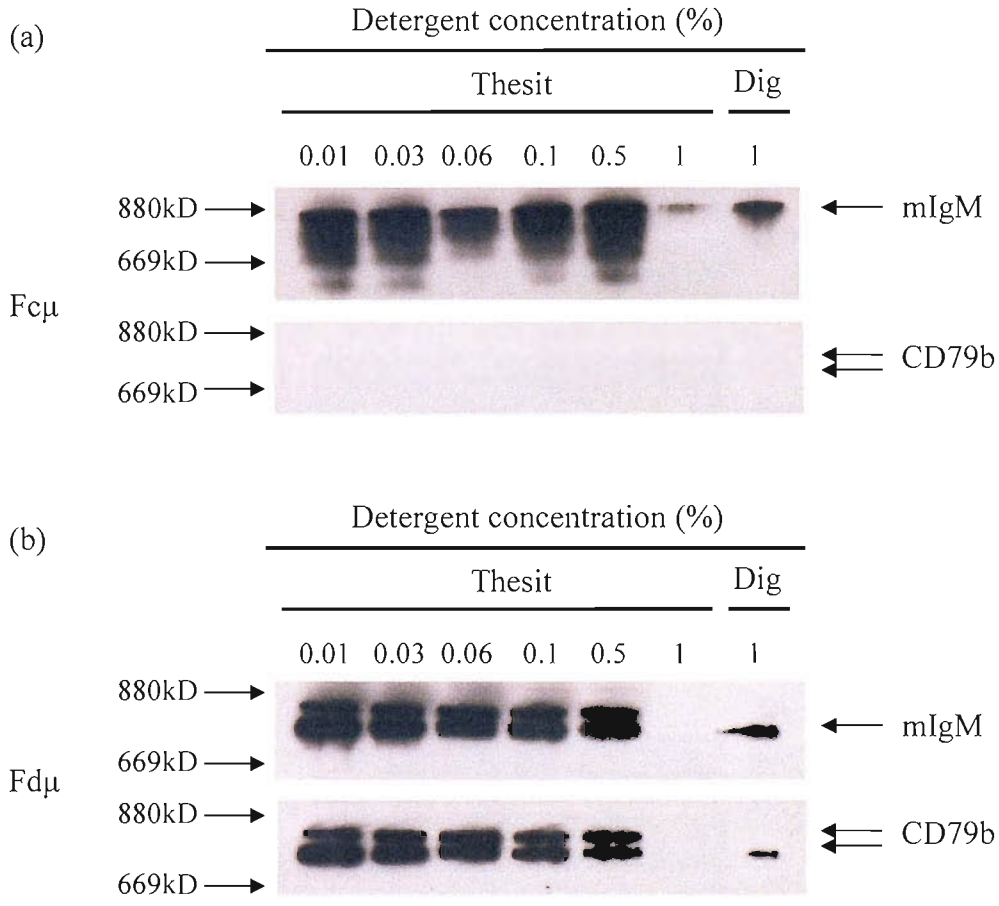

Figure 4.24 Use of thesit detergent on BCR complexes separated by BN-PAGE. 4x10^6 EHRB cells were incubated with either anti-Fcμ (M15/8, a) or Fdμ (XG9, b) mAb for 30 minutes on ice. Cells were lysed in various concentrations of thesit detergent or 1% digitonin buffer and BCR complexes were immunoprecipitated with protein A beads and separated on 12.5-5.5% BN-PAGE gels as detailed in Figure 4.20. The presence of BCR complexes was assessed by immunoblotting for either mIgM or CD79b. Cells were lysed in the following detergents; lane 1 is 1%Thesit, lane 2 is 0.5% Thesit, lane 3 is 0.1% Thesit, lane 4 is 0.06% Thesit, lane 5 is 0.03% Thesit, lane 6 is 0.01% Thesit and lane 7 is 1% digitonin. Representation of at least two independent experiments.

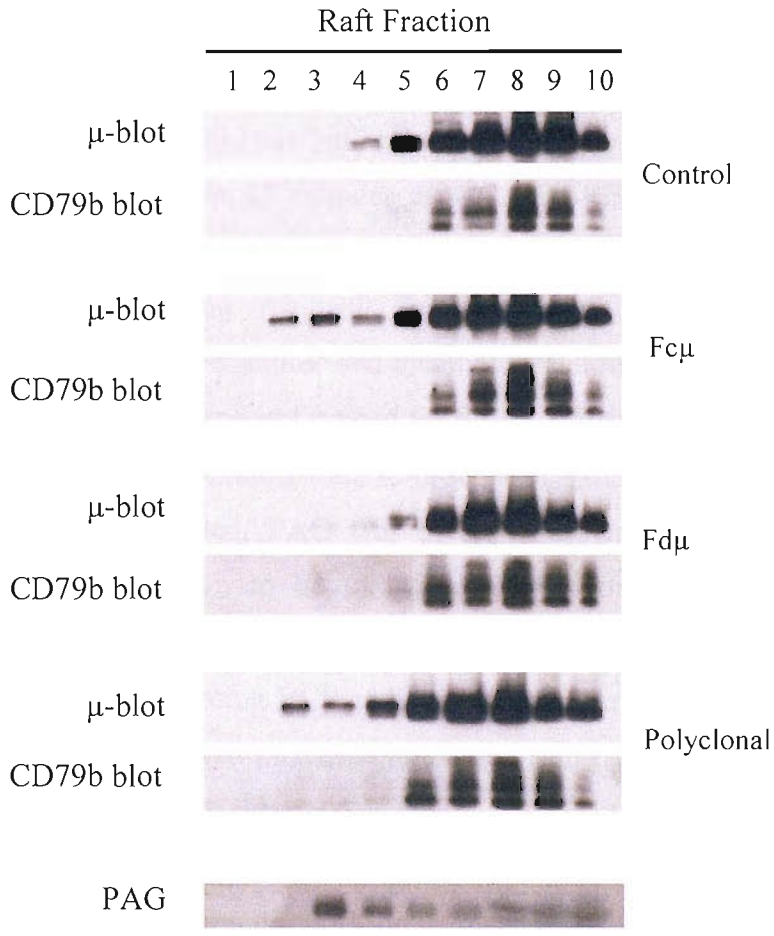

Figure 4.25 Lipid raft analysis of BCR complexes from EHRB cells stimulated with various mAb. $2x10^7$ EHRB cells were treated with various Ab ($25\mu g/10^6$ cells) for 30 minutes on ice, washed in PBS and incubated at 37°C for 5 minutes in a pre-warmed water bath. Samples were washed twice with ice cold PBS and followed by lysis in TX-100 MES lysis buffer. Samples were separated over continuous Optiprep gradients at 45,000rpm for 16 hours at 4°C. Equal fractions were removed, separated on 12.5% SDS-PAGE gels, transferred to PVDF membranes and immunoblotted for the presence of IgM and CD79b as detailed in Figure 4.7. Fractions containing the presence of lipid raft insoluble fractions were detected using anti-PAG mAb, followed by appropriate HRP labeled secondary Ab. Cells were treated with the following Ab; control is CP1/17, Fcμ is M15/8, Fdμ is XG9, and Polyclonal Ab. Representative of three independent experiments.

this area of the lipid raft assay contains the lipid insoluble fractions. The mIgM of cells treated with the anti-Fdμ mAb failed to translocate IgM into the lipid insoluble fractions. Interestingly, CD79b did not translocate into lipid insoluble fractions from cells stimulated with either the anti-Fcμ or polyclonal Ab, although IgM translocated with both treatments.

A more rapid, refined method used for investigating movement of proteins into lipid insoluble fractions was also employed as described by[153]. This method involves lysis of treated cells with 1% TX-100 lysis buffer and separation into pellet and lysate fractions by centrifugation at 16,000g for 15 minutes at 4°C. EHRB cells were treated with either control, anti-Fcμ, anti-Fdμ and as a positive control for raft redistribution, the anti-CD20 mAb Rituximab. Following treatment, lysis and separation, supernatant from treated samples was removed and the soluble and insoluble fractions were resolved by SDS-PAGE, transferred to PVDF membrane and probed for the BCR using anti-μ or anti-CD79b Ab. As a method and loading control, blots were re-probed for PAG, CD20 and β-actin. These data demonstrate that, as expected, PAG was present only in the insoluble pellet fraction. Similarly, CD20 was shown to be redistributed into the insoluble fraction following Rituximab treatment. Thus such, these data validate the technique for detecting redistribution events. Regarding BCR redistribution, Figure 4.26a shows that cells treated with the anti-Fcμ mAb showed increased amounts of mIgM in the insoluble/pellet fraction compared to cells treated with the anti-Fdμ mAb. Again, CD79b did not translocate into the insoluble fraction of cells treated with the anti-Fcμ mAb. In fact, the level of CD79b present in the insoluble fraction did not change regardless of which mAb was used to cross-link the BCR. Subsequently, the experiment was repeated several times and the amount of IgM and CD79b in the pellet or lysate fraction was quantitated using densitometry. These data are shown in Figure 4.26b, and demonstrate that about 20% of IgM was moved into the pellet fraction when cells were treated with the anti-Fcμ mAb, compared to cells treated with the other mAb, where the amount of IgM present in the pellet fraction did not change when compared to cells treated with the irrelevant control mAb.

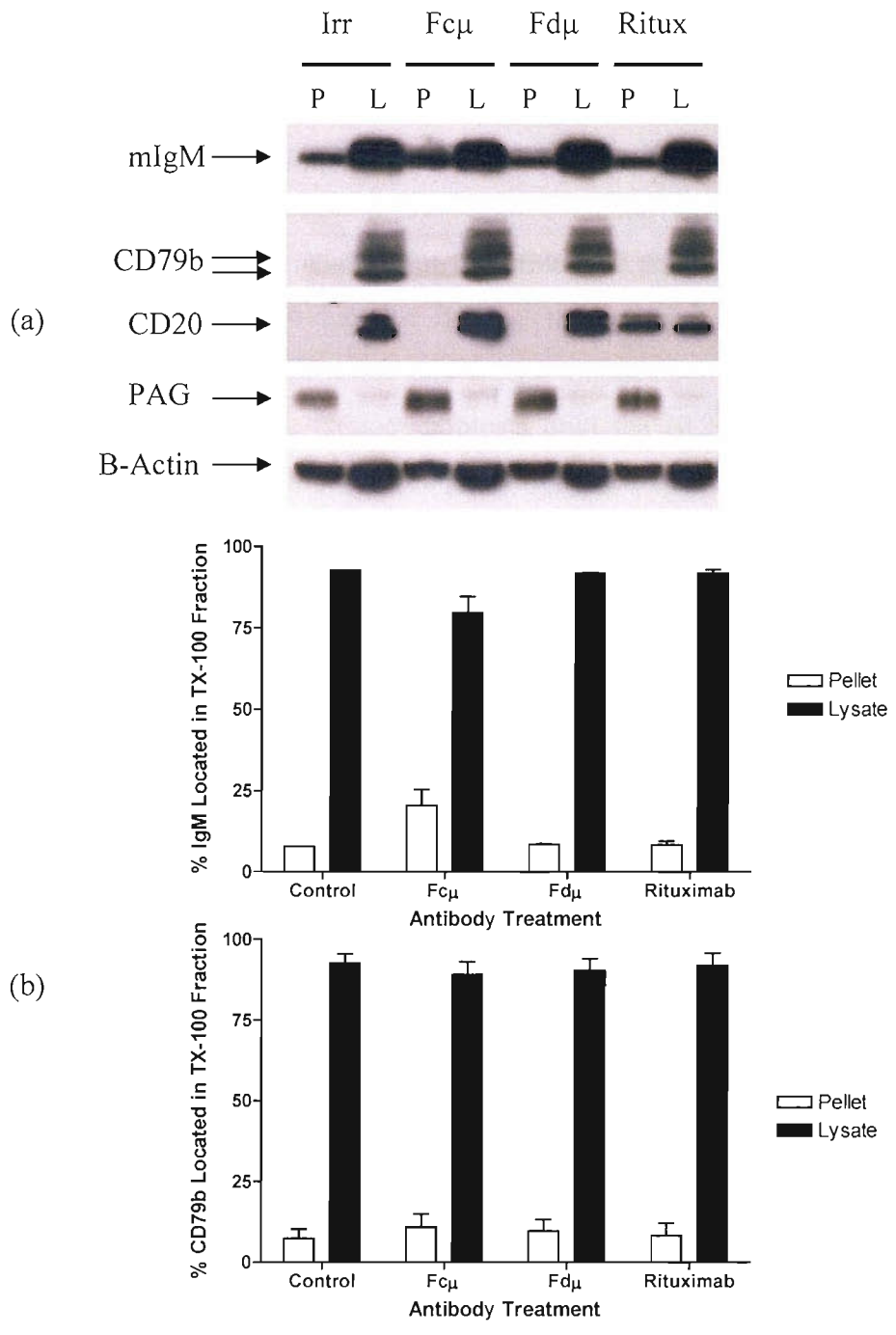

Figure 4.26 Analysis of BCR complexes in TX-100 insoluble and soluble fractions. $4x10^6$ EHRB cells were treated with various mAb (10μg/ml) for 30 minutes on ice. Samples were then lysed in TX-100 lysis buffer. Supernatant was removed (lysate, L) and pelleted (pellet, P) debris was washed four times in ice cold lysis buffer prior to solubalising in SDS-LB. (a) Protein was separated on 12% SDS-PAGE gels, and immunoblotted for presence of IgM and CD79b in pellet of lysate fractions as detailed previously. For controls blots were probed for the presence of CD20 (7D1, 1:100), anti-PAG, and anti β-Actin (1:14000), followed by addition of appropriate secondary Ab. Representative of three independent experiments. (b) Levels of IgM and CD79b present in lysate and pellet fractions were analysed using densitometry and calculated to percentage in each fraction, mean values ± SD from three independent experiments. Cells were treated with the following mAb; Control (Irr) is CP1/17, Fcμ is M15/8, Fdμ is XG9, and Ritux is Rituximab.

4.3 Discussion

The main aim of this chapter was to investigate the cellular mechanisms which allow the anti-Fcμ mAb to induce apoptosis when bound to the BCR. From the previous chapter, it is clear that there are differences in the length of signal induced by the binding of different anti-BCR mAb. One explanation for the prolonged signalling caused by anti-Fcμ mAb is that the mAb could be holding the BCR at the cell surface for a longer period of time, compared to other anti-BCR mAb that do not induce apoptosis. One possible explanation could be that mAb which induce apoptosis hold the BCR in lipid rafts for a prolonged period of time, leading to prolonged signalling and cell death. Therefore, we also wanted to investigate the nature of the BCR complex associated with the different mAb.

Initial experiments were set up to observe the level of mAb bound to the BCR. Interestingly, these results indicate that the anti-BCR mAb that do not induce apoptosis (anti-Fdμ, λ light chain and Id mAb); bound twice as much compared to the anti-Fcμ mAb that induces apoptosis. One explanation for this, suggests that the anti-Fdμ, λ or Id mAb may bind to a single BCR, whereas the anti-Fcμ mAb may bind to two separate BCR. These binding levels appear to fit in with observations made by Elliott, *et al.*,[179]. Their data suggest that anti-BCR mAb which bind between mIgM (bigamously), like the anti-Fcμ mAb, provide protection from lymphoma in animal models. Conversely, the anti-BCR mAb which bind to a single mIgM molecule (monogamous binding), fail to protect against *in-vivo* tumour challenge. Therefore, bigamously bound mAb could induce apoptosis by effectively cross-linking mIgM and holding the BCR at the cell surface for longer periods of time, allowing prolonged signalling.

One possible way of sustaining the intracellular signal would be to retain the BCR at the cell surface for a longer period of time. As mentioned above, the BCR held at the surface for a prolonged period of time could interact with an increased number of PTK located within the lipid raft as suggested by Pierce, *et al.*,[118] and this may lead to cellular apoptosis. Therefore, we wanted to know if this sustained signal was caused by the BCR being retained at the cell surface when cells were treated with the anti-Fcμ mAb. An important fact in B cell immunology is that BCR bound with antigen or Ab readily internalise, a process that allows antigen to be processed and presented to T cells via MHC class II molecules[3]. Interestingly, on the EHRB and BL-60 cell lines that are sensitive to apoptosis stimulated by anti-BCR mAb, polyclonal anti-μ Ab induced the quickest rate of mIgM

modulation. However, although a large proportion of mIgM was modulated when cells were treated with the anti-Fcμ mAb, the rate of mIgM modulation was not different from cells treated with the other anti-IgM mAb. Monoclonal Ab directed at the CD79 heterodimer had little effect on the amount of mIgM or CD79 modulated over short periods of time. However, a combination of both anti-CD79a and CD79b mAb led to an increased rate of mIgM modulation. These results suggest that the rate of mIgM modulation has little effect on the ability of anti-BCR mAb to induce apoptosis.

Next, we decided to investigate the modulation rate of the CD79 heterodimer on EHRB cells. Cells treated with the anti-Fcμ mAb showed a reduction in the amount of CD79a and CD79b modulated, compared to cells treated with anti-Fdμ or anti-λ light chain mAb. Therefore, it appears that although the anti-Fcμ mAb induces rapid modulation of bound mIgM from the cell surface, a proportion of the CD79 heterodimer may remain. In EHRB cells stimulated with anti-BCR mAb that induce apoptosis, the mIgM appears to also dissociate from the CD79 heterodimer. Previous studies have shown that mIgM of anergic B cells physically dissociate from the CD79 heterodimer, preventing generation of intracellular signals upon binding of antigen[180, 181]. However, as discussed in the previous chapter, cells treated with the anti-BCR mAb that induce apoptosis continue to signal for up to 1 hour following treatment with mAb. As mIgM may disassociate from the CD79 heterodimer, it is likely that mIgM is modulated leaving the CD79 heterodimer at the cell surface in contact with PTK. As the CD79 heterodimer is not internalised, the signalling cascade is not shut down, leading to prolonged signalling and apoptosis.

To confirm that the anti-Fcμ mAb causes disassociation of mIgM from the CD79 heterodimer, we devised a method that would allow immunoprecipitation of anti-BCR mAb along with bound BCR complexes. Cells were lysed with 1% digitonin lysis buffer. Digitonin allows whole BCR complexes to be isolated from the cell without disruption of the complete BCR complex[109].'

An interesting observation from the immunoprecipitation experiments was that different anti-BCR mAb bound to the cell surface immunoprecipitated different amounts of mIgM. Interestingly, complete BCR complexes were not immunoprecipitated when EHRB cells were treated with the anti-Fcμ mAb as large amounts of mIgM were immunoprecipitated that were not associated with CD79b. We knew that when the anti-Fcμ mAb was added to cell lysates whole BCR complexes could be immunoprecipitated, shown by the presence of

IgM and CD79b and therefore this defect was not due to an inability of the mAb to IP the whole BCR per se. As expected, the other anti-BCR mAb raised against the mIgM domain of the BCR bound the whole BCR complex, but the amount of mIgM immunoprecipitated was smaller than the amount immunoprecipitated with the anti-Fcμ mAb. When developing this immunoprecipitation method, differences in the amount of CD79b immunoprecipitated with mIgM were observed, depending on the number of times the Sepharose beads were washed in cold lysis buffer. This could be due to either free CD79b protein binding to the Sepharose beads, or the disruption of the BCR complex as CD79b is ionically bound to mIgM. Therefore, this method, although giving good preliminary data needs to be more thoroughly investigated for future use.

This phenomenon clearly acted independently of cellular mechanisms. Inhibition of cellular metabolic activity with specific inhibitors, or binding anti-BCR mAb on ice without warming the cells to 37°C, fails to prevent immunoprecipitation of these large mIgM complexes immunoprecipitated with the anti-Fcμ mAb. This suggests that these large immunoprecipitated mIgM complexes could be caused directly by binding of the mAb to the BCR, and not due to a cellular response.

Together, these results suggest that the anti-Fdμ, λ, or Id mAb immunoprecipitated single complete BCR complexes. This is due to the fact that these mAb immunoprecipitated less mIgM, probably because they bind monogamously to the BCR, with one Ab molecule binding to one mIgM molecule. Anti-Fcμ mAb that could bind bigamously between BCR complexes, immunoprecipitated more mIgM, as one Ab molecule can bind to two mIgM molecules. To help prove this theory, EHRB cells were incubated with concentrations of mAb that gave equal levels of bound mAb. However, the anti-Fcμ mAb still immunoprecipitated more mIgM compared to the other anti-BCR mAb, even when the same amount of mAb was bound at the cell surface as the other anti-BCR mAb.

Another theory for the large amounts of mIgM immunoprecipitated with anti-Fcμ mAb was that free mAb that had not bound to surface mIgM was available to bind to cytosolic IgM when the cells were lysed, prior to immunoprecipitation. To address this question, EHRB cells were surface radio-labelled with I^{125} and BCR complexes immunoprecipitated following binding of mAb to surface BCR, or addition of mAb to cell lysates. Results showed that the level of surface mIgM immunoprecipitated with the anti-Fcμ mAb was greater than that observed when cells were treated with the other anti-BCR mAb. Cell

lysates showed that all anti-BCR mAb directed at different regions of mIgM immunoprecipitated complete BCR complexes, shown by the presence of mIgM and the CD79 heterodimer.

Monoclonal Ab directed at the CD79 heterodimer did not immunoprecipitate any mIgM. CD79b could only be immunoprecipitated from cells treated with the anti-CD79b mAb and not the anti-CD79a mAb. This suggests that binding of CD79 mAb to the BCR could spatially disrupt the BCR complex, this may also account for the low levels of BCR internalised from the surface of different cell lines treated with either the anti-CD79a or anti-CD79b mAb alone. Interestingly, when combinations of the anti-CD79a and b mAb were used, an increase in the amount of internalised mIgM was observed. However, only very small amounts of mIgM were immunoprecipitated when EHRB cells were treated with a combination of the anti-CD79a and b mAb. This could imply that the anti-CD79 mAb causes a disassociation of mIgM from the CD79 heterodimer upon binding that does not induce apoptosis; this could be due to the anti-CD79 mAb failing to pull the BCR into lipid rafts or successfully disrupting an oligomaeric BCR. This aspect of BCR disruption at the cell surface needs to be investigated further; perhaps using fluorescent microscopy to observe what happens to the bound BCR complexes at the cell surface.

There have been two major theories recently proposed for initiation of intracellular signals upon BCR cross-linking. The first theory, proposed by Reth, *et al.*,[30, 42] suggests that upon binding of Ag, the BCR which exists as an oligomer on the cell surface is disrupted. The disruption of the BCR oligomer blocks the interaction of the PTP: SHP with the PTK: Syk, allowing Syk to phosphorylate and bind to the cytoplasmic ITAM motifs located on the CD79 heterodimer[30, 128], causing the initiation of the BCR signal. One way to investigate this theory is to use a new method of PAGE, known as BN-PAGE[155, 182], which has been adapted to allow separation of complete BCR complexes[30].

Therefore, BN-PAGE was adapted to allow us to investigate the nature of the BCR complexes immunoprecipitated by the different anti-BCR mAb. We were also interested to know if there were differences in the size of the BCR complex immunoprecipitated with the anti-Fcμ mAb, compared to BCR complexes immunoprecipitated with other anti-BCR mAb. BN-PAGE showed that the anti-Fcμ mAb immunoprecipitated a slightly larger complex than the anti-BCR mAb directed at other regions of mIgM. The size of the complete BCR complex immunoprecipitated with the anti-Fdμ, anti-λ and anti-Id mAb was in the

molecular range shown by Schamel and Reth[30] to be an oligomeric BCR. Therefore, the anti-BCR mAb that do not induce apoptosis could bind monomerically to a single complete BCR complex, this single BCR complex then remains part of an oligomeric complex containing more than one BCR. However, as shown with SDS-PAGE, the anti-Fcμ mAb did not immunoprecipitate complete BCR complexes when resolved on BN-PAGE. CD79b was shown not to be associated with mIgM immunoprecipitated with anti-Fcμ mAb, compared to the other anti-BCR mAb that co-immunoprecipitated both mIgM and CD79b. The large mIgM complex immunoprecipitated with the anti-Fcμ mAb could be accounted for by the fact that the mAb bind bigamously to two mIgM molecules. If the mIgM are still in an oligomeric complex, then one anti-Fcμ mAb could bind between complexes immunoprecipitating larger amounts of mIgM, as observed.

Our results suggest that the anti-Fcμ mAb may bind bigamously between BCR, disrupting the BCR oligomeric complex. This disruption could lead to the CD79 heterodimer disassociating from mIgM, allowing prolonged intracellular signalling and induction of apoptosis. This would fit in with the theory proposed by Reth, *et al.*,[30, 42, 128] who have shown that activation of intracellular signalling cascades of B cells involves BCR in an oligomeric complex. However, BN-PAGE has never been used to observe the effects of mAb bound to oligomeric BCR complexes. It has also never been reported that anti-BCR mAb can cause a disassociation of the CD79 heterodimer from mIgM. Another interesting observation from the BN-PAGE gels was that different mAb immunoprecipitated CD79b associated with mIgM that were of different sizes. This may be due to different glycosylation states of CD79b, which have been reported by Payelle-Brogard, *et al.*,[192]. Another theory is that CD79b could be differentially phosphorylated, depending upon the mAb used to cross-link the BCR complex. However, both of these ideas need to be investgated further beforte a conclusion can be reached.

The second, more popular theory to explain initiation of intracellular signalling cascades upon cross-linking BCR proposes that cross-linked BCR translocate into lipid raft domains of the plasma membrane[114]. Therefore, we decided to investigate the association of BCR complex with lipid rafts upon cross-linking with different anti-BCR mAb. Initial lipid raft immunoblots showed that a small amount of the BCR complex translocates into lipid rafts following ligation with the anti-Fcμ and polyclonal anti-μ Ab. This was compared to cells treated with the anti-Fdμ or control mAb, where the BCR remained in the lipid soluble fraction. However, lipid raft immunoblots showed that following incubation of cells with

either the anti-Fcμ or polyclonal anti-μ Ab, a proportion of the BCR remained in the soluble fractions. Previous work has suggested that only 30 to 40% of the BCR translocates into lipid rafts following cross-linking[114, 118], however, in our hands, the percentage appeared to be much lower. The reasons for this difference are uncertain.

Interestingly, the CD79b heterodimer did not translocate into lipid raft fractions following cross-linking BCR with anti-BCR mAb, assessed with both the sucrose density gradient and lipid/pellet methods. This suggests that the CD79 heterodimer remains outside lipid rafts in EHRB cells following BCR cross-linking with all of the anti-BCR mAb. This does not agree with Pierce's theory that complete BCR translocate into lipid rafts rich in the Src family kinase, Lyn, initiating BCR signalling following BCR cross-linking[114]. These results again add support to the oligomeric BCR complex theory proposed by Reth, *et al.*,[30, 128] that suggest BCR signalling is initiated by the PTK: Syk, upon BCR cross-linking.

In conclusion we have shown that anti-BCR mAb that induce apoptosis of the BCR sensitive cell line EHRB, leads to a physical disassociation of mIgM from the CD79 heterodimer. However, as discussed in the previous chapter, these anti-BCR mAb that induce apoptosis cause prolonged intracellular signalling for up to 1 hour after stimulation. Therefore, in this model we suggest that cross-linking the BCR with the anti-Fcμ mAb causes a disassociation of the CD79 heterodimer from mIgM, where the CD79 heterodimer remains at the cell surface signalling for a prolonged period of time. Further to this, we believe that mIgM translocates into lipid raft domains upon cross-linking with anti-Fcμ mAb, where it is internalised leaving activated CD79 heterodimers in the lipid soluble region of the cell membrane to continue signalling with the PTK: Syk, leading to apoptosis.

Chapter 5

Identification and characterisation of an alternative transcript of murine CD79b

5.1 Introduction

CD79b forms one half of the CD79 heterodimer which is vital for initiating intracellular signalling pathways following cross-linking of the BCR[4]. An alternative transcript of human CD79b has also been reported by Hashimoto, *et al.*,[138]. Alternative mRNA splicing is an important mechanism for allowing production of multiple proteins that have distinct functions from single genes[143]. In this truncated transcript the whole of exon three is deleted forming an alternative transcript that lacks the Ig-like extracellular domain (hΔCD79b).

Although there have been several mutations of human CD79b reported in the literature[134], the alternative transcript of CD79b is of most interest as its over-expression has been reported in human B-CLL samples[134, 140]. Work by Cragg *et al.*,[141] within this laboratory identified that hΔCD79b, when over-expressed in human B cell lines, inhibited BCR induced apoptosis. Therefore, the aim of this chapter was to investigate whether an alternative transcript of CD79b is present in murine B cells (mΔCD79b), and to observe whether it shares homology with hΔCD79b. If mΔCD79b does exist, it was decided to investigate whether expression of an alternative transcript had the same effect on inhibition of BCR induced apoptosis in murine B cells, as observed in human B cell lines, and to determine how it performs this function

5.2 Results

5.2.1 Identification of an alternative transcript of CD79b in murine B cells.

As increased levels of hΔCD79b have been reported in human B cell lymphomas, it was decided to base the preliminary investigation of mΔCD79b on two murine B lymphoma models extensively used in the laboratory. As such, mRNA was extracted from splenocytes of animals bearing the BCL_1 or A31 tumours, along with splenocytes from the two host strains of mice; Balb/c and CBA, respectively. To perform this analysis mRNA from $1x10^7$ splenocytes was isolated, converted to cDNA using first strand cDNA synthesis, and PCR performed using primers directed towards the full length molecule of mCD79b with *Taq* polymerase. As shown in Figure 5.1, a PCR product correlating to the full length molecule of mCD79b (~678bp) was identified in all cDNA samples. A further, smaller ~480bp PCR product was also apparent which correlates to the size predicted for a truncated transcript of mCD79b that lacks the whole of the extracellular Ig-like domain. Interestingly this smaller PCR product was also detected in naïve splenocytes from the host mice not inoculated with the tumour cells.

5.2.2 Sequence analysis of mΔCD79b.

To determine the sequence of mΔCD79b, PCR was again performed using BCL_1 and A31 cDNA and primers directed to full length CD79b but this time with *Pfu* polymerase, to minimise PCR errors. Both 678 and 480bp DNA bands were extracted from agarose gels, ligated into TOPO sequencing vectors and transformed into TOP10 pre-competent cells. 100 ng of each PCR product was then sequenced by fluorescent sequencing and analysed using Chromas software. Sequencing confirmed the larger PCR product to be mCD79b and that the 480bp product was indeed and alternative transcript of mCD79b, which lacks exon 3. The sequence obtained for mΔCD79b is shown in figure 5.2, together with the relevant sequences reported for full length murine CD79b[11], human CD79b[183] and hΔCD79b[138] (human sequences shown in blue text). It is clear from the sequence comparisons that mΔCD79b is highly analogous to hΔCD79b in its structure and also contains a potential splice site (**BOLD**), that leads to the exclusion of the whole of exon three.

Differences between human and murine sequence are indicated in red in the murine sequence. Figure 5.2 confirms that whilst the leader sequence (exon 1) and in particular the extracellular domains (exons 2 and 3) of mCD79b do not share extensive homology to hCD79b, the transmembrane (exon 4) and intracellular domains (exons 5 and 6) of both

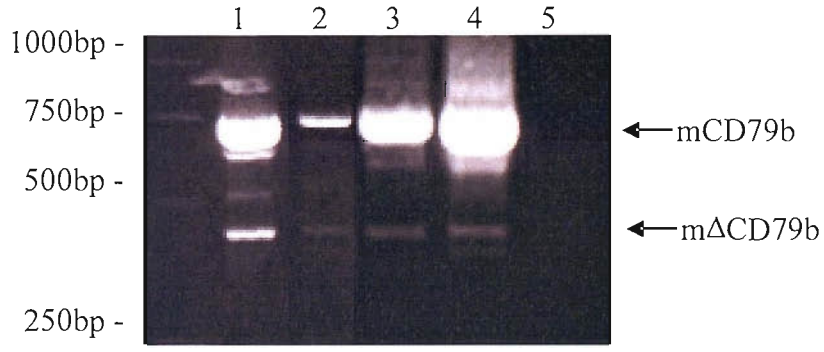

Figure 5.1 Identification of a truncated alternative transcript of mCD79b.
mRNA was extracted from $1x10^7$ splenocyes of mice bearing BCL_1 (lane 1), A31 (lane 2), or naïve splenocytes; Balb/c (lane 4), and CBA (lane 4) and converted to cDNA. Primers directed to full length mCD79b were used to identify both full length mCD79b (687bp) and a smaller PCR product correlating to that predicted for mΔCD79b compared to the no cDNA control (lane 5).

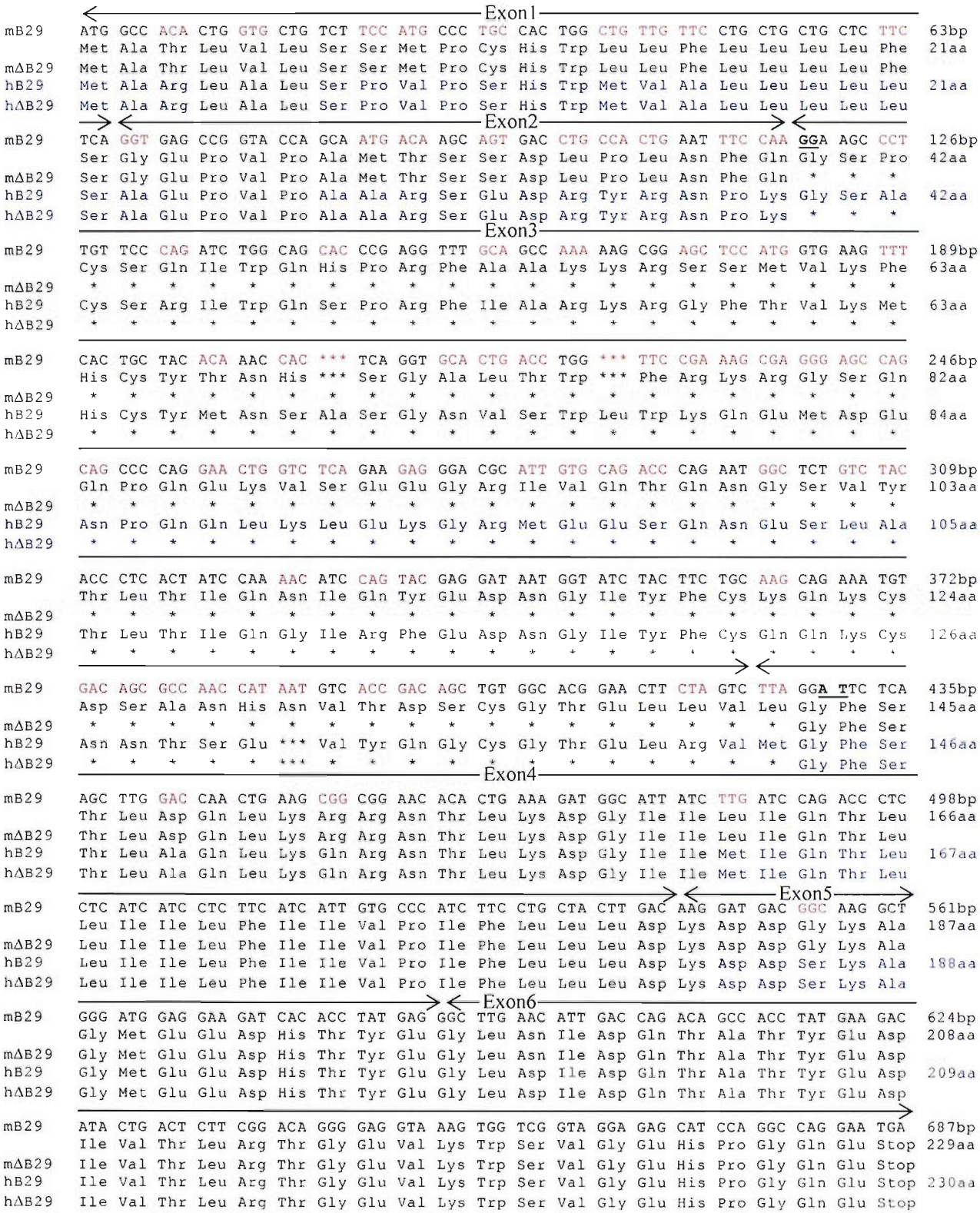

Figure 5.2 Sequence homology between mΔCD79b and the reported hΔCD79b sequence. Both truncated transcripts are compared to the published full-length sequences. Murine sequences are given in black along with nucleotide sequence, with differing amino acids to the human sequence (blue) shown by red nucleotides. Relevant base pairs and amino acid numbers are given down the right hand side. The arrow lines above nucleotide sequence give relevant exon numbers. mΔCD79b sequence was obtained from cDNA extracted from A31 lymphoma cells.

sequences share a high level of homology, indicating that these regions are important for the function of these proteins. Importantly, these conserved sequences are also present in the truncated proteins.

5.2.3 Identification of mΔCD79b at the protein level.

Following identification of mΔCD79b at the mRNA level in mouse cells it was decided to establish if mΔCD79b also existed as a protein. To address this question both full length and mΔCD79b PCR products were cloned into the pCI-puromycin (pCI-puro) expression vector (Appendix A). Following confirmation that the correct DNA sequence was inserted into the vector by sequencing, plasmid DNA was expanded using maxiprep kits as detailed in section 2.7.5 and 25 μg of maxiprep DNA transfected into COS-7 cells. Transfected COS-7 cells were then assessed 24 hours later following lysis of the cells in NP-40 lysis buffer, resolved by SDS-PAGE, protein transferred to PVDF membranes and immunoblotted for the presence of mCD79b.

Figure 5.3 shows that mCD79b and mΔCD79b were detected from lysates of COS-7 cells transiently transfected with both mCD79b and mΔCD79b pCI-puro expression vectors, compared to cells transfected with empty vector. The expression level for both proteins was similar, which may indicate a similar stability of the two transcripts. Transfected COS-7 lysates were probed with both the commercially available mAb HM79-11, raised against an extracellular peptide of mCD79b and the in-house mAb AT107/2, raised against a peptide in the cytoplasmic domain of hCD79b which shares homology with the mouse region. This antibody was raised in collaboration with Ms A Tutt and validated by its binding to peptide KLH in ELISA and its ability to immunoprecipitate the correct sized protein.

5.2.4 The presence of mΔCD79b in murine B cell lines.

Once the presence of mΔCD79b had been confirmed at the mRNA level in murine lymphoma cells and naive splenocytes, and at the protein level in an over-expression system (transfected COS-7 cells), it was decided to determine the endogenous level of mΔCD79b in a variety of murine B cell lines. The three cell lines chosen were WEHI-231, πBCL_1 and A20, which are thought to represent immature, mature and class-switched B cells, respectively. NB: πBCL_1 cells were derived from a variant of the BCL_1 tumour which had transformed and become capable of in vitro propagation. First, we assessed the level of CD79b mRNA transcripts. mRNA was extracted from the three cell lines and converted to cDNA prior to PCR using the primers detailed above. Figure 5.4a, indicates the presence of

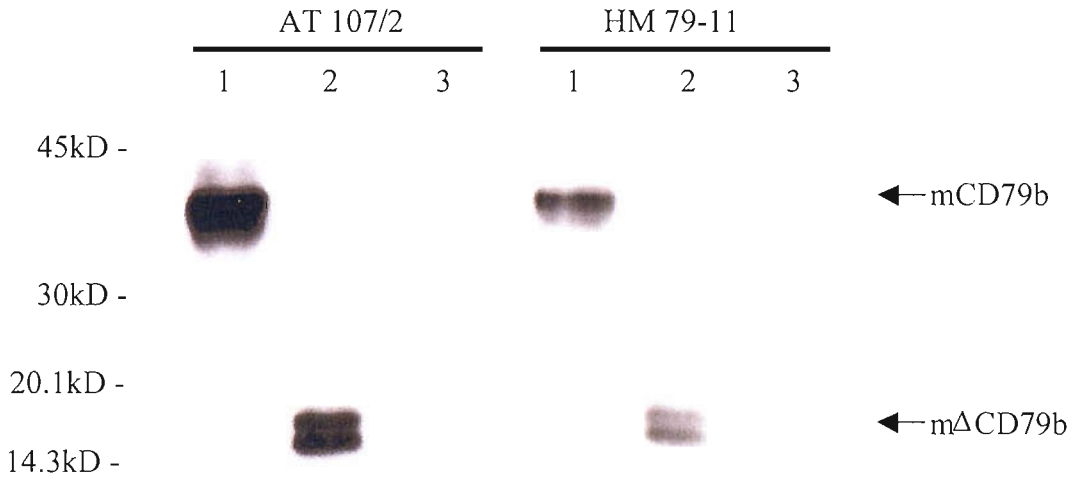

Figure 5.3 Identification of a truncated alternative transcript of mCD79b at the protein level. To observe if mΔCD79b is expressed at the protein level both full length mCD79b and mΔCD79b were cloned into the pCI-puromycin expression vector and subsequently transfected into COS-7 cell lines. Lysates were separated through 15% SDS-PAGE and membranes probed with AT107/2 and HM79-11 mAb to show the presence of both full length mCD79b (lane 1) and mΔCD79b (lane 2) compared to COS-7 cells transfected with an empty vector (lane 3).

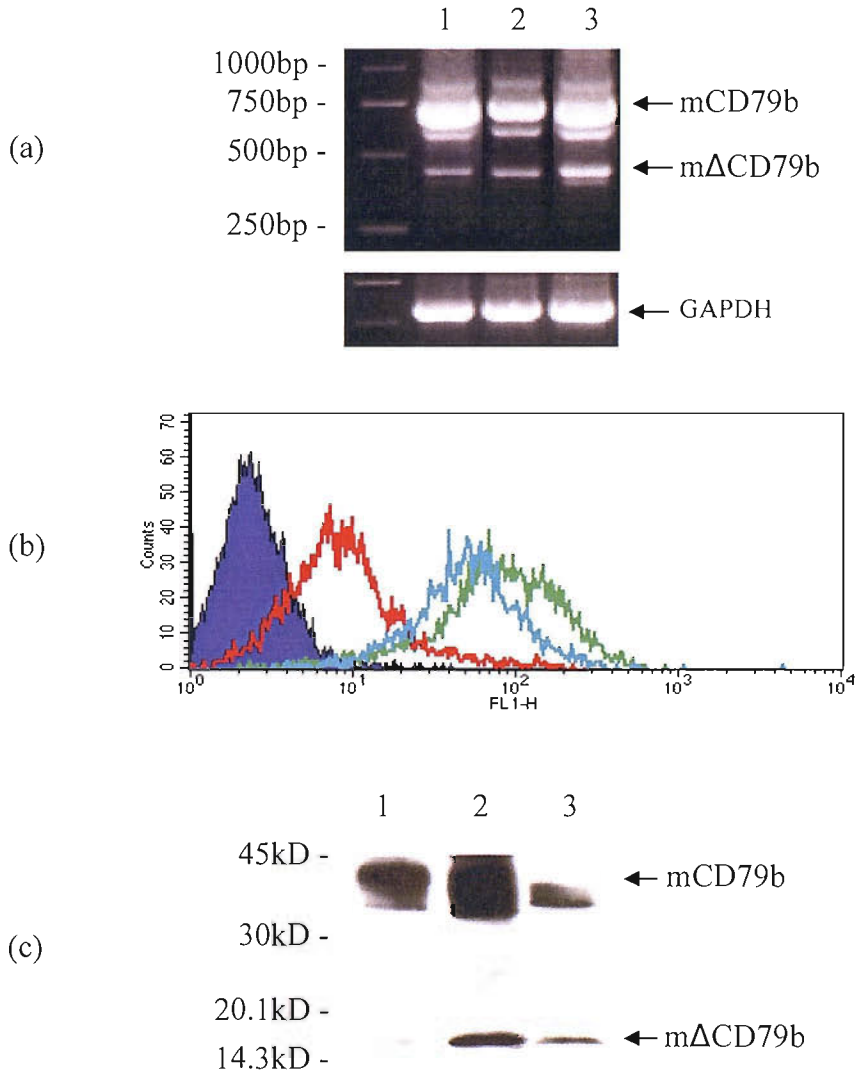

Figure 5.4 Identification of a mΔCD79b in various murine B cell lines. The level of expression of mΔCD79b was assessed in three *in vitro* murine B cell lines. Initially cDNA was obtained from 1x10^6 B cells and probed for the presence of mΔCD79b, Figure 5.4a, confirms varying levels of expression of mΔCD79b in the WEHI-231 (lane 1), πBCL$_1$ (lane 2) and A20 (lane 3) cell lines along with full length mCD79b at the mRNA level, compared to GAPDH controls. Next surface expression of mCD79b was assessed by flow cytometry (Figure 5.4b). Cells were stained with FITC conjugated HM79-11 and the level of expression assessed; irrelevant control (—), WEHI-231 (—), πBCL$_1$ (—), and A20 (—). The expression of both full length mCD79b and mΔCD79b was also assessed at the protein level in lysates from WEHI-231 (lane 1), πBCL$_1$ (lane 2) and A20 (lane 3) cell lines using the AT107/2 mAb (Figure 5.4c).

both full length mCD79b and mΔCD79b in all cell lines. A20 cells expressed the highest level of mΔCD79b followed by πBCL_1 cells, with slightly lower levels of expression observed in WEHI-231 cells. GAPDH PCR controls were used showing that for each sample a similar amount of mRNA was extracted and converted to cDNA.

Figure 5.4b, shows the surface expression of mCD79b on the murine B cell lines assessed by flow cytometry, using the FITC labelled mAb HM79-11. A20 cells expressed the lowest levels of surface mCD79b, WEHI-231 cells an intermediate level and πBCL_1 cells expressed the highest level.

Next, we assessed how the mRNA transcript levels related to the production of CD79b proteins in these cells. To perform these experiments, NP-40 lysates of the murine cell lines were prepared, separated on 15% SDS-PAGE gels and probed with AT107/2. πBCL_1 cells expressed the highest levels of mΔCD79b at the protein level, followed by A20 cells, with a faint protein band observed in WEHI-231 cells (Figure 5.4c). The levels of protein correlated with the mRNA expression levels shown above, in that the B cell lines πBCL_1 and A20 expressed the highest levels of mRNA for mΔCD79b with WEHI-231 cells expressing the lowest.

5.2.5 The effect of anti-μ mAb on BCR-induced apoptosis.

To address whether mΔCD79b has the same anti-apoptotic characteristics as shown for the human homolog, we needed to investigate if the B cell lines assessed above showed differences in their susceptibility to BCR-induced apoptosis. Before assessing the effect of BCR-induced apoptosis on the B cell lines, we first assessed whether the in-house anti-μ mAb (Mc39-12) could induce apoptosis upon cross-linking the BCR. The WEHI-231 cell line was used in preliminary experiments as it is reported that this cell line is sensitive to BCR induced apoptosis[184, 185]. Initially, $1x10^5$ cells were treated with 10 μg/ml of an isotype matched control (KT3) or the anti-μ mAb for 24 and 48 hours at 37°C. Cells were then assessed for levels of BCR induced apoptosis using the annexin V/PI flow cytometry assay. Figure 5.5a, shows that higher levels of BCR induced apoptosis were observed after incubation of WEHI-231 cells with the anti-μ mAb for 48 compared to 24 hours. For this reason, subsequent assays were performed for 48 hours.

To determine the optimal concentration of mAb, $1x10^5$ WEHI-231 cells were incubated with increasing concentrations of either the control or the anti-μ mAb for 48 hours at 37°C.

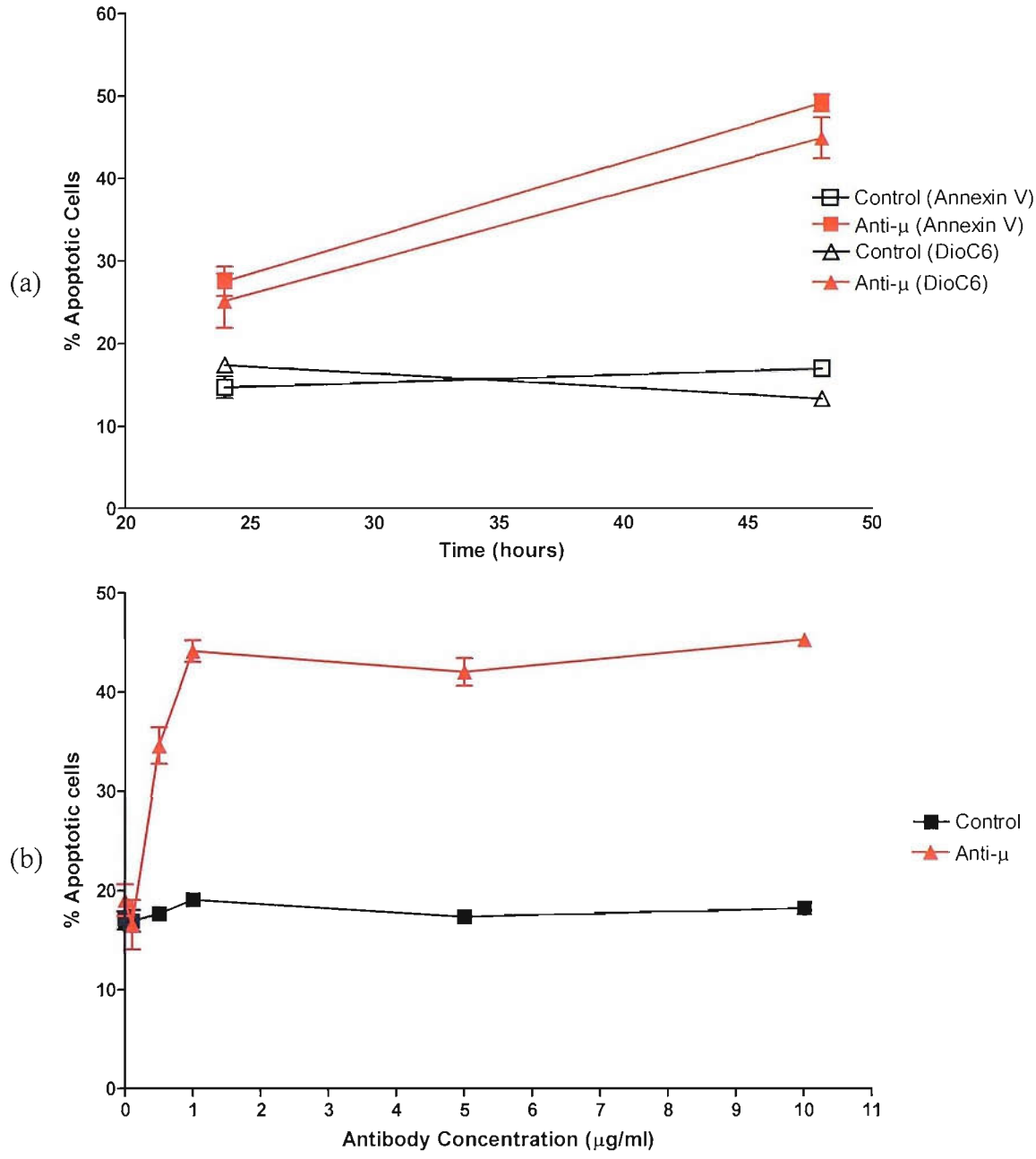

Figure 5.5 Effect of titrating anti-μ concentration on BCR induced apoptosis on WEHI-231 cell lines. (a) $1x10^5$ WEHI-231 cells were treated with either control (KT3) or anti-μ (Mc39-12) at 10 μg/ml for 24 or 48 hours, at 37°C and levels of BCR induced apoptosis assessed by flow cytometry using annexin V/PI (b) $1x10^5$ WEHI-231 cells were treated with various concentrations of either control (KT3) or anti-μ (Mc39-12) mAb for 48 hours at 37°C. Levels of apoptosis were assessed using annexin V/PI staining by flow cytometry. Results shown are mean values ± SD from three separate experiments.

Following stimulation, cells were again assessed for levels of BCR induced apoptosis using annexin V/PI by flow cytometry. Figure 5.5b, shows that WEHI-231 cells are sensitive to BCR induced apoptosis when the anti-μ mAb was used at concentrations above 1 μg/ml, compared to cells treated with the control mAb.

5.2.6 The effect of anti-BCR mAb on BCR-induced apoptosis on various murine B cell lines.

Following assessment of the anti-μ mAb on WEHI-231 cells, it was important to determine the levels of BCR-induced apoptosis on the other *in vitro* murine B cell lines. $2x10^5$ WEHI-231, πBCL_1 and A20 cells were treated with either: control (KT3), anti-μ or anti-κ (HB58) mAb at 10 μg/ml for 48 hours at 37°C. Cells were also treated with the anti-κ mAb, as A20 cells express mIgG and not mIgM like the other cell lines. Figure 5.6 shows that WEHI-231 cells are the most sensitive to BCR induced apoptosis, assessed by both annexin V/PI, with about 22% cells staining positive above controls, compared with BCL_1 cells, with only about 5% cells staining positive. A20 cells were more sensitive than πBCL_1 cells when the BCR was cross-linked with the anti-κ mAb, with 12% and 7% cells staining positive respectively, but again these cell lines were not as sensitive as WEHI-231 cells with more than 25% cells staining positive.

5.2.7 Altering the expression of mΔCD79b in WEHI-231 cells.

From the above data it was apparent that the levels of mΔCD79b expression may correlate with cellular susceptibility to BCR-induced apoptosis, at least in respect of the fact that the WEHI-231 cells expressed the lowest amount of mΔCD79b and were the most sensitive. Previous data has suggested that over-expression of hΔCD79b may account for a reduction in the expression of full length CD79b[138]. However, this was not observed in Ramos cell lines, where hΔCD79b was over-expressed[141]. From Figures 5.4 and 5.6 it is clear that the WEHI-231 cells that express the lowest levels of mΔCD79b are the most sensitive to anti-BCR-induced apoptosis. Therefore, it was decided to try and alter the expression of mΔCD79b in WEHI-231 cells to determine whether this would change their sensitivity to BCR induced apoptosis.

5.2.7.1 Over-expression of mΔCD79b in WEHI-231 cell line.

It was decided to over-express mΔCD79b in WEHI-231 cells, the hypothesis being that the cells would become resistant to BCR apoptosis. To achieve this, WEHI-231 cells were transfected with mΔCD79b:pCI-puro expression vector using electroporation. Clones were

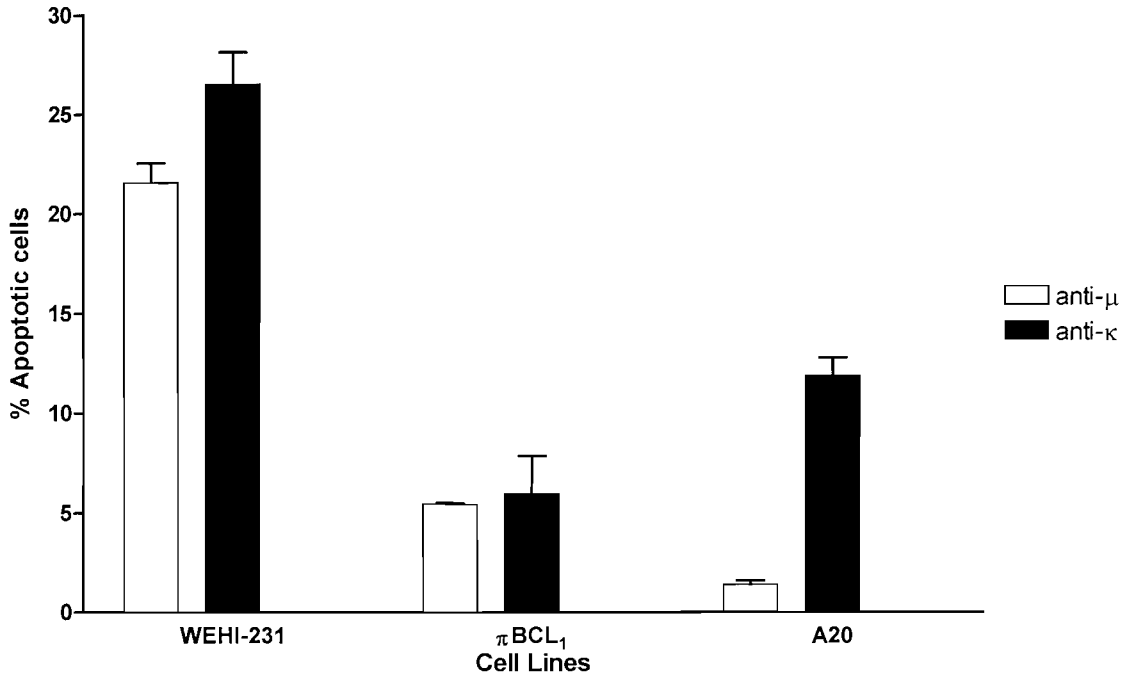

Figure 5.6 BCR induced apoptosis on various murine B cell lines. $2x10^5$ cells were treated with 10 μg/ml anti-μ (Mc39-12) or anti-κ (HB58) mAb for 48 hours at 37°C, levels of apoptosis was measured with Annexin V/PI by flow cytometry. Results shown are levels of induced apoptosis above cells treated with irrelevant control (KT3) and represent mean values ± SD from three separate experiments.

selected under puromycin and screened using RT-PCR. RT-PCR data (Figure 5.7a) shows that five clones of WEHI-231 that varied in levels of mΔCD79b expressed compared to wild type cells were obtained. GAPDH was used as a control for the amount of mRNA isolated. Previous data has suggested that over-expression of hΔCD79b may account for a reduction in the expression of full length CD79b[138]. However, this was not observed in Ramos cell lines, where hΔCD79b was over-expressed[141]. Interestingly, the surface expression of the BCR on these WEHI-231 clones also did not alter between the different clones and wild type cells, assessed by flow cytometry (Figure 5.7b) using the FITC labelled anti-μ and anti-CD79b mAb.

5.2.8 The effect of over-expressing mΔCD79b in WEHI-231 cells on BCR induced apoptosis.

The five different WEHI-231 clones which express increased concentrations of mΔCD79b were treated with either the control or the anti-μ mAb at 10 μg/ml for 48 hours at 37°C. Levels of BCR-induced apoptosis were assessed using annexin V/PI and DioC6 by flow cytometry. Figure 5.8 shows that WEHI-231 clones that express increased amounts of mΔCD79b are not as sensitive to BCR-induced apoptosis compared to wild type WEHI-231 cells. Interestingly, as the level of mΔCD79b expression increased so the sensitivity of the cells to BCR-induced apoptosis decreased, with clone Δ35 expressing the highest levels of mΔCD79b, being the least sensitive to BCR-induced apoptosis.

5.2.9 Cellular localisation of mΔCD79b.

It is clear that over-expression of mΔCD79b correlates with a reduction in cellular susceptibility to BCR induced apoptosis. As mΔCD79b contains an active ITAM motif which has been shown to be important for protecting human cell lines from BCR induced apoptosis[141], it was hypothesised that mΔCD79b must be situated at or near the plasma membrane, allowing it to interfere with PTK activation upon BCR cross-linking. To address this question, several experiments were devised to ascertain the cellular localisation of mΔCD79b.

5.2.9.1 Localisation of mΔCD79b tagged with YFP.

Both full length mCD79b and mΔCD79b cDNA were isolated from BCL_1 lymphoma cells using YFP primers containing the EcoR1 and BamH1 restriction sites (Table 2.1). Clones with the correct sequence of both full length and mΔCD79b were then ligated into the YFP expression vector, $pEYFP_{N1}$ (Appendix C). Following the use of restriction digests to

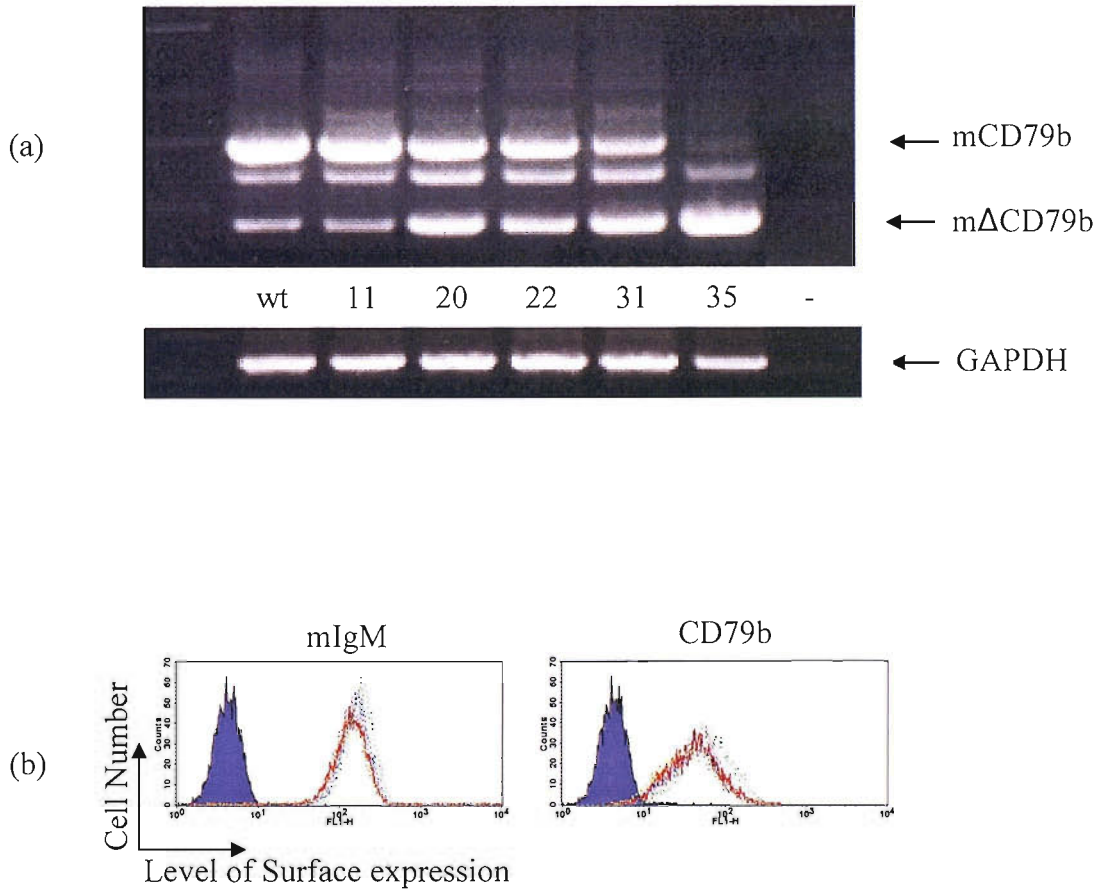

Figure 5.7 Over expression of mΔCD79b in WEHI-231 cell line does not affect BCR expression. WEHI-231 cells were transfected with mΔCD79b in the pCI-puromycin expression vector, and clones selected under puromycin. Five different clones were selected that expressed increasing levels of mΔCD79b compared to non-treated (wt) WEHI-231 cells, when analysed by RT-PCR. Figure 5.6 a, levels of mΔCD79b expressed in $1x10^6$ WEHI-231 clones assessed at the mRNA level compared to wt and GAPDH controls. Surface expression of the BCR receptor was assessed on all clones by flow cytometry (Figure 5.6 b). Cells were stained with either FITC conjugated anti-μ (Mc39-12) or anti-CD79b (HM79-11) as detailed in Figure 2, compared to wt control (—) and irrelevant mAb (—).

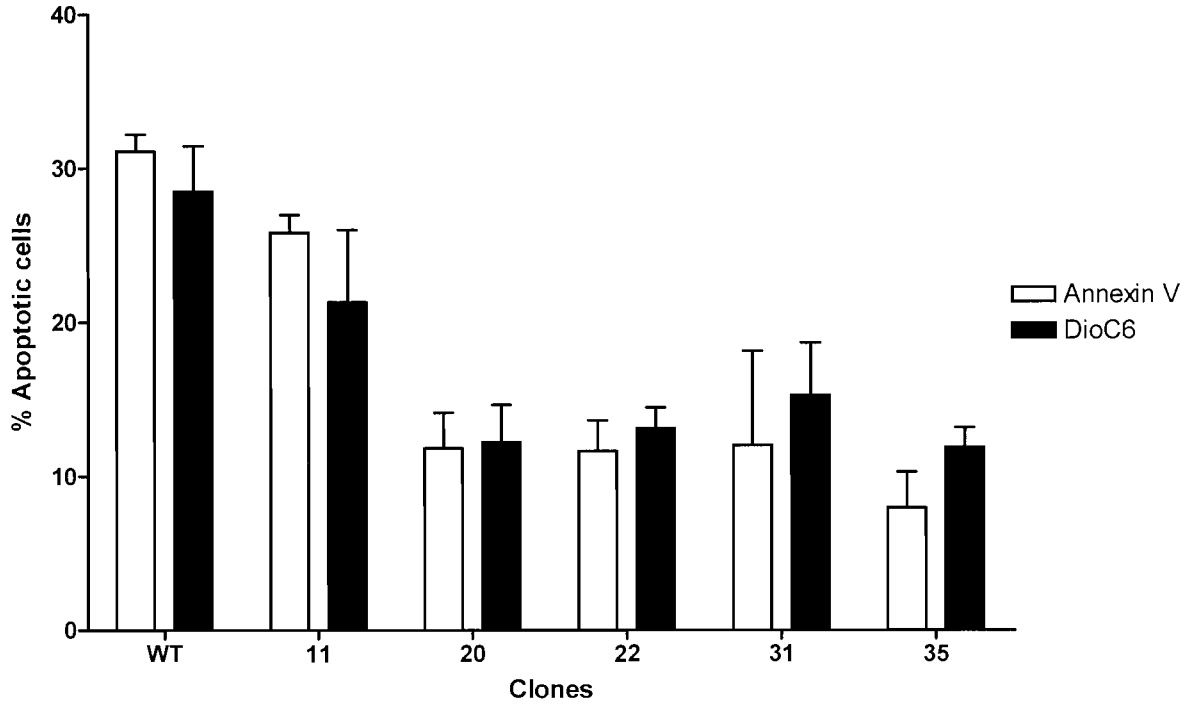

Figure 5.8 Effect of over expression of mΔCD79b in WEHI-231 cells on BCR-induced apoptosis. 2x10^5 WEHI-231 transfected clones were treated with anti-μ mAb for 48 hours at 37°C, in a humidified chamber. Cells were assessed for the effects of over expressed mΔCD79b on BCR induced apoptosis by Annexin V/PI and DioC6 staining. Results are mean values ± SD from three separate experiments.

confirm the construct and amplification of plasmid DNA using maxipreps, both full length mCD79b and mΔCD79b were transfected into 293T cells to assess their expression in a transient system. Fluorescent microscopy indicate that in this system, both full mCD79b and mΔCD79b are expressed at the plasma membrane, compared to cells transfected with an empty YFP vector (Figure 5.9a).

It was also decided to assess the expression of full length and mΔCD79b proteins in murine B cells. Therefore, WEHI-231 B cells were transfected with the same YFP expression vectors and selected utilising selection medium and expanded. To assess the overall level of YFP expression, cells were assessed by flow cytometry. This analysis demonstrated that 293T cells expressed much higher levels of YFP proteins than WEHI-231 cells (Figure 5.9a and 5.9b respectively). However, Figure 5.9b shows that although mΔCD79b:YFP staining in the selected WEHI-231 cells was much weaker and more diffuse compare to that observed in transiently transfected 293-T cells, it again appeared to show a plasma membrane orientation, in particular compared to the YFP control which showed weak diffuse cytoplasmic staining.

5.2.9.2 Assessment of surface expression of mΔCD79b.

Although the fluorescent image data allows us to visualise where mΔCD79b is expressed within the cell, it does not answer the question of whether the molecule is expressed on the cell surface. To address this, 293T cells were transfected with 1 μg of full length mCD79b and mΔCD79b in the pCI-puro expression vectors, and incubated for 24 hours at 37°C. Levels of mCD79b expressed at the cell surface were assessed using FITC labelled anti-CD79b (HM79-11), that has previously been shown to detect both full length and truncated proteins in COS-7 cell lysates (Figure 5.3). 293T cells were also co-transfected with empty pCI-puro vector as a control or mCD79a;pCI-puro, allowing formation of a stable CD79 heterodimer and increased surface expression in these non-B cells. Figure 5.10, shows that, CD79b was expressed at low levels: 3.2%, on the cell surface of 293T cells transfected with full length mCD79b. These levels were enhanced upon co-transfection with mCD79a (29.8%). However, mΔCD79b was not detected on the cell surface of 293T transfected cells. These data indicate that mΔCD79b is not expressed at the cell surface.

One concern from this experiment was that only a small portion of mΔCD79b (exon 2) is available at the plasma membrane, compared to full length mCD79b, to allow the mAb, HM79-11 to bind. This close proximity to the plasma membrane could hamper binding of

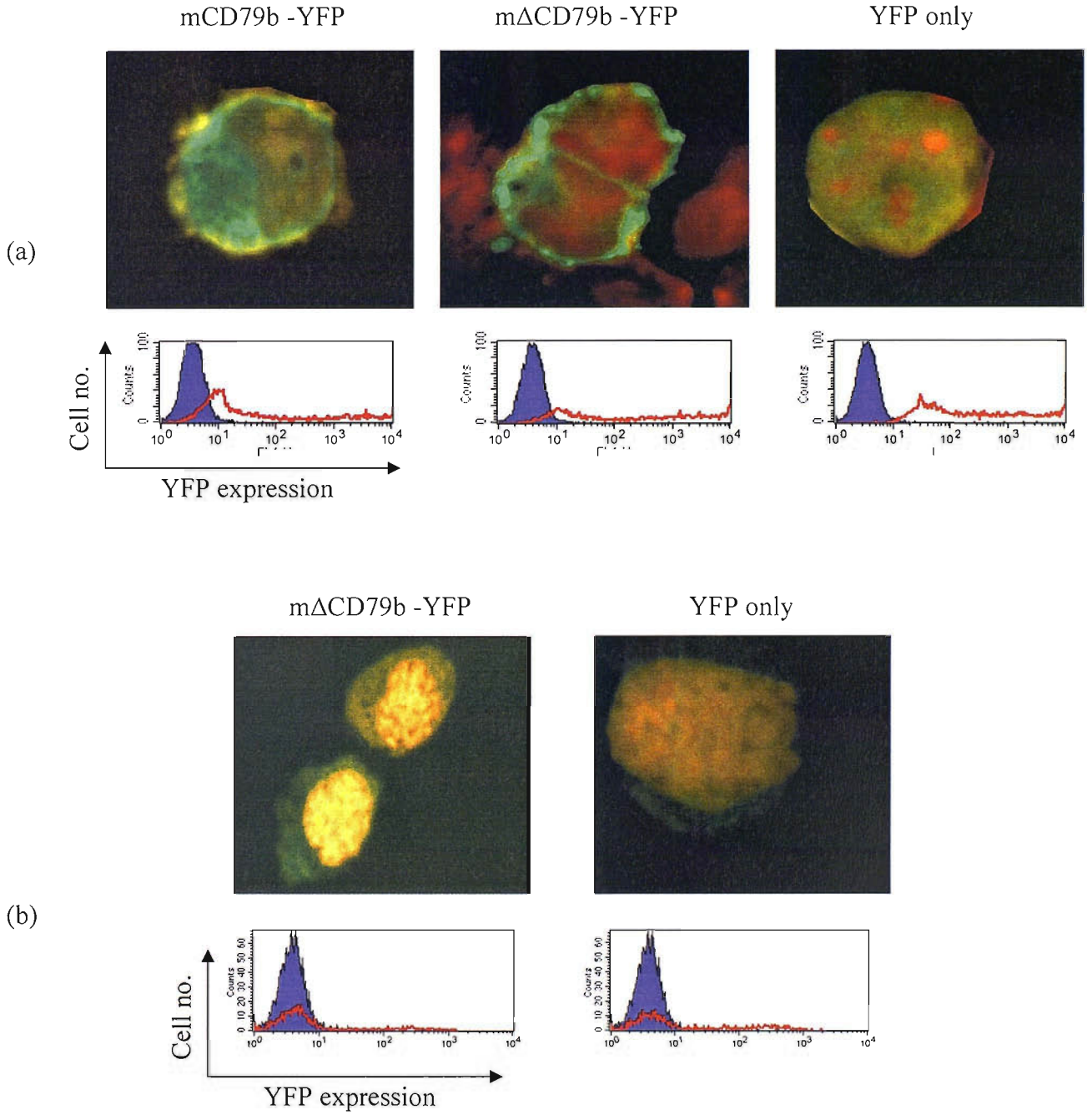

Figure 5.9 Cellular location of YFP tagged mΔCD79b in 293T cells. (a) 293T cell line was transiently transfected with mΔCD79b and full length mCD79b transformed into a YFP expression vector, images were obtained by fluorescent microscopy 24 hours post transfection. (b) WEHI-231 cell line was transfected by electroporation and cells selected under geneticin. Positive colonies were allowed to expand and checked under fluorescent microscopy. Level of YFP expressed in transfected cells was also assessed by flow cytometry as a methods control.

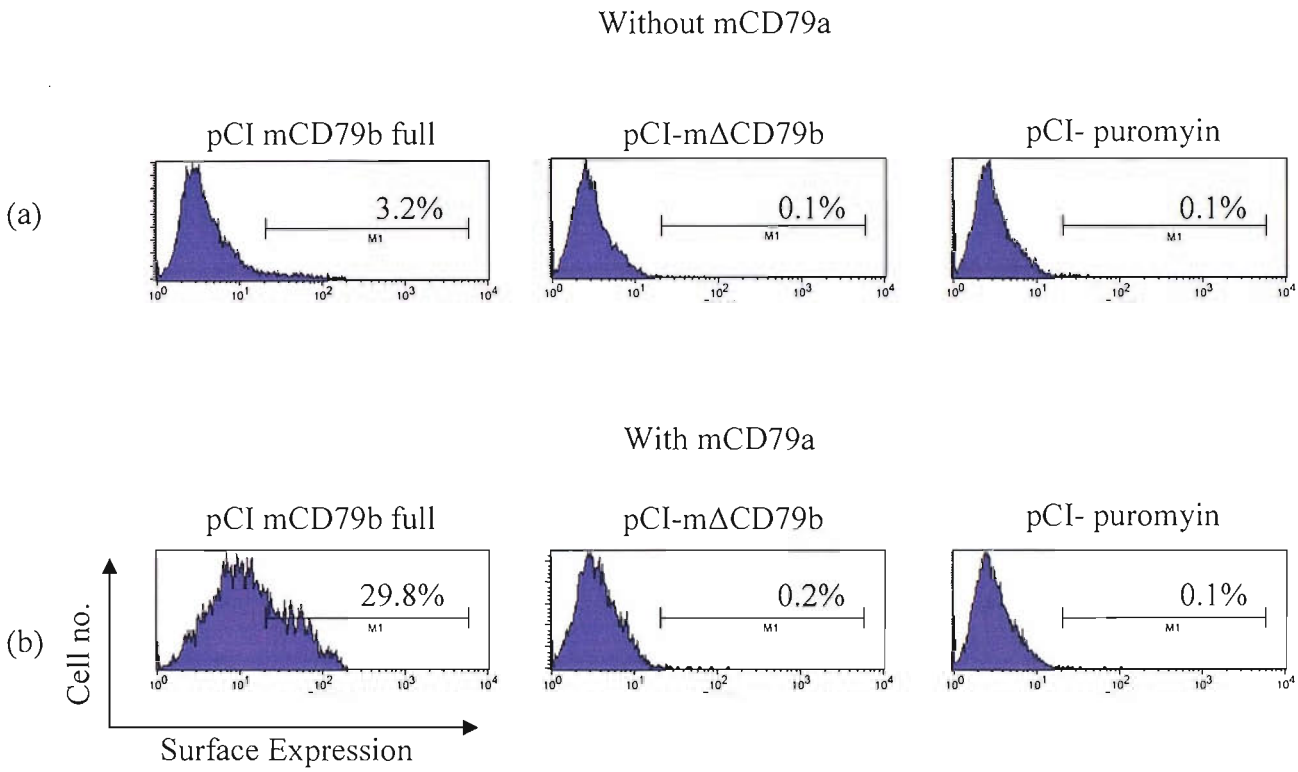

Figure 5.10 Surface expression of full length mCD79b and mΔCD79b in pCI-puromycin vectors on 293T cells. 293T cells were transfected with 1 μg mCD79b full, 1 μg mΔCD79b pCI-puromycin, or 1 μg empty pCI-puromycin vector (Figure 5.9a). 293T cells were also transfected with the above constructs in the presence of either 1 μg mCD79a pCI-puromycin vector (Figure 5.9b). Levels of mCD79b expressed at the plasma membrane were assessed using FITC labelled anti-CD79b (HM79-11) by flow cytometry 24 hours post transfection. Levels of expression are from gated viable cells, and a representative of at least three independent experiments.

HM79-11 mAb (Figure 5.11a). Therefore, it was decided to clone both full length and mΔCD79b into an expression vector containing rat CD4 Ig-like domains 3 and 4 (rCD4d3+4; Appendix D), allowing formation of rCD4d3+4-mCD79b/mΔCD79b fusion proteins that express a larger extracellular domain which can be detected by the rCD4d3+4 specific mAb, OX68[186]. It was also known that the rCD4d3+4 protien cannot be expressed at the cell surface, unless it is attached to a protein which is normally expressed at the cell surface. Once again 293T cells were co-transfected with 1 μg of the fusion protein along with either empty pCI-puro vector or mCD79a:pCI-puro vector. Surface expression of mCD79b was assessed using FITC labelled HM79-11 or OX68 mAb.

The mAb HM79-11, again showed the expression of full length mCD79b at the cell surface which was enhanced in the presence of mCD79a, but once again failed to detect mΔCD79b (Figure 5.11b, upper plots). The OX68 mAb showed the presence of full length mCD79b at the cell surface (11.5%), which was again enhanced in the presence of mCD79a (29.1%). However, surface expression of the rCD4d3+4-mΔCD79b fusion protein was also detected with the OX68 mAb: 9.3%. The surface expression of mΔCD79b was also, but surprisingly, enhanced in the presence of mCD79a to 30.6% (Figure 5.11b. lower plots). These data clearly indicate that mCD79b is expressed at the cell surface.

5.2.10 Protein tyrosine and threonine phosphorylation in wild type WEHI-231 and clone Δ35.

Following the findings that mΔCD79b not only inhibits BCR induced apoptosis, but it is also located near to the cell surface, it was decided to investigate if mΔCD79b interferes with PTK activation. Our hypothesis was that mΔCD79b inhibits activation of early PTKs and activation of downstream intracellular signals that result in cell death upon cross-linking the BCR. Initially, both wild type WEHI-231 and WEHI-231 clone Δ35 cells were stimulated with either the control, or the anti-μ mAb at 10 μg/ml for 5 minutes at 37°C. Cells were then lysed, protein separated on 12.5% SDS-PAGE gels, transferred to PVDF membranes and probed for phosphorylated tyrosine or threonine residues.

Figure 5.12 shows that there is little difference in levels of protein tyrosine phosphorylation upon cross-linking the BCR between the two different WEHI-231 cell lines. Protein threonine activation also differed little between cell lines, and cells treated with either the control or the anti-μ mAb.

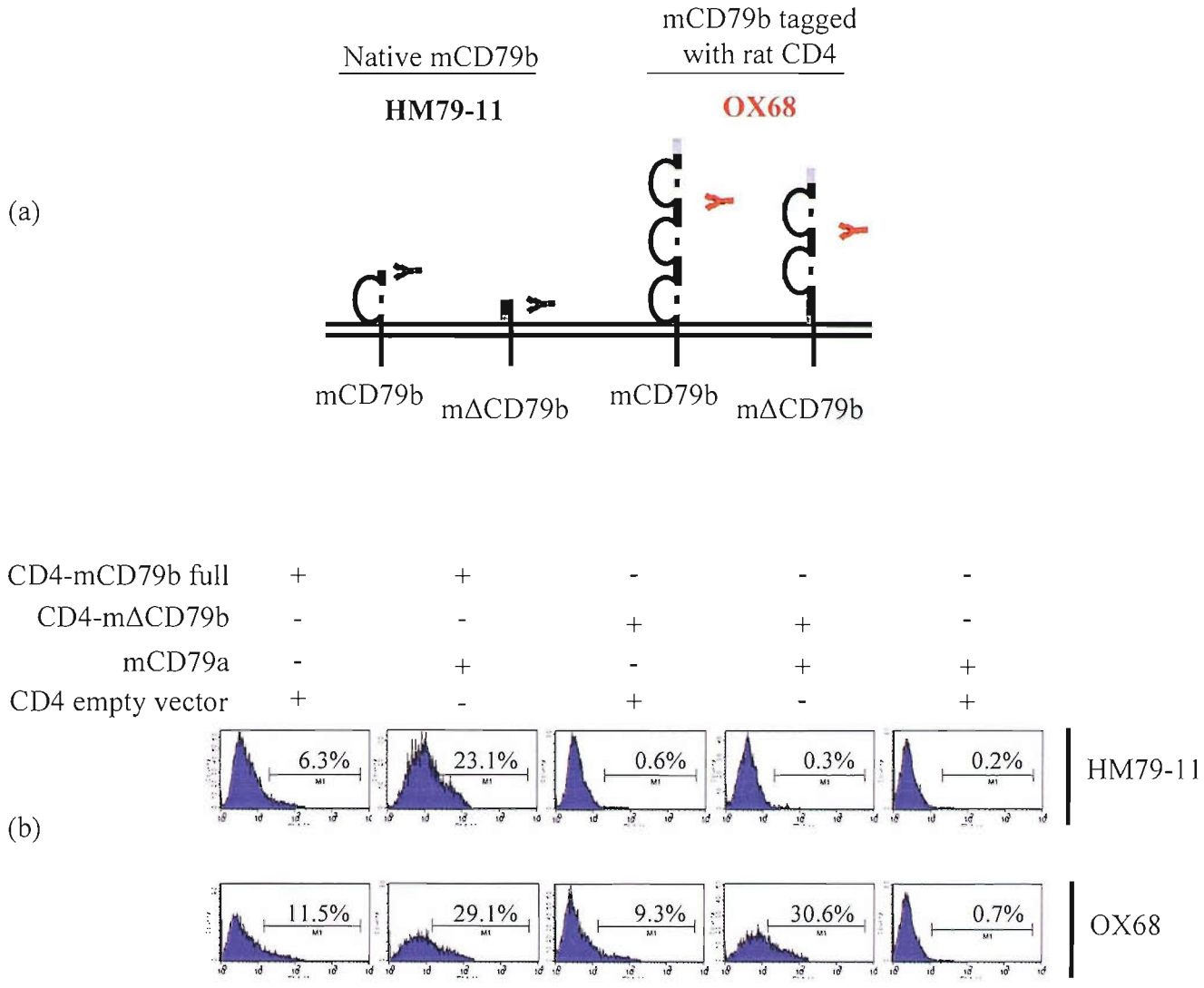

Figure 5.11 Surface expression of full length mCD79b and mΔCD79b in CD4d3,4+1 vectors on 293T cells. (a) Schematic representation for surface expression of mCD79b vectors, and detection with either anti-mCD79b (HM79-11) or anti-rCD4d3+4 (OX68). (b) 293T cells were co-transfected with 1 μg rCD4d3+4-mCD79b full or rCD4d3+4-mΔCD79b fusion proteins, again in the presence of 1 μg of mCD79a or empty rCD4d3+4 vector. Levels of surface expression were again assessed 24 hours post transfection by flow cytometry using antiCD79b (HM79-11) or anti rCD4d3+4 mAb (OX68). Levels of expression are from gated viable cells, and a representative of at least three independent experiments

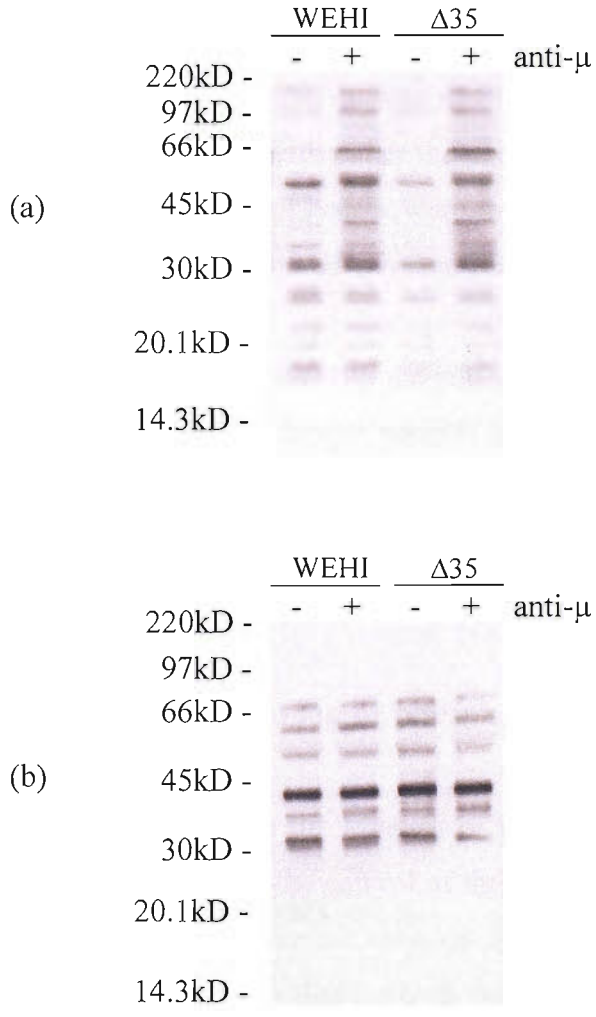

Figure 5.12 Tyrosine and threonine phosphorylation patterns of wild type WEHI-231 and clone Δ35 stimulated with mAb directed at the BCR. $4x10^6$ wild type WEHI-231 or WEHI-231 clone Δ35 cells were stimulated with either control (KT3, -) or anti-μ (Mc39-12, +) at 10 μg/ml for 5 minutes at 37°C. Cells were then lysed and protein separated on 12.5% SDS-PAGE gels, transferred to PVDF membrane and probed for the presence of phosphorylated tyrosine residues using the mAb 4G10 (1μg/ml) (a), or phosphorylated threonine residues using Ab p-Thr (1:1000) (b), and appropriate HRP conjugated secondary Ab. Representative of at least three independent experiments

5.2.11 The kinetics of protein tyrosine phosphorylation in wild type WEHI-231cells and clone Δ35.

In chapter 3 we demonstrated the importance of the kinetics of PTK activation for subsequent apoptosis via BCR-ligation. Therefore, after investigating initial PTK activation following cross-linking of the BCR, it was decided to investigate the kinetics of PTK activation upon ligating the BCR with either the control or the anti-μ mAb (10 μg/ml) for 1, 5, 15 and 60 minutes at 37°C. Cell lysates were then separated on SDS-PAGE and probed for proteins containing phosphorylated tyrosine residues. Figure 5.13 shows that there is little difference in the levels of tyrosine phosphorylated proteins observed following stimulation for 5 minutes stimulation with the anti-μ mAb between wild type and clone Δ35 WEHI-231 cells. However, with longer periods of stimulation (15 and 60 minutes) wild type WEHI-231 cells exhibit higher protein tyrosine phosphorylation than WEHI-231 clone Δ35 cells, with protein tyrosine phosphorylation appearing to decrease in the Δ35 cells after stimulation for 15 and 60 minutes.

5.2.12 The kinetics of protein threonine phosphorylation in wild type WEHI-231 and clone Δ35 cells.

It was also decided to investigate the kinetics of protein threonine phosphorylation upon cross-linking the BCR with either the control or the anti-μ mAb for 1, 5, 15 and 60 minutes as detailed above. Activated threonine residues were probed using Ab P-Thr-Polyclonal (1:1000). Figure 5.14 again shows that for both cell lines there appears to be no difference in levels of threonine activated on proteins treated with either the control or the anti-μ mAb over the time course. The level of threonine phosphorylated proteins between wild type and Δ35 WEHI-231 cells also appears not to differ following early stimulation times of 1 and 5 minutes. However, following longer periods of stimulation, for 15 and 60 minutes, specific phosphorylated threonine proteins were observed in wild type WEHI-231 cells at around 90kD and 20kD that were not observed in the clone Δ35 cells.

5.2.13 Activation of p38 and ERK in wild type WEHI-231 and clone Δ35

From previous studies investigating BCR-induced apoptosis in WEHI-231 cells, activation of the downstream signalling proteins, ERK and p38 has been shown to be important in governing cellular fate[172]. Therefore, we investigated the effects of cross-linking mIgM on the activation of ERK and p38 in the two cell lines. Initially we used the same kinetics as used for investigating total PTK activation in WEHI-231 cells. Cells were stimulated with either the control or the anti-μ mAb (10 μg/ml) for 1, 5, 15 and 60 minutes at 37°C.

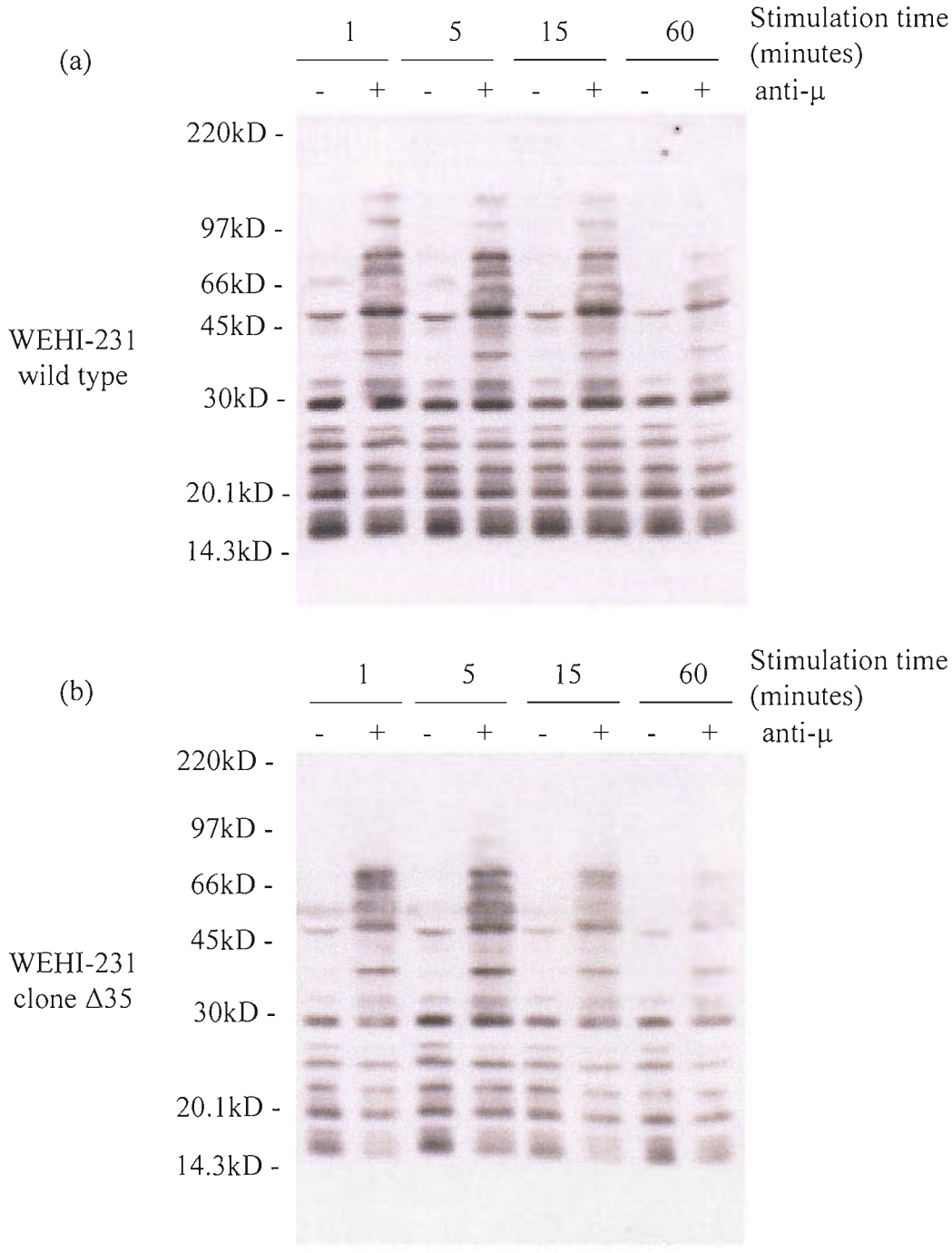

Figure 5.13 Tyrosine phosphorylation kinetics of wild type WEHI-231 and clone Δ35 stimulated with mAb directed at BCR. $4x10^6$ wild type WEHI-231 (a) or WEHI-231 clone Δ35 (b) were stimulated with either control (KT3, -) or anti-μ (Mc39-12) mAb (10μg/ml) for 1, 5, 15 or 60 minutes at 37°C, in a pre-warmed water bath. Cells lysates were separated by SDS-PAGE and PVDF membranes probed of phosphorylated tyrosine residues using the mAb 4G10 (1 μg/ml) and an appropriate HRP labelled secondary Ab. Representative of at least three independent experiments

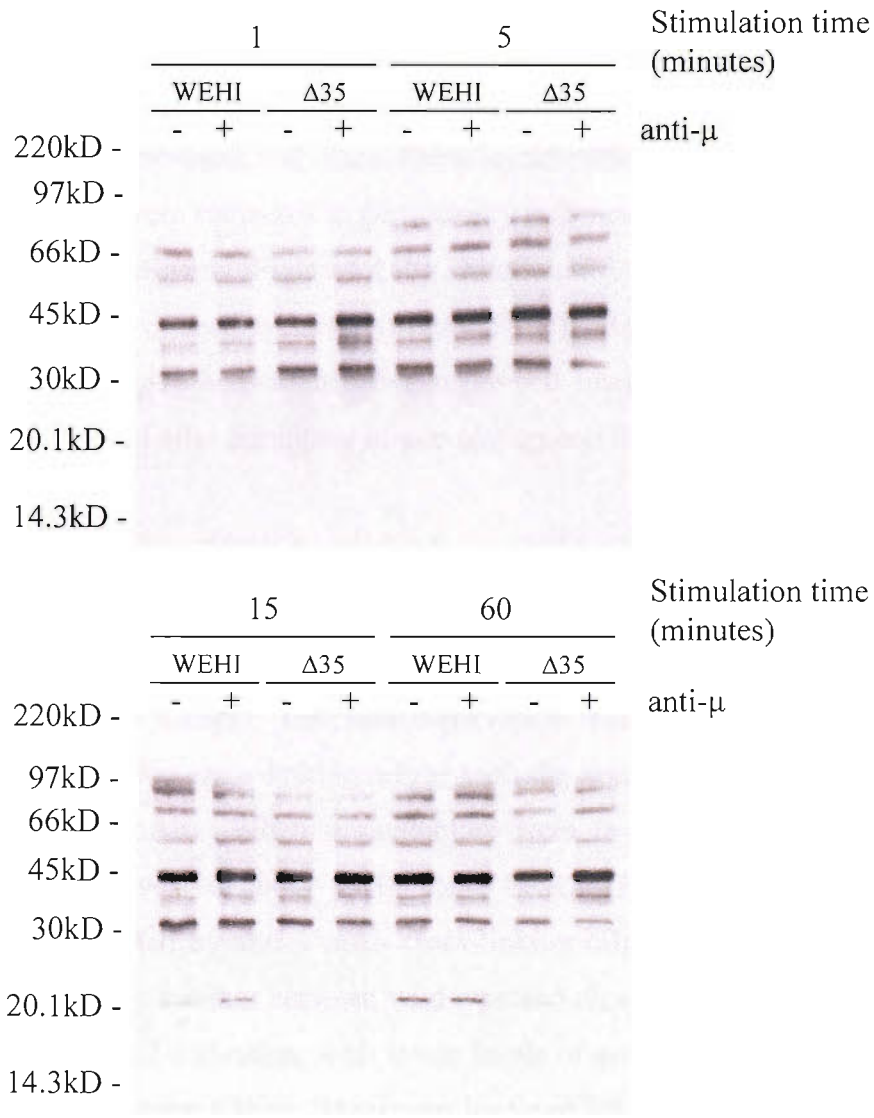

Figure 5.14 Threonine phosphorylation kinetics of wild type WEHI-231 and clone Δ35 stimulated with mAb directed at BCR. $4x10^6$ wild type WEHI-231 or WEHI-231 clone Δ35 were stimulated with either control (KT3, -) or anti-μ (Mc39-12) mAb (10μg/ml) for 1, 5, 15 or 60 minutes at 37°C, in a pre-warmed water bath. Cells lysates were separated by SDS-PAGE and PVDF membranes probed of phosphorylated threonine residues using the Ab p-Thr (1:1000) and an appropriate HRP labelled secondary Ab. Representative of at least three independent experiments

Samples were then lysed, and protein separated on 12.5% SDS-PAGE gels, and transferred to PVDF membranes. Membranes were then probed for the presence of active p38 (anti-active p38 1:2500) or active ERK (anti-active MAPK 1:5000). As a loading control membranes were re-probed for the presence of β-actin (p38) or total ERK (active ERK blots).

Figure 5.15a shows that between cell lines there is no difference in the level of p38 activation. Western blots were subjected to densitomtry and mean values ± SD were plotted for three independent experiments (Figure 5.15b). Maximum levels of p38 activation were then calculated as detailed in section 3.2.11 (Figure 5.15c). Results show that there is no difference in the levels of p38 activation between the cell lines. The maximum levels of activated p38 were observed after 5 minutes of stimulation and then decreased.

Figure 5.16a, shows the levels of ERK activation between the two cell lines. Again western blots were subjected to densitometry and mean values ± SD from three independent experiments were plotted (Figure 5.16b), and calculated as percentages of maximum activation of ERK (Figure 5.16c). The first observation was that in both, only ERK2 appeared to be activated upon cross-linking mIgM with the anti-μ mAb, compared to cells treated with the control mAb. When immunoblots were re-probed for total ERK, all samples showed equal levels of both ERK1 and ERK2 (Figure 5.16a). Therefore, intracellular signals generated by anti-μ mAb cross-linking mIgM appear to only activate ERK2 and not ERK1. Early kinetics between wild type and clone Δ35 WEHI-231 cell lines show similar levels of ERK2 activation, with lower levels of activation observed following stimulation for 1 minute (Figure 5.16b). Maximum levels of ERK activation were observed following stimulation for 5 minutes in both cell lines, and then decreased over time (Figure 5.16c). However, levels of activated ERK2 fall at a faster rate in the wild type WEHI-231 cells compared to the Δ35 WEHI-231 cells, where activated ERK2 was still observed following stimulation for 60 minutes.

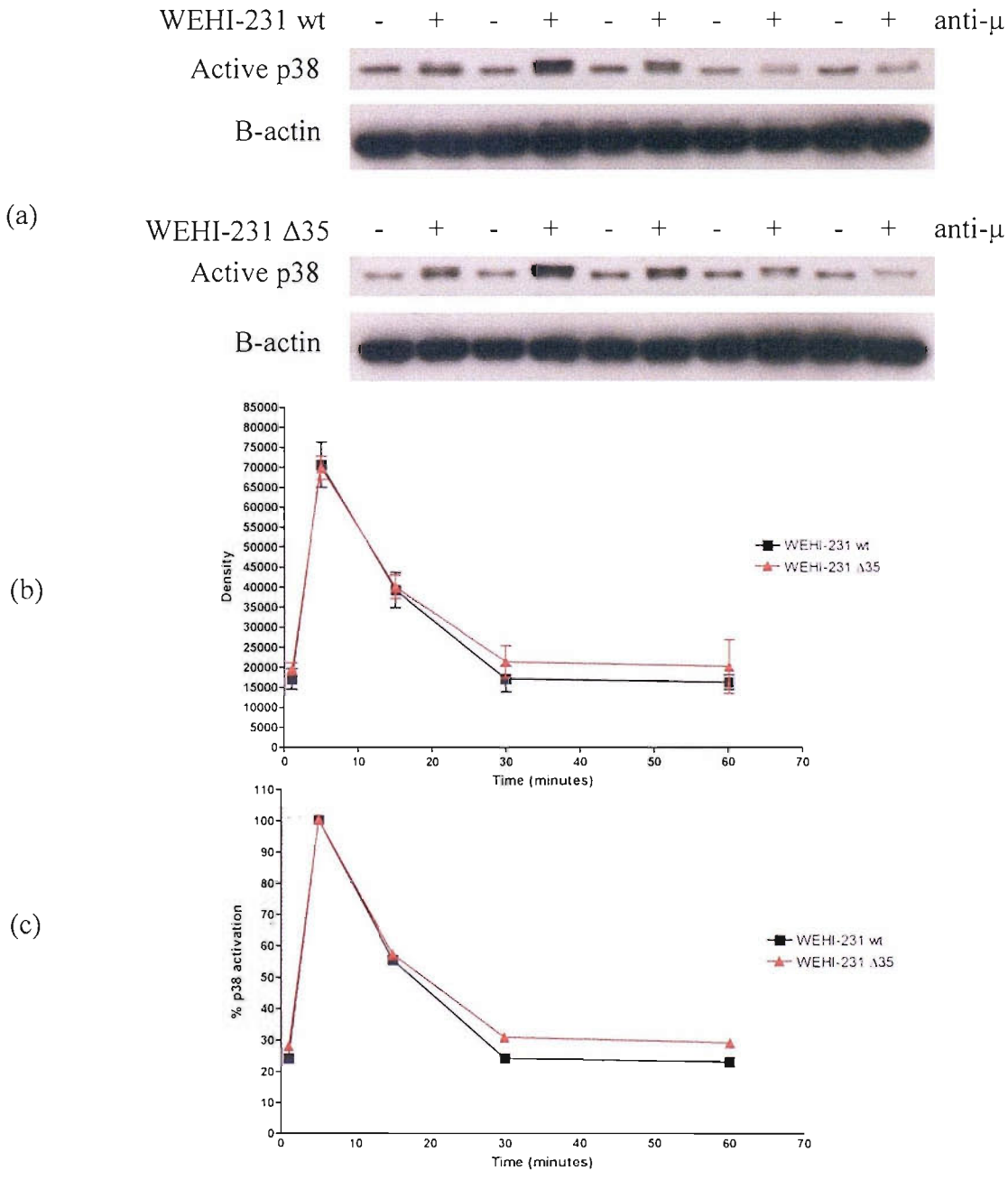

Figure 5.15 p38 activation kinetics of wild type WEHI-231 and WEHI-231 clone Δ35 stimulated with mAb directed at BCR. 4x10^6 wild type WEHI-231 or WEHI-231 clone Δ35 were stimulated with either control (KT3, -) or anti-μ (Mc39-12) mAb (10 μg/ml) for 1, 5, 15, 30 and 60 minutes 37°C in a pre-warmed water bath before being lysed. Proteins were separated on 12.5% SDS-PAGE gels, transferred to PVDF membrane and probed for the presence of activated p38 (top blot) using anti-active p38 Ab (1:2500), or β-Actin (bottom blot) as a loading control. Levels of p38 activation were quantitated using densitometry (b) mean values ± SD from three independent experiments. Levels of p38 activation were adjusted to maximum obtained when cells were treated with individual mAb (c).

(a)

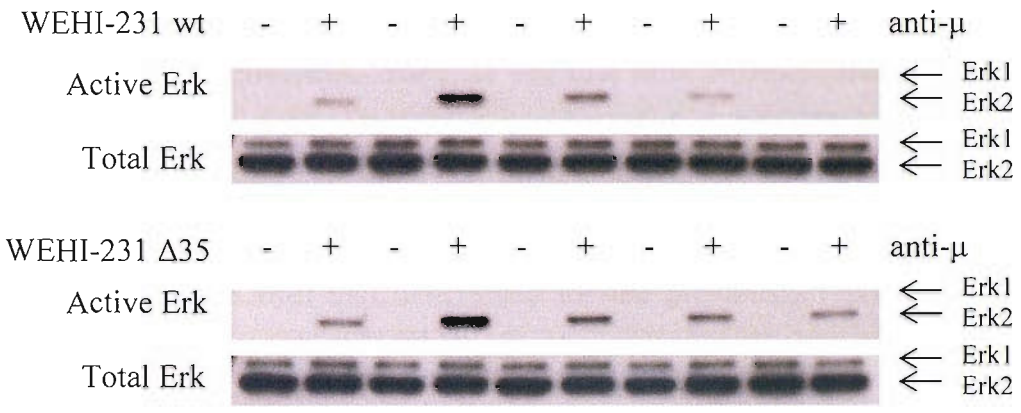

(b)

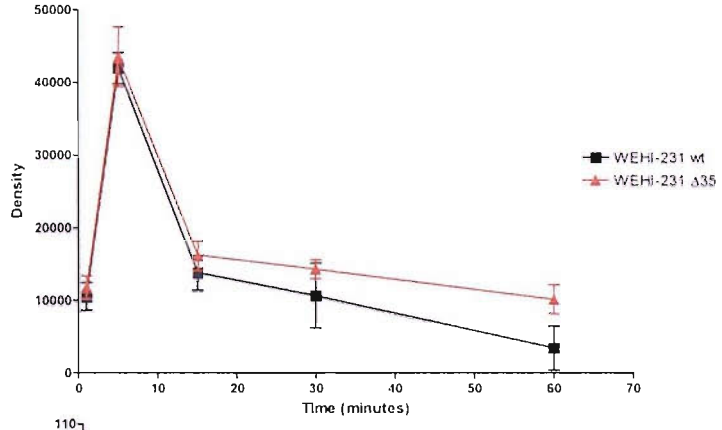

(c)

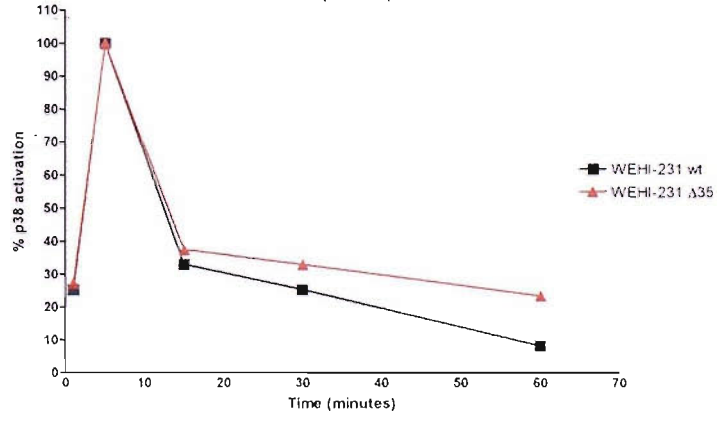

Figure 5.16 Erk activation kinetics of wild type WEHI-231 and WEHI-231 clone Δ35 stimulated with mAb directed at BCR. $4x10^6$ wild type WEHI-231 or WEHI-231 clone Δ35 were stimulated with either control (KT3, -) or anti-μ (Mc39-12) mAb (10 μg/ml) for 1, 5, 15, 30 and 60 minutes 37°C in a pre-warmed water bath before being lysed. Proteins were separated on 12.5% SDS-PAGE gels, transferred to PVDF membrane and probed for the presence of activated Erk (top blot) using anti-active MAPK Ab (1:5000), or total Erk (bottom blot) using anti-MAPK Ab (1:5000). Levels of Erk activation were quantitated using densitometry (b) mean values ± SD from three independent experiments. Levels of Erk activation were adjusted to maximum obtained when cells were treated with individual mAb (c).

5.3 Discussion

An alternative transcript of CD79b that lacks exon 3 has been reported in both normal and malignant human B cells, with an increased expression observed in human B cell malignancies including B-CLL[140, 141]. An alternative transcript of CD79b has never, to date, been reported in murine cells. Here for the first time we show that an alternative transcript of murine CD79b exists. Primers directed towards full length mCD79 indicated the presence of full length mCD79b and a smaller PCR product of about 480bp in murine B lymphoma cells and splenocytes from naïve mice. The size of the smaller PCR product of mCD79b is an accordance with that determined for the previously reported hΔCD79b, which lacks the whole of exon three[138, 140, 141].

Sequence analysis of the short PCR product confirmed that the transcript was an alternative form of mCD79b, with the whole of exon three deleted. Therefore, it is clear that mΔCD79b does exist, sharing homology with hΔCD79b in that both alternative transcripts lack exon three. The leader sequence (exon 1) and extracellular domain (exon 2) of mΔCD79b share very little homology with hCD79b and hΔCD79b, while the transmembrane domain (exon 4) and cytoplasmic domains of mΔCD79b (exons 5 and 6) share almost exact homology with the same domains of hCD79b and hΔCD79b as previously noted[16].

The expression of mΔCD79b was subsequently assessed in various murine B cell lines using RT-PCR. It was shown that the immature B cell line, WEHI-231, which is known to be sensitive to BCR-induced apoptosis, expressed lower levels of mΔCD79b compared with the mature class-switched murine B cell line A20, and the dual *in vivo/in vitro* cell line πBCL_1. When these cell lines were incubated with anti-BCR mAb it was clear that where WEHI-231 cells were sensitive to BCR-induced apoptosis, πBCL1 and A20 cells were less sensitive. The mRNA expression of mΔCD79b in murine B cell lines, therefore, appears to correlate with their sensitivity to BCR-induced apoptosis, similar to observations in the human B cell lines[141].

The protein expression of mΔCD79b was investigated using a commercially available mAb, HM79-11, that binds to the extracellular region of CD79b, and the in-house mAb AT107/2, raised against a peptide from the hCD79b cytoplasmic domain. The cytoplasmic domains of murine and human CD79b share homology and are almost identical in this region, and as expected the mAb recognised mCD79b in western blots of COS-7 cells transfected with

pCIpuro vectors encoding mCD79b. Furthermore, as the cytoplasmic domain is present in the alternative transcript, the mAb should also recognise mΔCD79b if it is expressed as a stable protein. Western blot analysis of lysates from COS-7 cells transfected with mΔCD79b in the pCI-puromycin expression vectors indicated that the alternative transcript is indeed capable of encoding for a mature, stable protein as both the mAb HM79-11 and AT107/2 could recognise it when over-expressed in COS-7 cell lines. Furthermore, the amount of full length and alternative protein detected appeared equivalent, possibly indicating that both full length and alternative transcripts have similar stability. The fact that the HM9-11 mAb was able to detect the alternative transcript indicates that this Ab is directed to the short peptide sequence encoded by exon 2 present in both full and truncated proteins, similar to the observation the mAb directed to human CD79b proteins recognise this region.

To confirm that endogenous levels of mΔCD79b are detectable in B cells, i.e. when not over-expressed in a non-B cell line, we analysed the protein expression of mΔCD79b in a selection of mouse B cell lines, and show that the mΔCD79b protein could be detected. Furthermore, its expression correlated with the level of mRNA produced, in that WEHI-231 murine B cell lines expressed the lowest level compared to A20 and πBCL_1 cells.

Signalling through the BCR is pivotal during B cell development[2, 187]. Signalling from a pre-BCR in the absence of an external ligand generates intracellular signals required to allow cellular proliferation, rearrangement of mIg light chain, and differentiation[87, 100]. In the absence of BCR signalling, pre-B cells die. However, at the immature stage of B cell development cross-linking the BCR generates intracellular signals that induce programmed cell death, apoptosis, preventing formation of self reactive B cells[187]. Although the fate of B cells at different stages of development are quite different, they are all generated from intracellular signals initiated from the BCR, in particular the CD79 heterodimer[4, 18].

At all stages of development it is thought that B cells contain the same basic signalling molecules, what has still to be shown are specific differences in signalling pathways between B cells at these different stages of development. In this study the WEHI-231 cell line, used extensively as a model of immature B cells[184, 185] expressed relatively low levels of mΔCD79b at both the mRNA and protein level but, was most sensitive to BCR induced apoptosis upon cross-linking the BCR, with as little as 1 μg/ml of the anti-μ mAb giving effective cross-linking. In contrast, A20 B cells, used as a mature B cell model[188] express

higher levels of mΔCD79b, and are not as sensitive to BCR-induced apoptosis. The *ex vivo* murine B lymphoma model, πBCL_1, also expressed higher levels of mΔCD79b compared to the WEHI-231 cells, and, like A20 cells, was less sensitive to apoptosis induced by cross linking the BCR. Therefore, it is possible that regulating the expression of mΔCD79b during B cell development could help in regulating B cell signalling and apoptosis. Furthermore, its over-expression could be a causative factor in disease states, such as certain types of B cell lymphoma, where it appears to be up-regulated[141].

To test this hypothesis it was decided to attempt to regulate the expression of mΔCD79b and observe the effects on BCR-induced apoptosis. Initially we attempted to utilise siRNA technology[189] to reduce the expression of mΔCD79b, and see if we could make cells more sensitive to BCR-induced apoptosis. siRNA primers were designed to span the splice site between exons two and four, which is present only in mΔCD79b and not the full length molecule. However, as the target region is relatively small, this severely limited the possible sequence of siRNA that could be used, and so we were only able to produce a single siRNA plasmid for mΔCD79b (data not shown). Experiments were devised to over-express full length and mΔCD79b-YFP tagged proteins in the 293T cell line together with the siRNA to mΔCD79b. If siRNA had worked, we would have observed a decrease in the fluorescence in cells transfected with the mΔCD79b-YFP protein. Unfortunately, no evidence of gene knock down was observed and due to the limited target region mentioned above, we did not pursue this avenue of investigation (data not shown).

Although we were unable to utilise siRNA to knock down the expression of mΔCD79b in transient cells, we did manage to over-express mΔCD79b in WEHI-231 cells which are sensitive to apoptosis. Five clones that expressed increasing levels of mΔCD79b compared to wild type WEHI-231 cells were obtained. Interestingly, as hypothesised, increasing the level of mΔCD79b decreased the susceptibility to BCR-induced apoptosis similar to results observed in sensitive Ramos cells over-expressing the human ΔCD79b[141]. Cragg, *et al.*,[141] also showed that the presence of ITAM motifs within the cytoplasmic domains of hΔCD79b was essential to prevent BCR-induced apoptosis. This data suggests that ΔCD79b interacts with PTK, via ITAM motifs located within the cytoplasmic domain, and that over-expression of ΔCD79b in cell lines or B-CLL cells prevents PTK interacting with normal CD79 proteins, preventing initiation of a complete intracellular signalling cascade.

The discovery of hΔCD79b expression has lead many groups to postulate whether this alternative transcript could have an effect on the physiology of B-CLL cells. It has been proposed that hΔCD79b, or other point mutations observed in the B29 gene in B-CLL, samples may lead to the decreased expression of surface BCR characteristic of B-CLL cells[134]. Gordon, *et al.*,[190] showed that transfection of the Jurkat T cell line with cDNA for mIgM, CD79a, and CD79b led to the expression of a complete BCR at the cell surface. If cDNA for CD79b was substituted with cDNA encoding ΔCD79b then BCR surface expression was lost. This indicates that ΔCD79b is not capable of allowing release of a complete BCR from the ER and transport to the cell surface, at least in these cells (non-B cells). Indraccalo, *et al.*,[191], also showed that in a transient expression system, transfection of increasing concentrations of cDNA encoding hΔCD79b together with cDNA encoding full length CD79b led to a reduced expression of surface BCR. However, this research is in disagreement with our data presented here. Our research indicates that over-expression of hΔCD79b in human B cell lines, or over-expression of mΔCD79b in WEHI-231 cells does not reduce surface BCR expression[141]. It should be noted that these other studies were performed in non-B cells commonly used for over-expression studies, which may have altered/deregulated intracellular trafficking, and utilised extremely high levels of transfected DNA to achieve these effects, which may not be achieved physiologically. Payelle-Brogard, *et al.*,[192, 193] have suggested that although there appears to be no defect in the assembly of CD79b and mIg in B-CLL samples, the loss of BCR surface expression is caused by a constant defect in BCR assembly within the cell, probably due to a defect in the glycosylation of CD79a, which is independent of the over-expression of hΔCD79b.

However, it must be noted that we did not fully characterise the WEHI-231 cell lines that over-expressed mΔCD79b. The protein expression of mΔCD79b was not investigated and so the surface expression of mΔCD79b as a protein cannot be taken into account. It should also be noted that for further experiments only clone 35, that expressed the greatest amount of mΔCD79b at the mRNA level was used, it would have been more ideal to use all of the clones, but time did not permit this.

Research by Tseng, *et al.*,[194] showing that BCR-induced apoptosis of WEHI-231 cells can only be achieved if both CD79a and CD79b are expressed as a heterodimer, may indicate that ΔCD79b could act by sequestering PTKs away from normal full length CD79b. This could prevent activation of a full signalling cascade leading to apoptosis. To test this theory

we investigated the cellular localisation of mΔCD79b, and assessed whether it could interfere with PTKs activated near to the plasma membrane upon BCR cross-linking.

The cellular localisation of mΔCD79b in cell lines was initially assessed by tagging a YFP reporter molecule to the N-terminal domain of both full length and mΔCD79b. mΔCD79b appears to be expressed within the cell, near to the surface in both transiently transfected 293T cells and stably transfected WEHI-231 cells. These results indicated that ΔCD79b could be expressed near to the plasma membrane of B cells, allowing close proximity to essential PTKs utilised by cross-linked BCR. However, as with flouresent microscopy the exact location of mΔCD79b cannot be assured and so this method only gives an approximate cellular location of the protein. We then used mAb directed at the extracellular domain of mCD79b to assess whether the proteins were actually expressed at the cell surface. We showed previously that the mAb raised against the extracellular domain of mCD79b (HM79-11) can recognise both the full length and mΔCD79b proteins. Interestingly, we were able to detect low levels of full length mCD79b at the cell surface of transfected 293T cells, which was enhanced when cells were co-transfected with mCD79a allowing the formation of a stable heterodimer, and increased expression at the cell surface.

However, we were unable to detect expression of mΔCD79b either in the presence or absence of CD79a. These data appear to indicate that mΔCD79b is not expressed at the cell surface. However, we reasoned that although the mAb may be capable of binding to the short peptide encoded by exon two of mΔCD79b, it may be impaired in this context when in close proximity to the plasma membrane. To test if this was the case we decided to create a fusion protein that contained domains three and four of rat CD4 tethered to the N-terminus of mΔCD79b (rCD4d3+4). The theory was that this should create a spacer region presenting the short peptide region of mΔCD79b away from the plasma membrane, thus allowing binding without interference from the close proximity of the plasma membrane.

293T cells were transfected with both full length (rCDd3+4-mCD79b) and mΔCD79b (rCD4d3+4-mΔCD79b) fusion proteins with or without mCD79a, and surface expression assessed using anti-mCD79b (HM79-11) or anti-rCD4 (OX68) mAb. As shown previously, the anti-mCD79b mAb could only recognise full-length mCD79b and not mΔCD79b. The surface expression of full-length mCD79b was once again enhanced when 293T cells were co-transfected with mCD79a. It was no surprise that anti-rCD4 mAb recognised rCD4d3+4-mCD79b expressed at the cell surface. However, mΔCD79b was also detected

at the cell surface, when expressed as the rCD4 fusion protein. Surprisingly, the surface expression of mΔCD79b was enhanced when cells were co-transfected with mCD79a, suggesting that mΔCD79b can form a stable heterodimer with mCD79a. This evidence underlines the findings of Koyama *et al.,*[91] showing the presence of a CD79 heterodimer on the surface of pro-B cells, although a pro-BCR has never been identified on human pro-B cells[93]. This suggests that CD79b could be expressed on the surface of pro-B cells, allowing the generation of intracellular signals that could drive B cell differentiation from the pro-B cell stage to the immature stage in the absence of an external ligand[92, 96, 97].

Surprisingly, the surface expression of rCD4d3+d-mΔCD79b fusion protein was enhanced when 293T cells were co-transfected with mCD79a. This is a surprise because the cysteine residues required to form disulphide bonds between CD79a and CD79b are deleted in mΔCD79b, due to the loss of exon three. Although it is likely that ΔCD79b is expressed as a monomer within the cell cytosol or possibly at the plasma membrane, association between CD79a and ΔCD79b, and mIg has never been examined. Therefore, ΔCD79b could associate with mIg due to the expression of polar transmembrane residues present on ΔCD79b, preventing full-length CD79b binding and the formation of a correct BCR[8]. It is also possible, that ΔCD79b could form a stable CD79 heterodimer, stabilising its expression at the cell surface and allowing the molecule to interfere with intracellular signalling cascades.

As the data indicated that mΔCD79b is located at the plasma membrane, it was predicted that mΔCD79b may be able to sequester important PTK needed to initiate cell death. At early stages of activation following BCR cross-linking, little difference was observed between wild type WEHI and clone Δ35 WEHI-231 cells over-expressing mΔCD79b in both tyrosine and threonine activation. However, at later time points it is clear that increased PTP is observed in wild type cells compared to clone Δ35 cell line. This indicates that the duration of signalling is reduced in resistant cells, presumably due to action of mΔCD79b. This prolonged signalling observed in wild type WEHI-231 cells could be similar to situation we observed in the human EHRB cell lines, where prolonged signalling was apparent in cells that undergo apoptosis.

We tried to utilise the immunopreciptation method used previously to isolate specific activated PTKs. However, the method could not be optimised for the WEHI-231 cell line (data not shown). Therefore, we decided to investigate the activation of downstream

signalling molecules that have previously been reported to be important in protecting WEHI-231 cell lines from BCR induced apoptosis [174, 195]. Harnett, *et al.*,[196] have recently shown that over-expression of the anti-apoptotic factor, Bcl-$_{XL}$ in WEHI-231 cells leads to prolonged activation of ERK2 and rescue from cell death. Other reports have also indicated that p38 has no effect on the cellular fate of WEHI-231 cells [43, 173, 195]. Our data shows that there is no difference in the level or kinetics of p38 activation between wild type or clone Δ35 WEHI-231 cells. However, when investigating activation of MAPK, we showed differences in activation of ERK2 and not ERK1, confirming previously reported data[174]. ERK2 appeared to remain activated for longer periods in clone Δ35 WEHI-231 cells compared to wild type cells. Previous data has shown that WEHI-231 cells rescued from BCR induced apoptosis by the addition of anti-CD40 mAb showed elevated levels of ERK2 activation[174, 197]. This data suggests that over-expression of mΔCD79b in the WEHI-231 cell line interferes with PTK activation following BCR cross-linking preventing cell death.

In conclusion, it has been shown that mΔCD79b expression occurs in both malignant and normal murine B cells, both *in-vivo* murine B lymphoma models and normal *in-vivo* B lymphocytes. mΔCD79b is expressed at both the mRNA and protein levels, as shown for hΔCD79b, with the level of protein expression correlating to mRNA expression. Importantly the protein expression of mΔCD79b was observed in a non-over expressing system. It is also clear that expression of mΔCD79b appears to correlate with cellular susceptibility to BCR induced apoptosis. Our hypothesis of how mΔCD79b interferes with BCR induced apoptosis predicts that mΔCD79b is situated at the plasma membrane and interferes with the signalling cascade. Expression of mΔCD79b at the plasma membrane was confirmed and may help in understanding how ΔCD79b interferes with pro-apoptotic signalling cascades. Although specific PTK activation could not be observed we did manage to confirm that wild type WEHI-231 cells do induce prolonged global PTP compared with cells that over express mΔCD79b, and that prolonged activation of ERK2 is observed, indicating that mΔCD79b does interfere with activation of specific PTK inhibiting BCR induced apoptosis.

Signalling through the BCR is crucial at all stages of B cell development allowing B cells respond to the situation[2]. In the case of immature cells, cross-linking of the BCR by self-Ag leads to signals that induce apoptosis and removal of the B cell from the gene pool[108]. Where, mature B cells require intracellular signals driven from the BCR to allow B cells to proliferate and differentiate into effector cells leading to removal of the invading pathogen from the host[111]. What is interesting is that the intracellular signals activated by cross-linking BCR are the same in all B cells, and what appears to be important is the kinetics of PTK activation that determine cellular fate.

Since the discovery and the application of mAb for curing hosts of disease such as lymphoma, research has focused on the production of mAb as curative agents[198, 199]. However, the production of tailor-made anti-Id mAb as a therapeutic agent is both time consuming and expensive, therefore, research has focused on the production of single mAb that can be used on a number of different patients as an effective remedy[160, 198]. The importance of intracellular signals initiated by cross-linking the BCR with mAb that may be able to induce cell death has also been of interest, since original research showed that B cells isolated from patients in remission from NHL, treated with anti-Id mAb, were capable of inducing intracellular signals [160].

Results from this thesis have shown that only mAb raised against the Fcμ domain of mIgM can effectively induce apoptosis of various *in vitro* B cell lines. However, all mAb can activate intracellular signalling cascades, shown by PTK phosphorylation and release of intracellular calcium upon binding to the BCR. It has previously been reported that only mAb which are effective at giving therapy can activate PTK[160]. However, it is now clear that the kinetics and type of PTK activated by cross-linking the BCR is important in deciding the fate of the cell. Cross-linking the BCR with anti-Fcμ mAb generates a prolonged level of PTK activation, compared to mAb raised against other domains of the BCR. mAb that cross-linked the BCR, but did not induce apoptosis caused a short period of intense PTK activation that quickly fell back to background levels. It appears that it is this prolonged kinetics of specific PTK activation which is important in inducing cell death. According to Reth, *et al.*,[30, 42, 128] it is the PTK Syk, which is important for initiating the activation of intracellular signalling cascades. Activation of Syk is vital for the activation of downstream PTK and release of intracellular calcium[171].

The basis for importance of Syk in the activation of intracellular signalling cascades is that B cells from Syk knockout (Syk $^{-/-}$) murine models cannot differentiate past the pro-B cell stage[44, 126]. However, B cells from Lyn knockout (Lyn -/-) murine models can differentiate to mature B cells, that appear auto-reactive[175, 176, 200, 201]. Therefore, it is apparent that where Lyn is important for tuning the immune response, Syk is vital for initiating and controlling activation of the intracellular signalling cascade upon cross-linking the BCR[39, 42]. Results here appear to confirm as this little difference was observed in kinetics of Lyn activation upon cross-linking the BCR with various mAb. However, anti-Fcμ mAb induced prolonged activation of Syk compared to other mAb that caused a rapid increase in levels of Syk activation, which fell quickly following activation.

The PTK Syk has been shown to be essential for the release of intracellular calcium stores and subsequent activation of nuclear transcription factors allowing B cells to respond to BCR cross-linking[172]. Cross-linking the BCR of immature B cells that contain a null Syk protein with Ag will still internalise, but fail to release intracellular calcium and subsequently will not differentiate into mature B cells[44]. These results have been confirmed by Ma, *et al.*,[127] who have shown by fluorescent microscopy showing Syk tagged with YFP is essential for allowing cross-linked BCR to cap and co-localise following treatment with mAb, where Lyn tagged with YFP does not allow BCR to co-localise, but is essential for allowing the BCR to internalise following cross-linking.

The differences in kinetics of Syk activation also appears to be important in determining the fate of B cell in response to cross-linking the BCR. Dolmetsch, *et al.*,[202] have shown that activation of specific nuclear transcription factors relies on differences in the kinetics of calcium release upon cross-linking the BCR. A sudden, elevated release of intracellular calcium results in the activation of NFAT, but activation of JNK and NF-κB are dependent on a moderate, but sustained release of calcium[44, 203]. Other research has shown that prolonged activation of calcium in B cell models leads to the activation of JNK and cellular apoptosis[204]. Benschop *et al.*,[108] have also shown that differences in the level of calcium release determines the fate of B cells at different stages of B cell development. Cross-linking the BCR of mature B cells with mAb leads to a quick elevated release of intracellular calcium, but does not induce cell death. However, cross-linking the BCR of immature B cells with mAb that induces cell death leads to a moderate and prolonged release in the levels of intracellular calcium[2, 108]. As activation of Syk directly correlate's

with the release of intracellular calcium, results in this thesis suggest that prolonged activation of Syk by anti-Fcμ mAb would result in the activation of JNK and NF-κB, resulting in cell death.

The prolonged activation of Syk resulting in cell death upon cross-linking the BCR with anti-Fcμ mAb is probably caused by a physical disassociation of the CD79 heterodimer from mIgM. Modulation experiments showed that the internalisation kinetics of mIgM were similar when BCR was cross-linked with mAb raised against different domains of mIgM. However, the internalisation kinetics of the CD79 heterodimer were slower when cells were incubated with anti-Fcμ mAb, compared to other mAb raised against the mIgM domain of the BCR. These results were confirmed by immunoprecipitation experiments which showed that anti-Fcμ mAb only bound to mIgM and not the complete BCR, as shown by the presence of the CD79 heterodimer which was co-immunoprecipitated with other mAb raised against the mIgM domain of the BCR.

Data presented in this thesis shows that mAb that induce apoptosis lead to a disassociation of mIgM from the CD79 heterodimer. This would suggest that the CD79 heterodimer would remain at the plasma membrane continuing to signal, leading to prolonged activation of PTKs, including Syk, resulting in cell death, as shown in figure 6.1. However, this would directly disagree with theories proposed by Pierce, *et al.,*[114, 116] that propose cross-linked BCR translocates into lipid raft domains of the plasma membrane. The rational behind this, is that sucrose density gradient analysis of cross-linked BCR show movement of BCR from TX-100 insoluble fractions into TX-100 insoluble raft fractions[118]. It has also been shown that the PTK Lyn is mainly located in raft fractions, and therefore would be able to activate the ITAM motifs of cross-linked BCR[118, 178]. However, there remain several key discoveries that argue against this theory. Firstly, as mentioned above $Lyn^{-/-}$ B cells are capable of differentiating into mature B cells, which are auto reactive[175, 176, 200, 201]. Secondly, research using *in-vitro* $Lyn^{-/-}$ and $Syk^{-/-}$ knock out models have shown that Lyn is important for internalisation of the BCR upon cross-linking and not activation of intracellular signalling cascades[44, 127].

Lipid raft analysis of BCR cross-linked with mAb shows that only polyclonal and anti-Fcμ mAb cause a translocation of mIgM into lipid raft domains. Surprisingly the CD79 heterodimer remains outside the lipid raft supporting our hypothesis that mAb which induce apoptosis lead to a physical disassociation of the CD79 heterodimer from mIgM upon BCR

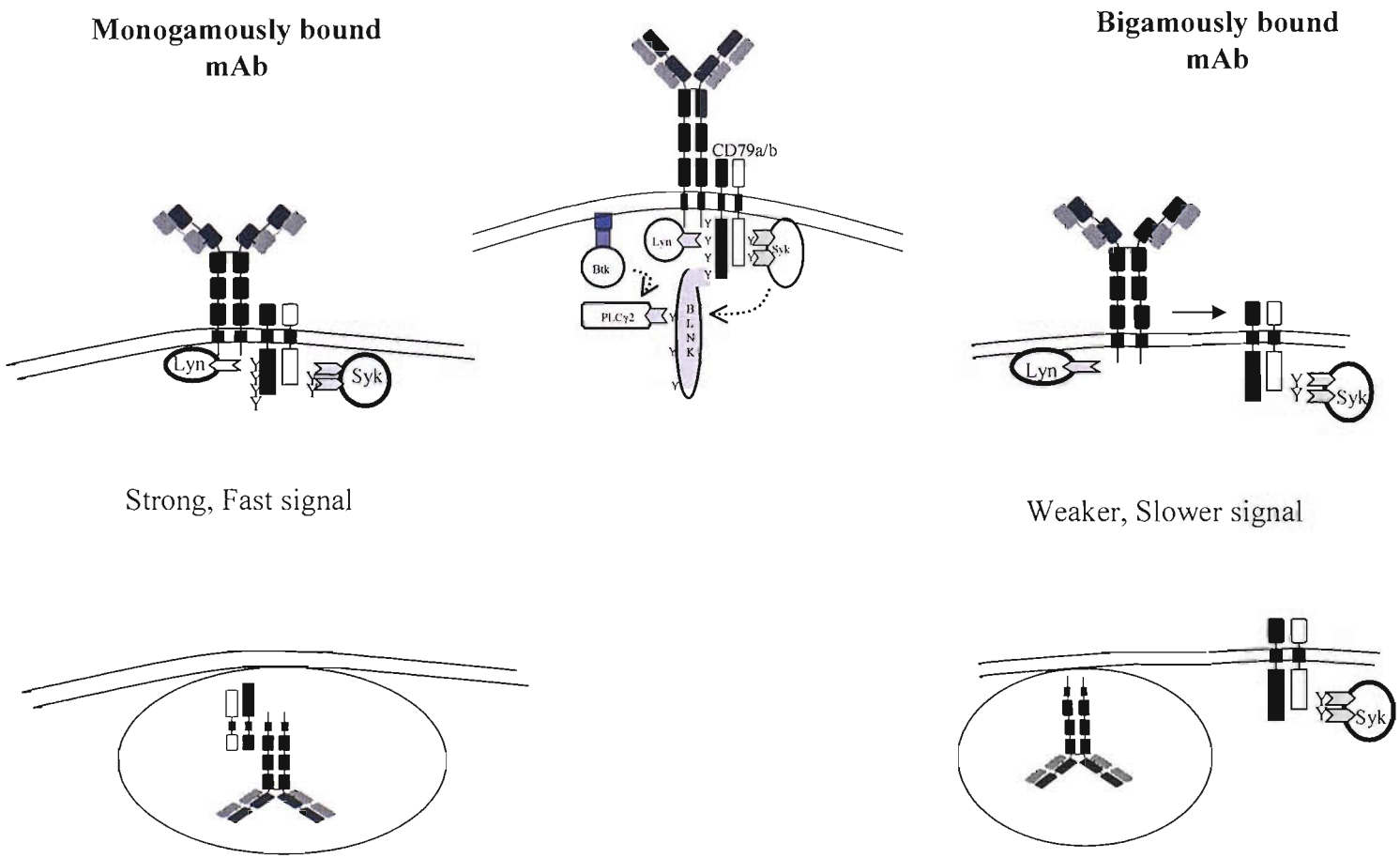

Figure 6.1 – Hypothetical prediction of how bigamously bound mAb leads to separation of mIgM from CD79 heterodimer and induction of cellular apoptosis, compared to bigamously bound mAb that does not.

cross-linking, allowing the CD79 heterodimer to remain at the plasma membrane and signal to induce apoptosis. These results have been supported by recently published data which shows that the CD79 heterodimer can drive B cell development from outside lipid rafts[205], and that a proportion of CD79b remains at the plasma membrane of primary human B cells following internalisation of mIgM upon cross-linking the BCR with polyclonal Ab[206].

The idea that anti-Fcμ mAb induce apoptosis may also be explained as they bind bigamously between BCR, compared to mAb that bind monogamously to a single BCR and do not induce apoptosis. Bigamously bound mAb may effectively disrupt the oligomeric structure of BCR as proposed by Reth *et al.*,[42]. This theory proposes that binding of Ag or Ab disrupts a pre-formed BCR oligomeric structure, releasing associated PTPs such as SHP1. SHP1 along with the PTK Syk, are believed to be constantly phosphorylating and de-phosphorylating tyrosine residues located within the CD79 heterodimer ITAM motifs generating a basal signal sustaining the life of the cell. mAb that bind to the Fc domain of mIgM could disrupt the oligomeric structure of the BCR resulting in the disassociation of the CD79 heterodimer from mIgM, allowing Syk to remain activated in the presence of the CD79 heterodimer at the plasma membrane.

The final area of research in this thesis involved investigating an alternative transcript of mCD79b that lacked the whole of the extracellular domain encoded by exon three; mΔCD79b. Results presented in this thesis confirmed the presence of mΔCD79b in both *in-vivo* murine B cells and *in-vitro* murine B cell lines. It was not surprising that mΔCD79b showed close homology to the alternative transcript of CD79b previously identified in human B cell lines and B cells isolated from B-CLL patients and normal individuals[134, 138, 141]. Therefore, it was also of little surprise to discover that over-expression of mΔCD79b in the WEHI-231 B cell line inhibited BCR induced apoptosis. From this we hypothesised, that mΔCD79b must interfere with PTK activation upon cross-linking the BCR, as shown in figure 6.2. The reasoning behind this hypothesis is that mutation of the tyrosine residues located in the ITAM motif of CD79b to threonine residues ablates the anti-apoptotic properties of ΔCD79b when over-expressed in a human B lymphoma cell line[141].

Experiments looking at the cellular localisation of mΔCD79b aided in trying to answer this hypothesis, suggesting that mΔCD79b may inhibit BCR induced apoptosis by interfering with the activation of early PTKs upon BCR cross-linking. Fluorescent microscopy data showed that mΔCD79b was located near to the plasma membrane of 293T and WEHI-231

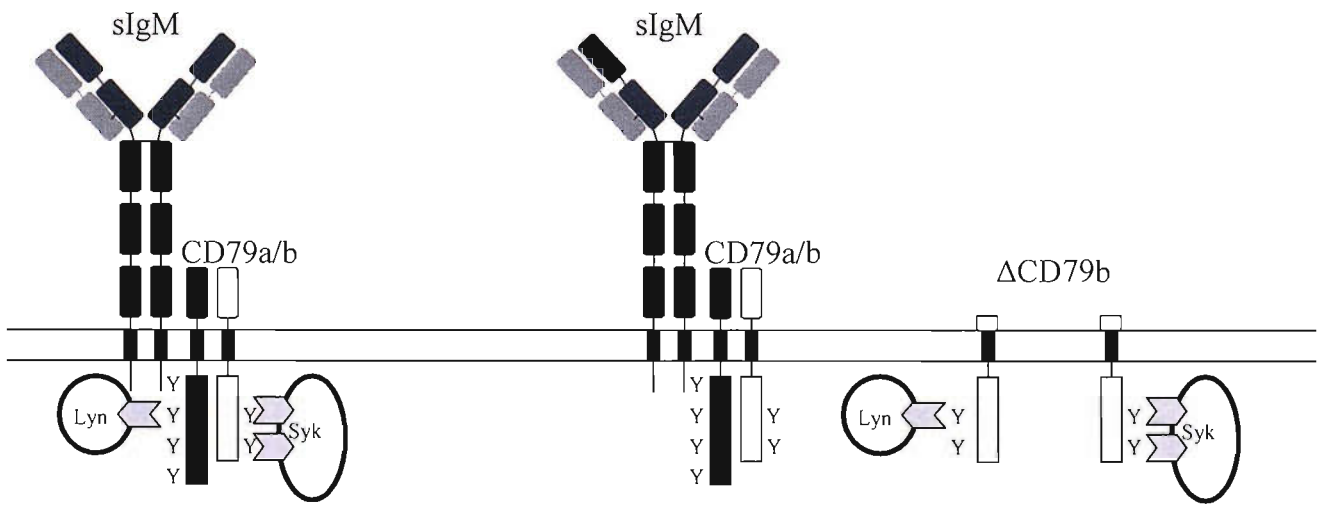

Figure 6.2 – How mΔCD79b could interact with PTK. Hypothetical diagram to show how we predict mΔCD79b could be located at the cell surface and interact with PTK preventing full activation of the B cell signalling pathways.

cell lines. This data was confirmed by flow cytometry data which showed the expression of mΔCD79b at the cell surface, when transfected with the rCD4d3+4-mΔCD79b fusion protein.

Therefore, over-expression and cellular localisation studies suggest that mΔCD79b is located at the plasma membrane of B cells where it can interfere with PTK activation upon BCR cross-linking. To address this, we investigated the activation of PTK upon BCR cross-linking in both wild type WEHI-231 and WEHI-231 cell line that over-expressed mΔCD79b (Δ35), and was shown to be resistant to BCR induced apoptosis. Immunoblot analysis shows that both the amount and kinetics of PTK were reduced upon BCR cross-linking in WEHI-Δ35 cell line compare to wild type WEHI-231. Surprisingly, although no difference was observed in the kinetics of activated p38, Erk2 was activated for prolonged periods in stimulated WEHI-Δ35 cell line.

Up-regulation of the MAPK; Erk, has been shown previously in WEHI-231 cell lines rescued from BCR induced apoptosis[174, 197]. WEHI-231 cell line stimulated to undergo apoptosis show short kinetics in Erk2 activation, which is extended if cells are rescued by the addition of anti-CD40 mAb[174]. Katz, *et al.*,[196] have recently shown that over-expression of the anti-apoptotic protein Bcl_{XL} inhibits BCR induced apoptosis, and that this correlates with extended kinetics of Erk2 activation, compared to wild type WEHI-231 cells. Therefore, results presented here suggest that mΔCD79b interferes with PTK activation, leading to prolonged activation of ERK2 and inhibition of apoptosis. It is most likely that mΔCD79b is situated near to the plasma membrane, allowing it to interfere with the early PTKs, preventing initiation of a full intracellular signal to induce cell death.

In conclusion, we have tried to show that at different stage of B cell development, the kinetics of PTK activation are important for determining the fate of B cells. In the case of mAb therapy, mAb that induce prolonged activation of the PTK; Syk, also led to the disassociation of the CD79 heterodimer from mIgM. This process allowed prolonged signalling and induction of apoptosis. In the murine model, not only did we show that an alternative transcript of mCD79b; mΔCD79b exists for the first time. We also clearly showed that over-expression of mΔCD79b leads to reduced PTK activation, prolongd activation of Erk2 and inhibited BCR induced apoptosis. Therefore, prolonging the kinetics of PTK activation by cross-linking the BCR leads to cell death of B cell by apoptosis.

6.2 Future Work

Research carried out in this thesis has not only aided in answering several important questions in the activation of PTK for inducing apoptosis, but, several interesting views have developed for future research. Firstly, now we understand how different mAb induce apoptosis by activation of early PTKs. However, we have only investigated the activation of the early PTKs Lyn and Syk in one cell line. It would be important to further investigate the activation of the other PTKs involved in the BCR signalling pathways, and also in the other human B cell lines. This could be achieved with the use of 2-D SDS-PAGE and proteomic mapping techniques to investigate global PTK activation. This should be performed at regular time points following cross-linking the BCR with different mAb. This technique could also be applied to investingating the activation of PTK in cell lines that overexpress the alternative transcript of CD79b, allowing a clearer understanding of the PTK actived, or not, by this molecule.

It would be interesting to investigate which genes are switched on during BCR induced apoptosis. Micro-array could be used to investigate which genes are differentially activated when B cells are stimulated with different mAb. This would aid in the future development of curative agents for lymphoma. As current mAb raised against the BCR cannot be used for therapy, the use of small molecules or inhibitors is a possible avenue for investigation. One interesting avenue would be the effects of compounds that induce prolonged activation of Syk. In breast carcinoma cell lines tested, moderate but constant activation of Syk was a trend observed in cell lines that underwent apoptosis[207]. There could be a number of possible ways for developing compounds, including molecules that inhibit the SHP-1 PTP, known to regulate the activation of Syk in basal resting cells.

It would be of interest to determine if mΔCD79b forms a stable heterodimer with mCD79a, as co-transfection of mΔCD79b with mCD79a increased the expression of mΔCD79b at the cell surface. It would also be of interest to determine what controls the expression of mΔCD79b in B cells. It is evident that the expression of mΔCD79b correlates with the B cells susceptibility to undergo BCR induced apoptosis. If the protein involved in regulating the expression of mΔCD79b could be located, using similar methods adapted by Konig, *et al.*,[208, 209] who located the regulating proteins for CD44, then these would prove valuable targets for therapy in B-CLL. Over-expression of ΔCD79b has been observed in B-CLL patients and is a possible causative factor for disease. Therefore, being able to control the expression of ΔCD79b by reducing its expression in B-CLL B cells may lead to cell death.

Finally to understand the functional role of mΔCD79b during B cell development it would be of interest to produce a transgenic murine model that over-expresses mΔCD79b, and to observe what the over-expression of mΔCD79b may have on B cell development. If the expression of mΔCD79b could be controlled by utilising a Cre-Lox system, then the effect of over-expressing mΔCD79b could be observed at different stages of B cell development ex-vivo. The effect of overexpresing mΔCD79b in murine B cells could be investigated at the protein level, by looking at PTK affected, and at the genetic level as described above.

(a)

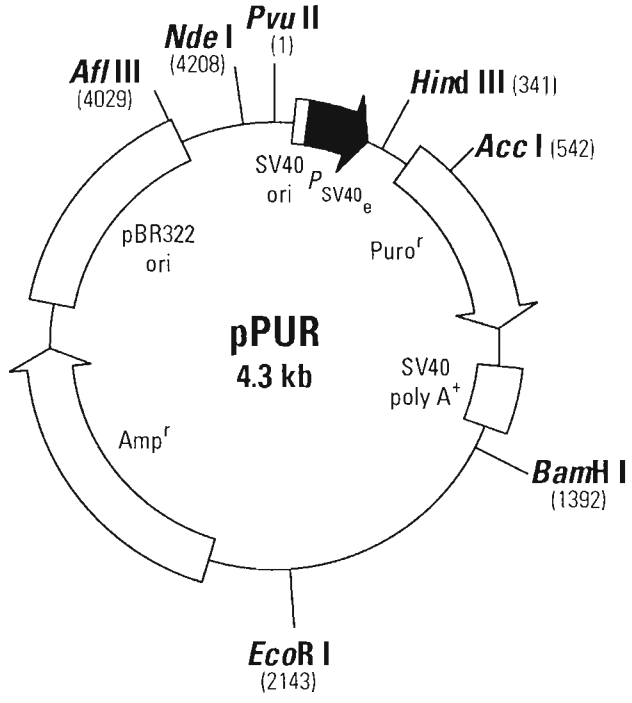

(b)

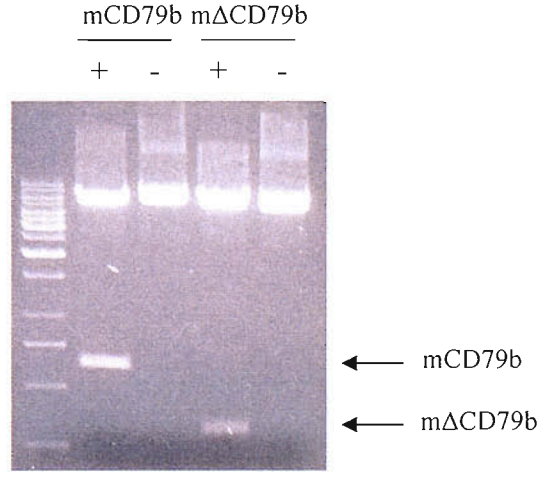

7.1 Appendix A – Cloning of full length mCD79b and mΔCD79b into pPUR vector. Following sequence analysis to confirm mCD79b and mΔCD79b were the correct PCR products, cDNA was extracted from agrose gels and ligated into the pPUR (pPuromincin) expression vector (a). Restrict digests were performed (b) to ensure the correct PCR product had been inserted before transfection of cell lines commenced.

(a)

Forward Primer
TTT CCA CGG ATT CAG CAC GTT CAA GAG ACG TGC TGA ATC CTT GGA AAT TTT TT

Reverse Primer
AAT TAA AAA ATT TCC AAG GAT TCA GCA CGT CTC TTG AAC GTG CTG AAT CCT TGG AAA GGC C

(b)

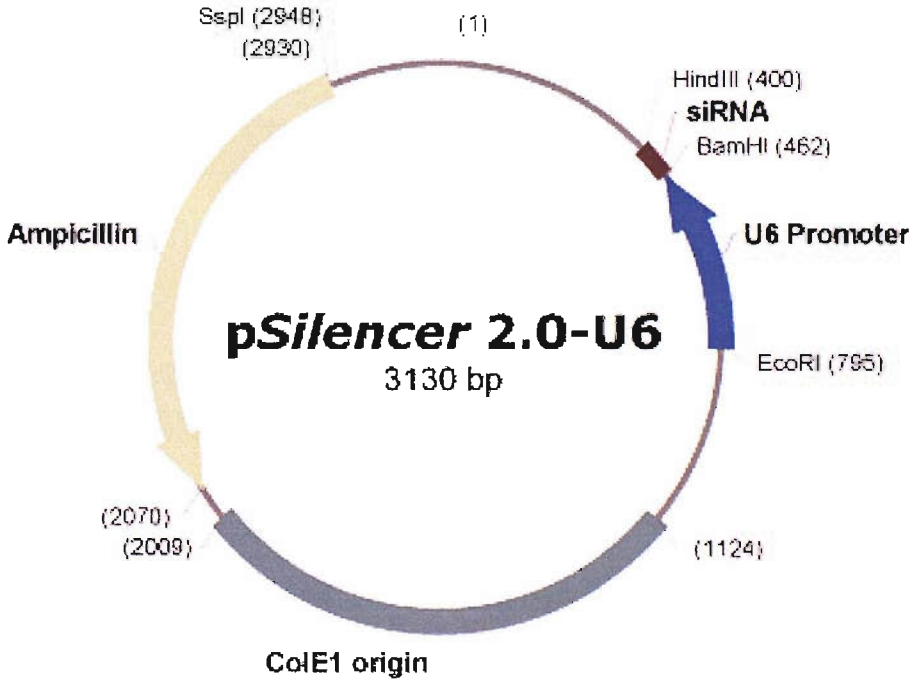

7.2 Appendix B – Designing siRNA for knockout of mΔCD79b from murine B cell lines. Primers were designed according to the Ambion protocol allowing the generation of stable siRNA that would span the splice site between exons two and four located on mΔCD79b (a). Primers were used to insert the desired sequence into the pSILENCER 2.0-U6 vector (b). Sequence analysis was utilised prior to transfections to confirm the correct sequence was inserted into the pSILENCER vector before experiments were performed.

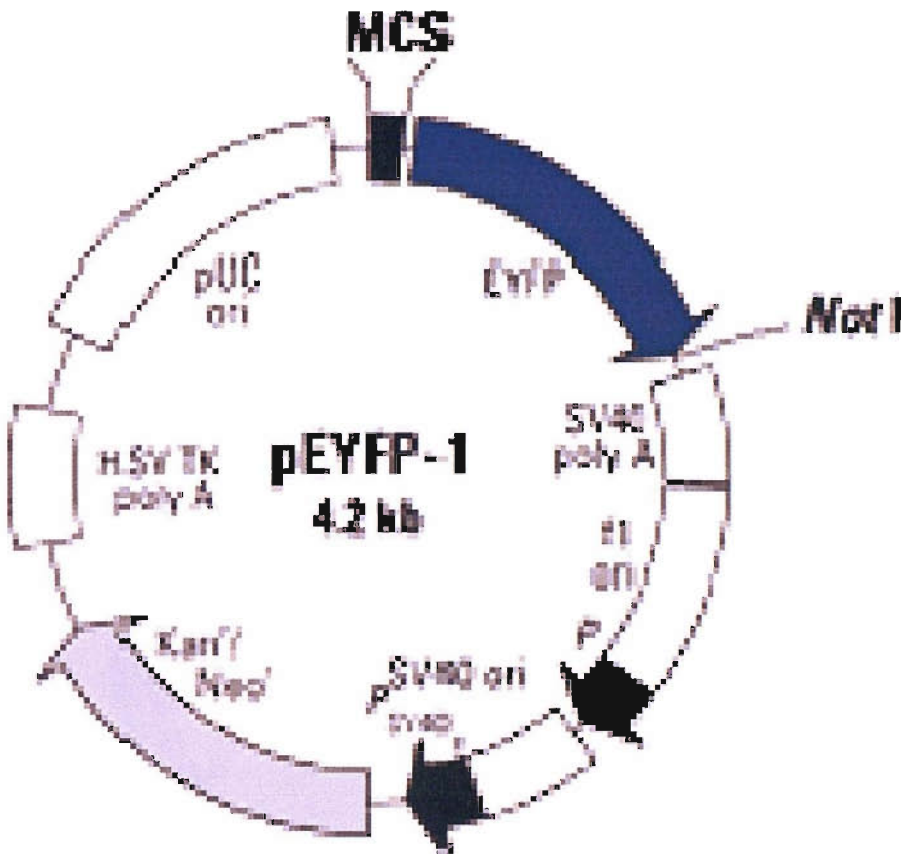

7.3 Appendix C – Cloning of full length mCD79b and mΔCD79b into pEYFP-1 vector. Following sequence analysis to confirm mCD79b and mΔCD79b were the correct PCR products, cDNA was extracted from agrose gels and ligated into the pEYFP-1 (Yellow fluorescent protein) expression vector. Restrict digests were performed to ensure the correct PCR product had been inserted before transfection of cell lines commenced.

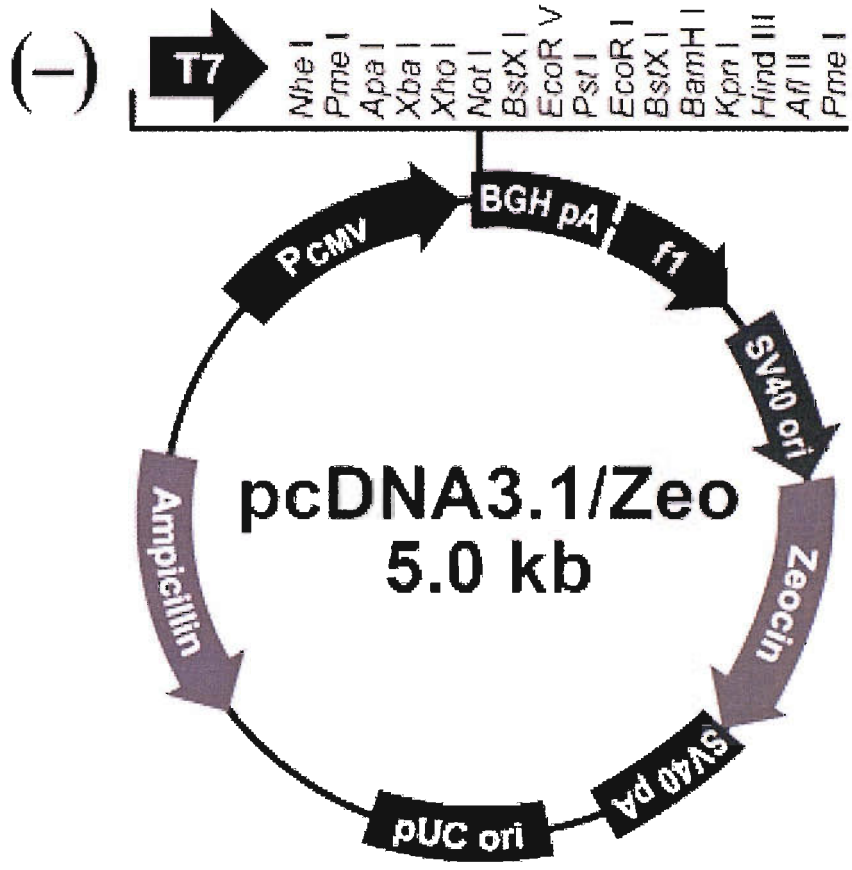

7.4 Appendix D – Cloning full length mCD79b and mΔCD79b into pcDNA3.1/Zeo with rCD4d3+4. Initially rCD4d3+4 was ligated into the pcDNA3.1/Zeo vector allowing the generation of a more stable expression system. Following this both full length mCD79b and mΔCD79b sequenced PCR products were ligated into the vector allowing the generation of fusion proteins with the rCD4d3+4 tagged to the N terminus of eiter mCD79b or mΔCD79b. Restriction digests were performed to confirm the presence of these proteins in the correct vector prior to experiments.

References

1. Gold, M. R. 2002. To make antibodies or not: signaling by the B-cell antigen receptor. *Trends Pharmacol Sci 23:316-24.*
2. Benschop, R. J., and J. C. Cambier. 1999. B cell development: signal transduction by antigen receptors and their surrogates. *Curr Opin Immunol 11:143-51.*
3. Parker, D. C. 1993. T cell-dependent B cell activation. *Annu Rev Immunol 11:331-60.*
4. Cambier, J. C. 1995. Antigen and Fc receptor signaling. The awesome power of the immunoreceptor tyrosine-based activation motif (ITAM). *J Immunol 155:3281-5.*
5. DeFranco, A. L. 1987. Transmembrane signaling reactions generated in B cells in response to anti-IgM or lipopolysaccharide. *Adv Exp Med Biol 213:189-93.*
6. Reth, M., J. Wienands, T. Tsubata, and J. Hombach. 1991. Identification of components of the B cell antigen receptor complex. *Adv Exp Med Biol 292:207-14.*
7. Pernis, B., L. Forni, and L. Amante. 1971. Immunoglobulins as cell receptors. *Ann N Y Acad Sci 190:420-31.*
8. Reth, M. 1992. Antigen receptors on B lymphocytes. *Annu Rev Immunol 10:97-121.*
9. Martin, S. W., and C. C. Goodnow. 2002. Burst-enhancing role of the IgG membrane tail as a molecular determinant of memory. *Nat Immunol 3:182-8.*
10. Reth, M., J. Hombach, J. Wienands, K. S. Campbell, N. Chien, L. B. Justement, and J. C. Cambier. 1991. The B-cell antigen receptor complex. *Immunol Today 12:196-201.*
11. Muller, B., L. Cooper, and C. Terhorst. 1992. Cloning and sequencing of the cDNA encoding the human homologue of the murine immunoglobulin-associated protein B29. *Eur J Immunol 22:1621-5.*
12. Kashiwamura, S., T. Koyama, T. Matsuo, M. Steinmetz, M. Kimoto, and N. Sakaguchi. 1990. Structure of the murine mb-1 gene encoding a putative sIgM-associated molecule. *J Immunol 145:337-43.*
13. Mason, D. Y., C. J. van Noesel, J. L. Cordell, W. M. Comans-Bitter, K. Micklem, A. G. Tse, R. A. van Lier, and J. J. van Dongen. 1992. The B29 and mb-1 polypeptides are differentially expressed during human B cell differentiation. *Eur J Immunol 22:2753-6.*
14. Kuwahara, K., T. Matsuo, J. Nomura, H. Igarashi, M. Kimoto, S. Inui, and N. Sakaguchi. 1994. Identification of a 52-kDa molecule (p52) coprecipitated with the Ig receptor-related MB-1 protein that is inducibly phosphorylated by the stimulation with phorbol myristate acetate. *J Immunol 152:2742-52.*
15. Williams, A. F., and A. N. Barclay. 1988. The immunoglobulin superfamily--domains for cell surface recognition. *Annu Rev Immunol 6:381-405.*
16. Hashimoto, S., N. Chiorazzi, and P. K. Gregersen. 1994. The complete sequence of the human CD79b (Ig beta/B29) gene: identification of a conserved exon/intron organization, immunoglobulin- like regulatory regions, and allelic polymorphism. *Immunogenetics 40:145-9.*
17. Letourneur, F., and R. D. Klausner. 1991. T-cell and basophil activation through the cytoplasmic tail of T-cell- receptor zeta family proteins. *Proc Natl Acad Sci U S A 88:8905-9.*
18. DeFranco, A. L. 1992. Tyrosine phosphorylation and the mechanism of signal transduction by the B-lymphocyte antigen receptor. *Eur J Biochem 210:381-8.*
19. Romeo, C., M. Amiot, and B. Seed. 1992. Sequence requirements for induction of cytolysis by the T cell antigen/Fc receptor zeta chain. *Cell 68:889-97.*
20. Letourneur, F., and R. D. Klausner. 1992. Activation of T cells by a tyrosine kinase activation domain in the cytoplasmic tail of CD3 epsilon. *Science 255:79-82.*

21. Cambier, J. C., C. M. Pleiman, and M. R. Clark. 1994. Signal transduction by the B cell antigen receptor and its coreceptors. *Annu Rev Immunol 12:457-86.*
22. Hombach, J., F. Sablitzky, K. Rajewsky, and M. Reth. 1988. Transfected plasmacytoma cells do not transport the membrane form of IgM to the cell surface. *J Exp Med 167:652-7.*
23. Hombach, J., L. Leclercq, A. Radbruch, K. Rajewsky, and M. Reth. 1988. A novel 34-kd protein co-isolated with the IgM molecule in surface IgM-expressing cells. *Embo J 7:3451-6.*
24. Sitia, R., M. S. Neuberger, and C. Milstein. 1987. Regulation of membrane IgM expression in secretory B cells: translational and post-translational events. *Embo J 6:3969-77.*
25. Venkitaraman, A. R., G. T. Williams, P. Dariavach, and M. S. Neuberger. 1991. The B-cell antigen receptor of the five immunoglobulin classes. *Nature 352:777-81.*
26. Shaw, A. C., R. N. Mitchell, Y. K. Weaver, J. Campos-Torres, A. K. Abbas, and P. Leder. 1990. Mutations of immunoglobulin transmembrane and cytoplasmic domains: effects on intracellular signaling and antigen presentation. *Cell 63:381-92.*
27. Grupp, S. A., K. Campbell, R. N. Mitchell, J. C. Cambier, and A. K. Abbas. 1993. Signaling-defective mutants of the B lymphocyte antigen receptor fail to associate with Ig-alpha and Ig-beta/gamma. *J Biol Chem 268:25776-9.*
28. Stevens, T. L., J. H. Blum, S. P. Foy, L. Matsuuchi, and A. L. DeFranco. 1994. A mutation of the mu transmembrane that disrupts endoplasmic reticulum retention. Effects on association with accessory proteins and signal transduction. *J Immunol 152:4397-406.*
29. Sanchez, M., Z. Misulovin, A. L. Burkhardt, S. Mahajan, T. Costa, R. Franke, J. B. Bolen, and M. Nussenzweig. 1993. Signal transduction by immunoglobulin is mediated through Ig alpha and Ig beta. *J Exp Med 178:1049-55.*
30. Schamel, W. W., and M. Reth. 2000. Monomeric and oligomeric complexes of the B cell antigen receptor. *Immunity 13:5-14.*
31. Burnet, F. M. 1962. The immunological significance of the thymus: an extension of the clonal selection theory of immunity. *Australas Ann Med 11:79-91.*
32. Campbell, K. S. 1999. Signal transduction from the B cell antigen-receptor. *Curr Opin Immunol 11:256-64.*
33. Kurosaki, T. 1999. Genetic analysis of B cell antigen receptor signaling. *Annu Rev Immunol 17:555-92.*
34. Tamir, I., J. M. Dal Porto, and J. C. Cambier. 2000. Cytoplasmic protein tyrosine phosphatases SHP-1 and SHP-2: regulators of B cell signal transduction. *Curr Opin Immunol 12:307-15.*
35. Clark, M. R., K. S. Campbell, A. Kazlauskas, S. A. Johnson, M. Hertz, T. A. Potter, C. Pleiman, and J. C. Cambier. 1992. The B cell antigen receptor complex: association of Ig-alpha and Ig- beta with distinct cytoplasmic effectors. *Science 258:123-6.*
36. Yamanashi, Y., T. Kakiuchi, J. Mizuguchi, T. Yamamoto, and K. Toyoshima. 1991. Association of B cell antigen receptor with protein tyrosine kinase Lyn. *Science 251:192-4.*
37. Burkhardt, A. L., M. Brunswick, J. B. Bolen, and J. J. Mond. 1991. Anti-immunoglobulin stimulation of B lymphocytes activates src-related protein-tyrosine kinases. *Proc Natl Acad Sci U S A 88:7410-4.*
38. Luisiri, P., Y. J. Lee, B. J. Eisfelder, and M. R. Clark. 1996. Cooperativity and segregation of function within the Ig-alpha/beta heterodimer of the B cell antigen receptor complex. *J Biol Chem 271:5158-63.*
39. Rolli, V., M. Gallwitz, T. Wossning, A. Flemming, W. W. Schamel, C. Zurn, and M. Reth. 2002. Amplification of B cell antigen receptor signaling by a Syk/ITAM positive feedback loop. *Mol Cell 10:1057-69.*

40. Plas, D. R., and M. L. Thomas. 1998. Negative regulation of antigen receptor signaling in lymphocytes. *J Mol Med 76:589-95.*
41. Matsuuchi, L., and M. R. Gold. 2001. New views of BCR structure and organization. *Curr Opin Immunol 13:270-7.*
42. Reth, M. 2001. Oligomeric antigen receptors: a new view on signaling for the selection of lymphocytes. *Trends Immunol 22:356-60.*
43. Jiang, A., A. Craxton, T. Kurosaki, and E. A. Clark. 1998. Different protein tyrosine kinases are required for B cell antigen receptor-mediated activation of extracellular signal-regulated kinase, c-Jun NH2-terminal kinase 1, and p38 mitogen-activated protein kinase. *J Exp Med 188:1297-306.*
44. Cornall, R. J., A. M. Cheng, T. Pawson, and C. C. Goodnow. 2000. Role of Syk in B-cell development and antigen-receptor signaling. *Proc Natl Acad Sci U S A 97:1713-8.*
45. Suzuki, H., Y. Terauchi, M. Fujiwara, S. Aizawa, Y. Yazaki, T. Kadowaki, and S. Koyasu. 1999. Xid-like immunodeficiency in mice with disruption of the p85alpha subunit of phosphoinositide 3-kinase. *Science 283:390-2.*
46. Fruman, D. A., S. B. Snapper, C. M. Yballe, L. Davidson, J. Y. Yu, F. W. Alt, and L. C. Cantley. 1999. Impaired B cell development and proliferation in absence of phosphoinositide 3-kinase p85alpha. *Science 283:393-7.*
47. Sasaki, T., A. Suzuki, J. Sasaki, and J. M. Penninger. 2002. Phosphoinositide 3-kinases in immunity: lessons from knockout mice. *J Biochem (Tokyo) 131:495-501.*
48. Lemmon, M. A., and K. M. Ferguson. 2000. Signal-dependent membrane targeting by pleckstrin homology (PH) domains. *Biochem J 350 Pt 1:1-18.*
49. Rameh, L. E., A. Arvidsson, K. L. Carraway, 3rd, A. D. Couvillon, G. Rathbun, A. Crompton, B. VanRenterghem, M. P. Czech, K. S. Ravichandran, S. J. Burakoff, D. S. Wang, C. S. Chen, and L. C. Cantley. 1997. A comparative analysis of the phosphoinositide binding specificity of pleckstrin homology domains. *J Biol Chem 272:22059-66.*
50. Hemmings, B. A. 1997. Akt signaling: linking membrane events to life and death decisions. *Science 275:628-30.*
51. Pogue, S. L., T. Kurosaki, J. Bolen, and R. Herbst. 2000. B cell antigen receptor-induced activation of Akt promotes B cell survival and is dependent on Syk kinase. *J Immunol 165:1300-6.*
52. Gold, M. R., M. P. Scheid, L. Santos, M. Dang-Lawson, R. A. Roth, L. Matsuuchi, V. Duronio, and D. L. Krebs. 1999. The B cell antigen receptor activates the Akt (protein kinase B)/glycogen synthase kinase-3 signaling pathway via phosphatidylinositol 3-kinase. *J Immunol 163:1894-905.*
53. Engels, N., B. Wollscheid, and J. Wienands. 2001. Association of SLP-65/BLNK with the B cell antigen receptor through a non-ITAM tyrosine of Ig-alpha. *Eur J Immunol 31:2126-34.*
54. Fu, C., C. W. Turck, T. Kurosaki, and A. C. Chan. 1998. BLNK: a central linker protein in B cell activation. *Immunity 9:93-103.*
55. Tsuji, S., M. Okamoto, K. Yamada, N. Okamoto, R. Goitsuka, R. Arnold, F. Kiefer, and D. Kitamura. 2001. B cell adaptor containing src homology 2 domain (BASH) links B cell receptor signaling to the activation of hematopoietic progenitor kinase 1. *J Exp Med 194:529-39.*
56. Ishiai, M., M. Kurosaki, R. Pappu, K. Okawa, I. Ronko, C. Fu, M. Shibata, A. Iwamatsu, A. C. Chan, and T. Kurosaki. 1999. BLNK required for coupling Syk to PLC gamma 2 and Rac1-JNK in B cells. *Immunity 10:117-25.*
57. Siemasko, K., B. J. Skaggs, S. Kabak, E. Williamson, B. K. Brown, W. Song, and M. R. Clark. 2002. Receptor-facilitated antigen presentation requires the recruitment of B cell linker protein to Igalpha. *J Immunol 168:2127-38.*

58. Pappu, R., A. M. Cheng, B. Li, Q. Gong, C. Chiu, N. Griffin, M. White, B. P. Sleckman, and A. C. Chan. 1999. Requirement for B cell linker protein (BLNK) in B cell development. *Science 286:1949-54.*
59. Hayashi, K., R. Nittono, N. Okamoto, S. Tsuji, Y. Hara, R. Goitsuka, and D. Kitamura. 2000. The B cell-restricted adaptor BASH is required for normal development and antigen receptor-mediated activation of B cells. *Proc Natl Acad Sci U S A 97:2755-60.*
60. Fukuda, M., T. Kojima, H. Kabayama, and K. Mikoshiba. 1996. Mutation of the pleckstrin homology domain of Bruton's tyrosine kinase in immunodeficiency impaired inositol 1,3,4,5-tetrakisphosphate binding capacity. *J Biol Chem 271:30303-6.*
61. Salim, K., M. J. Bottomley, E. Querfurth, M. J. Zvelebil, I. Gout, R. Scaife, R. L. Margolis, R. Gigg, C. I. Smith, P. C. Driscoll, M. D. Waterfield, and G. Panayotou. 1996. Distinct specificity in the recognition of phosphoinositides by the pleckstrin homology domains of dynamin and Bruton's tyrosine kinase. *Embo J 15:6241-50.*
62. Mohamed, A. J., B. F. Nore, B. Christensson, and C. I. Smith. 1999. Signalling of Bruton's tyrosine kinase, Btk. *Scand J Immunol 49:113-8.*
63. Suzuki, H., S. Matsuda, Y. Terauchi, M. Fujiwara, T. Ohteki, T. Asano, T. W. Behrens, T. Kouro, K. Takatsu, T. Kadowaki, and S. Koyasu. 2003. PI3K and Btk differentially regulate B cell antigen receptor-mediated signal transduction. *Nat Immunol 4:280-6.*
64. Hendriks, R. W., M. F. de Bruijn, A. Maas, G. M. Dingjan, A. Karis, and F. Grosveld. 1996. Inactivation of Btk by insertion of lacZ reveals defects in B cell development only past the pre-B cell stage. *Embo J 15:4862-72.*
65. Kang, S. W., M. I. Wahl, J. Chu, J. Kitaura, Y. Kawakami, R. M. Kato, R. Tabuchi, A. Tarakhovsky, T. Kawakami, C. W. Turck, O. N. Witte, and D. J. Rawlings. 2001. PKCbeta modulates antigen receptor signaling via regulation of Btk membrane localization. *Embo J 20:5692-702.*
66. Hashimoto, A., K. Hirose, T. Kurosaki, and M. Iino. 2001. Negative control of store-operated Ca2+ influx by B cell receptor cross- linking. *J Immunol 166:1003-8.*
67. Sugawara, H., M. Kurosaki, M. Takata, and T. Kurosaki. 1997. Genetic evidence for involvement of type 1, type 2 and type 3 inositol 1,4,5-trisphosphate receptors in signal transduction through the B-cell antigen receptor. *Embo J 16:3078-88.*
68. Beals, C. R., N. A. Clipstone, S. N. Ho, and G. R. Crabtree. 1997. Nuclear localization of NF-ATc by a calcineurin-dependent, cyclosporin- sensitive intramolecular interaction. *Genes Dev 11:824-34.*
69. Rawlings, D. J. 1999. Bruton's tyrosine kinase controls a sustained calcium signal essential for B lineage development and function. *Clin Immunol 91:243-53.*
70. Su, T. T., B. Guo, Y. Kawakami, K. Sommer, K. Chae, L. A. Humphries, R. M. Kato, S. Kang, L. Patrone, R. Wall, M. Teitell, M. Leitges, T. Kawakami, and D. J. Rawlings. 2002. PKC-beta controls I kappa B kinase lipid raft recruitment and activation in response to BCR signaling. *Nat Immunol 3:780-6.*
71. Senftleben, U., Y. Cao, G. Xiao, F. R. Greten, G. Krahn, G. Bonizzi, Y. Chen, Y. Hu, A. Fong, S. C. Sun, and M. Karin. 2001. Activation by IKKalpha of a second, evolutionary conserved, NF-kappa B signaling pathway. *Science 293:1495-9.*
72. Ren, H., A. Schmalstieg, D. Yuan, and R. B. Gaynor. 2002. I-kappa B kinase beta is critical for B cell proliferation and antibody response. *J Immunol 168:577-87.*
73. DeFranco, A. L. 2001. Vav and the B cell signalosome. *Nat Immunol 2:482-4.*
74. Tedford, K., L. Nitschke, I. Girkontaite, A. Charlesworth, G. Chan, V. Sakk, M. Barbacid, and K. D. Fischer. 2001. Compensation between Vav-1 and Vav-2 in B cell development and antigen receptor signaling. *Nat Immunol 2:548-55.*
75. Hashimoto, A., H. Okada, A. Jiang, M. Kurosaki, S. Greenberg, E. A. Clark, and T. Kurosaki. 1998. Involvement of guanosine triphosphatases and phospholipase C-

gamma2 in extracellular signal-regulated kinase, c-Jun NH2-terminal kinase, and p38 mitogen-activated protein kinase activation by the B cell antigen receptor. *J Exp Med 188:1287-95.*

76. O'Rourke, L. M., R. Tooze, M. Turner, D. M. Sandoval, R. H. Carter, V. L. Tybulewicz, and D. T. Fearon. 1998. CD19 as a membrane-anchored adaptor protein of B lymphocytes: costimulation of lipid and protein kinases by recruitment of Vav. *Immunity 8:635-45.*
77. Li, N., A. Batzer, R. Daly, V. Yajnik, E. Skolnik, P. Chardin, D. Bar-Sagi, B. Margolis, and J. Schlessinger. 1993. Guanine-nucleotide-releasing factor hSos1 binds to Grb2 and links receptor tyrosine kinases to Ras signalling. *Nature 363:85-8.*
78. Wienands, J., J. Schweikert, B. Wollscheid, H. Jumaa, P. J. Nielsen, and M. Reth. 1998. SLP-65: a new signaling component in B lymphocytes which requires expression of the antigen receptor for phosphorylation. *J Exp Med 188:791-5.*
79. Brummer, T., P. E. Shaw, M. Reth, and Y. Misawa. 2002. Inducible gene deletion reveals different roles for B-Raf and Raf-1 in B-cell antigen receptor signalling. *Embo J 21:5611-22.*
80. Mikula, M., M. Schreiber, Z. Husak, L. Kucerova, J. Ruth, R. Wieser, K. Zatloukal, H. Beug, E. F. Wagner, and M. Baccarini. 2001. Embryonic lethality and fetal liver apoptosis in mice lacking the c-raf- 1 gene. *Embo J 20:1952-62.*
81. Huser, M., J. Luckett, A. Chiloeches, K. Mercer, M. Iwobi, S. Giblett, X. M. Sun, J. Brown, R. Marais, and C. Pritchard. 2001. MEK kinase activity is not necessary for Raf-1 function. *Embo J 20:1940-51.*
82. Ogimoto, M., Y. Arimura, T. Katagiri, K. Mitomo, J. R. Woodgett, A. R. Nebreda, K. Mizuno, and H. Yakura. 2001. Opposing regulation of B cell receptor-induced activation of mitogen- activated protein kinases by CD45. *FEBS Lett 490:97-101.*
83. Mizuno, K., Y. Tagawa, K. Mitomo, N. Watanabe, T. Katagiri, M. Ogimoto, and H. Yakura. 2002. Src homology region 2 domain-containing phosphatase 1 positively regulates B cell receptor-induced apoptosis by modulating association of B cell linker protein with Nck and activation of c-Jun NH2-terminal kinase. *J Immunol 169:778-86.*
84. Brauweiler, A. M., I. Tamir, and J. C. Cambier. 2000. Bilevel control of B-cell activation by the inositol 5-phosphatase SHIP. *Immunol Rev 176:69-74.*
85. Hata, A., H. Sabe, T. Kurosaki, M. Takata, and H. Hanafusa. 1994. Functional analysis of Csk in signal transduction through the B-cell antigen receptor. *Mol Cell Biol 14:7306-13.*
86. Parnes, J. R., and C. Pan. 2000. CD72, a negative regulator of B-cell responsiveness. *Immunol Rev 176:75-85.*
87. Carsetti, R. 2000. The development of B cells in the bone marrow is controlled by the balance between cell-autonomous mechanisms and signals from the microenvironment. *J Exp Med 191:5-8.*
88. Era, T., S. Nishikawa, T. Sudo, F. H. Wang, M. Ogawa, T. Kunisada, and S. Hayashi. 1994. How B-precursor cells are driven to cycle. *Immunol Rev 137:35-51.*
89. Wei, C., L. Lai, and I. Goldschneider. 2002. Pre-pro-B cell growth-stimulating factor (PPBSF) upregulates IL-7Ralpha chain expression and enables pro-B cells to respond to monomeric IL-7. *J Interferon Cytokine Res 22:823-32.*
90. Meffre, E., E. Davis, C. Schiff, C. Cunningham-Rundles, L. B. Ivashkiv, L. M. Staudt, J. W. Young, and M. C. Nussenzweig. 2000. Circulating human B cells that express surrogate light chains and edited receptors. *Nat Immunol 1:207-13.*
91. Koyama, M., K. Ishihara, H. Karasuyama, J. L. Cordell, A. Iwamoto, and T. Nakamura. 1997. CD79 alpha/CD79 beta heterodimers are expressed on pro-B cell surfaces without associated mu heavy chain. *Int Immunol 9:1767-72.*
92. Nagata, K., T. Nakamura, F. Kitamura, S. Kuramochi, S. Taki, K. S. Campbell, and H. Karasuyama. 1997. The Ig alpha/Igbeta heterodimer on mu-negative proB cells is

competent for transducing signals to induce early B cell differentiation. *Immunity 7:559-70.*
93. Benlagha, K., P. Guglielmi, M. D. Cooper, and K. Lassoued. 1999. Modifications of Igalpha and Igbeta expression as a function of B lineage differentiation. *J Biol Chem 274:19389-96.*
94. Li, Y. S., R. Wasserman, K. Hayakawa, and R. R. Hardy. 1996. Identification of the earliest B lineage stage in mouse bone marrow. *Immunity 5:527-35.*
95. Gray Parkin, K., R. P. Stephan, R. G. Apilado, D. A. Lill-Elghanian, K. P. Lee, B. Saha, and P. L. Witte. 2002. Expression of CD28 by bone marrow stromal cells and its involvement in B lymphopoiesis. *J Immunol 169:2292-302.*
96. Gong, S., and M. C. Nussenzweig. 1996. Regulation of an early developmental checkpoint in the B cell pathway by Ig beta. *Science 272:411-4.*
97. Meffre, E., and M. C. Nussenzweig. 2002. Deletion of immunoglobulin beta in developing B cells leads to cell death. *Proc Natl Acad Sci U S A 99:11334-9.*
98. Pelanda, R., U. Braun, E. Hobeika, M. C. Nussenzweig, and M. Reth. 2002. B cell progenitors are arrested in maturation but have intact VDJ recombination in the absence of Ig-alpha and Ig-beta. *J Immunol 169:865-72.*
99. Bannish, G., E. M. Fuentes-Panana, J. C. Cambier, W. S. Pear, and J. G. Monroe. 2001. Ligand-independent signaling functions for the B lymphocyte antigen receptor and their role in positive selection during B lymphopoiesis. *J Exp Med 194:1583-96.*
100. Hess, J., A. Werner, T. Wirth, F. Melchers, H. M. Jack, and T. H. Winkler. 2001. Induction of pre-B cell proliferation after de novo synthesis of the pre-B cell receptor. *Proc Natl Acad Sci U S A 98:1745-50.*
101. Kurosaki, T. 2002. Regulation of B cell fates by BCR signaling components. *Curr Opin Immunol 14:341-7.*
102. Bradl, H., and H. M. Jack. 2001. Surrogate light chain-mediated interaction of a soluble pre-B cell receptor with adherent cell lines. *J Immunol 167:6403-11.*
103. Fang, W., B. C. Weintraub, B. Dunlap, P. Garside, K. A. Pape, M. K. Jenkins, C. C. Goodnow, D. L. Mueller, and T. W. Behrens. 1998. Self-reactive B lymphocytes overexpressing Bcl-xL escape negative selection and are tolerized by clonal anergy and receptor editing. *Immunity 9:35-45.*
104. Torres, R. M., and K. Hafen. 1999. A negative regulatory role for Ig-alpha during B cell development. *Immunity 11:527-36.*
105. Reichlin, A., Y. Hu, E. Meffre, H. Nagaoka, S. Gong, M. Kraus, K. Rajewsky, and M. C. Nussenzweig. 2001. B cell development is arrested at the immature B cell stage in mice carrying a mutation in the cytoplasmic domain of immunoglobulin beta. *J Exp Med 193:13-23.*
106. Melamed, D., and D. Nemazee. 1997. Self-antigen does not accelerate immature B cell apoptosis, but stimulates receptor editing as a consequence of developmental arrest. *Proc Natl Acad Sci U S A 94:9267-72.*
107. Hsueh, R. C., and R. H. Scheuermann. 2000. Tyrosine kinase activation in the decision between growth, differentiation, and death responses initiated from the B cell antigen receptor. *Adv Immunol 75:283-316.*
108. Benschop, R. J., E. Brandl, A. C. Chan, and J. C. Cambier. 2001. Unique signaling properties of B cell antigen receptor in mature and immature B cells: implications for tolerance and activation. *J Immunol 167:4172-9.*
109. Schamel, W. W., and M. Reth. 2000. Stability of the B cell antigen receptor complex. *Mol Immunol 37:253-9.*
110. Kelsoe, G. 1995. The germinal center reaction. *Immunol Today 16:324-6.*
111. Liu, Y. J., D. E. Joshua, G. T. Williams, C. A. Smith, J. Gordon, and I. C. MacLennan. 1989. Mechanism of antigen-driven selection in germinal centres. *Nature 342:929-31.*

112. Galibert, L., N. Burdin, C. Barthelemy, G. Meffre, I. Durand, E. Garcia, P. Garrone, F. Rousset, J. Banchereau, and Y. J. Liu. 1996. Negative selection of human germinal center B cells by prolonged BCR cross-linking. *J Exp Med 183:2075-85.*
113. Guzman-Rojas, L., J. C. Sims-Mourtada, R. Rangel, and H. Martinez-Valdez. 2002. Life and death within germinal centres: a double-edged sword. *Immunology 107:167-75.*
114. Pierce, S. K. 2002. Lipid rafts and B-cell activation. *Nat Rev Immunol 2:96-105.*
115. van Meer, G. 2002. Cell biology. The different hues of lipid rafts. *Science 296:855-7.*
116. Cheng, P. C., A. Cherukuri, M. Dykstra, S. Malapati, T. Sproul, M. R. Chen, and S. K. Pierce. 2001. Floating the raft hypothesis: the roles of lipid rafts in B cell antigen receptor function. *Semin Immunol 13:107-14.*
117. Awasthi-Kalia, M., P. P. Schnetkamp, and J. P. Deans. 2001. Differential effects of filipin and methyl-beta-cyclodextrin on B cell receptor signaling. *Biochem Biophys Res Commun 287:77-82.*
118. Cheng, P. C., M. L. Dykstra, R. N. Mitchell, and S. K. Pierce. 1999. A role for lipid rafts in B cell antigen receptor signaling and antigen targeting. *J Exp Med 190:1549-60.*
119. Petrie, R. J., P. P. Schnetkamp, K. D. Patel, M. Awasthi-Kalia, and J. P. Deans. 2000. Transient translocation of the B cell receptor and Src homology 2 domain-containing inositol phosphatase to lipid rafts: evidence toward a role in calcium regulation. *J Immunol 165:1220-7.*
120. Dykstra, M. L., R. Longnecker, and S. K. Pierce. 2001. Epstein-Barr virus coopts lipid rafts to block the signaling and antigen transport functions of the BCR. *Immunity 14:57-67.*
121. Guo, B., R. M. Kato, M. Garcia-Lloret, M. I. Wahl, and D. J. Rawlings. 2000. Engagement of the human pre-B cell receptor generates a lipid raft- dependent calcium signaling complex. *Immunity 13:243-53.*
122. Sproul, T. W., S. Malapati, J. Kim, and S. K. Pierce. 2000. Cutting edge: B cell antigen receptor signaling occurs outside lipid rafts in immature B cells. *J Immunol 165:6020-3.*
123. Stoddart, A., M. L. Dykstra, B. K. Brown, W. Song, S. K. Pierce, and F. M. Brodsky. 2002. Lipid rafts unite signaling cascades with clathrin to regulate BCR internalization. *Immunity 17:451-62.*
124. Salisbury, J. L., J. S. Condeelis, and P. Satir. 1980. Role of coated vesicles, microfilaments, and calmodulin in receptor- mediated endocytosis by cultured B lymphoblastoid cells. *J Cell Biol 87:132-41.*
125. Putnam, M. A., A. E. Moquin, M. Merrihew, C. Outcalt, E. Sorge, A. Caballero, T. A. Gondre-Lewis, and J. R. Drake. 2003. Lipid raft-independent B cell receptor-mediated antigen internalization and intracellular trafficking. *J Immunol 170:905-12.*
126. Turner, M., A. Gulbranson-Judge, M. E. Quinn, A. E. Walters, I. C. MacLennan, and V. L. Tybulewicz. 1997. Syk tyrosine kinase is required for the positive selection of immature B cells into the recirculating B cell pool. *J Exp Med 186:2013-21.*
127. Ma, H., T. M. Yankee, J. Hu, D. J. Asai, M. L. Harrison, and R. L. Geahlen. 2001. Visualization of Syk-antigen receptor interactions using green fluorescent protein: differential roles for Syk and Lyn in the regulation of receptor capping and internalization. *J Immunol 166:1507-16.*
128. Reth, M., J. Wienands, and W. W. Schamel. 2000. An unsolved problem of the clonal selection theory and the model of an oligomeric B-cell antigen receptor. *Immunol Rev 176:10-8.*
129. Kaplan, D., H. Meyerson, and K. Lewandowska. 2001. High resolution immunophenotypic analysis of chronic lymphocytic leukemic cells by enzymatic amplification staining. *Am J Clin Pathol 116:429-36.*

130. Caligaris-Cappio, F., and T. J. Hamblin. 1999. B-cell chronic lymphocytic leukemia: a bird of a different feather. *J Clin Oncol 17:399-408.*
131. Dighiero, G., E. Bodega, R. Mayzner, and J. L. Binet. 1980. Individual cell-by-cell quantitation of lymphocyte surface membrane Ig in normal and CLL lymphocyte and during ontogeny of mouse B lymphocytes by immunoperoxidase assay. *Blood 55:93-100.*
132. Zomas, A. P., E. Matutes, R. Morilla, K. Owusu-Ankomah, B. K. Seon, and D. Catovsky. 1996. Expression of the immunoglobulin-associated protein B29 in B cell disorders with the monoclonal antibody SN8 (CD79b). *Leukemia 10:1966-70.*
133. Hamblin, T. J., Z. Davis, A. Gardiner, D. G. Oscier, and F. K. Stevenson. 1999. Unmutated Ig V(H) genes are associated with a more aggressive form of chronic lymphocytic leukemia. *Blood 94:1848-54.*
134. Thompson, A. A., J. A. Talley, H. N. Do, H. L. Kagan, L. Kunkel, J. Berenson, M. D. Cooper, A. Saxon, and R. Wall. 1997. Aberrations of the B-cell receptor B29 (CD79b) gene in chronic lymphocytic leukemia. *Blood 90:1387-94.*
135. Payelle-Brogard, B., C. Magnac, F. R. Mauro, F. Mandelli, and G. Dighiero. 1999. Analysis of the B-cell receptor B29 (CD79b) gene in familial chronic lymphocytic leukemia. *Blood 94:3516-22.*
136. Verschuren, M. C., W. M. Comans-Bitter, C. A. Kapteijn, D. Y. Mason, G. S. Brouns, J. Borst, H. G. Drexler, and J. J. van Dongen. 1993. Transcription and protein expression of mb-1 and B29 genes in human hematopoietic malignancies and cell lines. *Leukemia 7:1939-47.*
137. Rassenti, L. Z., and T. J. Kipps. 2000. Expression of Ig-beta (CD79b) by chronic lymphocytic leukemia B cells that lack immunoglobulin heavy-chain allelic exclusion. *Blood 95:2725-7.*
138. Hashimoto, S., N. Chiorazzi, and P. K. Gregersen. 1995. Alternative splicing of CD79a (Ig-alpha/mb-1) and CD79b (Ig-beta/B29) RNA transcripts in human B cells. *Mol Immunol 32:651-9.*
139. Koyama, M., T. Nakamura, M. Higashihara, B. Herren, S. Kuwata, Y. Shibata, K. Okumura, and K. Kurokawa. 1995. The novel variants of mb-1 and B29 transcripts generated by alternative mRNA splicing. *Immunol Lett 47:151-6.*
140. Alfarano, A., S. Indraccolo, P. Circosta, S. Minuzzo, A. Vallario, R. Zamarchi, A. Fregonese, F. Calderazzo, A. Faldella, M. Aragno, C. Camaschella, A. Amadori, and F. Caligaris-Cappio. 1999. An alternatively spliced form of CD79b gene may account for altered B- cell receptor expression in B-chronic lymphocytic leukemia. *Blood 93:2327-35.*
141. Cragg, M. S., H. T. Chan, M. D. Fox, A. Tutt, A. Smith, D. G. Oscier, T. J. Hamblin, and M. J. Glennie. 2002. The alternative transcript of CD79b is overexpressed in B-CLL and inhibits signaling for apoptosis. *Blood 100:3068-76.*
142. Venter, J. C., M. D. Adams, E. W. Myers, P. W. Li, R. J. Mural, G. G. Sutton, H. O. Smith, M. Yandell, C. A. Evans, R. A. Holt, J. D. Gocayne, P. Amanatides, R. M. Ballew, D. H. Huson, J. R. Wortman, Q. Zhang, C. D. Kodira, X. H. Zheng, L. Chen, M. Skupski, G. Subramanian, P. D. Thomas, J. Zhang, G. L. Gabor Miklos, C. Nelson, S. Broder, A. G. Clark, J. Nadeau, V. A. McKusick, N. Zinder, A. J. Levine, R. J. Roberts, M. Simon, C. Slayman, M. Hunkapiller, R. Bolanos, A. Delcher, I. Dew, D. Fasulo, M. Flanigan, L. Florea, A. Halpern, S. Hannenhalli, S. Kravitz, S. Levy, C. Mobarry, K. Reinert, K. Remington, J. Abu-Threideh, E. Beasley, K. Biddick, V. Bonazzi, R. Brandon, M. Cargill, I. Chandramouliswaran, R. Charlab, K. Chaturvedi, Z. Deng, V. Di Francesco, P. Dunn, K. Eilbeck, C. Evangelista, A. E. Gabrielian, W. Gan, W. Ge, F. Gong, Z. Gu, P. Guan, T. J. Heiman, M. E. Higgins, R. R. Ji, Z. Ke, K. A. Ketchum, Z. Lai, Y. Lei, Z. Li, J. Li, Y. Liang, X. Lin, F. Lu, G. V. Merkulov, N. Milshina, H. M. Moore, A. K. Naik, V. A. Narayan, B. Neelam, D. Nusskern, D. B. Rusch, S. Salzberg, W. Shao, B. Shue, J. Sun, Z. Wang, A.

Wang, X. Wang, J. Wang, M. Wei, R. Wides, C. Xiao, C. Yan, A. Yao, J. Ye, M. Zhan, W. Zhang, H. Zhang, Q. Zhao, L. Zheng, F. Zhong, W. Zhong, S. Zhu, S. Zhao, D. Gilbert, S. Baumhueter, G. Spier, C. Carter, A. Cravchik, T. Woodage, F. Ali, H. An, A. Awe, D. Baldwin, H. Baden, M. Barnstead, I. Barrow, K. Beeson, D. Busam, A. Carver, A. Center, M. L. Cheng, L. Curry, S. Danaher, L. Davenport, R. Desilets, S. Dietz, K. Dodson, L. Doup, S. Ferriera, N. Garg, A. Gluecksmann, B. Hart, J. Haynes, C. Haynes, C. Heiner, S. Hladun, D. Hostin, J. Houck, T. Howland, C. Ibegwam, J. Johnson, F. Kalush, L. Kline, S. Koduru, A. Love, F. Mann, D. May, S. McCawley, T. McIntosh, I. McMullen, M. Moy, L. Moy, B. Murphy, K. Nelson, C. Pfannkoch, E. Pratts, V. Puri, H. Qureshi, M. Reardon, R. Rodriguez, Y. H. Rogers, D. Romblad, B. Ruhfel, R. Scott, C. Sitter, M. Smallwood, E. Stewart, R. Strong, E. Suh, R. Thomas, N. N. Tint, S. Tse, C. Vech, G. Wang, J. Wetter, S. Williams, M. Williams, S. Windsor, E. Winn-Deen, K. Wolfe, J. Zaveri, K. Zaveri, J. F. Abril, R. Guigo, M. J. Campbell, K. V. Sjolander, B. Karlak, A. Kejariwal, H. Mi, B. Lazareva, T. Hatton, A. Narechania, K. Diemer, A. Muruganujan, N. Guo, S. Sato, V. Bafna, S. Istrail, R. Lippert, R. Schwartz, B. Walenz, S. Yooseph, D. Allen, A. Basu, J. Baxendale, L. Blick, M. Caminha, J. Carnes-Stine, P. Caulk, Y. H. Chiang, M. Coyne, C. Dahlke, A. Mays, M. Dombroski, M. Donnelly, D. Ely, S. Esparham, C. Fosler, H. Gire, S. Glanowski, K. Glasser, A. Glodek, M. Gorokhov, K. Graham, B. Gropman, M. Harris, J. Heil, S. Henderson, J. Hoover, D. Jennings, C. Jordan, J. Jordan, J. Kasha, L. Kagan, C. Kraft, A. Levitsky, M. Lewis, X. Liu, J. Lopez, D. Ma, W. Majoros, J. McDaniel, S. Murphy, M. Newman, T. Nguyen, N. Nguyen, M. Nodell, S. Pan, J. Peck, M. Peterson, W. Rowe, R. Sanders, J. Scott, M. Simpson, T. Smith, A. Sprague, T. Stockwell, R. Turner, E. Venter, M. Wang, M. Wen, D. Wu, M. Wu, A. Xia, A. Zandieh, and X. Zhu. 2001. The sequence of the human genome. *Science 291:1304-51.*

143. Akker, S. A., P. J. Smith, and S. L. Chew. 2001. Nuclear post-transcriptional control of gene expression. *J Mol Endocrinol 27:123-31.*
144. Chabot, B. 1996. Directing alternative splicing: cast and scenarios. *Trends Genet 12:472-8.*
145. Sorek, R., and G. Ast. 2003. Intronic sequences flanking alternatively spliced exons are conserved between human and mouse. *Genome Res 13:1631-7.*
146. Lopez, A. J. 1998. Alternative splicing of pre-mRNA: developmental consequences and mechanisms of regulation. *Annu Rev Genet 32:279-305.*
147. Blencowe, B. J. 2000. Exonic splicing enhancers: mechanism of action, diversity and role in human genetic diseases. *Trends Biochem Sci 25:106-10.*
148. Smith, C. W., and J. Valcarcel. 2000. Alternative pre-mRNA splicing: the logic of combinatorial control. *Trends Biochem Sci 25:381-8.*
149. Maniatis, T., and B. Tasic. 2002. Alternative pre-mRNA splicing and proteome expansion in metazoans. *Nature 418:236-43.*
150. Caceres, J. F., and A. R. Kornblihtt. 2002. Alternative splicing: multiple control mechanisms and involvement in human disease. *Trends Genet 18:186-93.*
151. Proudfoot, N. 2000. Connecting transcription to messenger RNA processing. *Trends Biochem Sci 25:290-3.*
152. Slavin, S., and S. Strober. 1978. Spontaneous murine B-cell leukaemia. *Nature 272:624-6.*
153. Li, H., L. M. Ayer, M. J. Polyak, C. M. Mutch, R. J. Petrie, L. Gauthier, N. Shariat, M. J. Hendzel, A. R. Shaw, K. D. Patel, and J. P. Deans. 2004. The CD20 calcium channel is localized to microvilli and constitutively associated with membrane rafts: antibody binding increases the affinity of the association through an epitope-dependent cross-linking-independent mechanism. *J Biol Chem 279:19893-901.*
154. Gordon, J. A. 1991. Use of vanadate as protein-phosphotyrosine phosphatase inhibitor. *Methods Enzymol 201:477-82.*

155. Schagger, H., W. A. Cramer, and G. von Jagow. 1994. Analysis of molecular masses and oligomeric states of protein complexes by blue native electrophoresis and isolation of membrane protein complexes by two-dimensional native electrophoresis. *Anal Biochem 217:220-30.*
156. Nicoletti, I., G. Migliorati, M. C. Pagliacci, F. Grignani, and C. Riccardi. 1991. A rapid and simple method for measuring thymocyte apoptosis by propidium iodide staining and flow cytometry. *J Immunol Methods 139:271-9.*
157. Cragg, M. S., R. R. French, and M. J. Glennie. 1999. Signaling antibodies in cancer therapy. *Curr Opin Immunol 11:541-7.*
158. Cragg, M. S., L. Zhang, R. R. French, and M. J. Glennie. 1999. Analysis of the interaction of monoclonal antibodies with surface IgM on neoplastic B-cells. *Br J Cancer 79:850-7.*
159. Zhang, L., R. R. French, H. T. Chan, T. L. O'Keefe, M. S. Cragg, M. J. Power, and M. J. Glennie. 1995. The development of anti-CD79 monoclonal antibodies for treatment of B- cell neoplastic disease. *Ther Immunol 2:191-202.*
160. Vuist, W. M., R. Levy, and D. G. Maloney. 1994. Lymphoma regression induced by monoclonal anti-idiotypic antibodies correlates with their ability to induce Ig signal transduction and is not prevented by tumor expression of high levels of bcl-2 protein. *Blood 83:899-906.*
161. Kaminski, M. S., K. Kitamura, D. G. Maloney, M. J. Campbell, and R. Levy. 1986. Importance of antibody isotype in monoclonal anti-idiotype therapy of a murine B cell lymphoma. A study of hybridoma class switch variants. *J Immunol 136:1123-30.*
162. Lowder, J. N., T. C. Meeker, M. Campbell, C. F. Garcia, J. Gralow, R. A. Miller, R. Warnke, and R. Levy. 1987. Studies on B lymphoid tumors treated with monoclonal anti-idiotype antibodies: correlation with clinical responses. *Blood 69:199-210.*
163. Li, Y. S., K. Hayakawa, and R. R. Hardy. 1993. The regulated expression of B lineage associated genes during B cell differentiation in bone marrow and fetal liver. *J Exp Med 178:951-60.*
164. Gold, M. R., D. A. Law, and A. L. DeFranco. 1990. Stimulation of protein tyrosine phosphorylation by the B-lymphocyte antigen receptor. *Nature 345:810-3.*
165. Mongini, P. K., Q. Liu, M. A. Vilensky, P. F. Highet, and J. K. Inman. 1998. Evidence for an upper affinity threshold for anti-IgM-induced apoptosis in a human B-cell lymphoma. *Blood 92:3756-71.*
166. Finke, J., R. Fritzen, P. Ternes, P. Trivedi, K. J. Bross, W. Lange, R. Mertelsmann, and G. Dolken. 1992. Expression of bcl-2 in Burkitt's lymphoma cell lines: induction by latent Epstein-Barr virus genes. *Blood 80:459-69.*
167. Dillon, S. R., M. Mancini, A. Rosen, and M. S. Schlissel. 2000. Annexin V binds to viable B cells and colocalizes with a marker of lipid rafts upon B cell receptor activation. *J Immunol 164:1322-32.*
168. Dillon, S. R., A. Constantinescu, and M. S. Schlissel. 2001. Annexin V binds to positively selected B cells. *J Immunol 166:58-71.*
169. Mongini, P. K., M. A. Vilensky, P. F. Highet, and J. K. Inman. 1998. Membrane IgM-stimulated human B lymphocytes succumb to activation- related apoptosis at a G1-->S transition: influence of ligand affinity and valency. *Cell Immunol 188:137-50.*
170. Otipoby, K. L., K. E. Draves, and E. A. Clark. 2001. CD22 regulates B cell receptor-mediated signals via two domains that independently recruit Grb2 and SHP-1. *J Biol Chem 276:44315-22.*
171. Winslow, M. M., J. R. Neilson, and G. R. Crabtree. 2003. Calcium signalling in lymphocytes. *Curr Opin Immunol 15:299-307.*
172. Jun, J. E., and C. C. Goodnow. 2003. Scaffolding of antigen receptors for immunogenic versus tolerogenic signaling. *Nat Immunol 4:1057-64.*

173. Lee, J. R., and G. A. Koretzky. 1998. Extracellular signal-regulated kinase-2, but not c-Jun NH2-terminal kinase, activation correlates with surface IgM-mediated apoptosis in the WEHI 231 B cell line. *J Immunol 161:1637-44.*
174. Gauld, S. B., D. Blair, C. A. Moss, S. D. Reid, and M. M. Harnett. 2002. Differential roles for extracellularly regulated kinase-mitogen-activated protein kinase in B cell antigen receptor-induced apoptosis and CD40-mediated rescue of WEHI-231 immature B cells. *J Immunol 168:3855-64.*
175. Xu, Y., K. W. Harder, N. D. Huntington, M. L. Hibbs, and D. M. Tarlinton. 2005. Lyn tyrosine kinase: accentuating the positive and the negative. *Immunity 22:9-18.*
176. Chan, V. W., F. Meng, P. Soriano, A. L. DeFranco, and C. A. Lowell. 1997. Characterization of the B lymphocyte populations in Lyn-deficient mice and the role of Lyn in signal initiation and down-regulation. *Immunity 7:69-81.*
177. Takeshita, H., I. Taniuchi, J. Kato, and T. Watanabe. 1998. Abrogation of autoimmune disease in Lyn-deficient mice by the mutation of the Btk gene. *Int Immunol 10:435-44.*
178. Cheng, P. C., B. K. Brown, W. Song, and S. K. Pierce. 2001. Translocation of the B cell antigen receptor into lipid rafts reveals a novel step in signaling. *J Immunol 166:3693-701.*
179. Elliott, T. J., M. J. Glennie, H. M. McBride, and G. T. Stevenson. 1987. Analysis of the interaction of antibodies with immunoglobulin idiotypes on neoplastic B lymphocytes: implications for immunotherapy. *J Immunol 138:981-8.*
180. Vilen, B. J., S. J. Famiglietti, A. M. Carbone, B. K. Kay, and J. C. Cambier. 1997. B cell antigen receptor desensitization: disruption of receptor coupling to tyrosine kinase activation. *J Immunol 159:231-43.*
181. Vilen, B. J., T. Nakamura, and J. C. Cambier. 1999. Antigen-stimulated dissociation of BCR mIg from Ig-alpha/Ig-beta: implications for receptor desensitization. *Immunity 10:239-48.*
182. Schagger, H., H. Bentlage, W. Ruitenbeek, K. Pfeiffer, S. Rotter, C. Rother, A. Bottcher-Purkl, and E. Lodemann. 1996. Electrophoretic separation of multiprotein complexes from blood platelets and cell lines: technique for the analysis of diseases with defects in oxidative phosphorylation. *Electrophoresis 17:709-14.*
183. Hashimoto, S., P. K. Gregersen, and N. Chiorazzi. 1993. The human Ig-beta cDNA sequence, a homologue of murine B29, is identical in B cell and plasma cell lines producing all the human Ig isotypes. *J Immunol 150:491-8.*
184. Benhamou, L. E., P. A. Cazenave, and P. Sarthou. 1990. Anti-immunoglobulins induce death by apoptosis in WEHI-231 B lymphoma cells. *Eur J Immunol 20:1405-7.*
185. Hasbold, J., and G. G. Klaus. 1990. Anti-immunoglobulin antibodies induce apoptosis in immature B cell lymphomas. *Eur J Immunol 20:1685-90.*
186. Brown, M. H., K. Boles, P. A. van der Merwe, V. Kumar, P. A. Mathew, and A. N. Barclay. 1998. 2B4, the natural killer and T cell immunoglobulin superfamily surface protein, is a ligand for CD48. *J Exp Med 188:2083-90.*
187. Harnett, M. M., E. Katz, and C. A. Ford. 2005. Differential signalling during B-cell maturation. *Immunol Lett 98:33-44.*
188. Mizuguchi, J., W. Tsang, S. L. Morrison, M. A. Beaven, and W. E. Paul. 1986. Membrane IgM, IgD, and IgG act as signal transmission molecules in a series of B lymphomas. *J Immunol 137:2162-7.*
189. Tang, G. 2005. siRNA and miRNA: an insight into RISCs. *Trends Biochem Sci 30:106-14.*
190. Gordon, M. S., R. M. Kato, F. Lansigan, A. A. Thompson, R. Wall, and D. J. Rawlings. 2000. Aberrant B cell receptor signaling from B29 (Igbeta, CD79b) gene mutations of chronic lymphocytic leukemia B cells. *Proc Natl Acad Sci U S A 97:5504-9.*

191. Indraccolo, S., S. Minuzzo, R. Zamarchi, F. Calderazzo, E. Piovan, and A. Amadori. 2002. Alternatively spliced forms of Igalpha and Igbeta prevent B cell receptor expression on the cell surface. *Eur J Immunol 32:1530-40.*
192. Payelle-Brogard, B., C. Magnac, A. Alcover, P. Roux, and G. Dighiero. 2002. Defective assembly of the B-cell receptor chains accounts for its low expression in B-chronic lymphocytic leukaemia. *Br J Haematol 118:976-85.*
193. Vuillier, F., G. Dumas, C. Magnac, M. C. Prevost, A. I. Lalanne, P. Oppezzo, E. Melanitou, G. Dighiero, and B. Payelle-Brogard. 2005. Lower levels of surface B-cell-receptor expression in chronic lymphocytic leukemia are associated with glycosylation and folding defects of the mu and CD79a chains. *Blood 105:2933-40.*
194. Tseng, J., B. J. Eisfelder, and M. R. Clark. 1997. B-cell antigen receptor-induced apoptosis requires both Ig alpha and Ig beta. *Blood 89:1513-20.*
195. Sutherland, C. L., A. W. Heath, S. L. Pelech, P. R. Young, and M. R. Gold. 1996. Differential activation of the ERK, JNK, and p38 mitogen-activated protein kinases by CD40 and the B cell antigen receptor. *J Immunol 157:3381-90.*
196. Katz, E., C. Lord, C. A. Ford, S. B. Gauld, N. A. Carter, and M. M. Harnett. 2004. Bcl-(xL) antagonism of BCR-coupled mitochondrial phospholipase A(2) signaling correlates with protection from apoptosis in WEHI-231 B cells. *Blood 103:168-76.*
197. Reid, S. D., and M. M. Harnett. 1997. CD40 signalling in B cell apoptosis and rescue. *Biochem Soc Trans 25:299S.*
198. Glennie, M. J., and P. W. Johnson. 2000. Clinical trials of antibody therapy. *Immunol Today 21:403-10.*
199. Miller, R. A., D. G. Maloney, R. Warnke, and R. Levy. 1982. Treatment of B-cell lymphoma with monoclonal anti-idiotype antibody. *N Engl J Med 306:517-22.*
200. Hibbs, M. L., D. M. Tarlinton, J. Armes, D. Grail, G. Hodgson, R. Maglitto, S. A. Stacker, and A. R. Dunn. 1995. Multiple defects in the immune system of Lyn-deficient mice, culminating in autoimmune disease. *Cell 83:301-11.*
201. Nishizumi, H., I. Taniuchi, Y. Yamanashi, D. Kitamura, D. Ilic, S. Mori, T. Watanabe, and T. Yamamoto. 1995. Impaired proliferation of peripheral B cells and indication of autoimmune disease in lyn-deficient mice. *Immunity 3:549-60.*
202. Dolmetsch, R. E., R. S. Lewis, C. C. Goodnow, and J. I. Healy. 1997. Differential activation of transcription factors induced by Ca2+ response amplitude and duration. *Nature 386:855-8.*
203. Healy, J. I., R. E. Dolmetsch, L. A. Timmerman, J. G. Cyster, M. L. Thomas, G. R. Crabtree, R. S. Lewis, and C. C. Goodnow. 1997. Different nuclear signals are activated by the B cell receptor during positive versus negative signaling. *Immunity 6:419-28.*
204. Jiang, A., A. Craxton, T. Kurosaki, and E. A. Clark. 1998. Different protein tyrosine kinases are required for B cell antigen receptor-mediated activation of extracellular signal-regulated kinase, c-Jun NH2-terminal kinase 1, and p38 mitogen-activated protein kinase. *J Exp Med 188:1297-306.*
205. Fuentes-Panana, E. M., G. Bannish, D. van der Voort, L. B. King, and J. G. Monroe. 2005. Ig alpha/Ig beta complexes generate signals for B cell development independent of selective plasma membrane compartmentalization. *J Immunol 174:1245-52.*
206. Kremyanskaya, M., and J. G. Monroe. 2005. Ig-independent Ig beta expression on the surface of B lymphocytes after B cell receptor aggregation. *J Immunol 174:1501-6.*
207. Coopman, P. J., M. T. Do, M. Barth, E. T. Bowden, A. J. Hayes, E. Basyuk, J. K. Blancato, P. R. Vezza, S. W. McLeskey, P. H. Mangeat, and S. C. Mueller. 2000. The Syk tyrosine kinase suppresses malignant growth of human breast cancer cells. *Nature 406:742-7.*

208. Konig, H., J. Moll, H. Ponta, and P. Herrlich. 1996. Trans-acting factors regulate the expression of CD44 splice variants. *Embo J 15:4030-9.*
209. Matter, N., P. Herrlich, and H. Konig. 2002. Signal-dependent regulation of splicing via phosphorylation of Sam68. *Nature 420:691-5.*